NATIONAL ADVISORY COMMITTEE FOR AERONAUTICS

WARTIME REPORT

ORIGINALLY ISSUED

January 1946 as
Memorandum Report A5L07

THE HIGH-SPEED CHARACTERISTICS OF SEVERAL FLAPS AND SPOILERS ON THE UPPER SURFACE OF THE HORIZONTAL STABILIZER OF A MODEL OF A RADIAL-ENGINE PURSUIT AIRPLANE

By Lee E. Boddy

Ames Aeronautical Laboratory
Moffett Field, California

NACA

WASHINGTON

MR No. A5L07

NATIONAL ADVISORY COMMITTEE FOR AERONAUTICS

MEMORANDUM REPORT

for the

Air Technical Service Command, U. S. Army Air Forces

THE HIGH-SPEED CHARACTERISTICS OF SEVERAL FLAPS AND SPOILERS ON THE UPPER SURFACE OF THE HORIZONTAL STABILIZER OF A MODEL OF A RADIAL-ENGINE PURSUIT AIRPLANE

By Lee E. Boddy

SUMMARY

An investigation was made in the Ames 16-foot high-speed wind tunnel of several types and sizes of flaps and spoilers located immediately forward of the elevators on the upper surface of the horizontal stabilizer of a model of a radial-engine pursuit airplane. The elevator characteristics, the elevator-fixed and elevator-free balance lift coefficient, and the trim drag coefficient of the model are given through a Mach number range of 0.20 to 0.815 for all the flaps and spoilers tested. In addition, the effect of the largest flap on the maneuver forces, the stick-fixed and stick-free neutral point, and the chordwise pressure distribution on the horizontal tail at a station through the flap are given.

Throughout the Mach number range of the tests, except for small deflections, the flaps and spoilers produced a download on the tail and caused the elevators to float more negatively, thus increasing the trim lift coefficient. A reversal of the trim lift coefficient existed for small flap deflections and was caused largely by the fact that the elevators tended to float more positively until the flaps were extended above the critical height. Any of the devices having a projected area normal to the stabilizer surface of about 2 percent of the horizontal-tail area should provide satisfactory recovery of the airplane from a dive at 0.815

Mach number. However, the acceleration available decreased rapidly with increased Mach number above the Mach number at which the pitching-moment characteristics of the model diverged. Although the flaps and spoilers were suitable as a dive-recovery device, the reversal of their effectiveness with small deflections and their detrimental effect upon the stick-free stability of the model rendered them unsatisfactory as a longitudinal trim device.

INTRODUCTION

The pitching-moment characteristics of a conventional airplane traveling at speeds approaching those of sound differ widely from the characteristics at lower speeds. The most important effects of high speed, from the standpoint of stability and control, are a decrease of the slope of the lift curve of the airplane, a subsequent increase of the static longitudinal stability, and a shift of the longitudinal trim. Most current combat airplanes employing relatively high wing loadings encounter this divergence of characteristics in high-speed dives, the usual result being that the pilot experiences difficulty in making the recovery from the dive. It has been necessary, therefore, to equip many airplanes with some sort of auxiliary control device.

Up to the present time, the most popular method of gaining additional longitudinal control has been the use of dive-recovery flaps on the lower surface of the wing. (The results of tests of the radial-engine pursuit airplane model equipped with this type of flap are reported in reference 1.) It is possible, however, to control the trim of an airplane by means of any device which will vary the load on the horizontal tail - provided, of course, that the wing retains its ability to develop the necessary lift.

In a program of low-speed tests directed toward the development of a lateral-control device suitable for use with full-span flaps (reference 2), and during an investigation aimed at the improvement of the lateral-control characteristics of high-speed aircraft (reference 3), the NACA tested several arrangements of spoiler and spoiler-aileron combinations. The results of these tests indicated the possibility of applying spoilers to the horizontal tail of an airplane to gain sufficient longitudinal control in high-speed flight. The present investigation was undertaken, at the request of the Air Technical Service Command, U.S. Army Air Forces, in order to ascertain the suitability of such an arrangement.

The model of this radial-engine pursuit airplane was chosen for the tests because it was already available, and because the U.S. Army Air Forces had initiated flight tests of an airplane fitted with auxiliary flaps on the horizontal stabilizer.

MODEL AND APPARATUS

Throughout the tests of the flaps and spoilers, the standard configuration of the model (fig. 1) conformed to that of the radial-engine pursuit airplane with the propeller removed. The wing, fuselage, horizontal stabilizer, and vertical fin were built up of steel spars covered with mahogany; the elevators and rudder were cast aluminum alloy; and the engine cowl was formed from sheet aluminum. In order to determine the nature of the air flow ahead of and behind the flaps, a band of pressure orifices was built into the horizontal tail at a station 10.00 inches from the center line of the model. The elevator deflection was controlled remotely through a unit which incorporated an electric motor for power, an electric strain gage to measure the elevator hinge moment, and a selsyn motor to indicate the elevator deflection.

The pertinent model dimensions were as follows:

Wing

Area, sq ft	27.000
Span, ft.	12.233
Mean aerodynamic chord, ft.	2.187
Section	modified NACA 230-series section
Thickness at root, percent chord	15.0

Incidence at root relative to fuselage reference line, deg	1.00
Incidence at tip relative to fuselage reference line, deg	-2.96

Horizontail tail

Area, sq ft	4.95
Span, ft.	4.80
Length (center of gravity to elevator hinge line), ft	6.79
Thickness, percent chord.	9.0
Incidence relative to fuselage reference line, deg	2.8

Elevators (two)

Area forward of the hinge line, sq ft	0.404
Area aft of the hinge line, sq ft	1.614
Span (twice the hinge-line span of one elevator), ft	4.536
Mean-square chord aft of the hinge line, sq ft .	0.1369

The elevators on this airplane model are of the blunt-nose type, incorporating an average aerodynamic balance (ratio of the area forward of the hinge line to that aft of the hinge line) of approximately 25 percent, and an average nose gap with the elevators neutral of about 1.7 percent of the horizontal tail chord. The basic airfoil shape of the horizontal tail was similar to the NACA 0009 except that the leading-edge radius was considerably decreased and the section forward of the 25-percent-chord point was correspondingly thinner.

All the flaps and spoilers, locations on the model and dimensions of which are given in figure 2, were located so that the trailing edge of the undeflected surface would coincide with the center line of the rear stabilizer spar of the airplane.

The flaps were rectangular in plan form, and are designated in this report by the chord and span of a single flap and its angular deflection from the surface of the stabilizer. The flaps representing deflections of a 7.5° and 15° were hardwood wedges screwed to the stabilizer spar; those representing deflections of 30°, 45°, and 60° were 1/16-inch steel plate held to the spar by brackets on the underside of the flap. Two modifications were tested in addition to the standard split-type flaps: (1) a flap having one-third of its area removed from the leading edge so that a gap was formed as the flap was deflected, and (2) a flap placed as though hinged at its trailing edge. Details of these two flaps are shown in figures 2(b) and 2(c), respectively.

The spoilers were projected normal to the stabilizer surface and were of two types: (1) those having a projection at every point along the span of approximately a constant percent of the local tail-plane chord, and (2) those tapering from a maximum projection at the inboard end to zero projection at the outboard end. The former are referred to as constant-percent-chord spoilers and their projection is given in percent of the local tail-plane chord; the latter are referred to as tapered spoilers and their projection is given in percent of the tail-plane chord at the inboard end of the spoilers.

Support for the model in the wind-tunnel test section (fig. 3) was provided by two 5-percent-thick unshielded struts connected to the wing 40 inches either side of the center line of the model, and a single 7-percent-thick unshielded strut connected to the after part of the fuselage. Angle-of-attack control was obtained by vertical movement of the rear strut.

SYMBOLS

The symbols used in this report are defined as follows:

V free-stream velocity, feet per second

M free-stream Mach number $\left(\frac{V}{\text{speed of sound}}\right)$

ρ free-stream mass density, slugs per cubic foot

q free-stream dynamic pressure ($\frac{1}{2}\rho V^2$), pounds per square foot

p_o static pressure in test section, pounds per square foot

p local static pressure on the surface, pounds per square foot

S wing area, square feet

S_T horizontal-tail area, square feet

$S_{f'}$ projected area of flap normal to the stabilizer surface, square feet

M.A.C. mean aerodynamic chord of the wing, feet

b_e elevator span, feet

$\overline{c_e^2}$ mean-square chord of the elevator aft of the hinge line, square feet

W gross weight of airplane, pounds

C_L lift coefficient $\left(\frac{\text{lift}}{qS}\right)$

C_D drag coefficient $\left(\frac{\text{drag}}{qS}\right)$

$C_{m_{c.g.}}$ pitching-moment coefficient about the center of gravity $\left(\frac{\text{pitching moment}}{qS\ \text{M.A.C.}}\right)$

$\Delta C_{m_{c.g.}}$ increase of pitching-moment coefficient about the center of gravity

C_{h_e} elevator hinge-moment coefficient $\left(\frac{\text{hinge moment}}{q\ b_e\ \overline{c_e^2}}\right)$

P pressure coefficient $\left(\frac{p - p_o}{q}\right)$

P_U pressure coefficient on the upper surface

P_L pressure coefficient on the lower surface

P_{cr} critical pressure coefficient (P at which the local speed equals the local speed of sound)

α angle of attack of the fuselage reference line, degrees

α_u angle between the fuselage reference line and the tunnel center line, degrees

δ_e elevator deflection relative to the horizontal-tail-chord plane (positive with the trailing edge down), degrees

$\Delta\delta_e$ increase of elevator floating angle due to flap deflection, degrees

δ_f flap deflection relative to the surface of the stabilizer, degrees

δ_t elevator tab deflection (positive with the trailing edge down), degrees

REDUCTION OF DATA

The results of the tests have been corrected for tunnel-wall effects by adding the following:

$$\Delta\alpha \text{ (deg)} = 1.052\ C_L$$

$$\Delta C_D = 0.0184\ C_L^2$$

$$\Delta C_m = 0.0189\ C_L \quad \text{(tail on)}$$

In addition, tare corrections due to the support struts have been applied to the drag, pitching moment, and angle of attack. The tare forces and moments were obtained from tests with the struts in place, but with the model removed from the tunnel, while the angle-of-attack correction was obtained from upright and inverted tests of a model similar in size and plan form to this model. Because of the complicated structure and rigging involved, no attempt was made to account for the mutual interference between the model and the support struts. For the same reason, the inclination of the air stream at the horizontal-tail plane due to the support system was not evaluated but was assumed to be the same at the tail as at the wing.

The average Mach number throughout the space in the test section normally occupied by the wing was measured, with the struts in place and model removed, by means of a multiple-boom static-pressure survey wing. (See reference 4.) This calibration was then corrected for the constriction effects of the model in a manner similar to that described in reference 4, using the dimensions and equations given in the appendix. The dynamic pressure was computed from the corrected Mach number and the known total pressure in the test section.

No attempt was made to account for the difference of the Mach number and dynamic pressure at the tail plane from that at the wing. Due to the arrangement of the support system and the model components, both the local velocity with the model removed and the effect of the model constriction were undoubtedly less in the region of the tail than they were near the wing, with the result that the tail probably was operating in a slower region of air than indicated.

All the data were reduced to dimensionless coefficients, the pitching-moment coefficients being referred to a center-of-gravity location which was 1.650 inches below the fuselage reference line and directly above the 27.5-percent point of the M.A.C.

DISCUSSION

Characteristics of the Standard Model

The three-component aerodynamic characteristics of the radial-engine pursuit airplane model are shown in figures 4 to 8, inclusive. For Mach numbers from 0.20 to 0.815, no important change of angle of attack for zero lift was detected, and the increase of the tail-off lift-curve slope from 0.080 per degree at a Mach number of 0.20 to 0.97 per degree at a Mach number of 0.69 was only about 60 percent of that predicted from Glauert's theoretical factor $(1/\sqrt{1-M^2})$. Since the trim and the static longitudinal stability depend upon the angle of attack for zero lift and the lift-curve slope, it is desirable that changes of these two factors be as small as possible.

For small values of the lift coefficient, the drag coefficient of the model increased rapidly with Mach number above a Mach number of about 0.75. If inertia forces and propeller thrust are neglected (so that in a vertical dive the drag of the airplane is equal to and opposes the weight), the results indicate a maximum attainable Mach number at 10,000 feet altitude of 0.825 for a wing loading of 45 pounds per square foot. (See fig. 6.) At an altitude of 20,000 feet, the maximum predicted Mach number is about 0.84. Figures 7, 8, and 9 show that this is considerably above the Mach number at which the pitching-moment characteristics diverge from those at low speed.

Above a Mach number of about 0.75 and a lift coefficient of 0.2, or above a Mach number of about 0.63 and a lift coefficient of 0.6, the rate of change of pitching-moment coefficient with Mach number became highly negative. Similarly, the rate of change of pitching-moment coefficient with lift coefficient (static longitudinal stability) suddenly increased to three or four times the low-speed value. At these Mach numbers and lift coefficients, then, a slight increase of speed would cause the airplane to tend to nose down, which in turn would result in a further increase of speed, the instability progressing until the airplane finally trimmed in a nearly vertical dive. The condition is further aggravated by the fact that the large increase of the static longitudinal stability greatly reduces the ability of the elevators to control the airplane.

It is significant that one-third to one-half the total divergence of the pitching-moment characteristics was present with the tail removed, indicating that the wing-fuselage combination contributes directly a large proportion of the adverse effects.

The elevator characteristics of the airplane model are given for three different elevator-tab angles in figures 10, 11, and 12. At low values of the lift coefficient and for moderate elevator deflections, the elevator effectiveness $(\partial C_m/\partial \delta_e)_{C_L}$ was independent of Mach number up to a Mach number of 0.815, the maximum obtained with the complete model. However, the rate of change of hinge-moment coefficient with lift coefficient changed from a small negative value at low Mach numbers to a small positive value at high Mach numbers. No radical change of elevator characteristics was apparent which might appreciably alter the divergence of the pitching-moment characteristics detected in the results of the elevator-fixed tests.

Characteristics of the Flaps and Spoilers

Comparison of the various flaps and spoilers.- The pitching-moment characteristics of this pursuit airplane model fitted with various flaps and spoilers are shown in figures 13 to 32 in the form of plots of pitching-moment coefficient and elevator hinge-moment coefficient as a function of elevator angle. A brief résumé of the increments of pitching-moment coefficient and elevator floating angle due to the flaps and spoilers is given in figure 33. Figures 34 to 37 are plots showing the lift coefficient for balance ($C_m = 0$) and the trim lift coefficient (balance with elevators free, or $C_m = 0$, $C_{h_e} = 0$) of the model as a function of the deflection of the flaps and spoilers.

With the elevators fixed, except for small deflections at low speed, all the flaps and spoilers produced a download on the tail which was approximately proportional to their projected area normal to the stabilizer surface. Furthermore, the elevator hinge-moment characteristics indicate that, except for small deflections, the flaps and spoilers caused the elevators to float more negatively, resulting in an additional favorable effect. The tendency of the elevators to float more positively with small flap deflections is examined in detail in the section concerning the pressure distribution on the horizontal tail.

The faired curves of figure 33, although derived from too few points to be considered entirely accurate, indicate the effectiveness of the various flaps and spoilers in producing a download on the tail and in decreasing the elevator floating angle. The solid curves were obtained from tests of all the flaps and spoilers having average projected heights of approximately 2 percent of the horizontal-tail chord, the projected area then being a function of the span of the device. Data for the dashed curves and dotted curves were obtained from tests of the 12-inch-span flaps so that the projected area was determined by the deflection of the flaps. Since the solid curves include no data from tests with small flap deflections, the characteristic reversal is not shown.

The power of the flaps to produce a download on the tail increased with Mach number up to a value of 0.815, and the maximum change of elevator floating angle was about 25 percent less at a Mach number of 0.815 than it was at low speed. Nevertheless, above the lift coefficient and Mach number at which the pitching-moment characteristics of the standard model diverged widely (fig. 9) the power of the flaps and spoilers to balance the model was greatly reduced. For example, at a Mach number of 0.60, a 45° deflection of the 1.2- by 12-inch flaps trimmed the model at a lift coefficient of about 0.82; at a Mach number of 0.815 the trim lift coefficient was only 0.39. Similarly, only 1.8° travel of the elevators was required at low speed in order to increase the balance lift coefficient of the standard model from 0.00 to 0.30; whereas 8.0° travel was required at a Mach number of 0.815. This increase is due almost entirely to the increased static longitudinal stability of the model at high speed, and demonstrates clearly the need for additional control.

The results of tests of the modified flaps are shown in figure 34 as single points, since each modification was tested with only one deflection. Hinging the flap at its trailing edge had very little effect upon its characteristics, at least for the deflection tested. The 33-percent gap, however, reduced the elevator-fixed effectiveness slightly, and diminished the effect on the elevator floating angle about 50 to 60 percent, the over-all effect of the gap being to reduce the trim lift coefficient by about 0.06 at all Mach numbers from 0.60 to 0.815. The gap, although detrimental to the effectiveness of a device of this type, may alleviate the violent turbulence in the flap wake so as to be desirable for reducing tail buffeting. Unfortunately, the mass and rigidity of the model prevented observations concerning tail buffeting during the present tests.

Compared on a basis of the projected area of the device normal to the stabilizer surface, the 0.6- by 12-inch flaps and the 12-inch-span, constant-percent-chord spoilers were slightly more effective than the remainder of the flaps and spoilers tested. It appears then, that portions of the device near the tip of the horizontal tail were not quite as effective as those portions nearer the center of the semispan, and that the large-chord flaps with moderate deflections were slightly less powerful than spoilers or the small-chord flaps with compensatingly larger deflections. The latter effect may be due to the fact that the spoilers and small-chord flaps presented a sharper discontinuity of the surface for a given projected area, resulting in less tendency of the air flow to return to the surface aft of the device. For all practical purposes, however, all the devices tested were so effective that in most cases structural considerations would be of more consequence than the aerodynamic advantages of one or the other.

Trim drag coefficient.- The drag coefficients due to the flaps and spoilers may be obtained from figures 38 and 39. In order to provide a fair means of comparison, the drag coefficient of the model was determined for each deflection of the various trim devices and was plotted against the lift coefficient at which that deflection would trim the model. In other words, each point on figure 39 represents the drag coefficient with the model trimmed. This was done for the tabs as well as for the flaps and spoilers. The dashed curves represent the drag coefficient with the model balanced by the elevators but with all other trim devices undeflected. For moderate lift coefficients, the increment of drag coefficient due to trimming the model with the flaps or spoilers was about 0.0030. The drag due to the tab was of course zero near zero lift, but was about one-half that of the flaps and spoilers at moderate lift coefficients.

If the reversal of the elevator-free characteristics of the flaps and spoilers were eliminated, the drag coefficient for trim would be reduced considerably, since small deflections of the devices would then yield a positive increment of trim lift coefficient.

Chordwise pressure distribution on tail.- The chordwise pressure distribution on the horizontal tail is given in figure 40 for several deflections of the 1.2- by 12-inch flaps. Due to the similarity of the pressure distribution with all the devices tested, results are presented herein for this flap only.

Up to a Mach number of 0.815, the pressure induced by the flaps was positive on the upper surface ahead of the flap and slightly negative on the lower surface. Aft of the flap the flow appeared to be separated. For small flap deflections, however, the pressures aft of the flap tended to recover, indicating that the flow was returning to the surface after it had once been separated. The chordwise point on the surface to which the flow appeared to return moved aft as the flap angle was increased.

The section load on the horizontal tail arising from the pressures induced by the flaps is given by the arrows in figure 41. The fact that the download induced ahead of the flaps is partially canceled by the upload induced aft of the flaps indicates the desirability of locating the device as far aft as possible. However, a practical limit to this procedure is reached if the flow tends to separate from the after part of the airfoil with the device undeflected, such as is often encountered at high Mach numbers.

An examination of the load distribution on the elevator offers an explanation of the reversal of the elevator floating angle with small flap deflections. It appears that with small deflections, the flow is separated for only a small distance aft of the flap, resulting in a large upload on the balance portion of the elevator and very little effect on the portion aft of the elevator hinge line. For small flap deflections, then, the tendency is for the elevators to float positively. As the flaps are deflected farther, the portion of the elevators aft of the hinge line also comes under the influence of the induced upload, and the elevators float more negatively. This reasoning suggests the possibility of eliminating the reversal of the elevator floating angle by incorporating an elevator without nose balance with the flaps in the present location, or by locating the flaps at the elevator hinge line if a nose balance is used. With the latter arrangement, the nose balance would be under the influence of the download induced ahead of the flaps, and the surface aft of the elevator hinge line would be under the influence of the upload induced aft of the flap, both effects causing a tendency of the elevators to float negatively. Such an arrangement should be considerably more effective than either the present one or one incorporating an elevator without nose balance.

Application of the Flaps to the Airplane

Dive-recovery device.- The control forces for the airplane were computed from the model test results for several deflections of the 1.2- by 12-inch flaps (model size), and are presented in figure 42 for three different Mach numbers at sea level. In figure 43 the control forces are given for three different altitudes at a Mach number of 0.815. The values given are for a wing loading of 45 pounds per square foot and a center-of-gravity location at 27.5 percent of the M.A.C. Since it is realized that the elevator tabs might be relatively ineffective at high Mach numbers, especially with the flaps deflected, the control forces were computed only for a tab angle of zero.

The results indicate that at least up to a Mach number of 0.815 the flaps were sufficiently powerful to provide satisfactory recovery from a dive, a 30° deflection resulting in a 5.2g pull-up at 10,000 feet altitude or a 3.7g pull-up at 20,000 feet altitude. It appears that a smaller chord flap could be used with compensatingly larger deflections. However, in view of the decreased power of the flaps above the Mach number of divergence, it is considered wise to retain a fairly large margin of control, since no data were obtained at Mach numbers equal to the maximum obtainable in a vertical dive (about 0.84 Mach number at 20,000 ft altitude).

The flaps should be connected to the elevator control system so that they become operative when the control force exceeds a predetermined amount. This arrangement has the advantage over a separate control system (as the tabs) of allowing rapid retraction of the flaps in order to avoid exceedingly high accelerations as the Mach number decreases during the recovery from the dive. Differentially connecting the flaps to the elevators would not provide a satisfactory dive-recovery device because of the reversal of the flap effectiveness at small deflections, and because a flap-deflection to elevator-deflection ratio which provided sufficiently light control forces at diving speeds probably would result in an unstable variation of control force with normal acceleration at low speed.

If the flaps are used solely as a dive-recovery device (connected to the elevator system as suggested) their detrimental effect upon the stick-free stability of the airplane (fig. 44) would not be critical, since they would be deflected only above the Mach number at which the pitching-moment characteristics of the airplane diverged. (At these Mach numbers the stability is three or four times that desired.) Furthermore, the reversal of the effectiveness of the flaps with small deflections is not considered objectionable, since they could be deflected rapidly. The pilot probably would feel an initial negative acceleration which would quickly disappear, the magnitude and duration of the negative acceleration depending upon how quickly the control force was applied. It may be possible for the control force to be applied suddenly enough so that the duration of the reversal would not be sufficient to overcome the inertia of the airplane.

Longitudinal trim device.- The plots of trim lift coefficient (fig. 34) and of control force (figs. 42 and 43) illustrate the power of the flaps to trim the model. Were it not for the reversal of their effectiveness for small deflections and their detrimental effect upon the stick-free stability of the model, the flaps could satisfactorily replace trim tabs and balance tabs. By virtue of their chordwise location on the tail, the flaps should not be as susceptible as tabs to loss of effectiveness due to separation of the flow from the after part of the tail surface. Also, the elevator-fixed effect of the flaps is a favorable one; whereas the elevator-fixed effect of a tab is unfavorable. Slightly heavier elevator control forces could be expected at flight speeds requiring a moderate deflection of the flaps to trim the airplane. (See fig. 42)

The characteristics of the flaps used to replace the elevators for longitudinal control may be obtained from figure 34 (using the curve for elevators neutral). A 45° deflection of the 1.2- by 12-inch flaps (model size) was only as effective as a 6° or 7° deflection of the elevators, indicating that much larger flaps would have to be used for this purpose. The increased drag of such large flaps might prove prohibitive.

CONCLUSIONS

The following statements may be made from the results of the tests:

1. Any of the devices having a projected area normal to the stabilizer surface of approximately 2 percent of the horizontal-tail area were sufficiently powerful to provide satisfactory recovery of the radial-engine pursuit airplane from a dive at 0.815 Mach number (about 3.5g pull-out at 20,000 ft altitude).

2. The acceleration available from the flaps decreased rapidly with increased Mach number above the Mach number at which the pitching-moment characteristics of the model diverged.

3. The flaps would not be satisfactory as a longitudinal trim device due to a reversal of their effectiveness for small deflections and their detrimental effect upon the elevator-free stability of the model.

4. The flaps were not powerful enough to replace the elevators as a longitudinal control device.

5. Further tests should be made in order to develop a flap arrangement free from reversal of effectiveness at small deflections. Also, the range of the tests should be expanded to include a wider range of lift coefficients and elevator angles in order to predict characteristics throughout the range of normal flight speeds.

Ames Aeronautical Laboratory,
National Advisory Committee for Aeronautics,
Moffett Field, Calif.

APPENDIX

The constriction effects of the radial-engine pursuit airplane model were calculated from the following equation, a complete development of which is given in reference 5:

$$M/M_o = 1 + \left[\epsilon_{wing} + \epsilon_{fuselage} + \epsilon_{wake} \right] \left[1 + \frac{\gamma - 1}{2} M_o^2 \right]$$

where

M_o	observed Mach number
M	Mach number corrected for constriction effects
γ	ratio of specific heats
ϵ_{wing}	$K_W \left[\dfrac{\text{wing volume}}{(\text{jet area})^{3/2} \quad (1-M_o^2)^{\eta/2}} \right]$
$\epsilon_{fuselage}$	$K_F \left[\dfrac{\text{fuselage volume}}{(\text{jet area})^{3/2} \quad (1-M_o^2)^{\eta/2}} \right]$
ϵ_{wake}	$\dfrac{1}{4} \left[\dfrac{(\text{model drag coefficient})(\text{Model wing area})}{(\text{jet area})(1-M_o^2)^{\eta/2}} \right]$

The following values were used in computing the several factors:

Ratio of specific heats, γ	1.4
Wing volume, cu ft	5.6
Fuselage volume, cu ft	12.4
Jet area (cross-sectional area of test section less boundary layer), sq ft	186.0
Wing constant, K_W	0.90

Fuselage constant, K_F 0.96

A value of $\eta = 3$ was used in determining the factor for the wing, the fuselage, and the wake.

Upon substitution of the above values, the equation becomes:

$$M/M_o = 1 + \left[\frac{(0.00668 + 0.0363\, C_D)}{(1 - M_o^2)^{3/2}}\right]\left[1 + 0.2\, M_o^2\right]$$

Using values of M_o determined from a survey of the test section with the struts in place, and values of the drag coefficient of the model near 0.2 lift coefficient, the following values of corrected Mach number were obtained:

M_o	0.20	0.395	0.59	0.675	0.72	0.765	0.785	0.80
M	.20	.40	.60	.69	.74	.79	.815	.84

REFERENCES

1. Hamilton, William T., and Boddy, Lee E.: High-Speed Wind-Tunnel Tests of Dive-Recovery Flaps on a 0.3-Scale Model of the P-47D Airplane. NACA ACR No. 5D19, 1945.

2. Wenzinger, Carl J., and Rogallo, Francis M.: Wind-Tunnel Investigation of Spoiler, Deflector, and Slot Lateral-Control Devices on Wings with Full-Span Split and Slotted Flaps. NACA Rep. No 706, 1941.

3. Laitone, Edmond V.: An Investigation of the High-Speed Lateral-Control Characteristics of a Spoiler. NACA ACR No. 4C23, 1944.

4. Nissen, James M., Gadeberg, Burnett L., and Hamilton, William T.: Correlation of the Drag Characteristics of a P-51B Airplane Obtained from High-Speed Wind-Tunnel and Flight Tests. NACA ACR No. 4K02, 1945.

5. Thom, A.: Blockage Corrections and Choking in the R.A.E. High-Speed Tunnel. Rep. No. Aero. 1891, R.A.E. (British/U.S. Confidential) Nov. 1943.

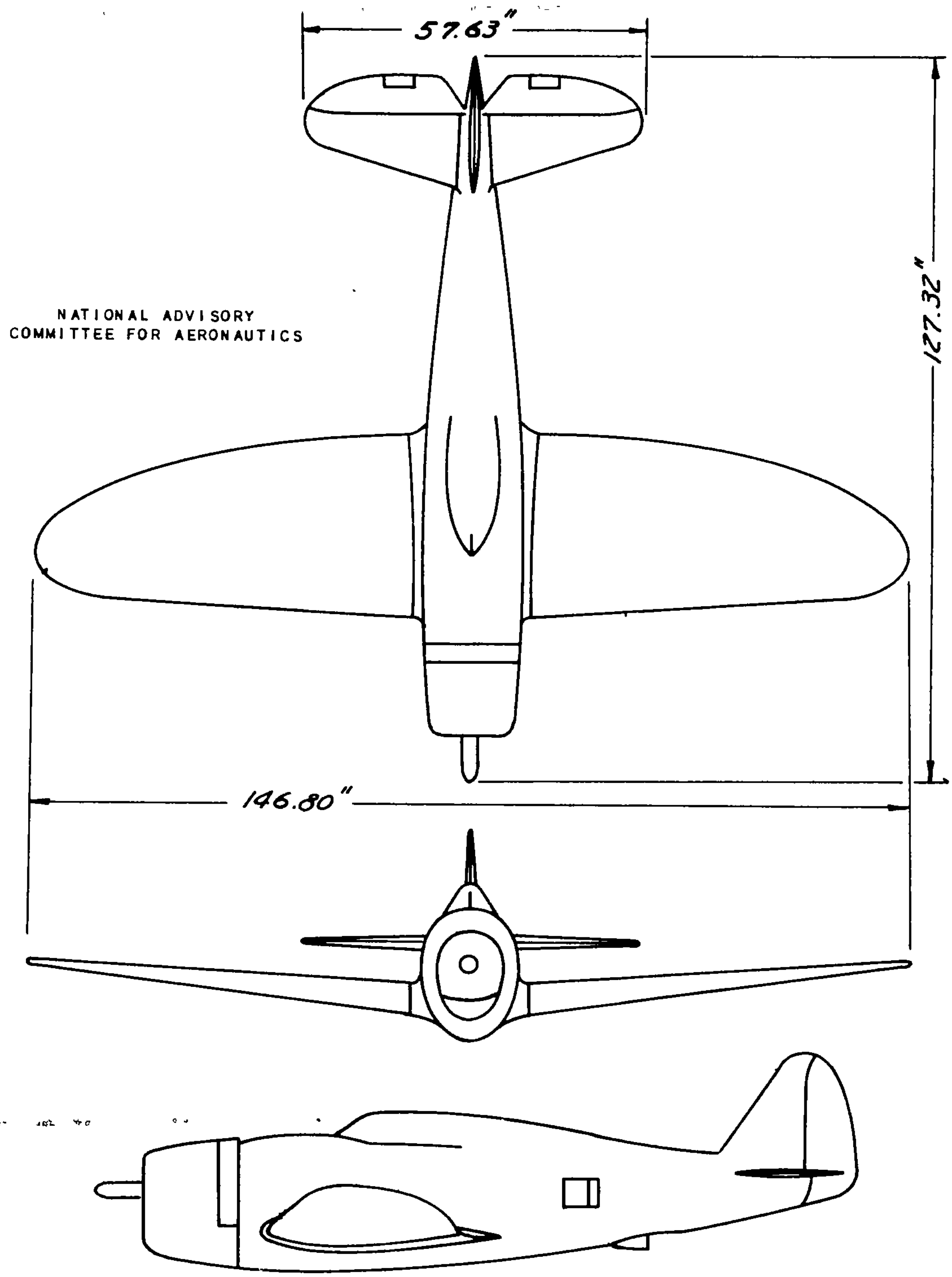

FIGURE 1.- THREE VIEWS OF THE MODEL OF THE RADIAL-ENGINE PURSUIT AIRPLANE.

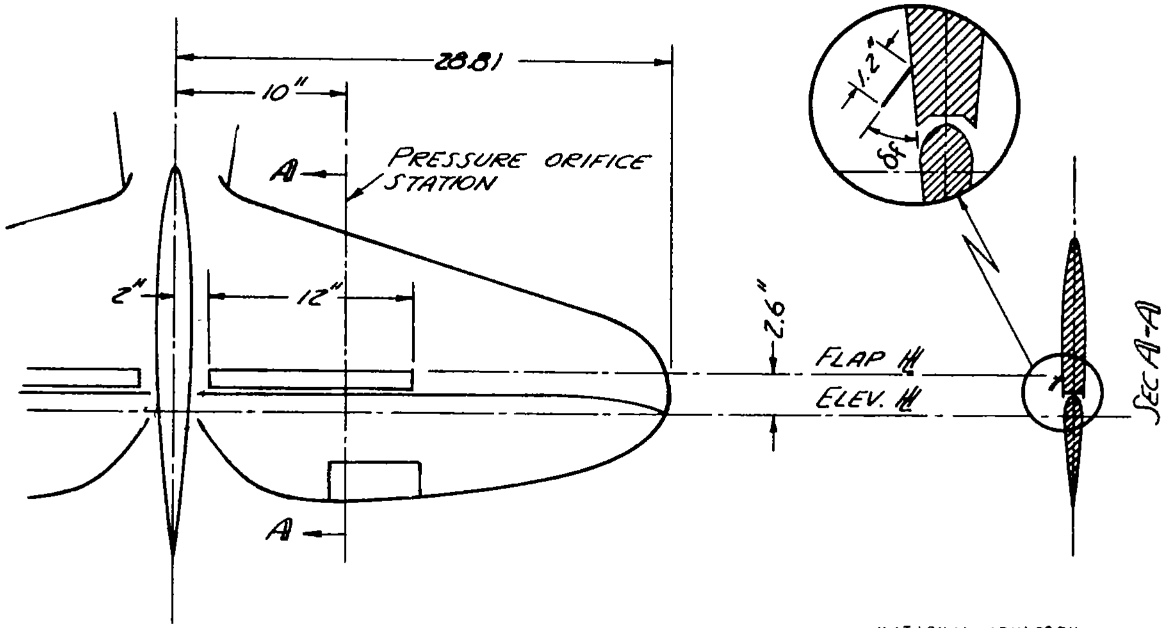

(a) 1.2-BY 12-INCH FLAP

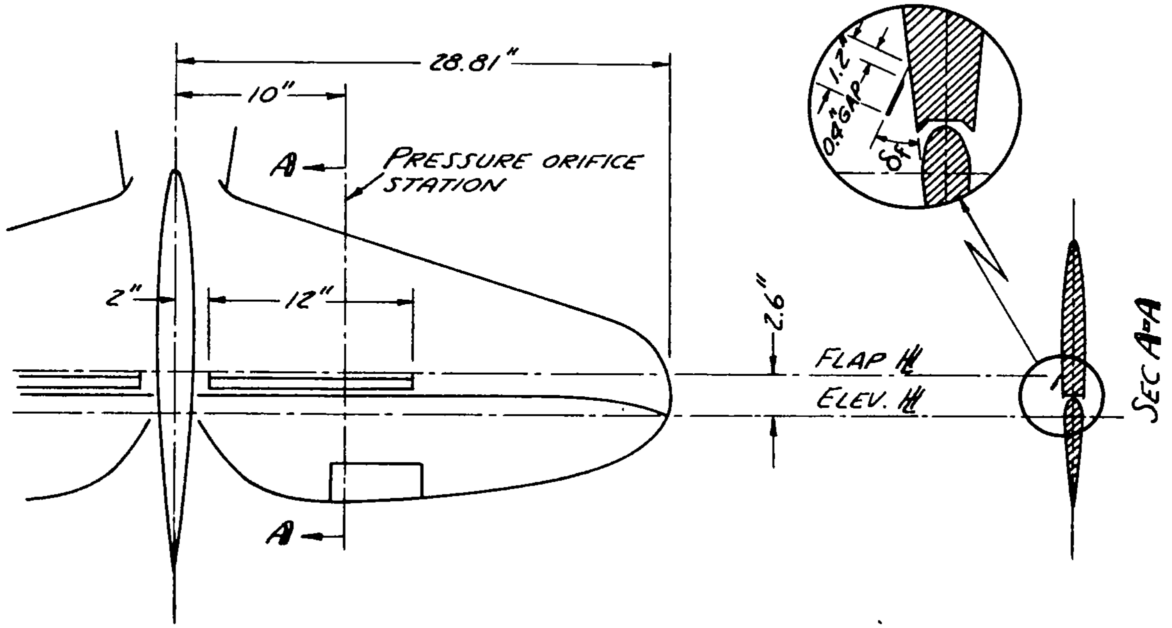

(b) 1.2-BY 12-INCH FLAP WITH 0.4-INCH GAP

FIGURE 2.- LOCATIONS AND DIMENSIONS OF THE FLAPS AND SPOILERS ON THE UPPER SURFACE OF THE STABILIZER.

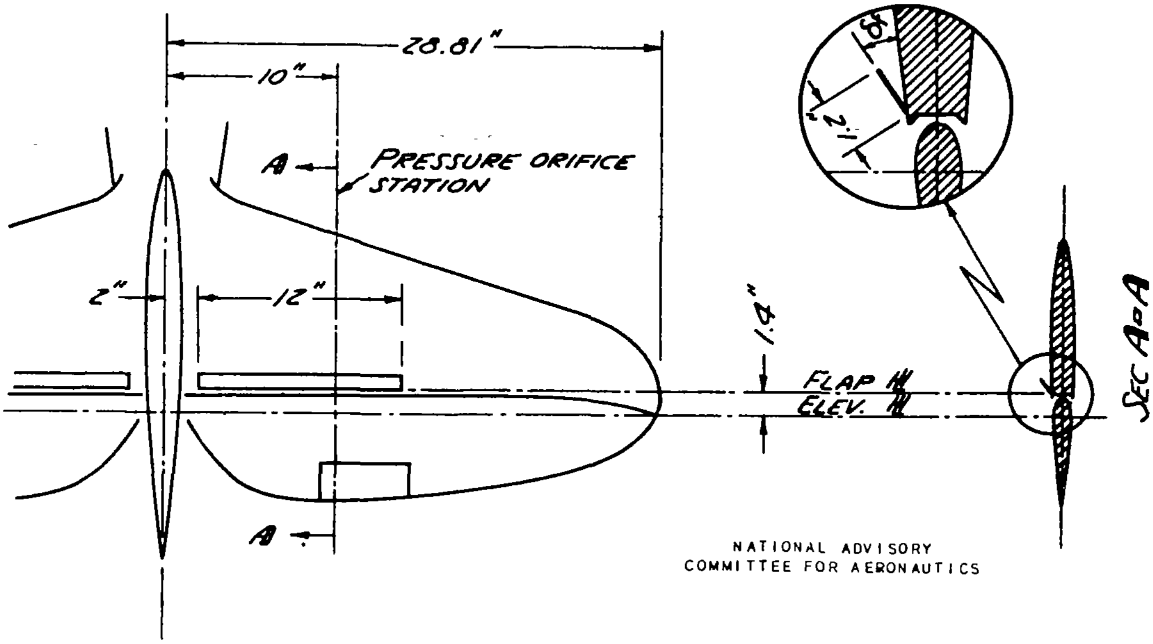

(C) 1.2-BY 12-INCH FLAP HINGED AT FLAP TRAILING EDGE.

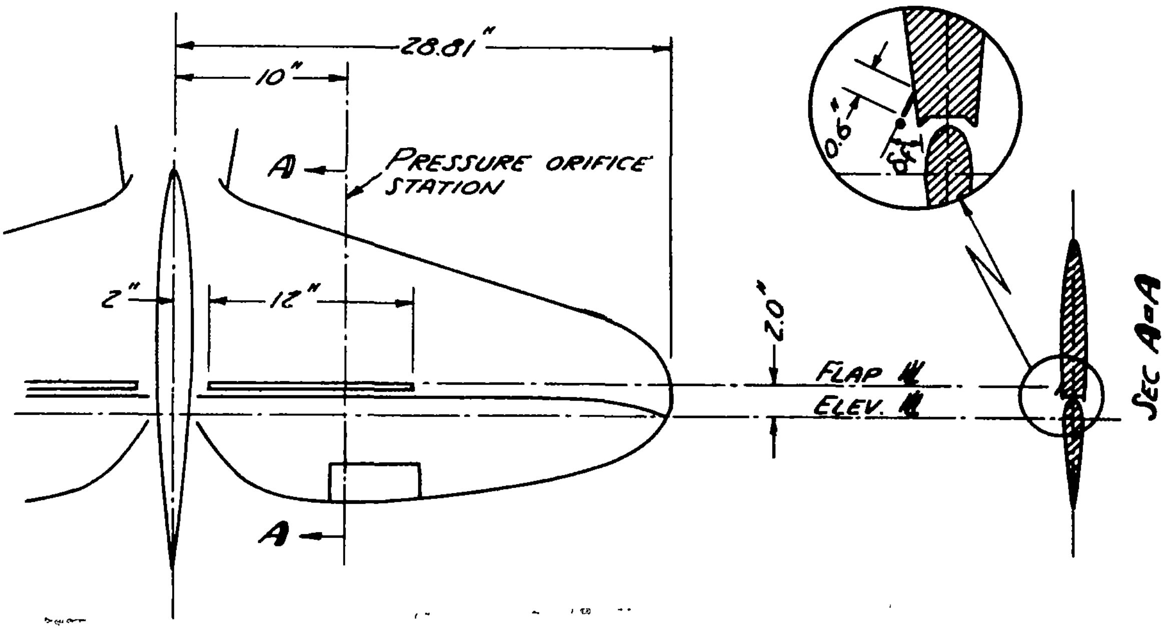

(d) 0.6-BY 12-INCH FLAP

FIGURE 2.- (CONTINUED)

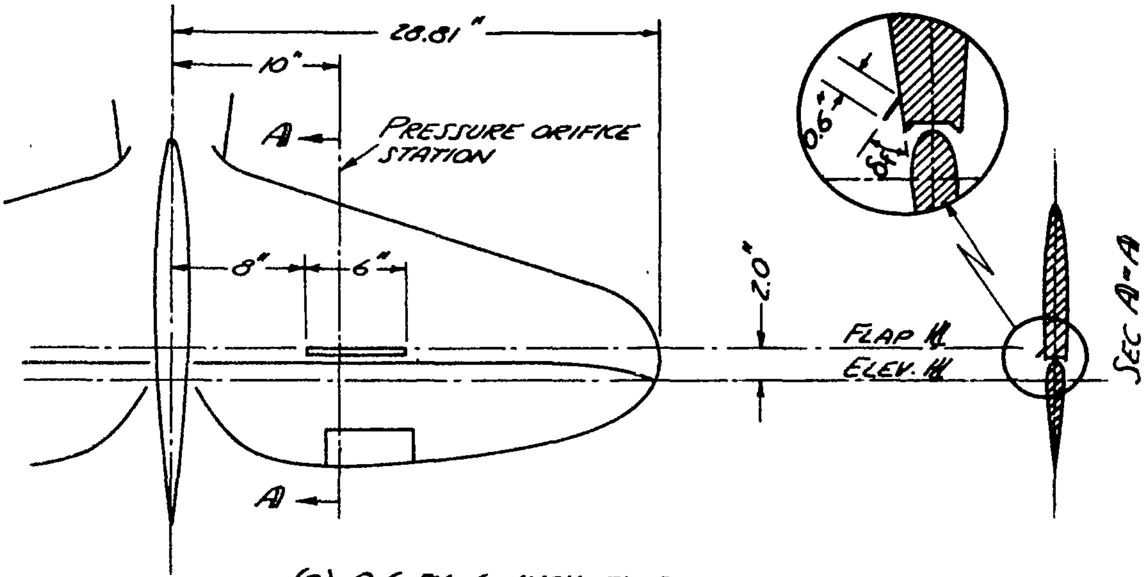

(e) 0.6-BY 6-INCH FLAP

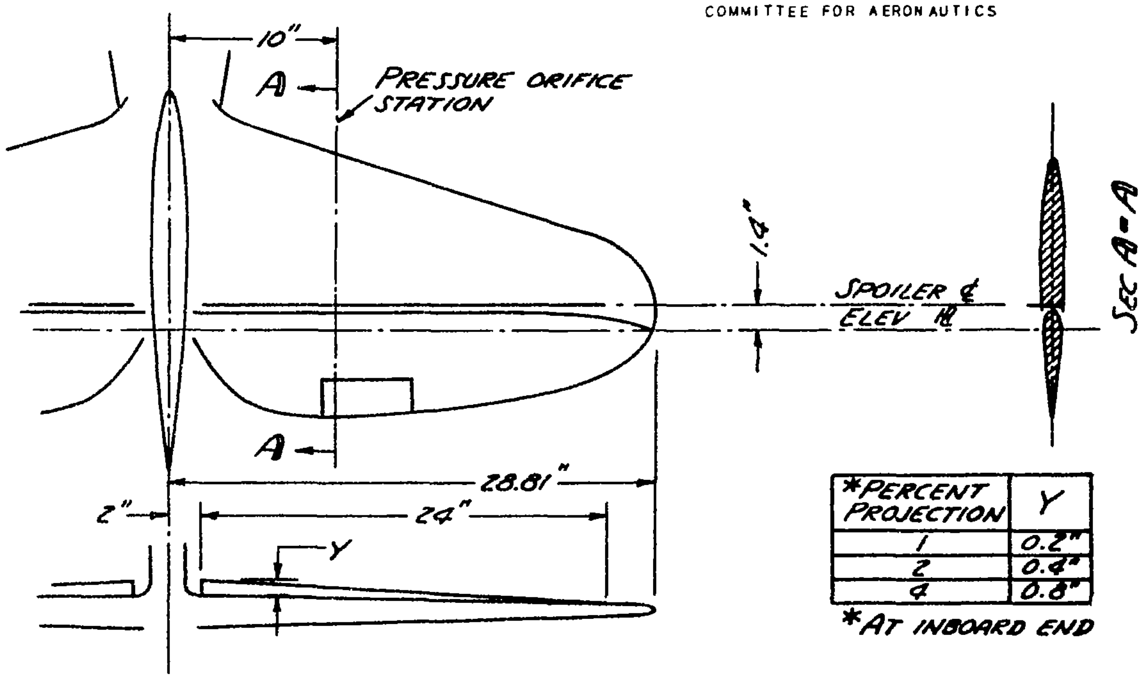

*PERCENT PROJECTION	Y
1	0.2"
2	0.4"
4	0.8"

*AT INBOARD END

(f) 24-INCH-SPAN TAPERED SPOILER

FIGURE 2. - (CONTINUED)

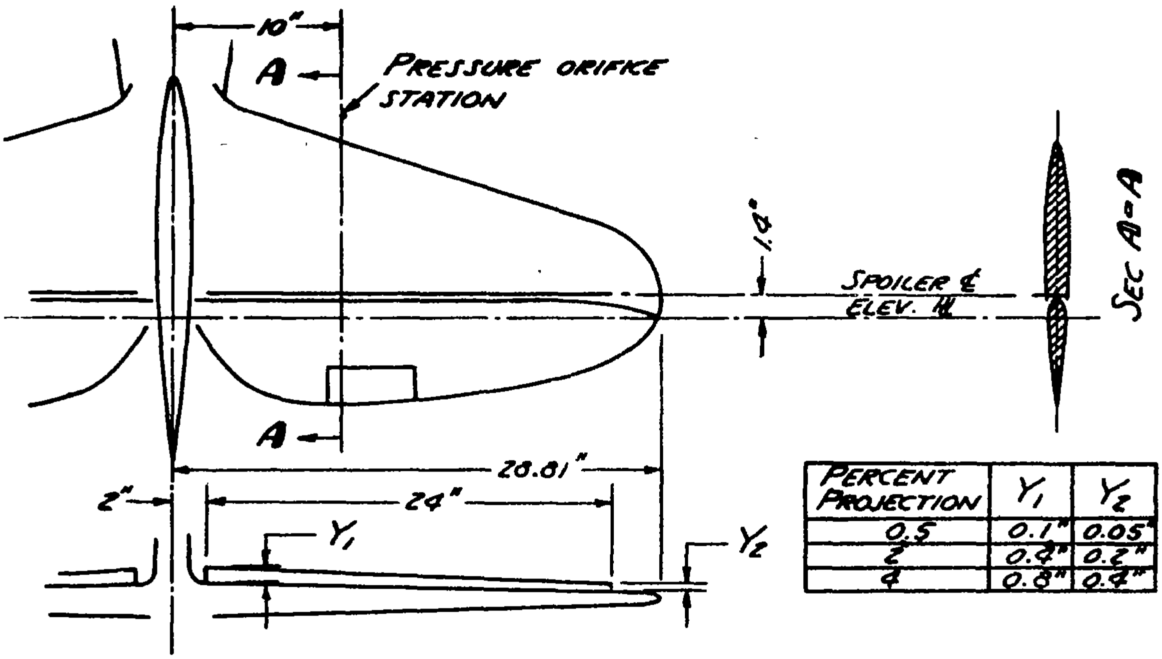

Percent Projection	Y_1	Y_2
0.5	0.1"	0.05"
2	0.4"	0.2"
4	0.8"	0.4"

(g) 24-inch-span constant-percent-chord spoiler

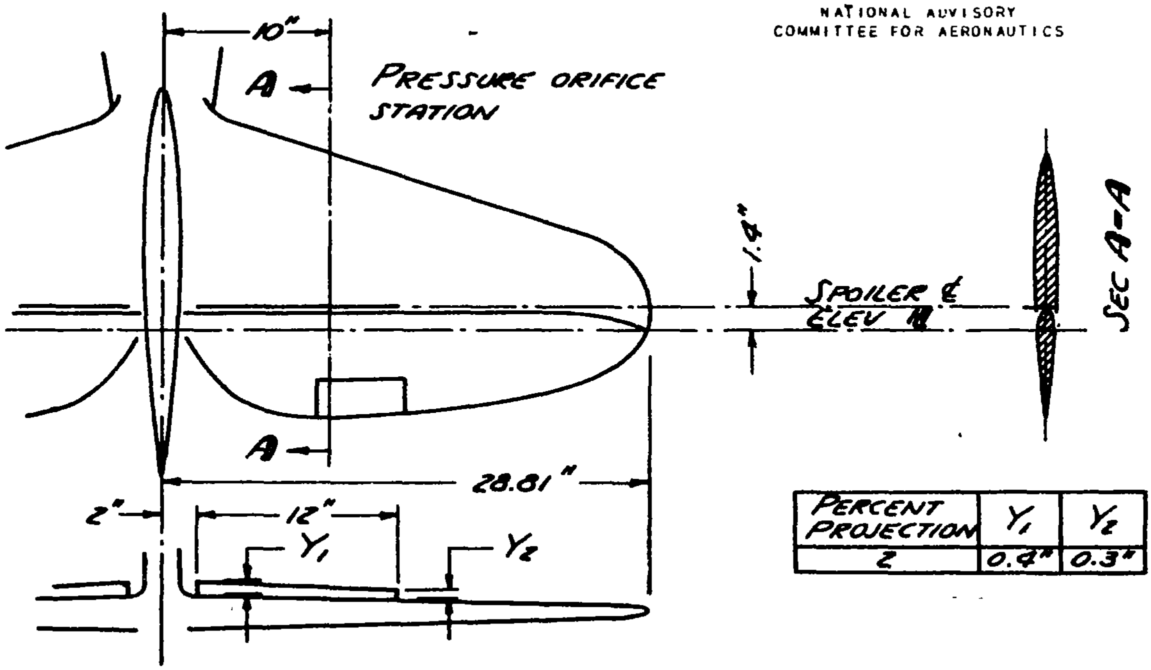

Percent Projection	Y_1	Y_2
2	0.4"	0.3"

(h) 12-inch-span constant-percent-chord spoiler

Figure 2.-(concluded)

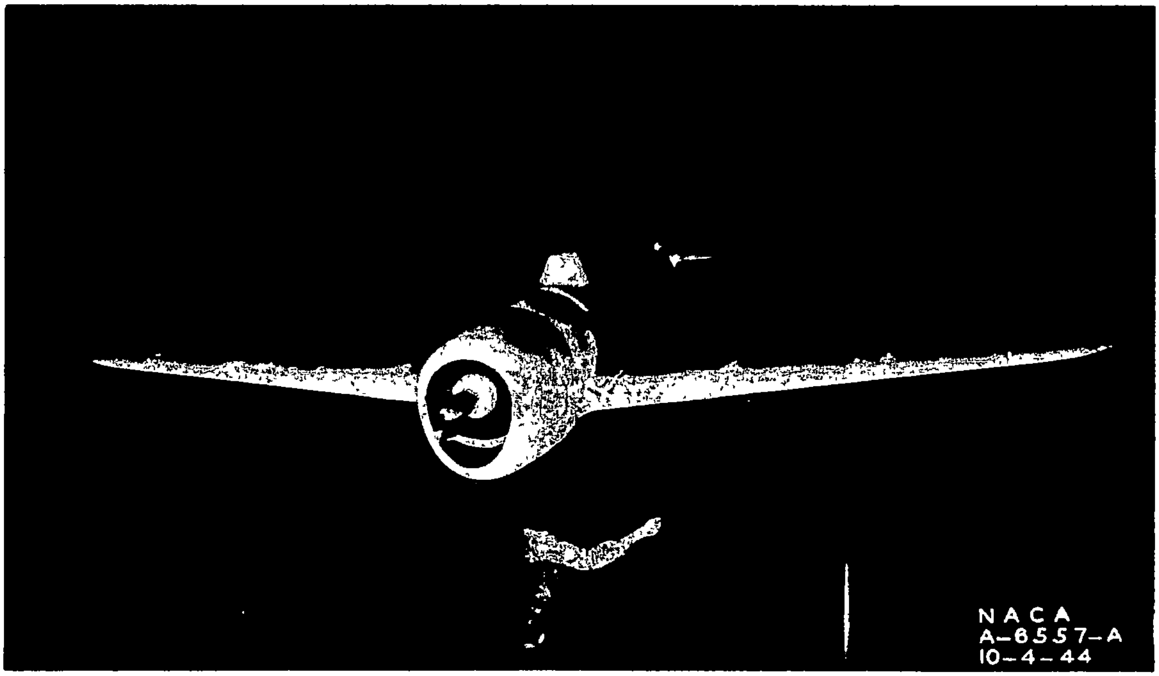

(a) Front view of the model mounted in the Ames 16-foot high-speed wind-tunnel.

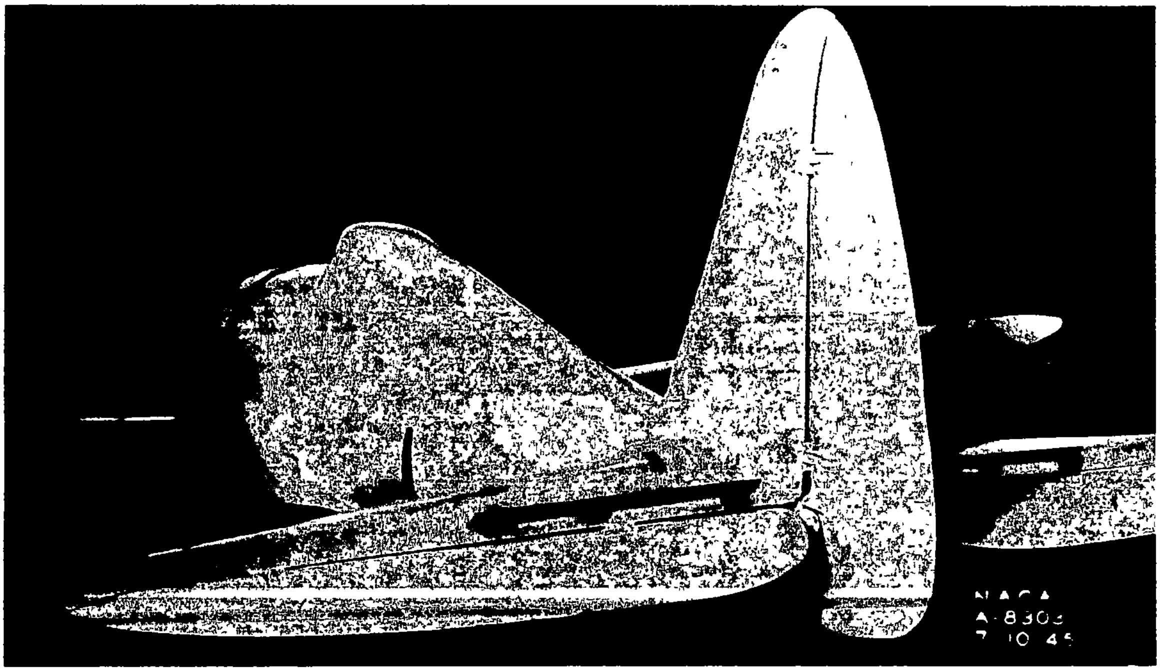

(b) Rear view showing the 1.2- by 12-inch flaps with gap.

Figure 3.- Front and rear view of the model of the radial-engine pursuit airplane.

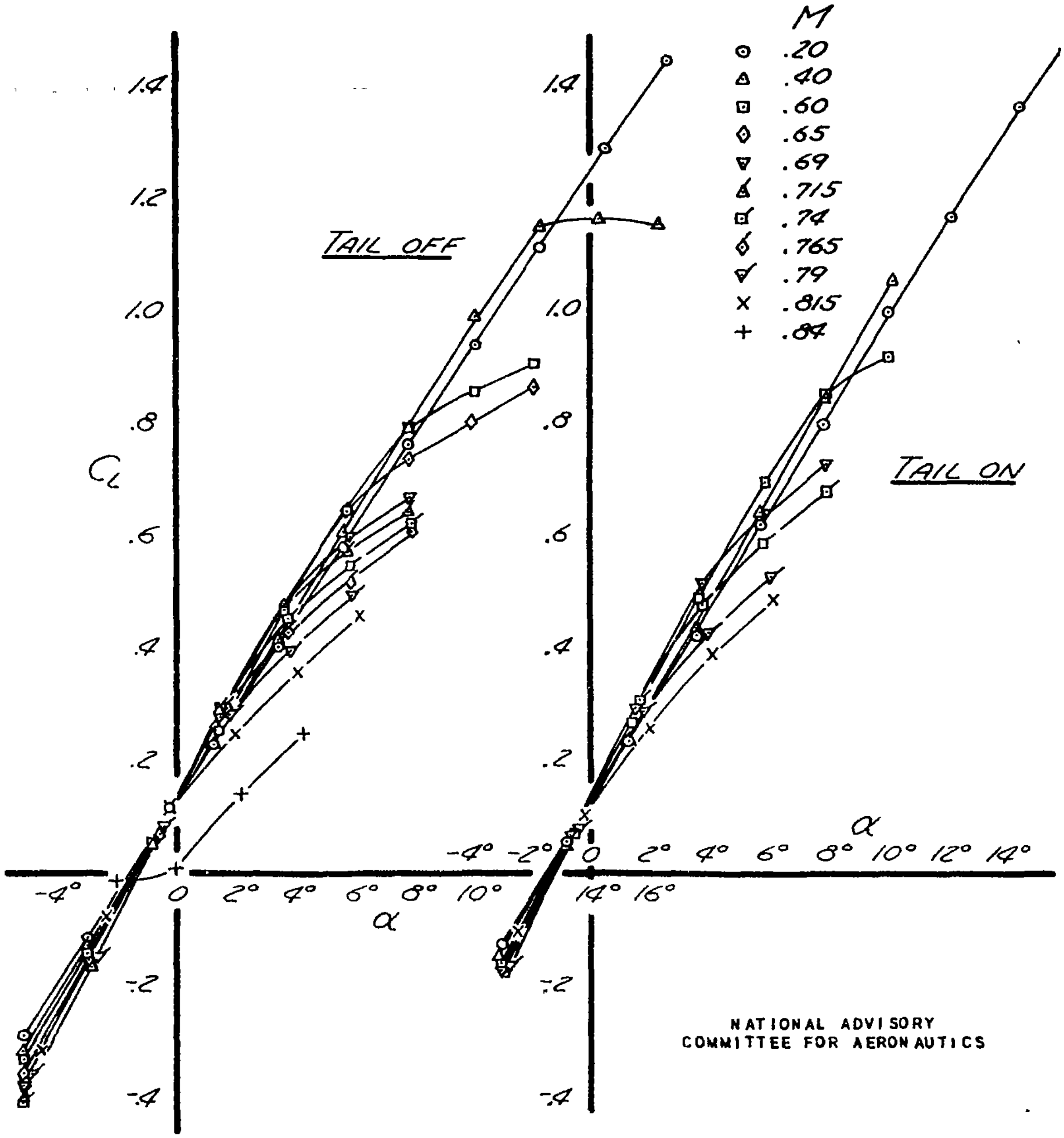

NATIONAL ADVISORY COMMITTEE FOR AERONAUTICS

FIGURE 4.- VARIATION OF LIFT COEFFICIENT WITH ANGLE OF ATTACK FOR THE STANDARD MODEL WITH ELEVATORS NEUTRAL AND FOR THE MODEL WITH THE TAIL REMOVED.

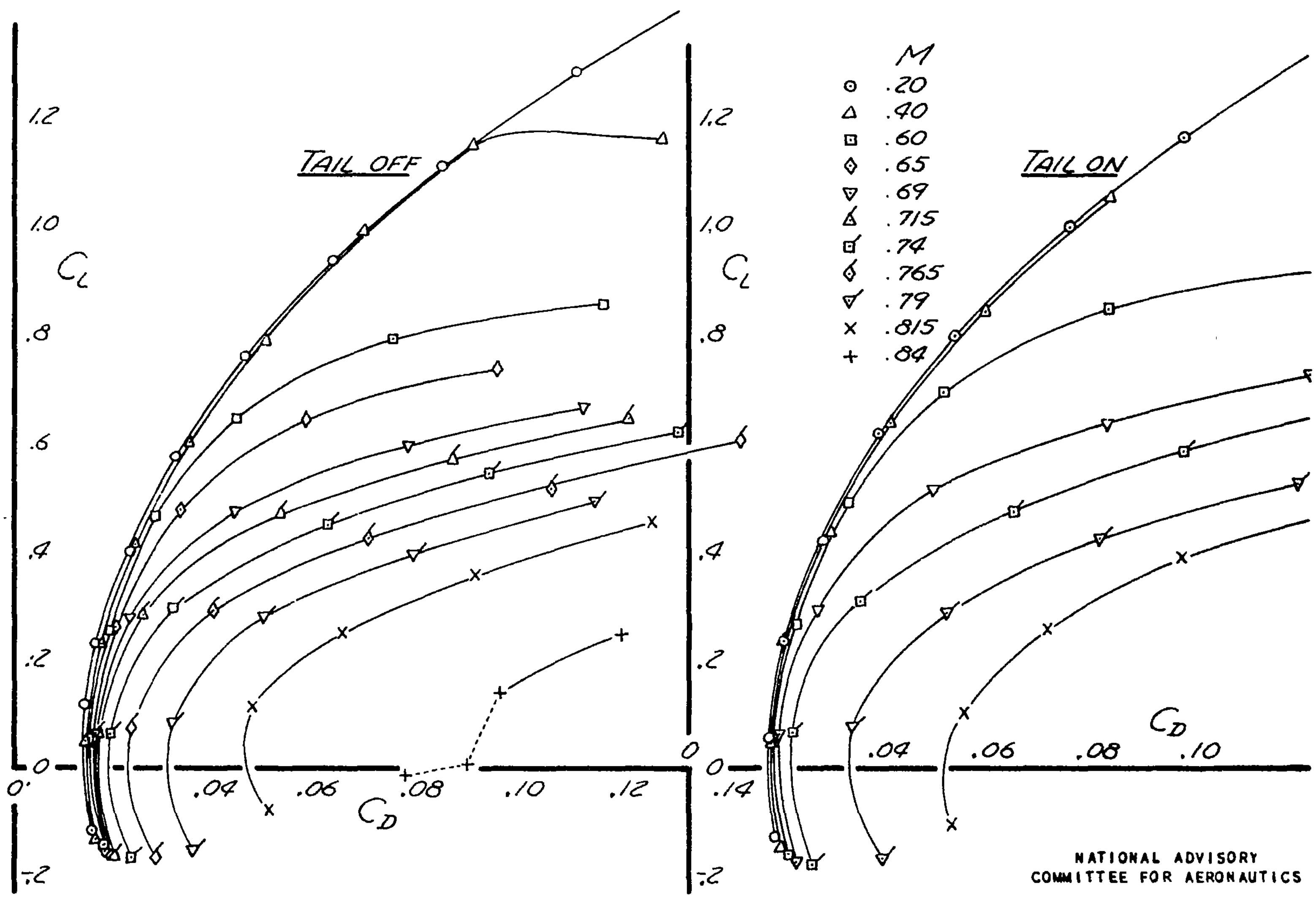

FIGURE 5.- VARIATION OF DRAG COEFFICIENT WITH LIFT COEFFICIENT FOR THE STANDARD MODEL WITH ELEVATORS NEUTRAL AND FOR THE MODEL WITH THE TAIL REMOVED

NATIONAL ADVISORY
COMMITTEE FOR AERONAUTICS

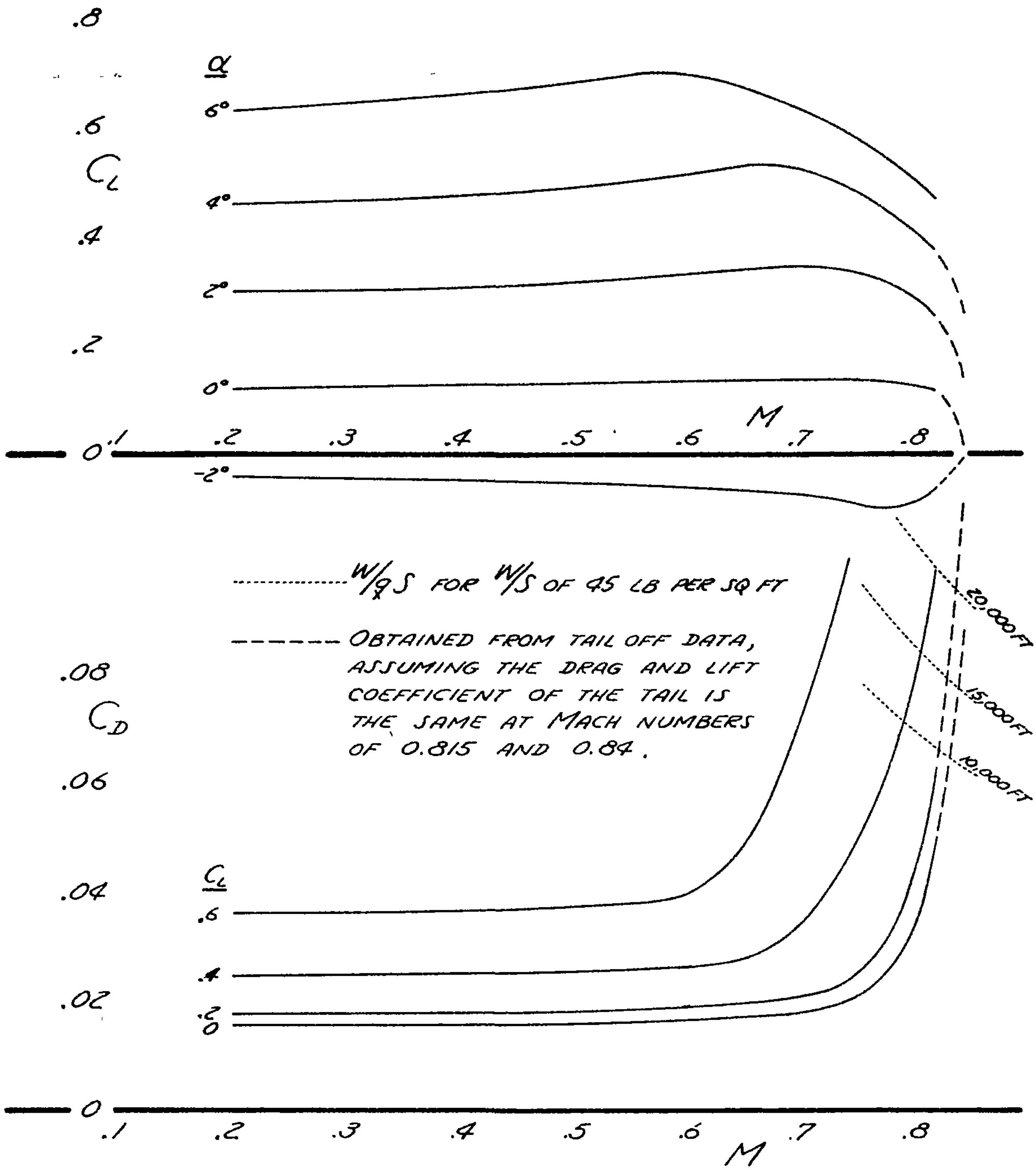

FIGURE 6.– VARIATION OF LIFT COEFFICIENT AND DRAG COEFFICIENT WITH MACH NUMBER FOR THE STANDARD MODEL WITH ELEVATORS NEUTRAL

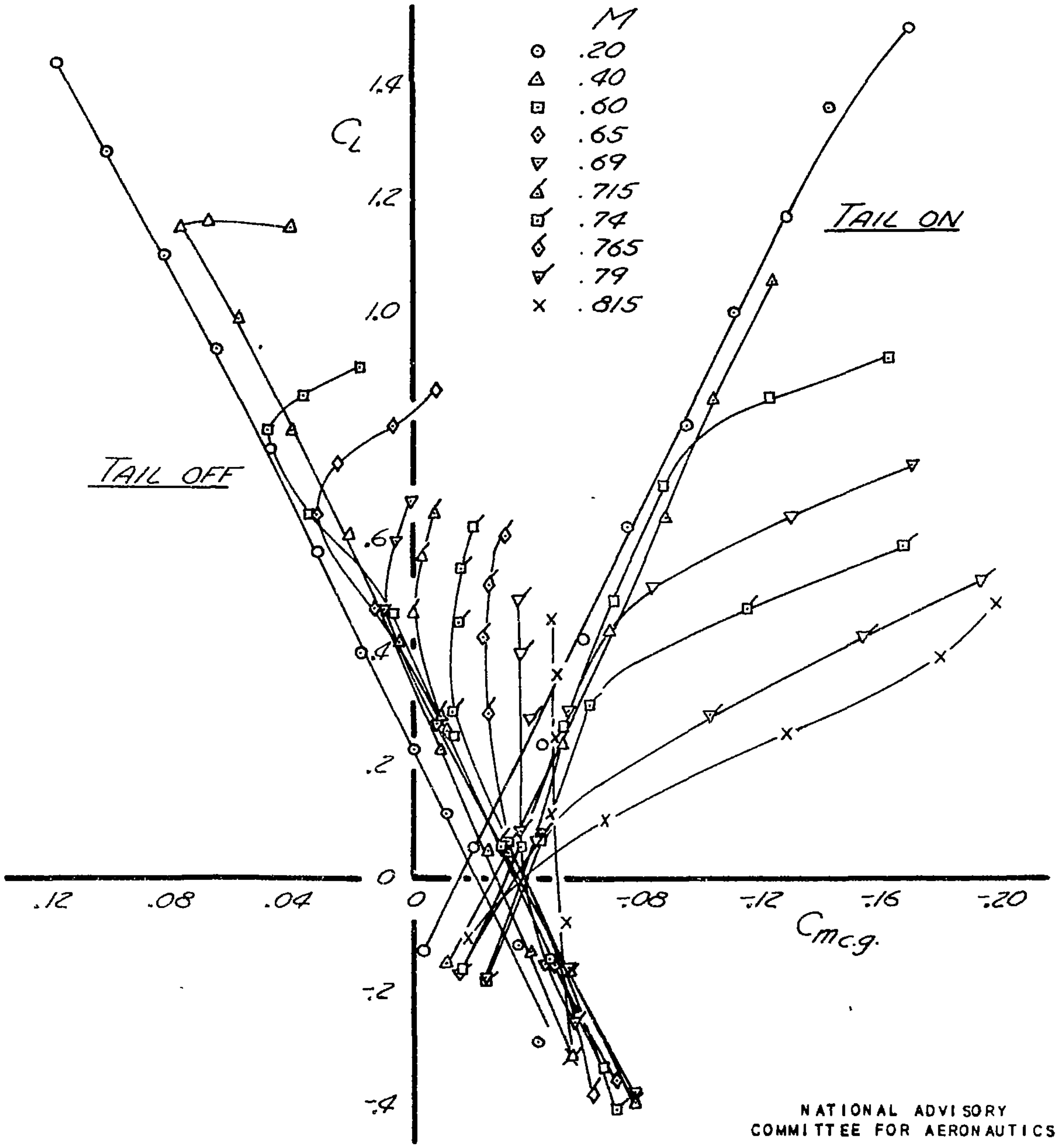

FIGURE 7.- VARIATION OF PITCHING-MOMENT COEFFICIENT WITH LIFT COEFFICIENT FOR THE STANDARD MODEL WITH ELEVATORS NEUTRAL AND FOR THE MODEL WITH THE TAIL REMOVED.

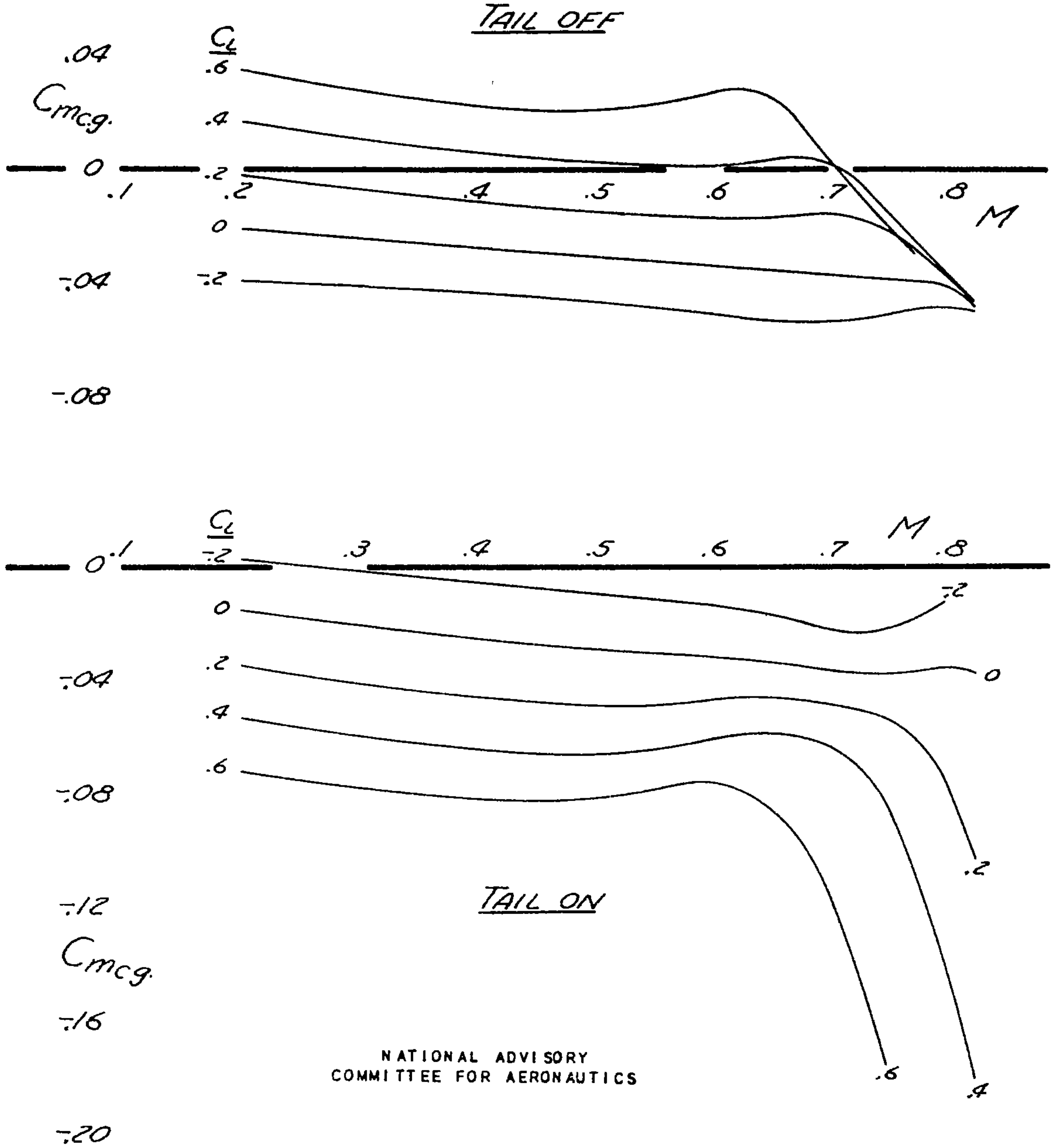

FIGURE 8.- VARIATION OF PITCHING-MOMENT COEFFICIENT WITH MACH NUMBER FOR THE STANDARD MODEL WITH ELEVATORS NEUTRAL AND FOR THE MODEL WITH THE TAIL REMOVED.

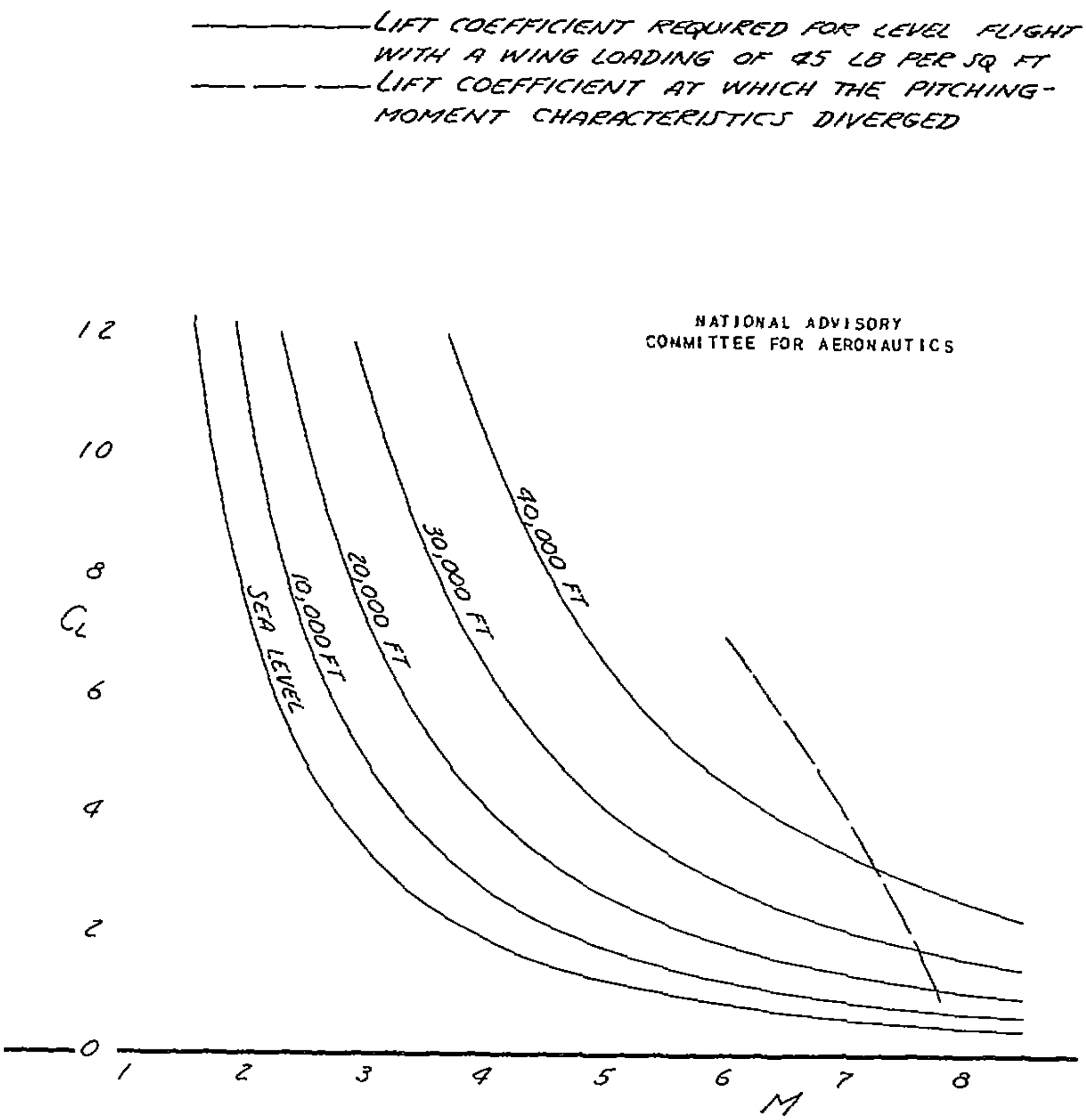

FIGURE 9 – LIFT COEFFICIENT FOR LEVEL FLIGHT WITH A WING LOADING OF 45 POUNDS PER SQUARE FOOT COMPARED TO THE LIFT COEFFICIENT AT WHICH THE PITCHING-MOMENT CHARACTERISTICS OF THE STANDARD MODEL DIVERGE WIDELY FROM THOSE AT LOW SPEED

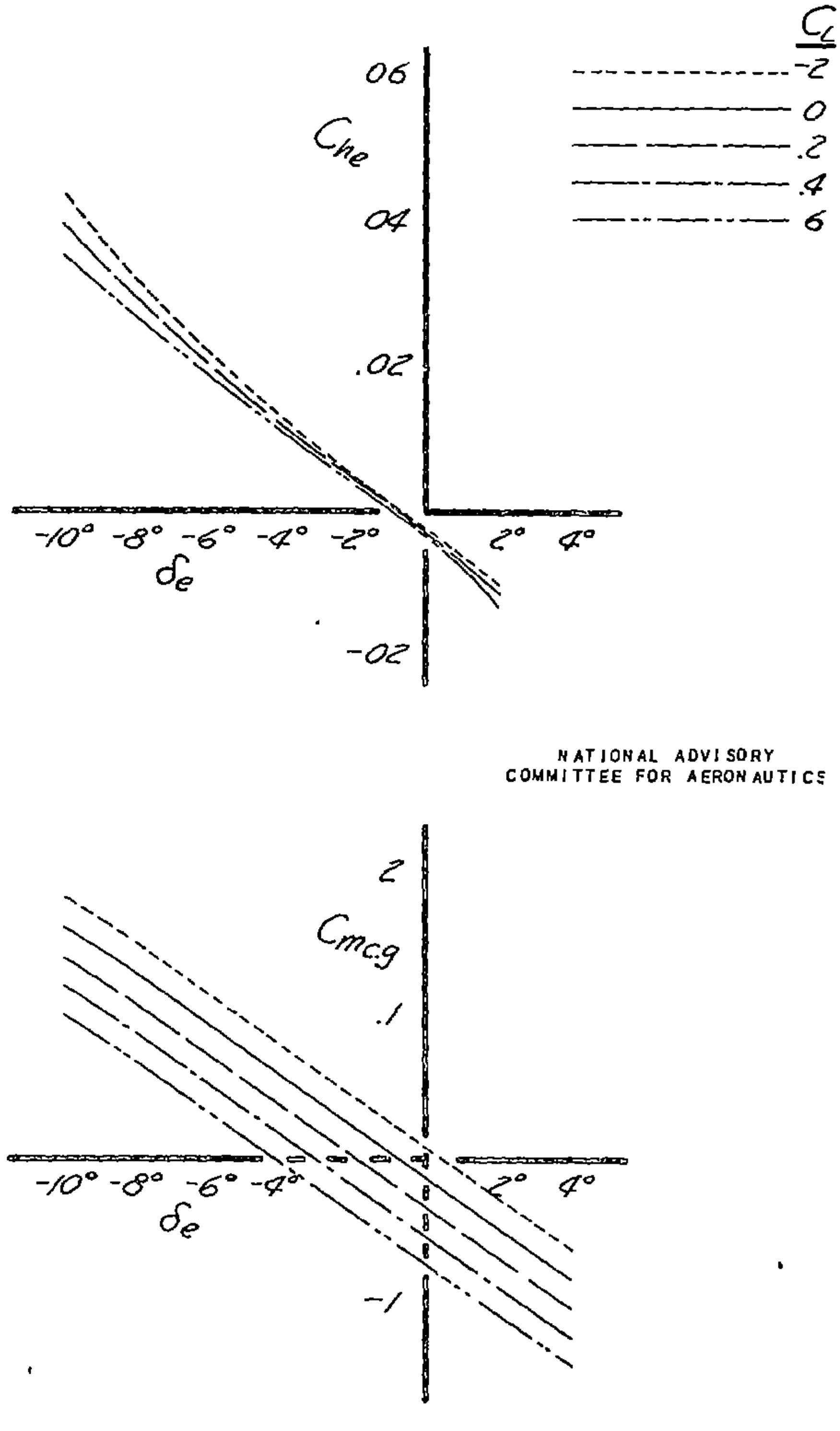

(a) M= 0.20

FIGURE 10 – ELEVATOR CHARACTERISTICS FOR THE STANDARD MODEL

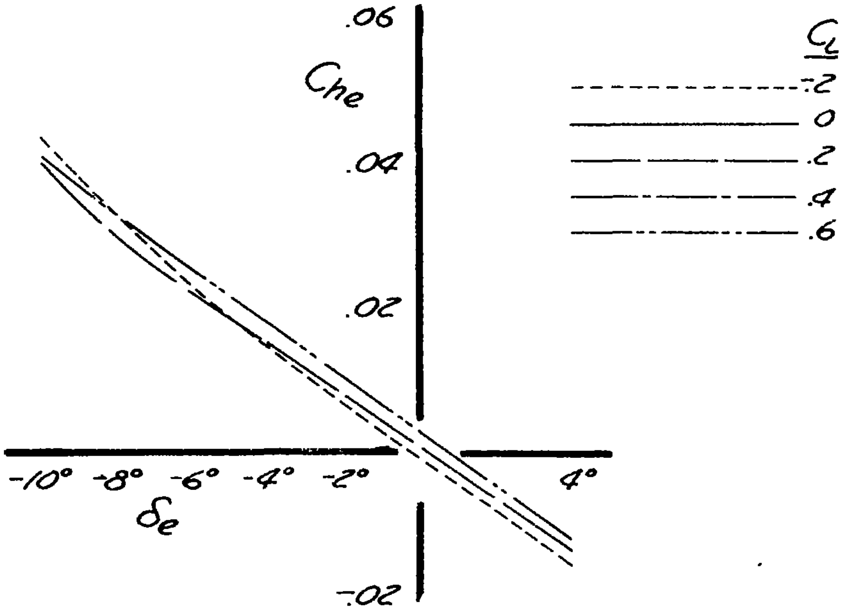

NATIONAL ADVISORY
COMMITTEE FOR AERONAUTICS

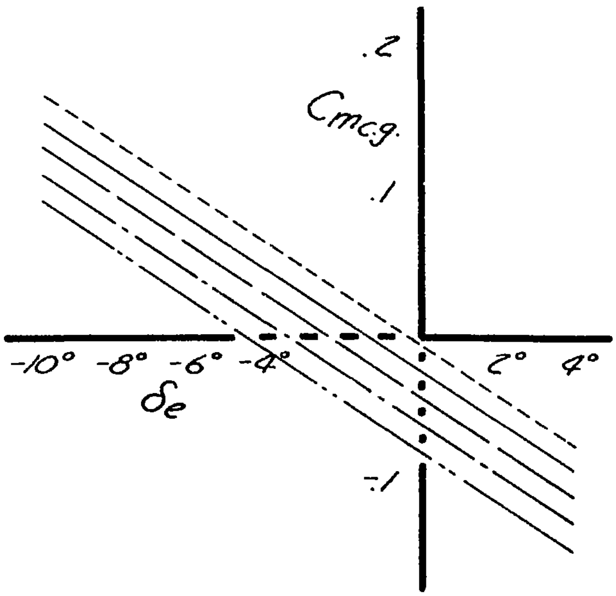

(b) M = 0.40

FIGURE 10.-(CONTINUED) STANDARD MODEL

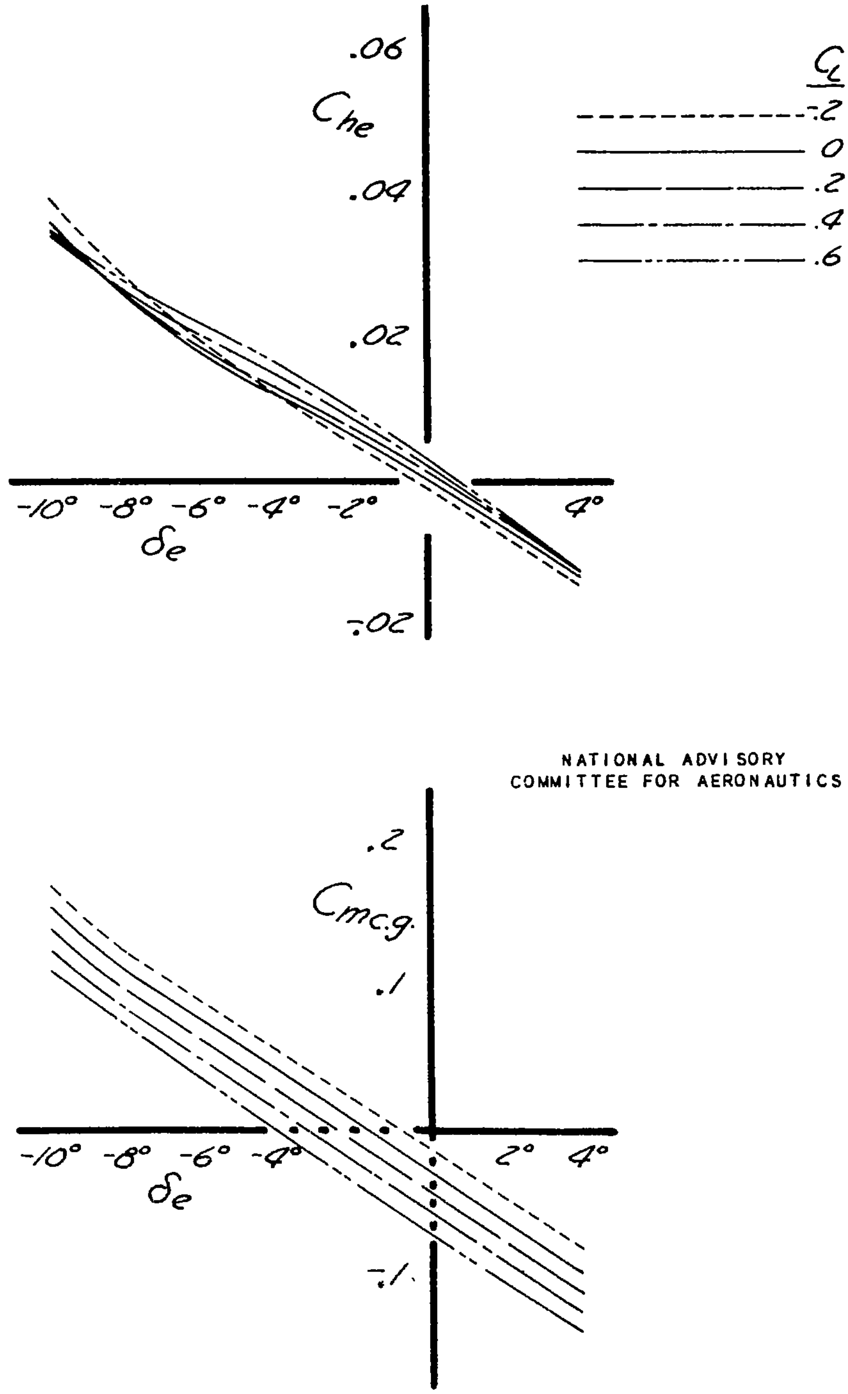

(c) M=0.60

FIGURE 10.- (CONTINUED) STANDARD MODEL

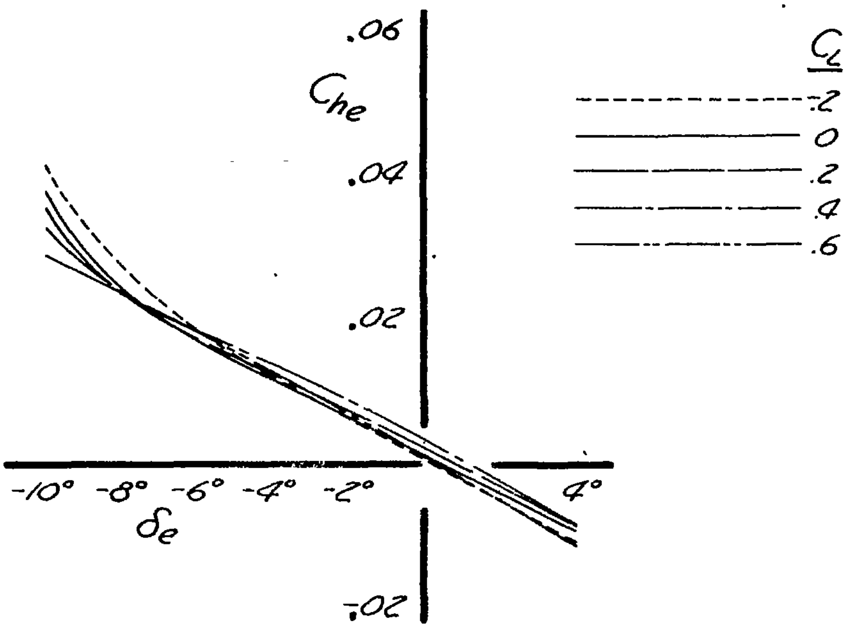

NATIONAL ADVISORY
COMMITTEE FOR AERONAUTICS

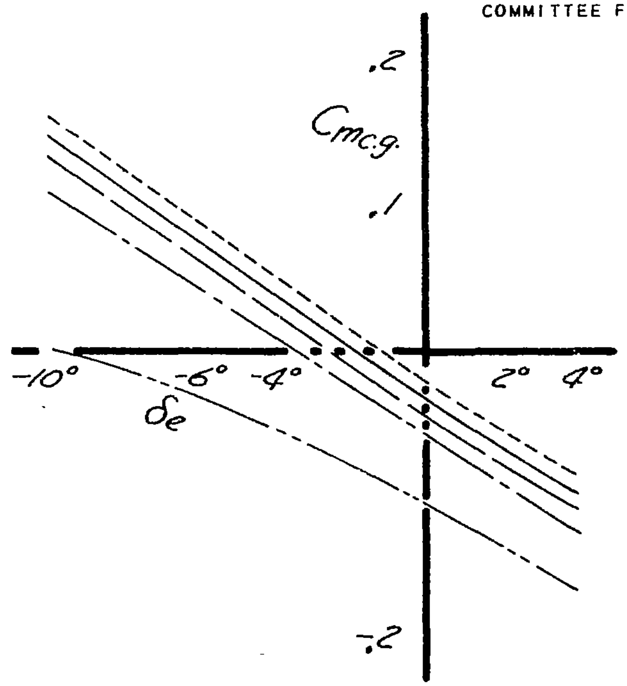

(d) M = 0.69

FIGURE 10.– (CONTINUED) STANDARD MODEL

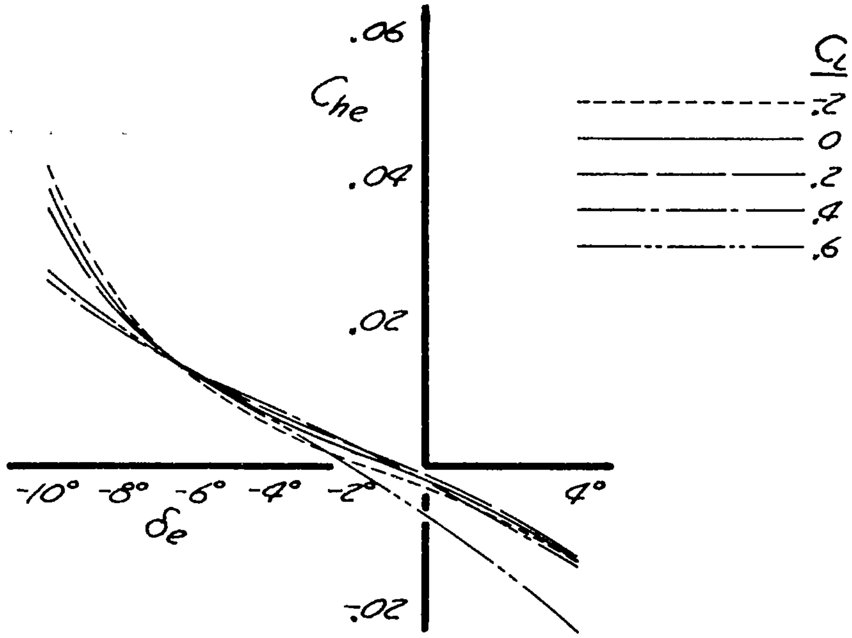

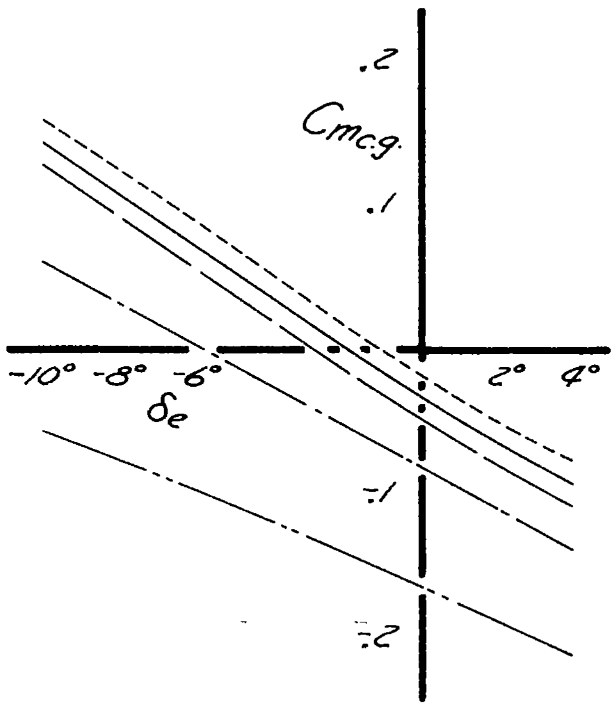

(e) M = 0.74

FIGURE 10. – (CONTINUED) STANDARD MODEL

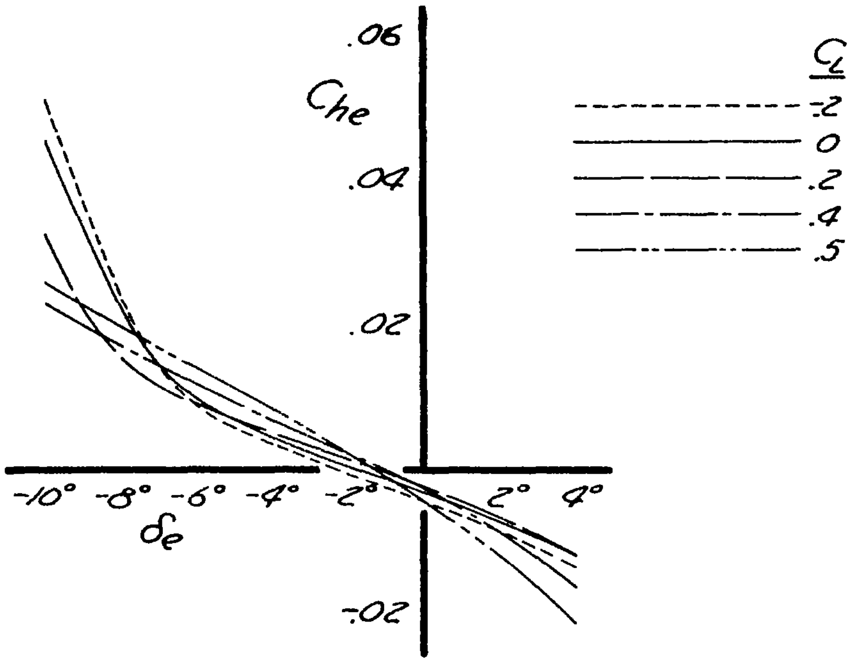

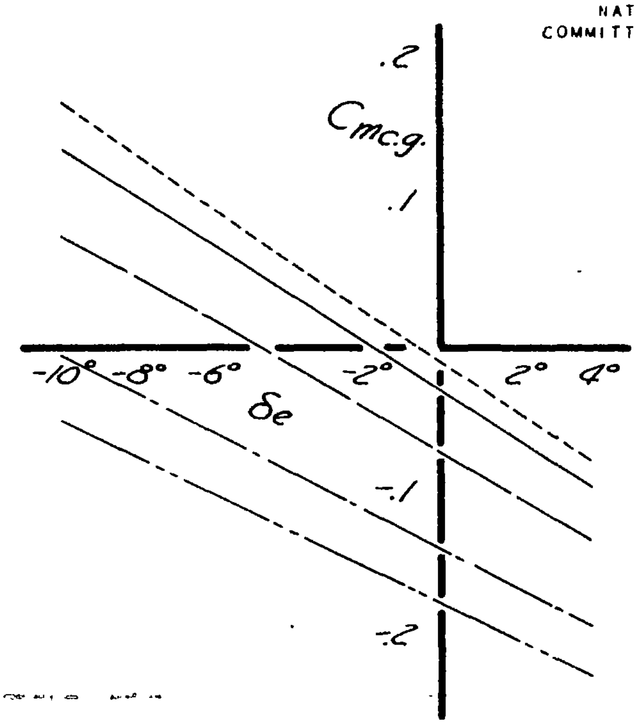

(f) M = 0.79

FIGURE 10.– (CONTINUED) STANDARD MODEL

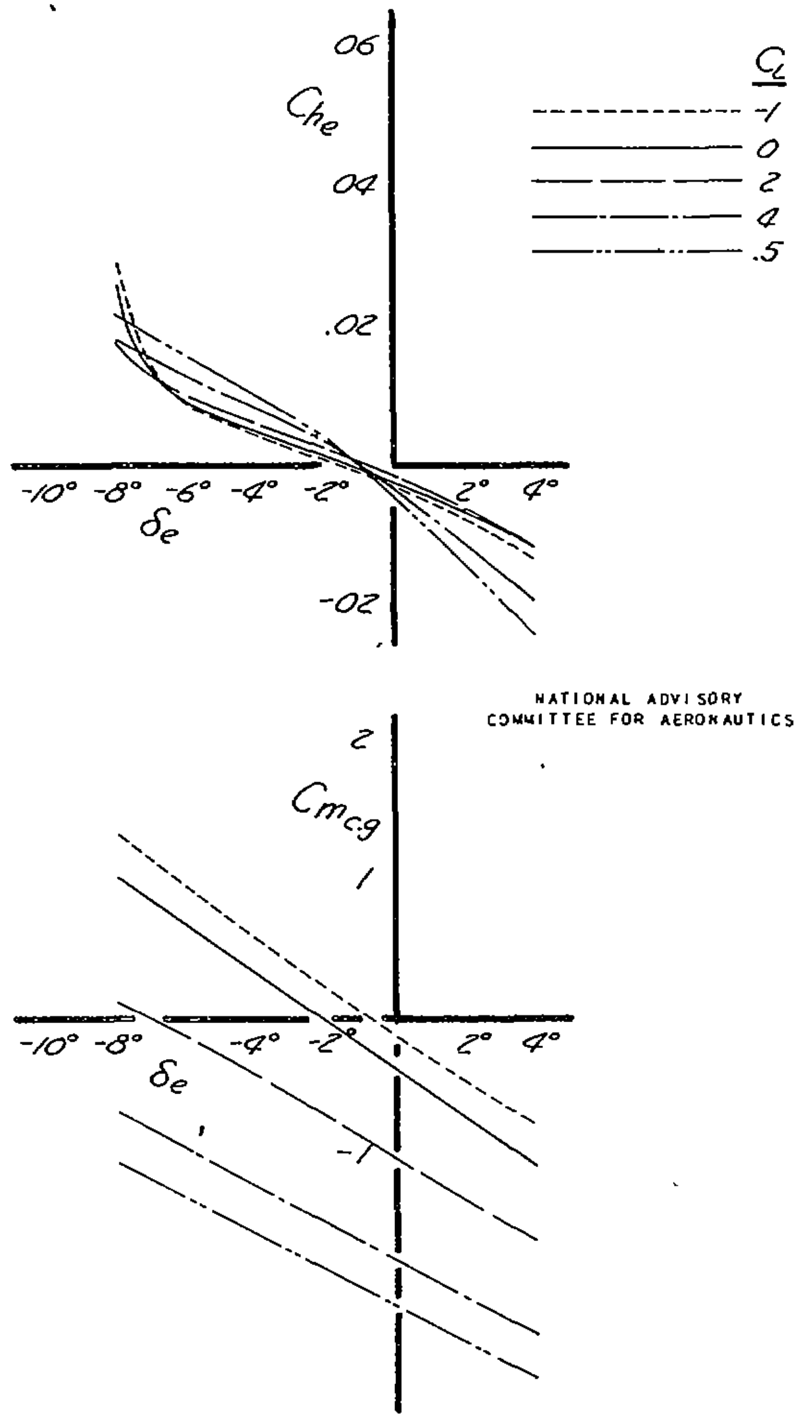

(g) M = 0.815

FIGURE 10 - (CONCLUDED) STANDARD MODEL

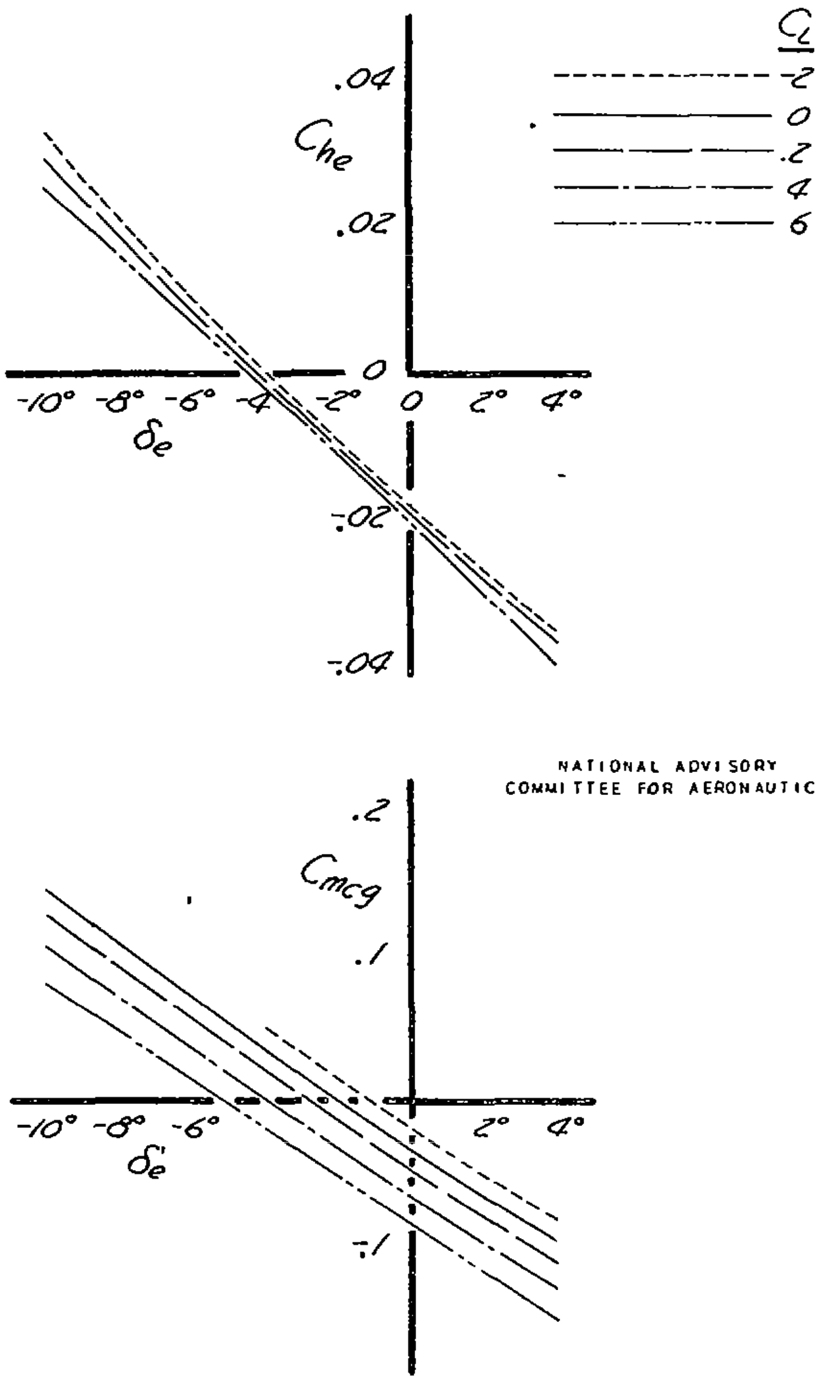

(a) M = 0.20

FIGURE 11 - ELEVATOR CHARACTERISTICS WITH THE ELEVATOR TABS DEFLECTED 5°

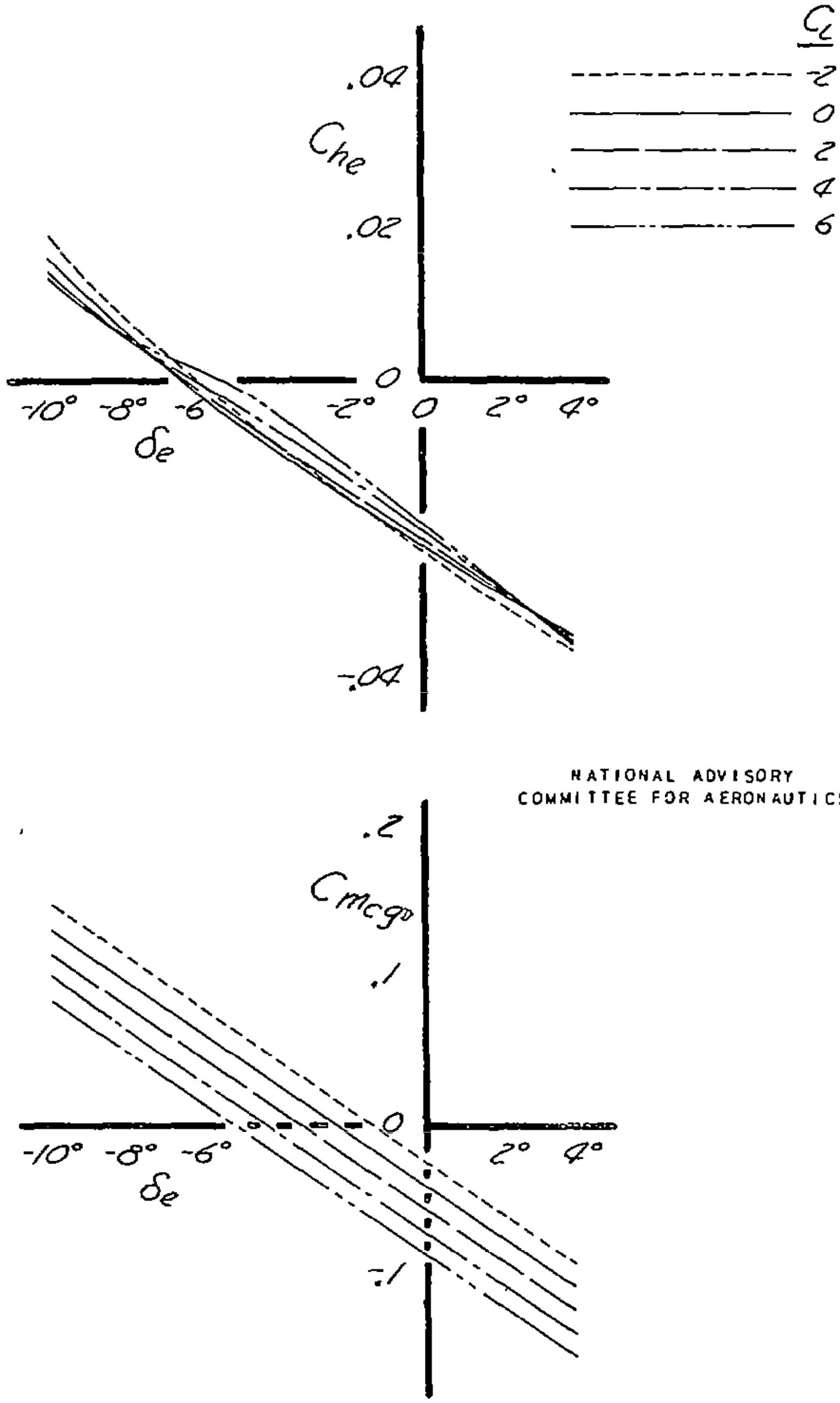

(b) M= 0.60

FIGURE 11.– (CONTINUED) ELEVATOR TABS DEFLECTED 5°

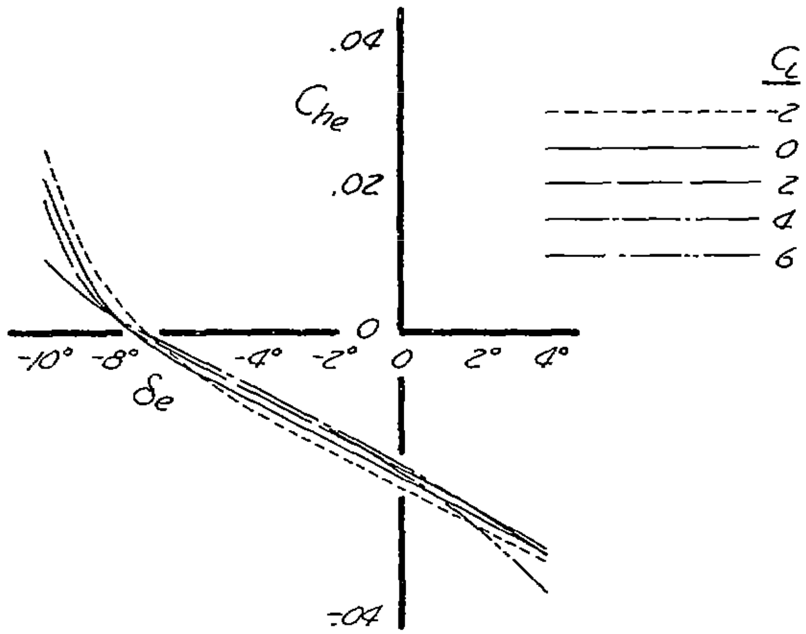

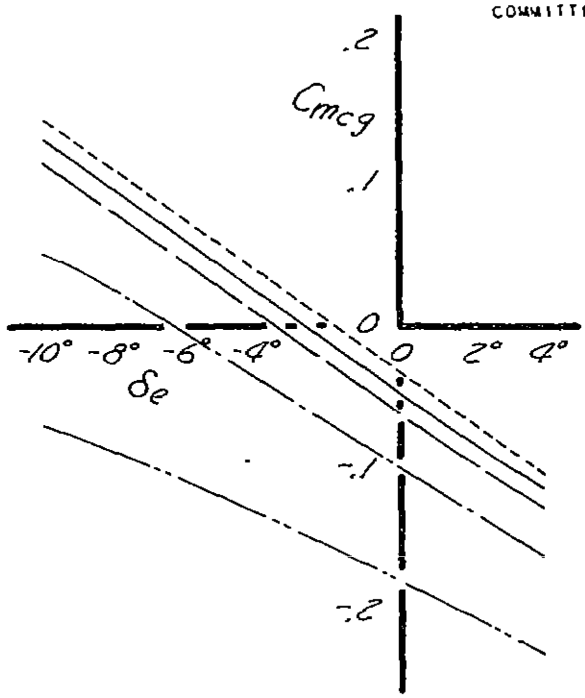

(c) M = 0.74

FIGURE 11 -(CONTINUED) ELEVATOR TABS DEFLECTED 5°

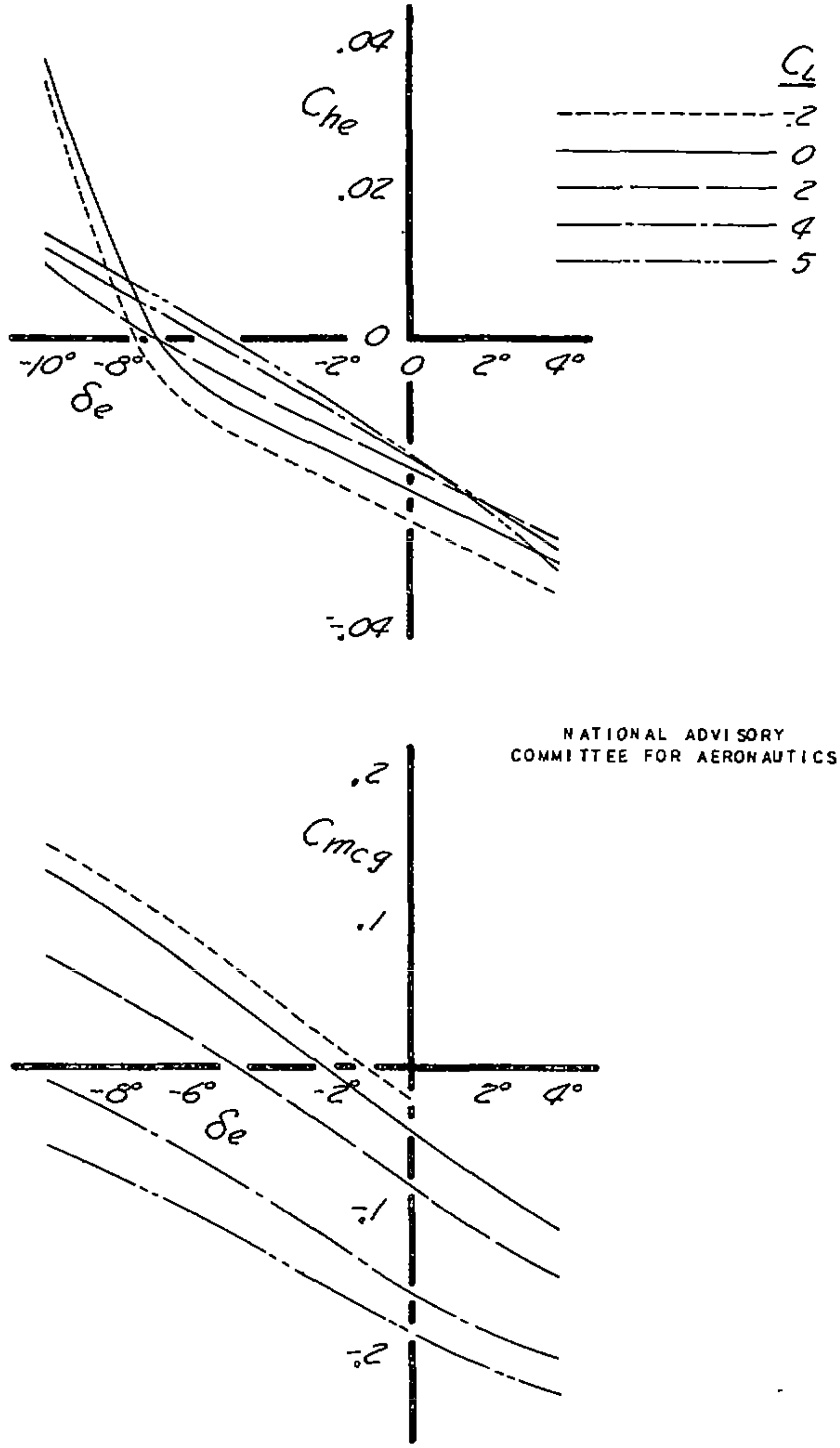

NATIONAL ADVISORY COMMITTEE FOR AERONAUTICS

(d) M=0.79

FIGURE 11.-(CONTINUED) ELEVATOR TABS DEFLECTED 5°

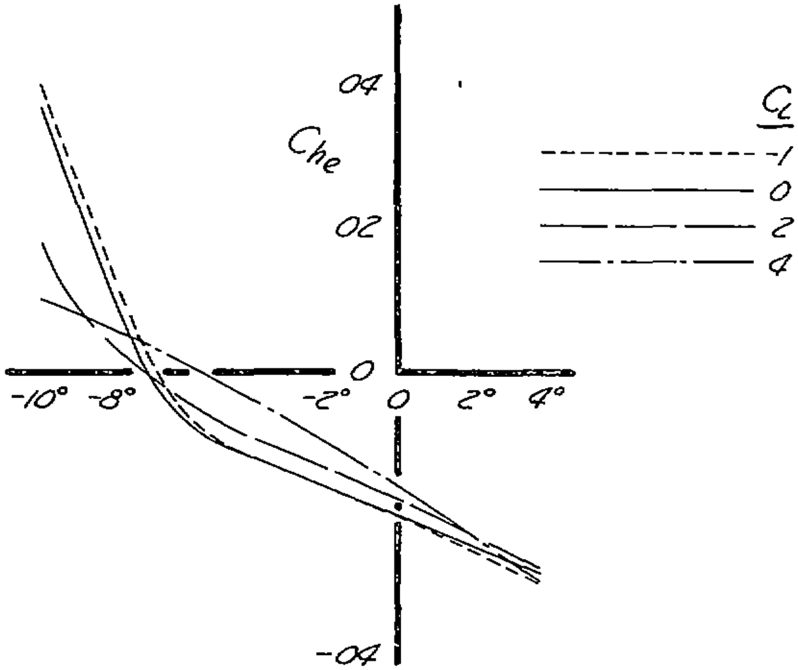

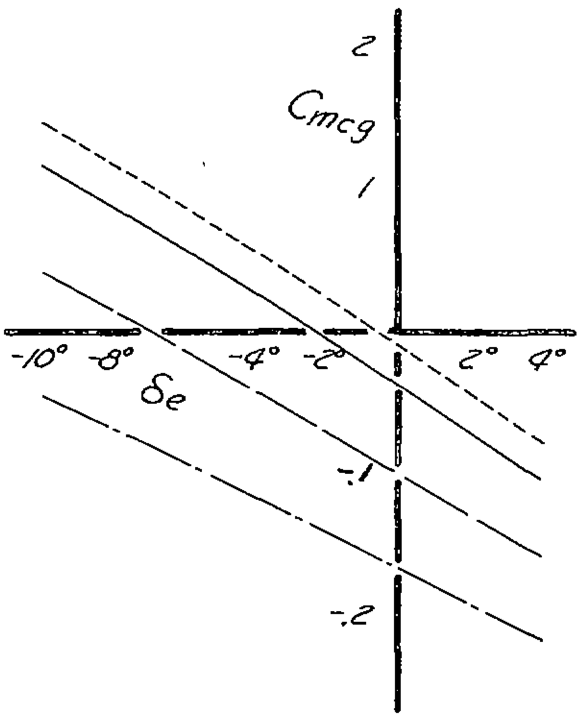

(e) M = 0.815

FIGURE 11.- (CONCLUDED) ELEVATOR TABS DEFLECTED 5°

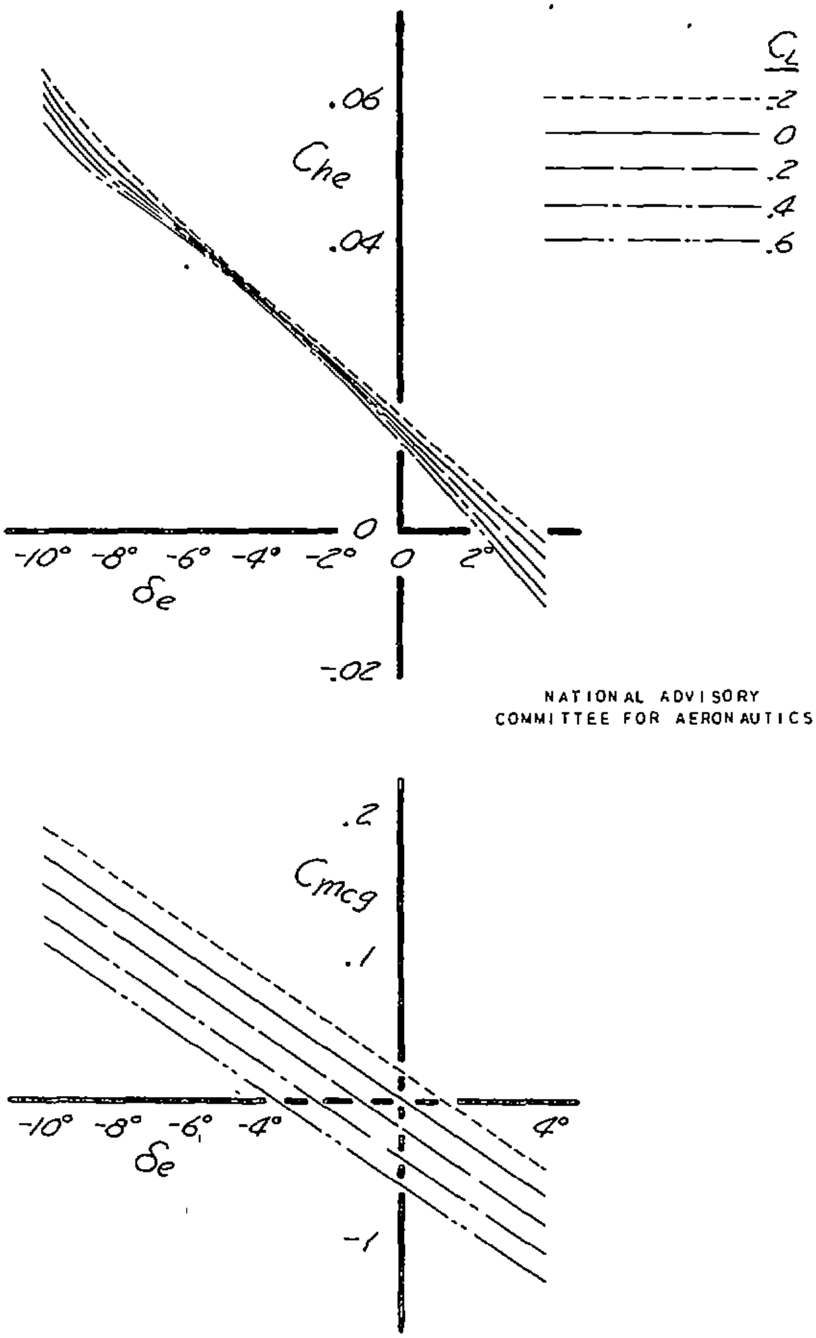

NATIONAL ADVISORY
COMMITTEE FOR AERONAUTICS

(a) $M = 0.20$

FIGURE 12 – ELEVATOR CHARACTERISTICS WITH THE ELEVATOR TABS DEFLECTED –5°

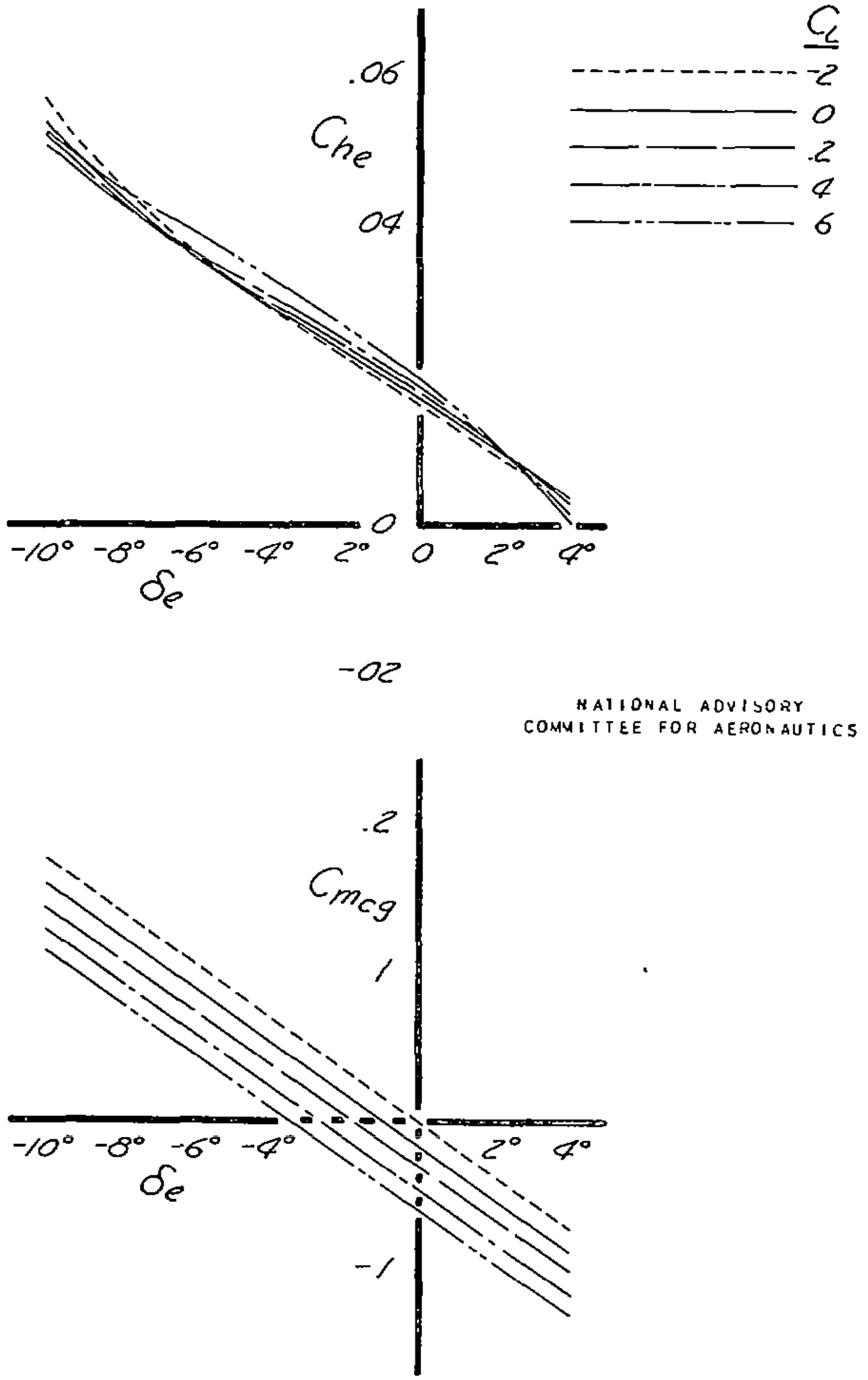

(b) M= 0.60

FIGURE 12.-(CONTINUED) ELEVATOR TABS DEFLECTED -5°

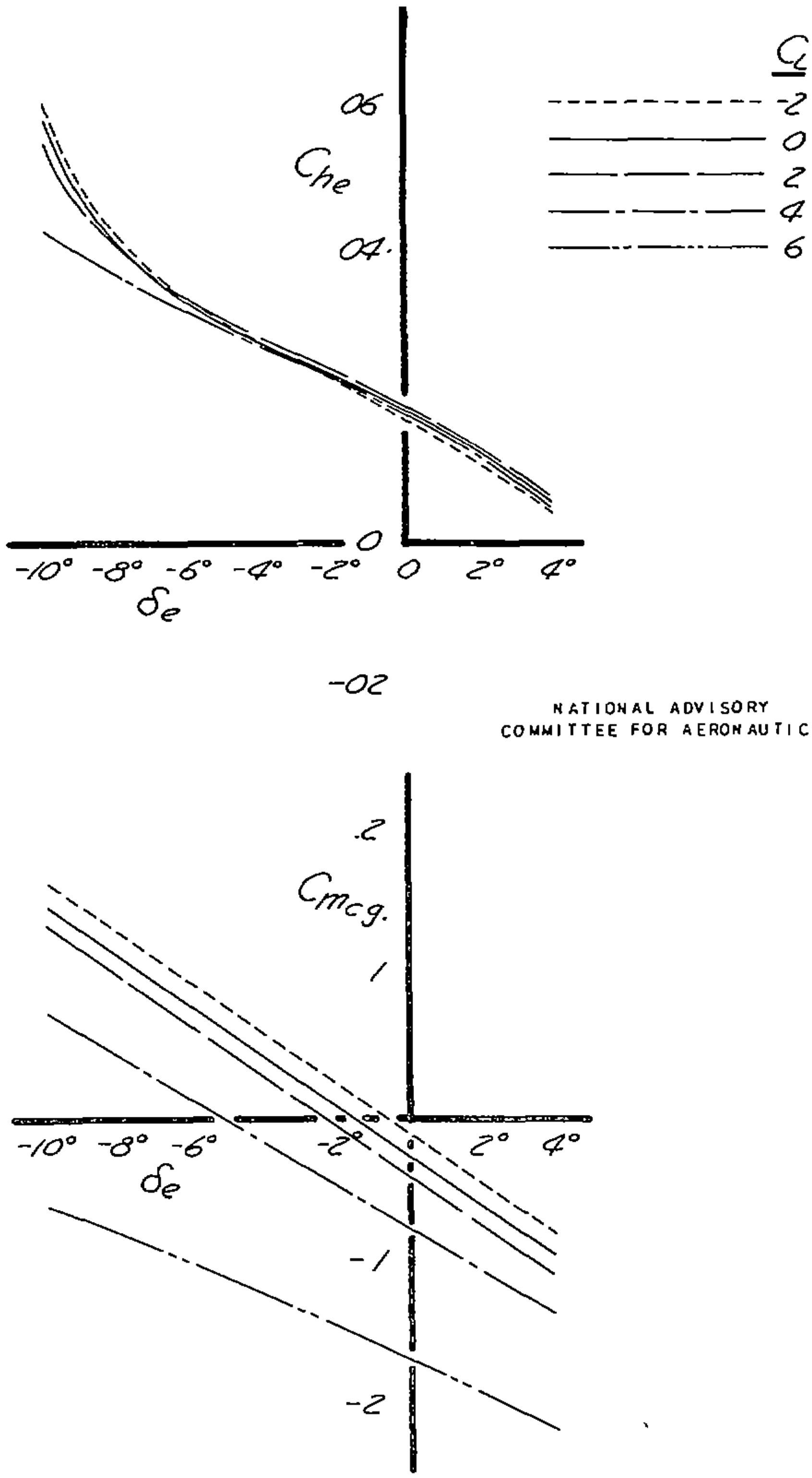

(c) M = 0.74

FIGURE 12 - (CONTINUED) ELEVATOR TABS DEFLECTED -5°

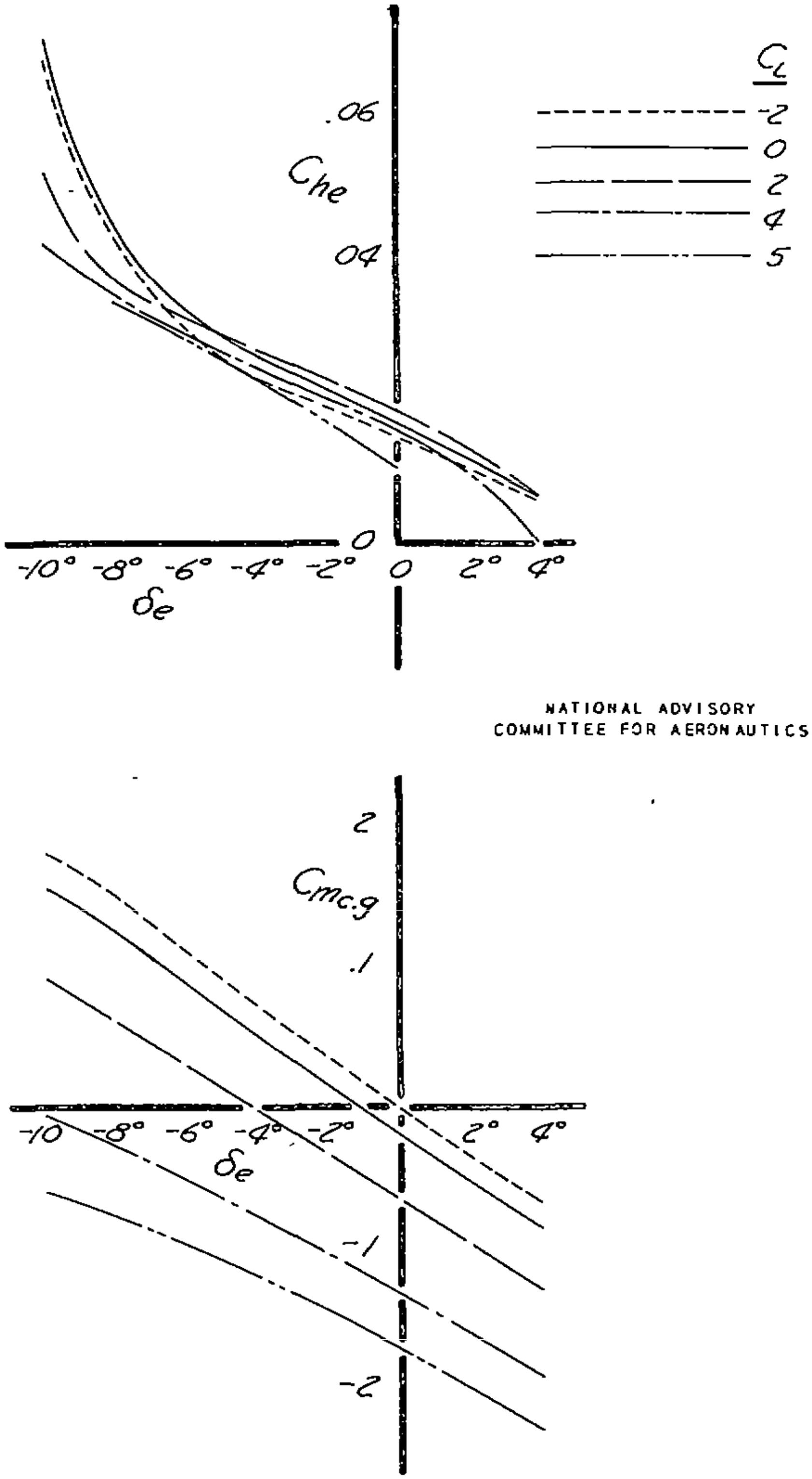

(d) M = 0.79

FIGURE 12.– (CONTINUED) ELEVATOR TABS DEFLECTED –5°

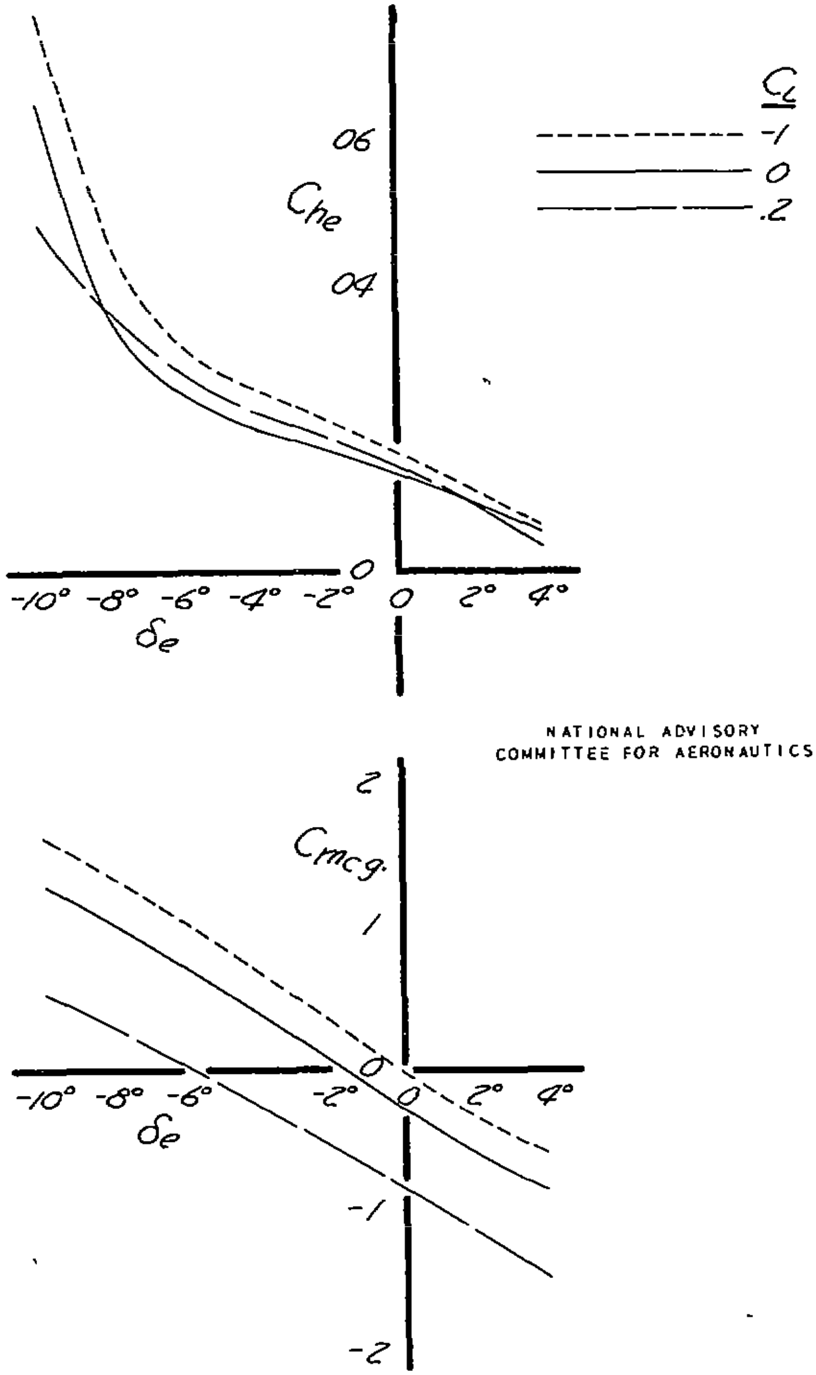

(e) M = 0.815

FIGURE 12 – (CONCLUDED) ELEVATOR TABS DEFLECTED –5°

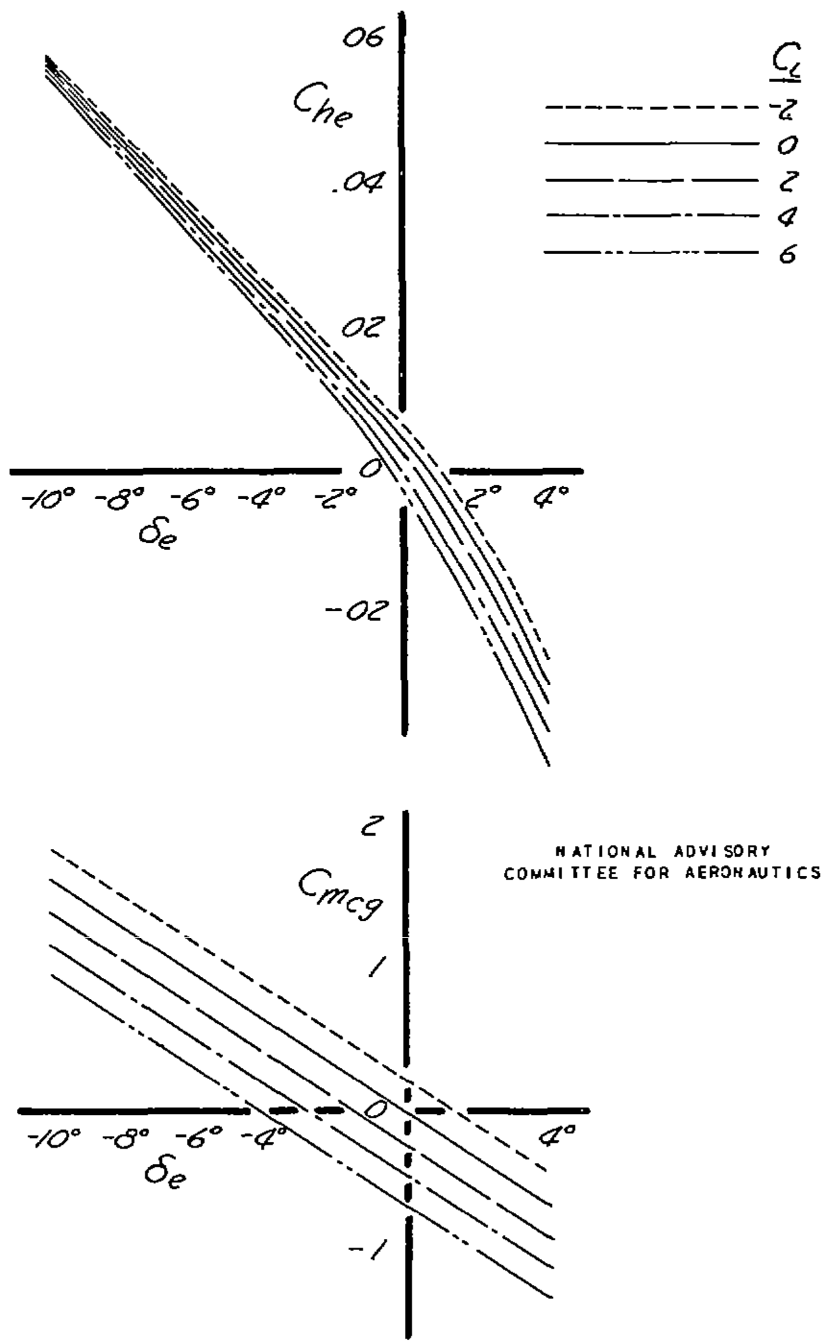

(a) $M = 0.20$

FIGURE 13.- ELEVATOR CHARACTERISTICS WITH THE 1.2-BY 12-INCH FLAPS DEFLECTED 7.5°

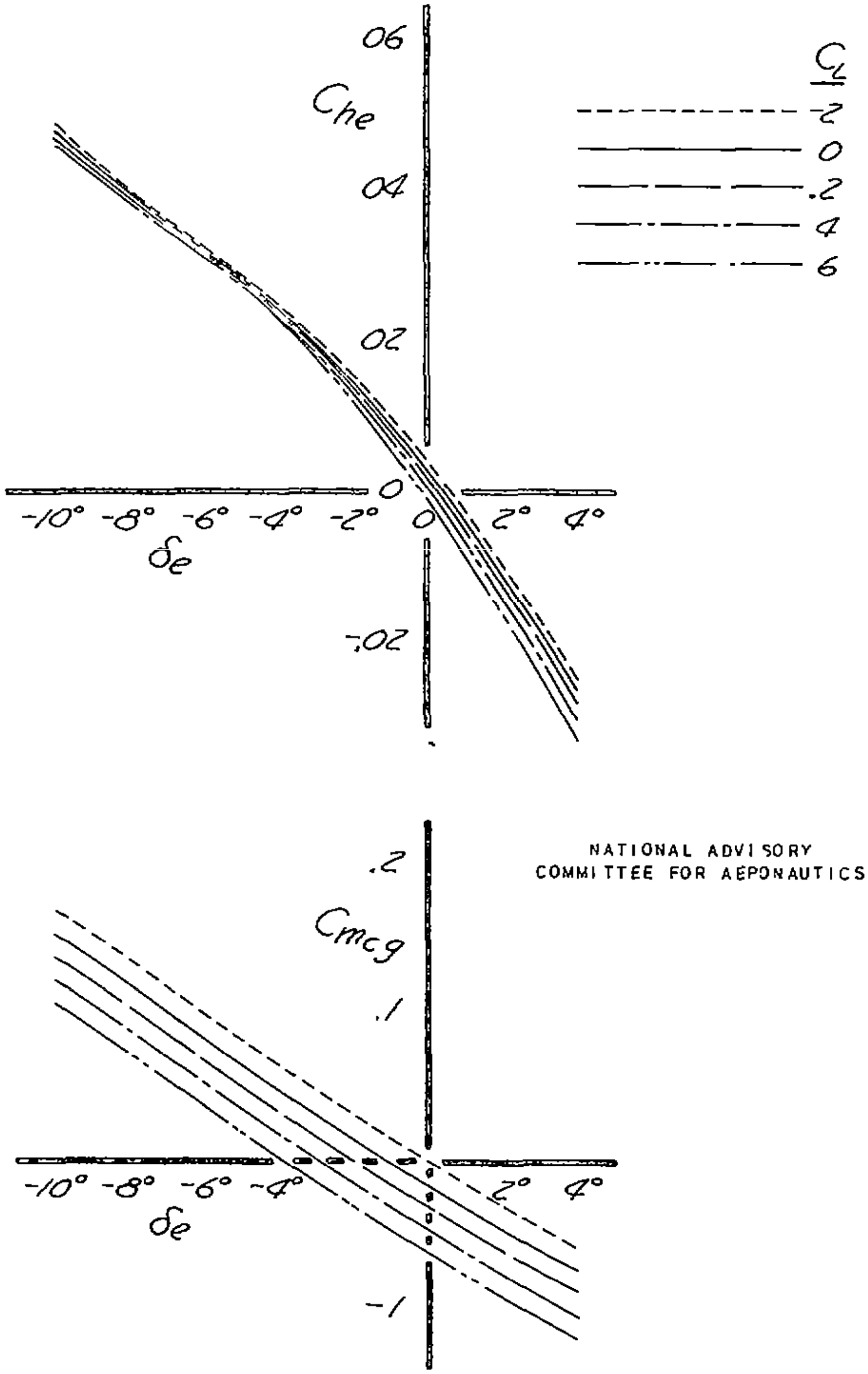

(b) M = 0.60

FIGURE 13 — (CONTINUED) 12-BY 12-INCH FLAPS DEFLECTED 75°

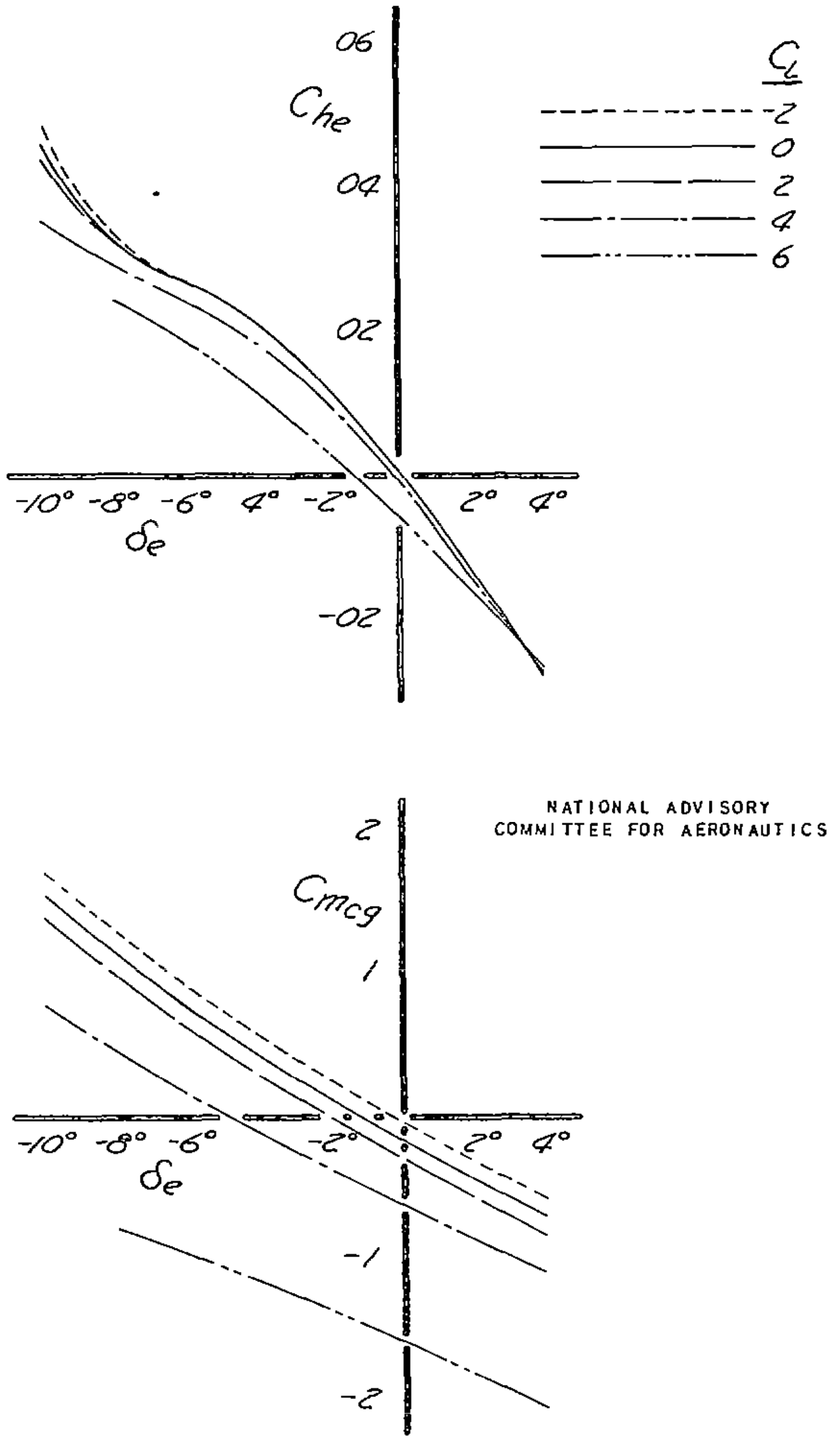

(c) M= 0 74

FIGURE 13 - (CONTINUED) 12-BY 12-INCH FLAPS DEFLECTED 75°

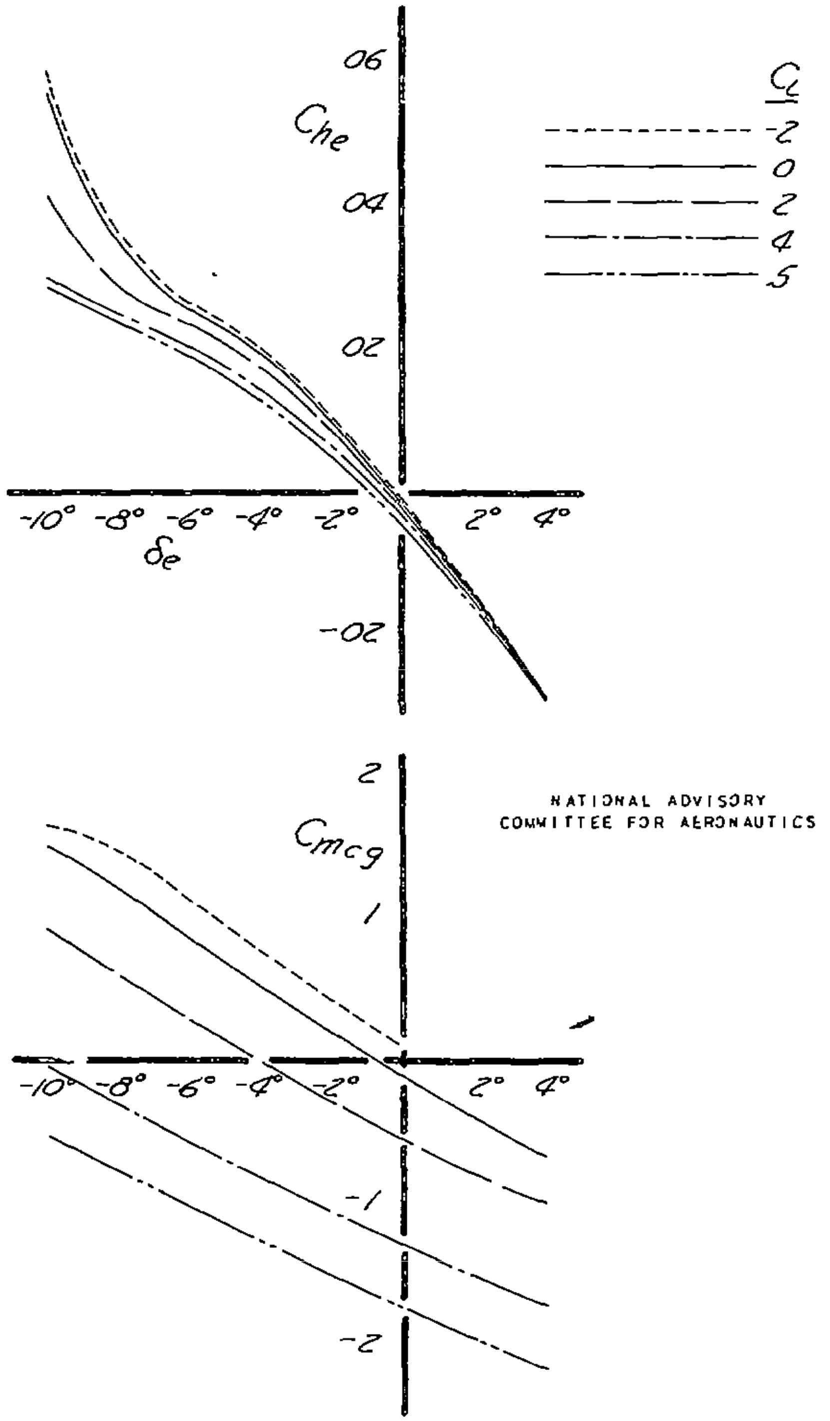

(d) M = 0 79

FIGURE 13 – (CONTINUED) 12-BY 12-INCH FLAPS DEFLECTED 75°

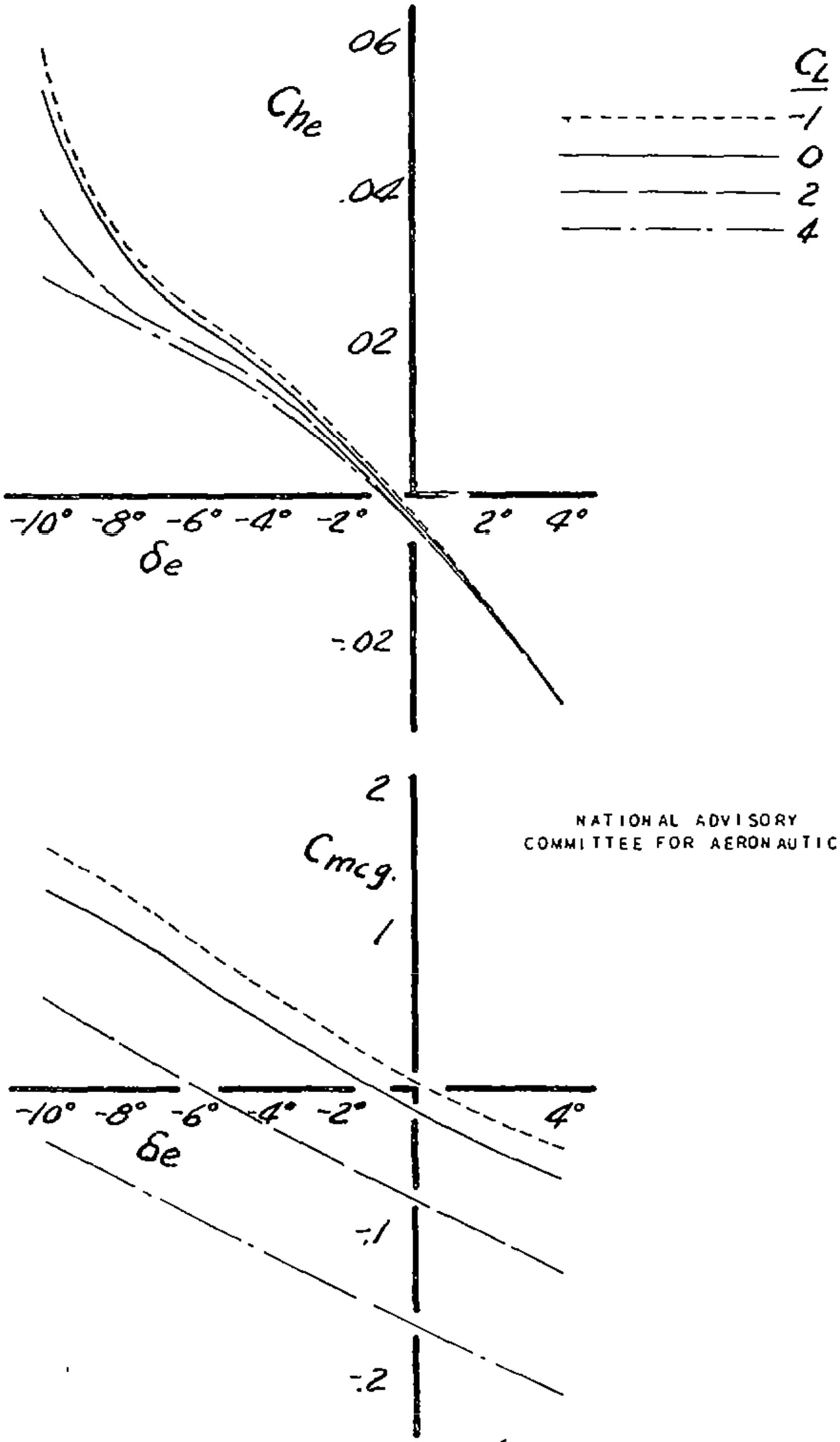

(e) M = 0.815

FIGURE 13 — (CONCLUDED) 1.2-BY 12-INCH FLAPS DEFLECTED 7.5°

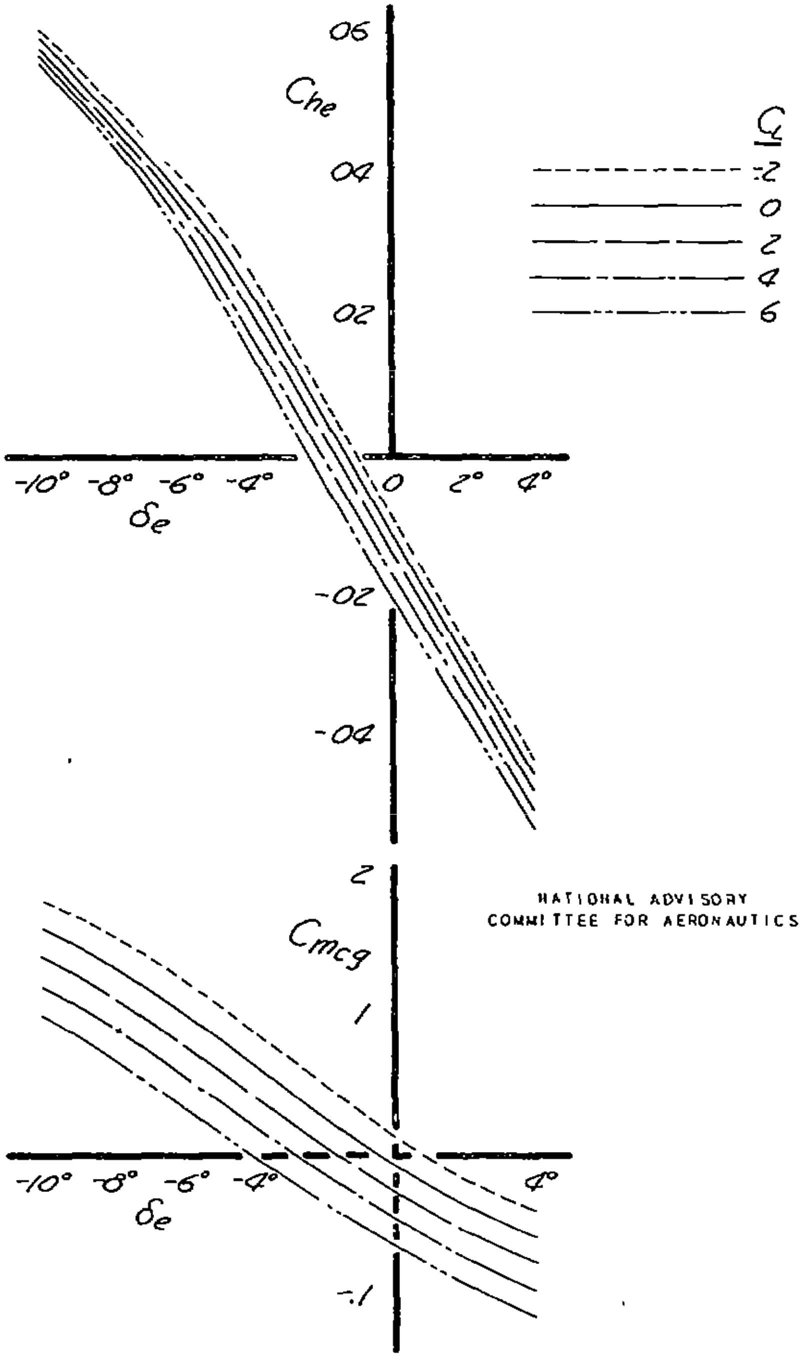

(a) M = 0.20

FIGURE 14 - ELEVATOR CHARACTERISTICS WITH THE 12-BY 12-INCH FLAPS DEFLECTED 15°

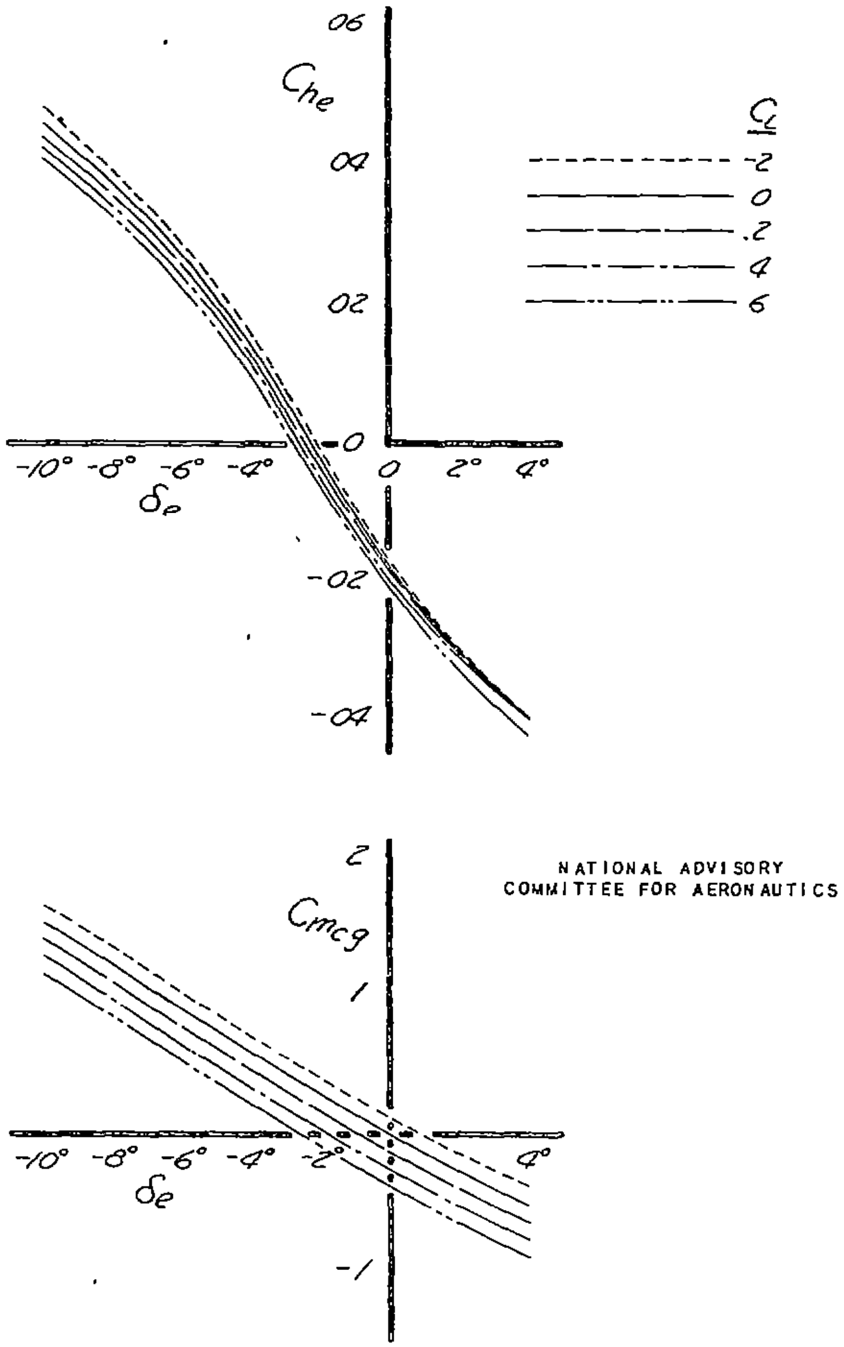

NATIONAL ADVISORY COMMITTEE FOR AERONAUTICS

(b) M = 0.60

FIGURE 14 – (CONTINUED) 12-BY 12-INCH FLAPS DEFLECTED 15°

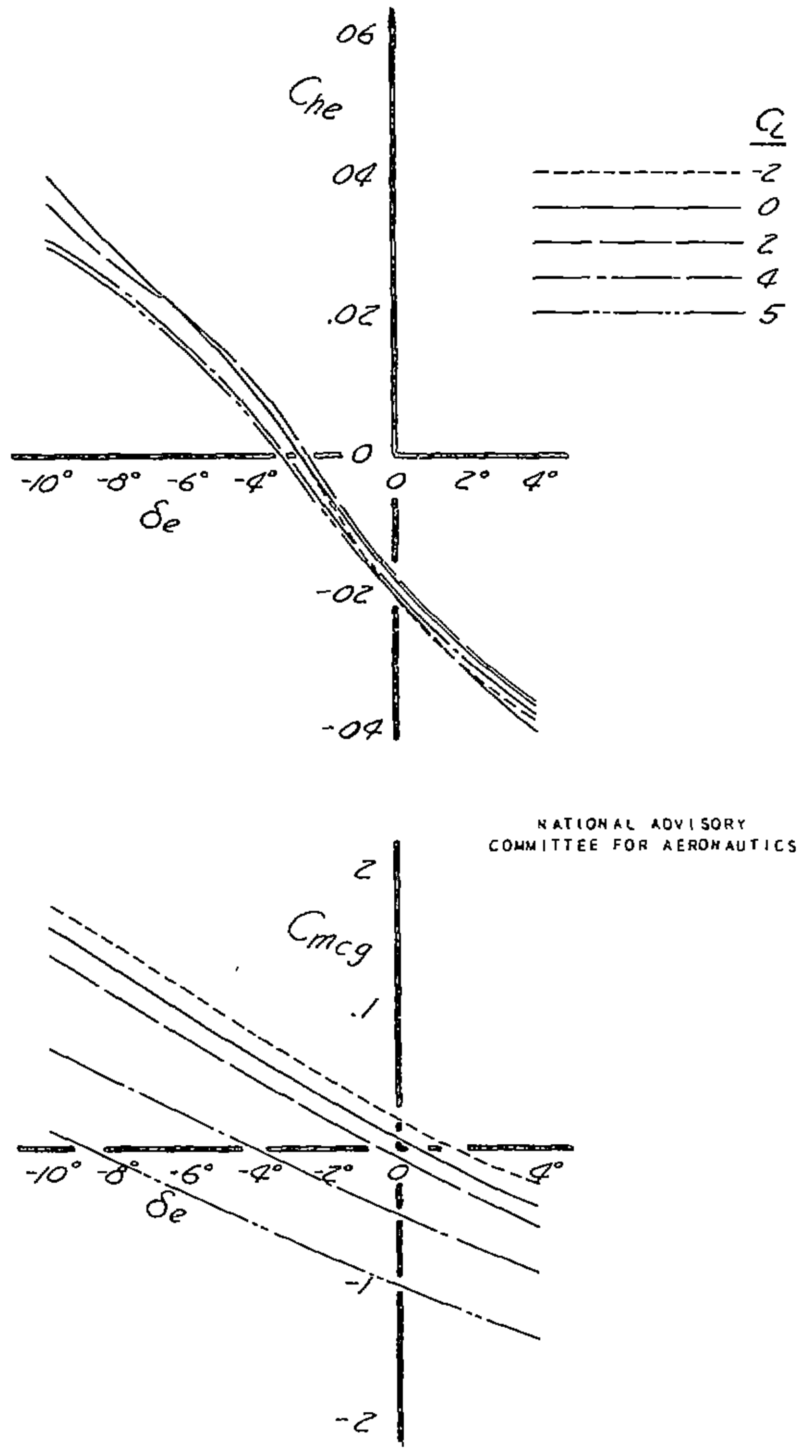

(c) $M = 0.74$

FIGURE 14 – (CONTINUED) 12-BY 12-INCH FLAPS DEFLECTED 15°

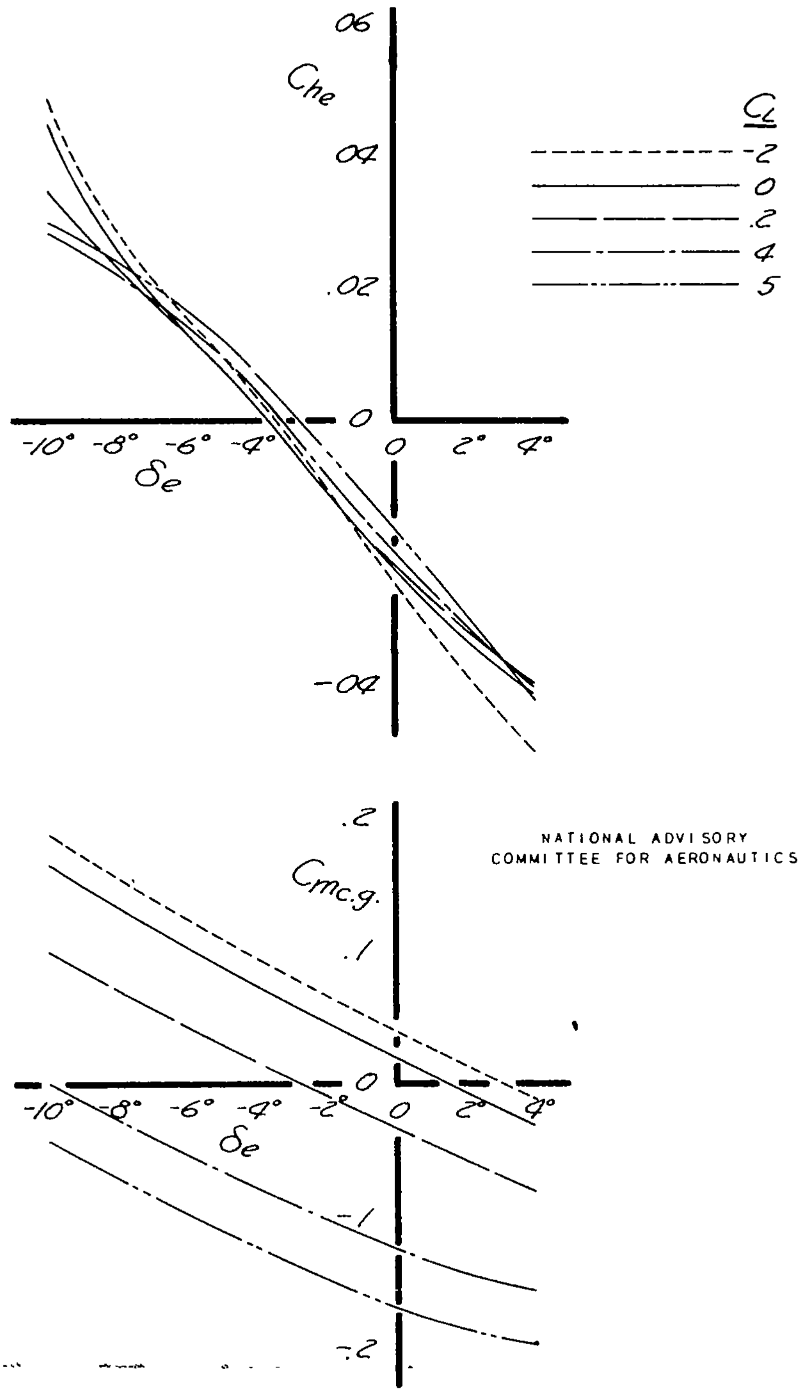

(d) $M = 0.79$

FIGURE 14.— (CONTINUED) 1.2-BY 12-INCH FLAPS DEFLECTED 15°

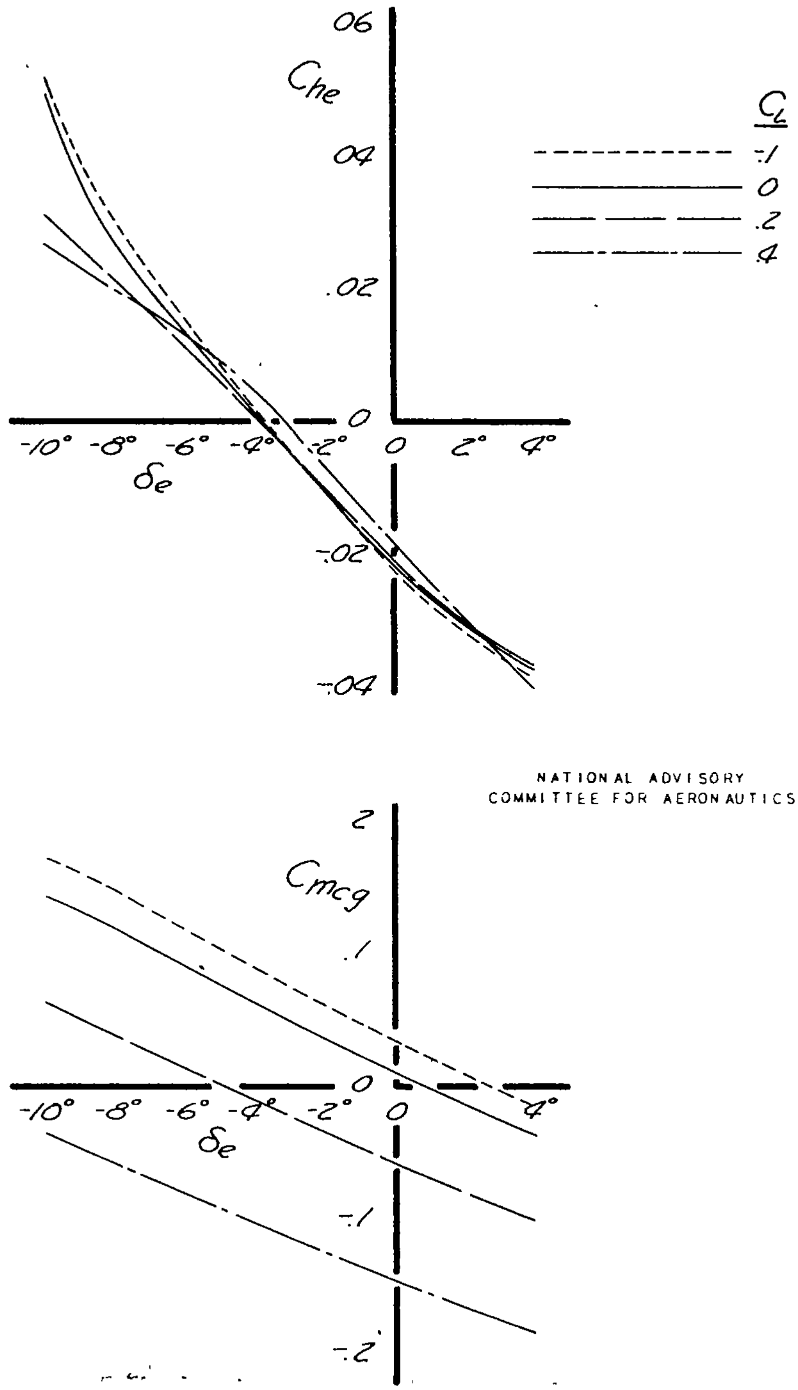

(e) M = 0.815

FIGURE 14.– (CONCLUDED) 1.2-BY 12-INCH FLAPS DEFLECTED 15°

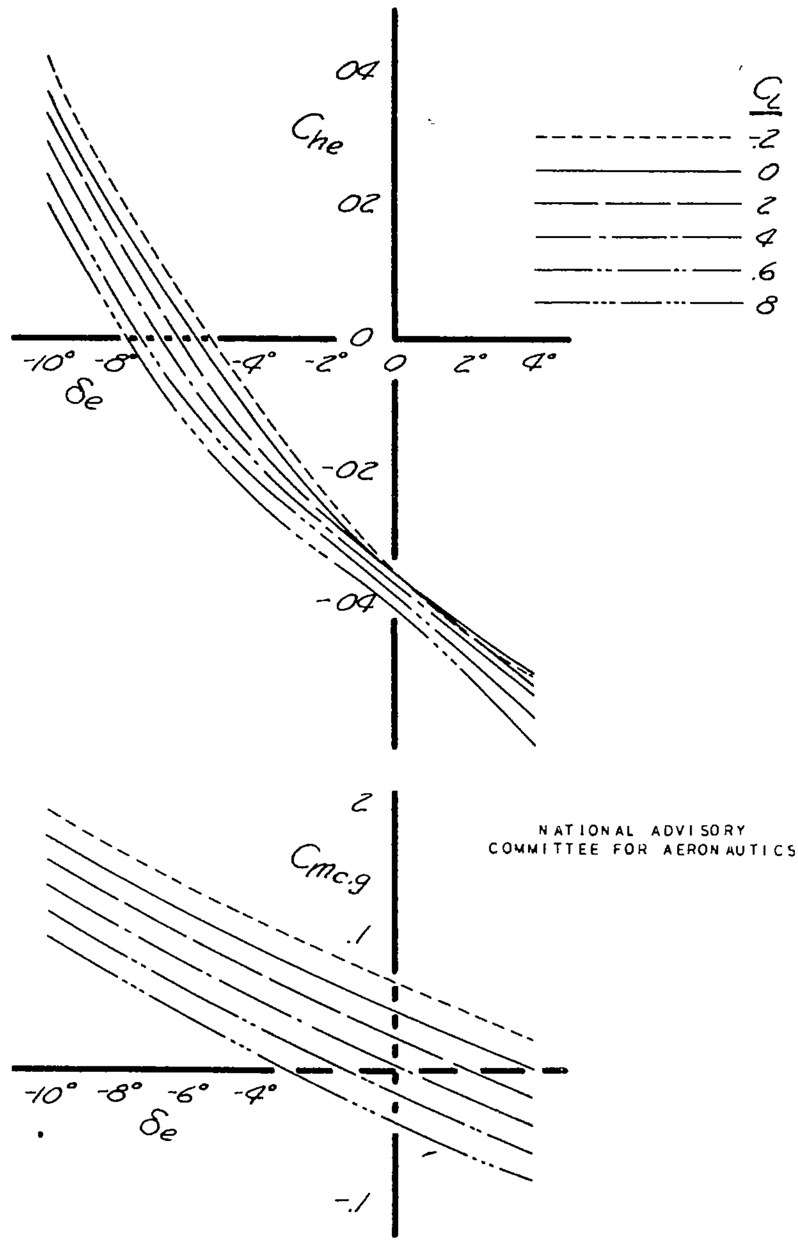

(a) M = 0.20

FIGURE 15.– ELEVATOR CHARACTERISTICS WITH THE 1.2-BY 12-INCH FLAPS DEFLECTED 30°

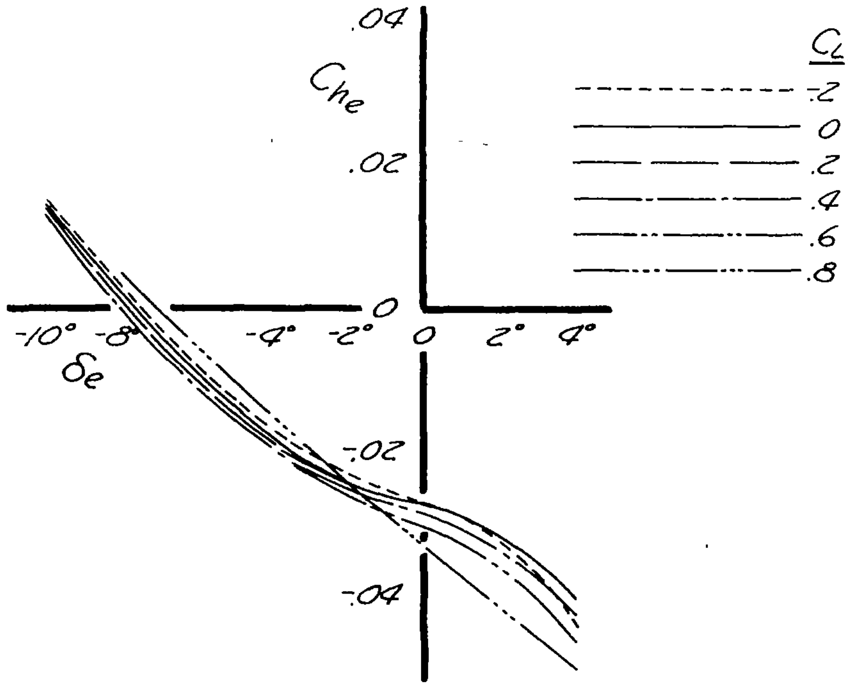

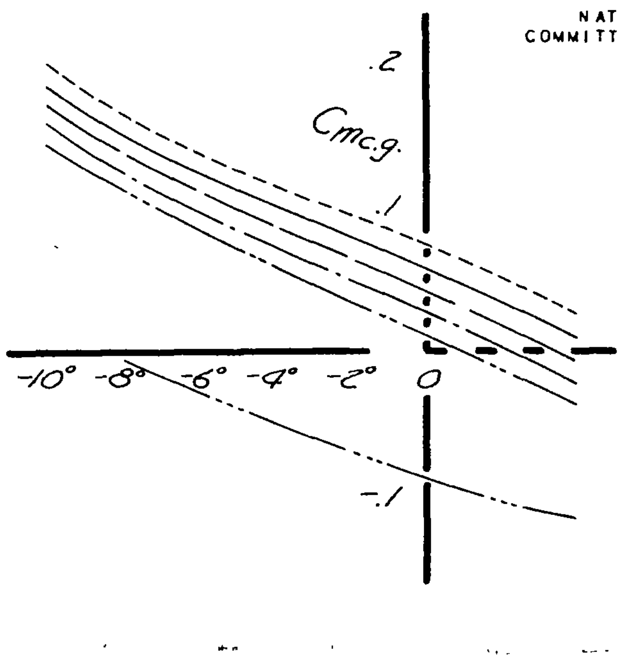

NATIONAL ADVISORY COMMITTEE FOR AERONAUTICS

(b) M = 0.60

FIGURE 15.- (CONTINUED) 1.2-BY 12-INCH FLAPS DEFLECTED 30°

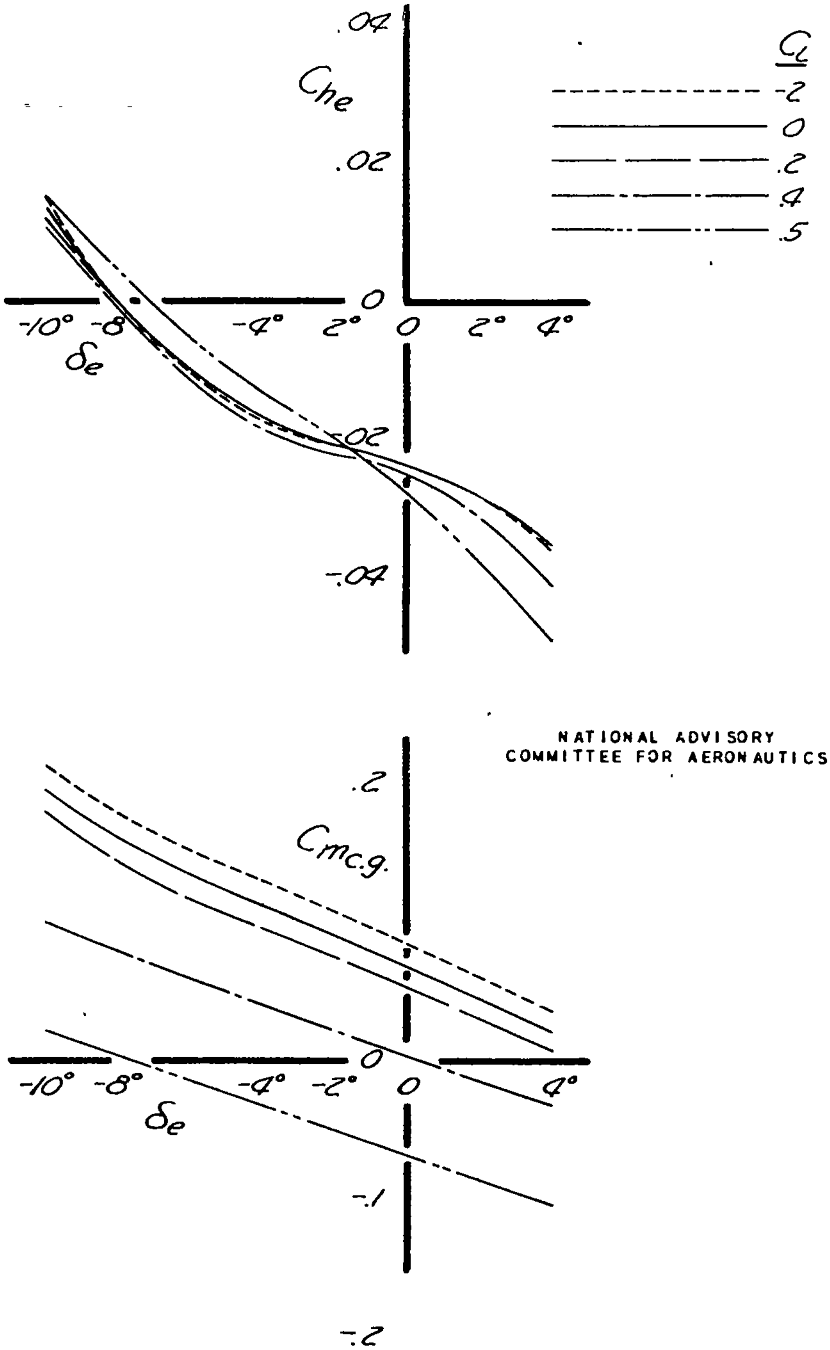

(c) M = 0.74

FIGURE 15.– (CONTINUED) 1.2-BY 12-INCH FLAPS DEFLECTED 30°

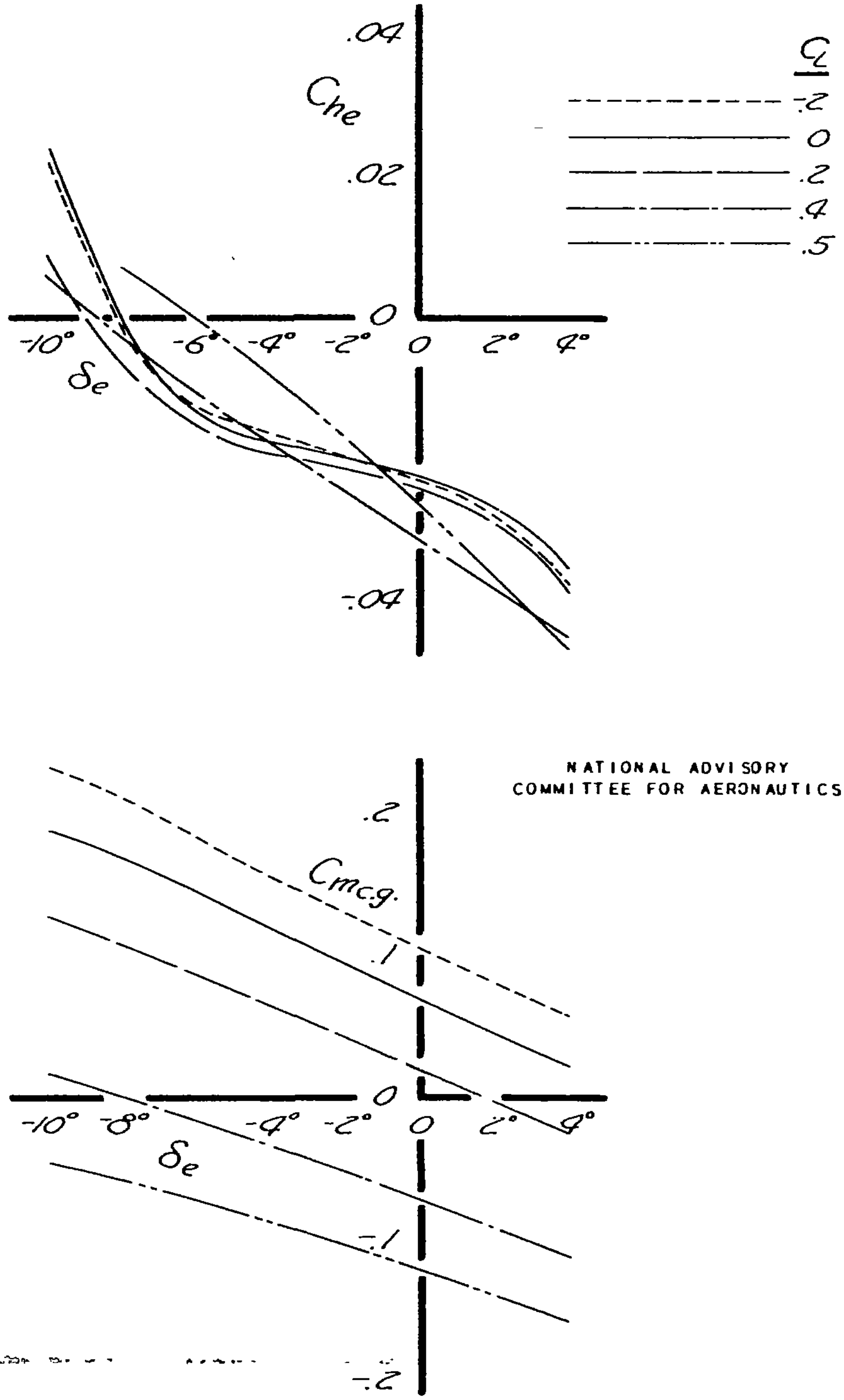

NATIONAL ADVISORY COMMITTEE FOR AERONAUTICS

(d) M = 0.79

FIGURE 15.- (CONTINUED) 1.2-BY 12-INCH FLAPS DEFLECTED 30°

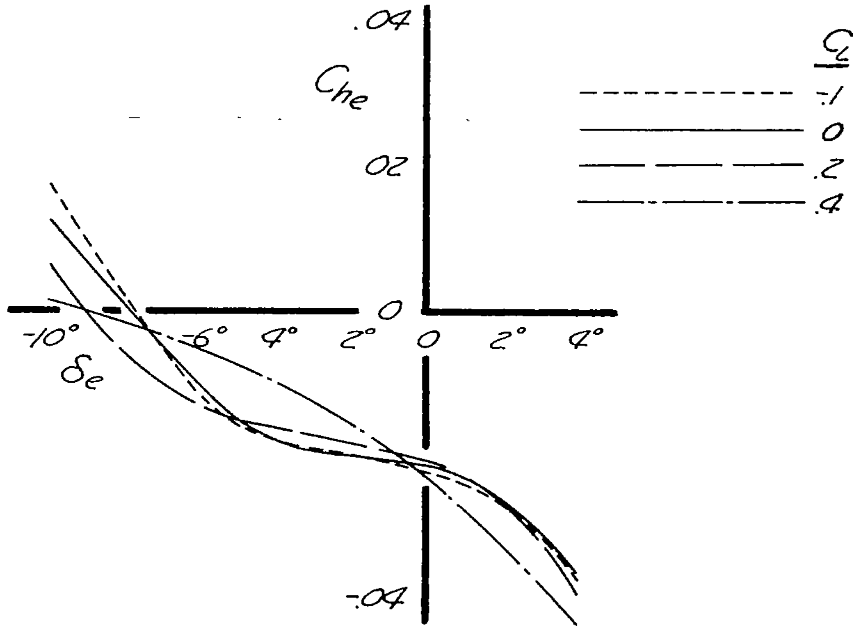

NATIONAL ADVISORY
COMMITTEE FOR AERONAUTICS

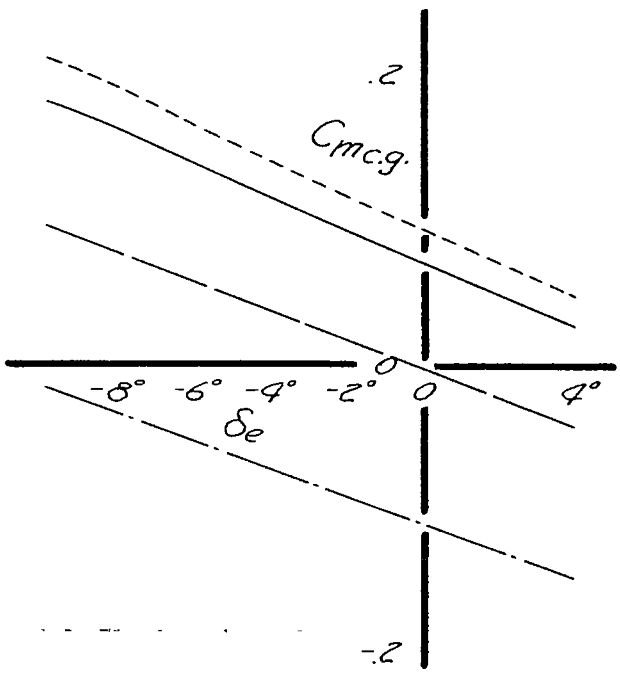

(e) M= 0.815

FIGURE 15.- (CONCLUDED) 1.2-BY 12-INCH FLAPS DEFLECTED 30°

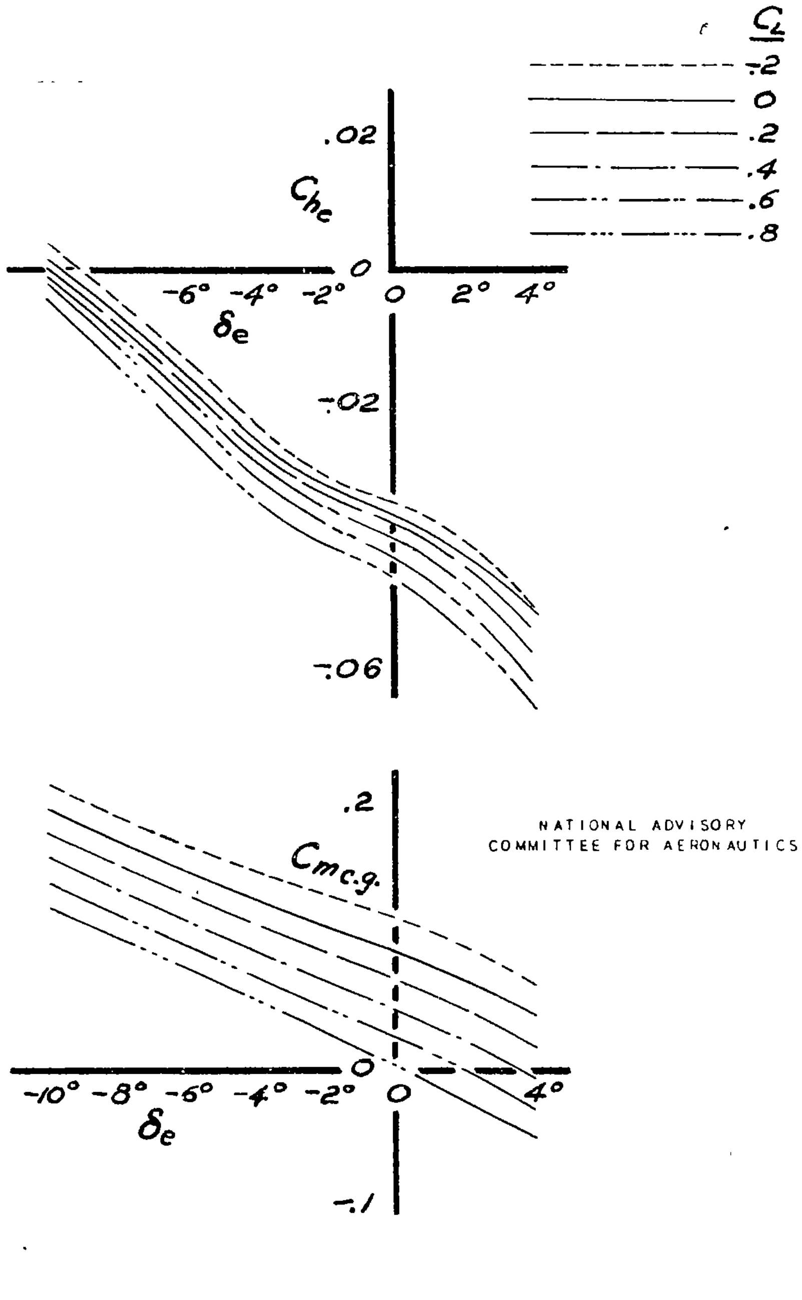

(a) $M = 0.20$

FIGURE 16.—ELEVATOR CHARACTERISTICS WITH THE 1.2-BY 12 INCH FLAPS DEFLECTED 45°

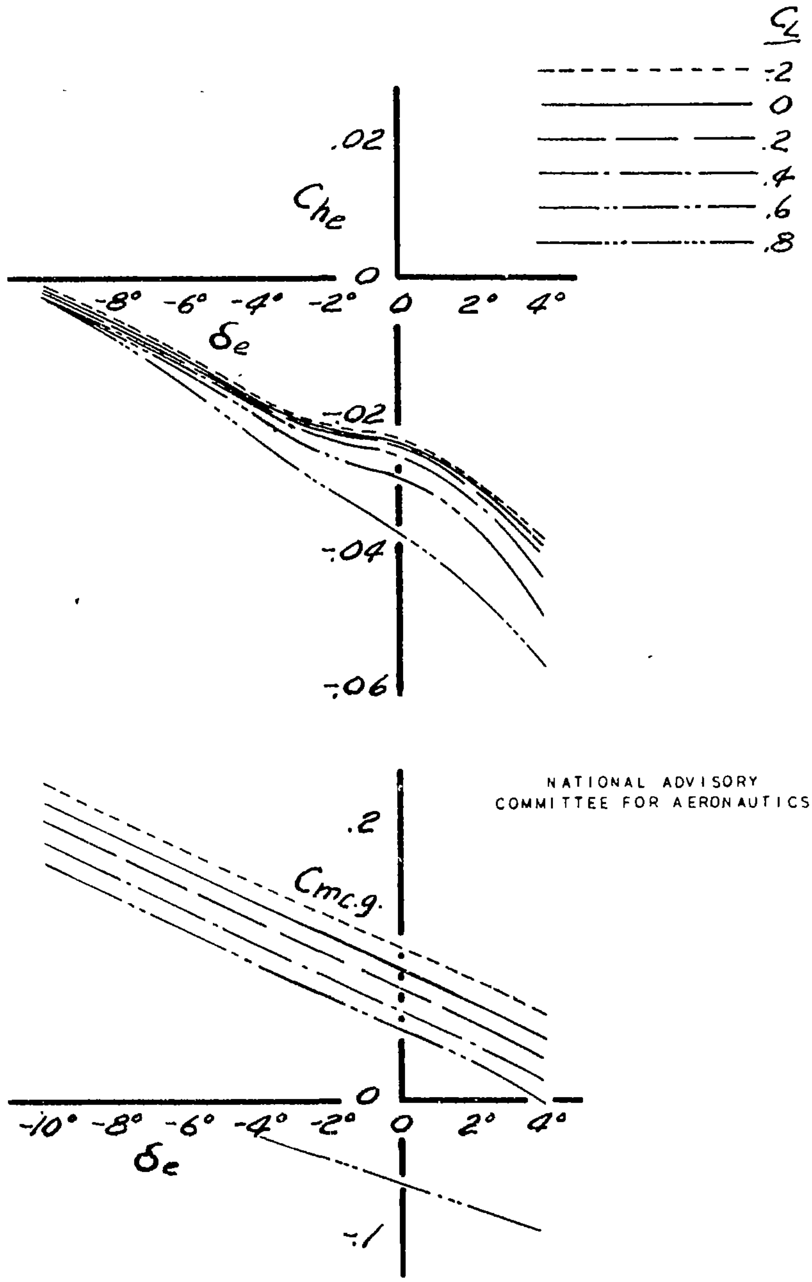

(b) M = 0.60

FIGURE 16.- (CONTINUED) 1.2-BY 12-INCH FLAPS DEFLECTED 45°

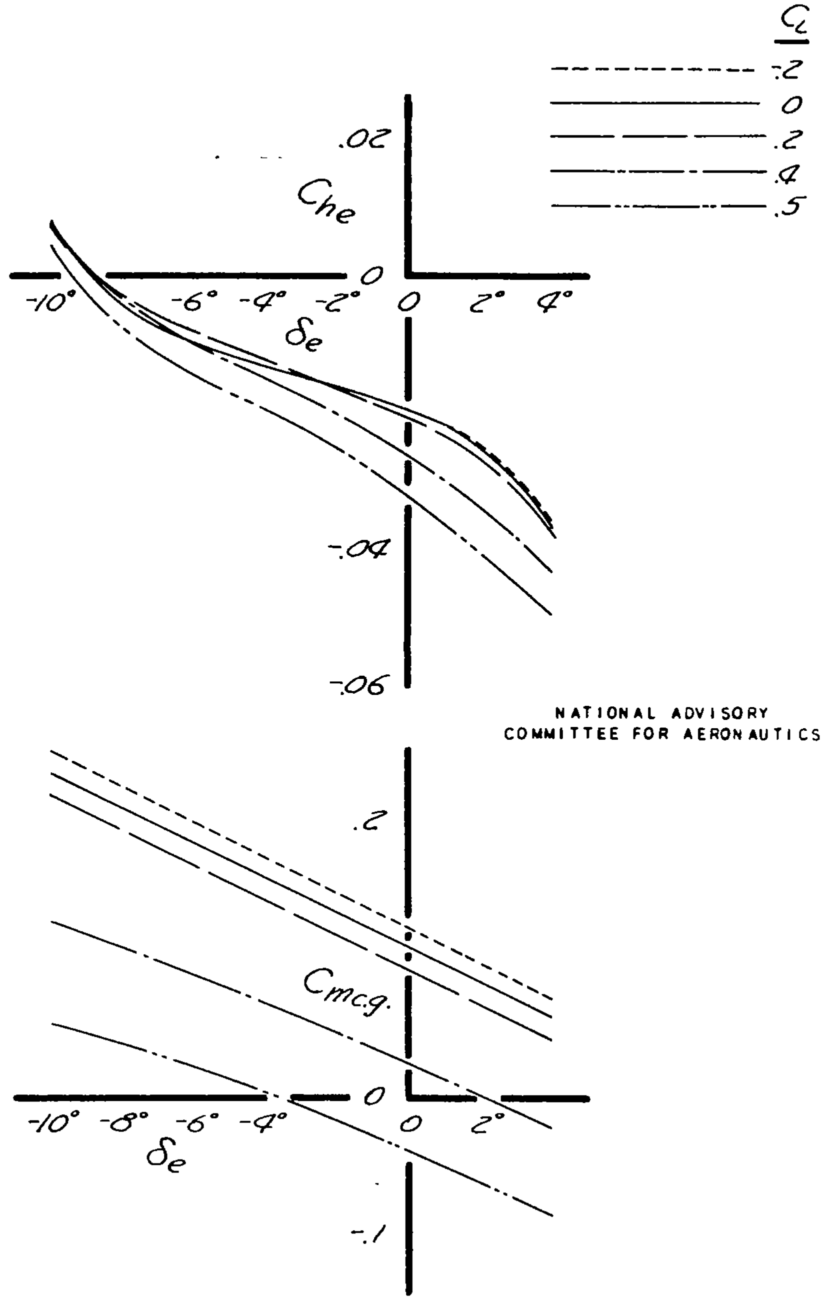

(c) M = 0.74

FIGURE 16.- (CONTINUED) 1.2-BY 12-INCH FLAPS DEFLECTED 45°

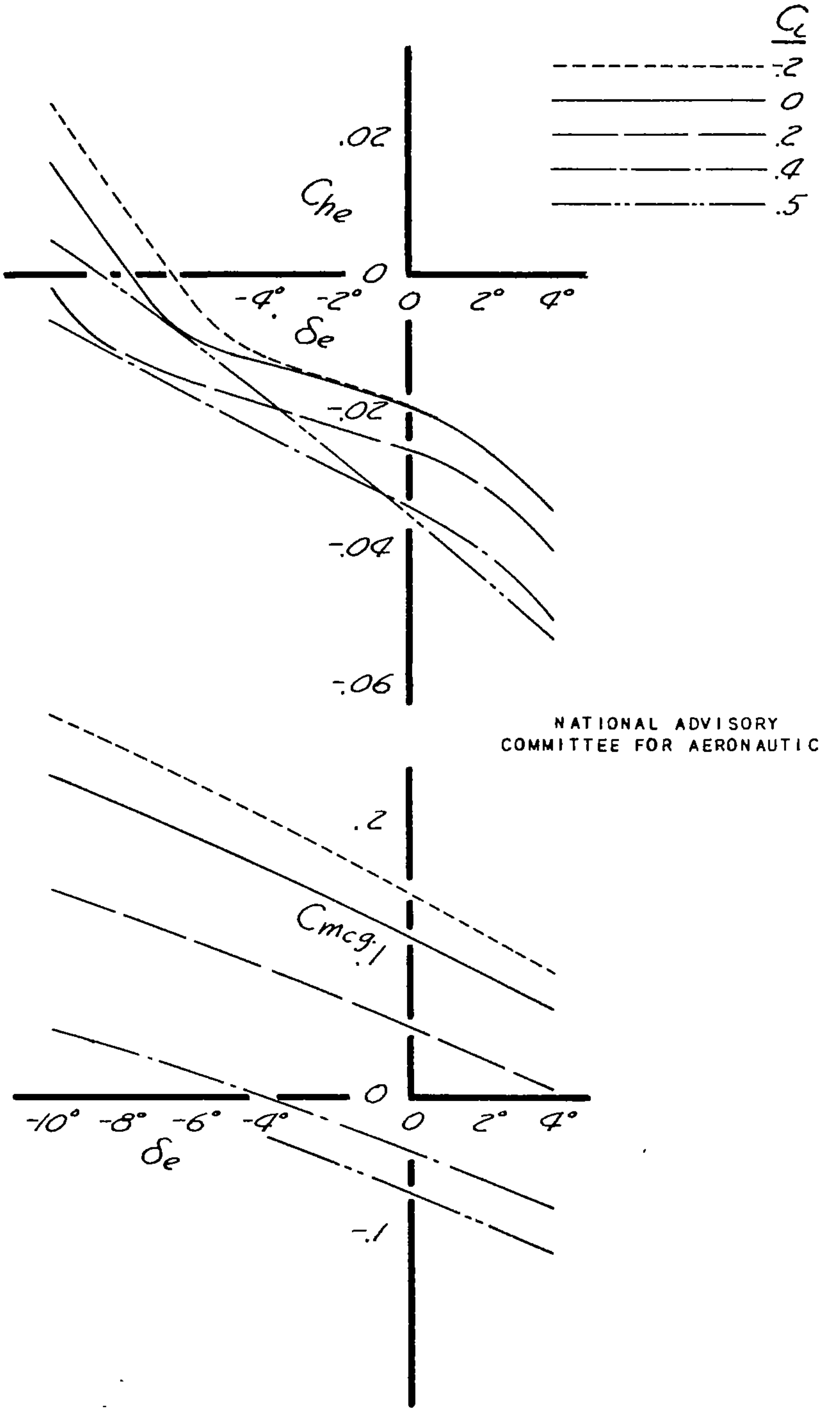

NATIONAL ADVISORY COMMITTEE FOR AERONAUTICS

(d) M = 0.79

FIGURE 16.– (CONTINUED) 1.2-BY 12-INCH FLAPS DEFLECTED 45°

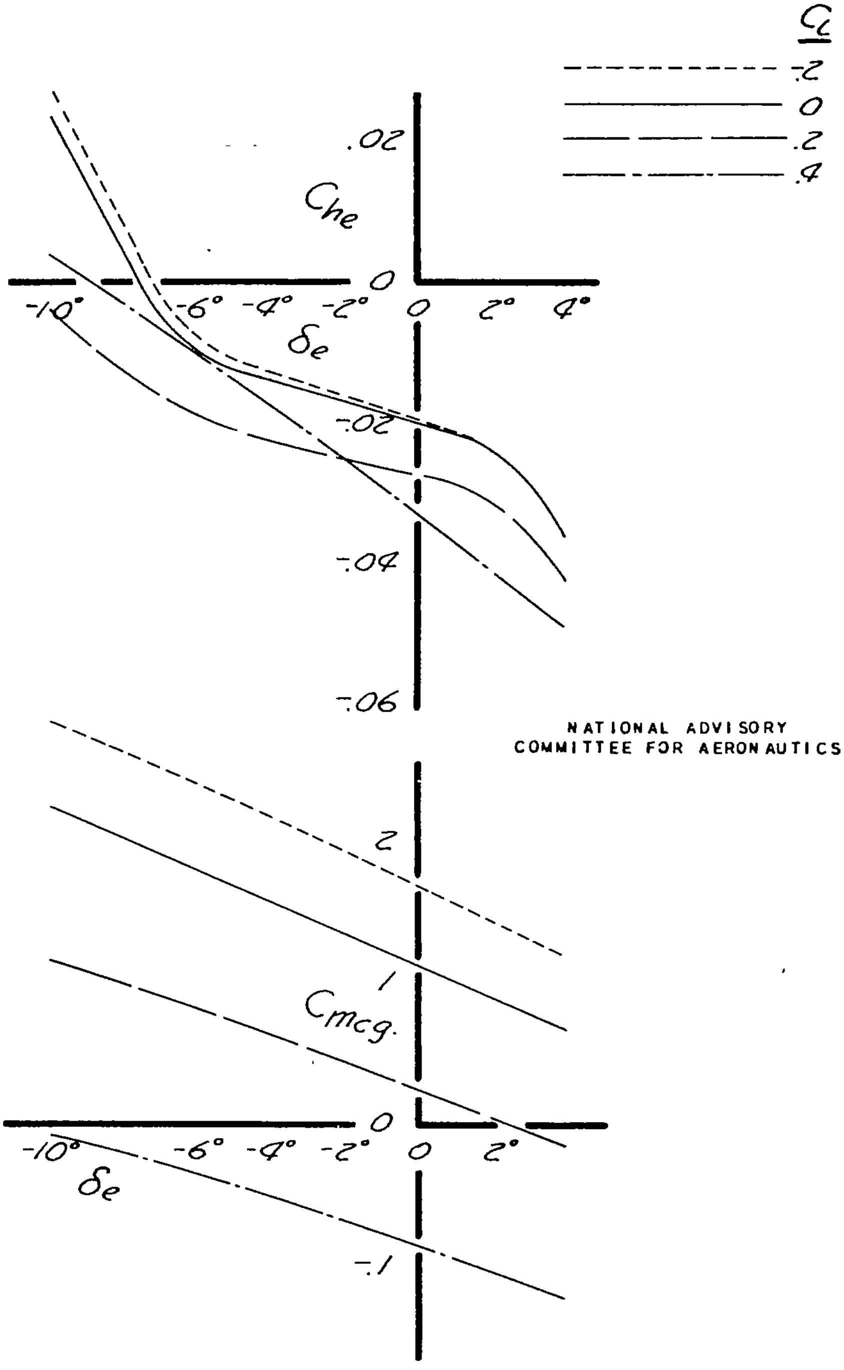

(e) M = 0.815

FIGURE 16.- (CONCLUDED) 1.2-BY 12-INCH FLAPS DEFLECTED 45°

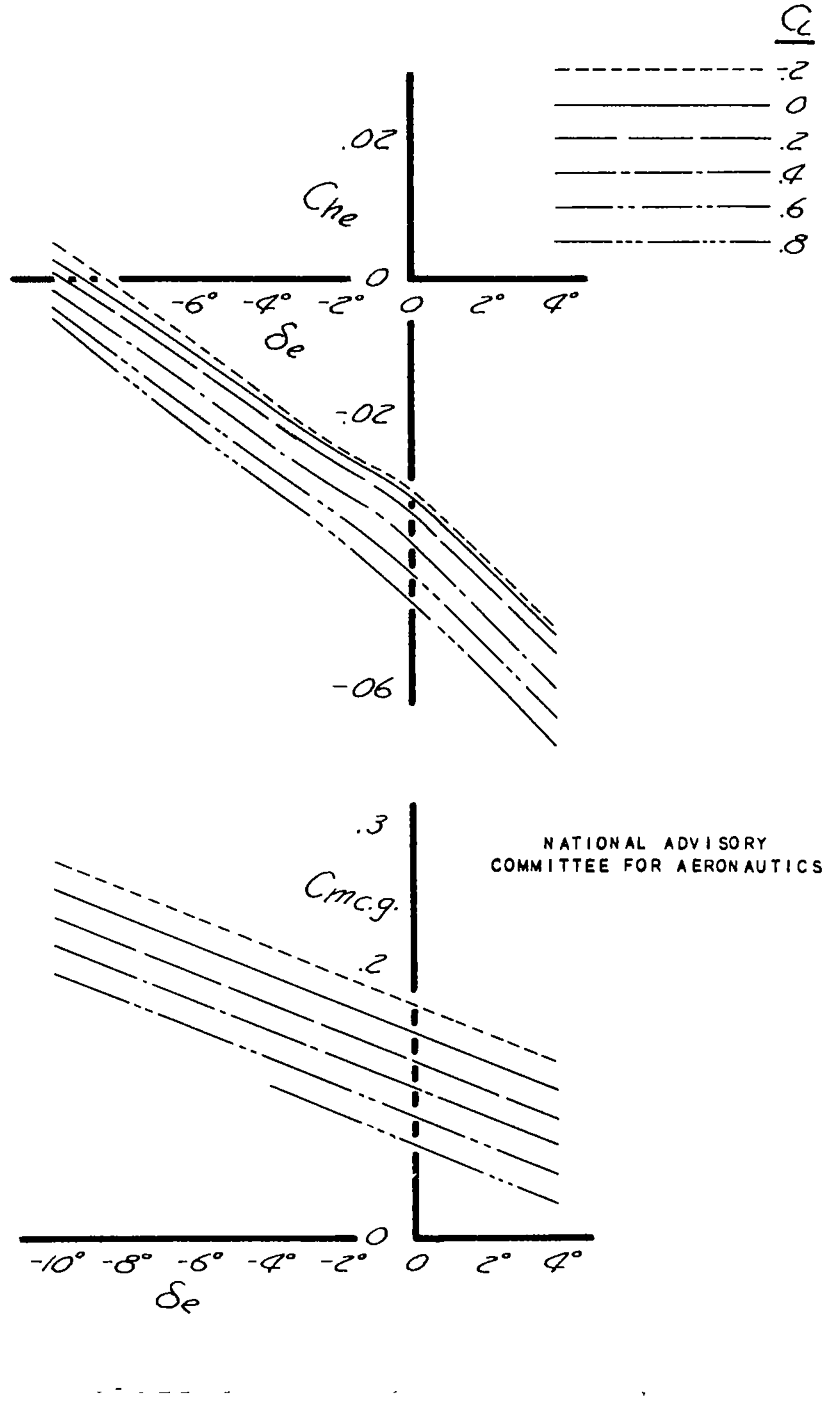

NATIONAL ADVISORY COMMITTEE FOR AERONAUTICS

(a) M = 0.20

FIGURE 17.– ELEVATOR CHARACTERISTICS WITH THE 1.2-BY 12-INCH FLAPS DEFLECTED 60°

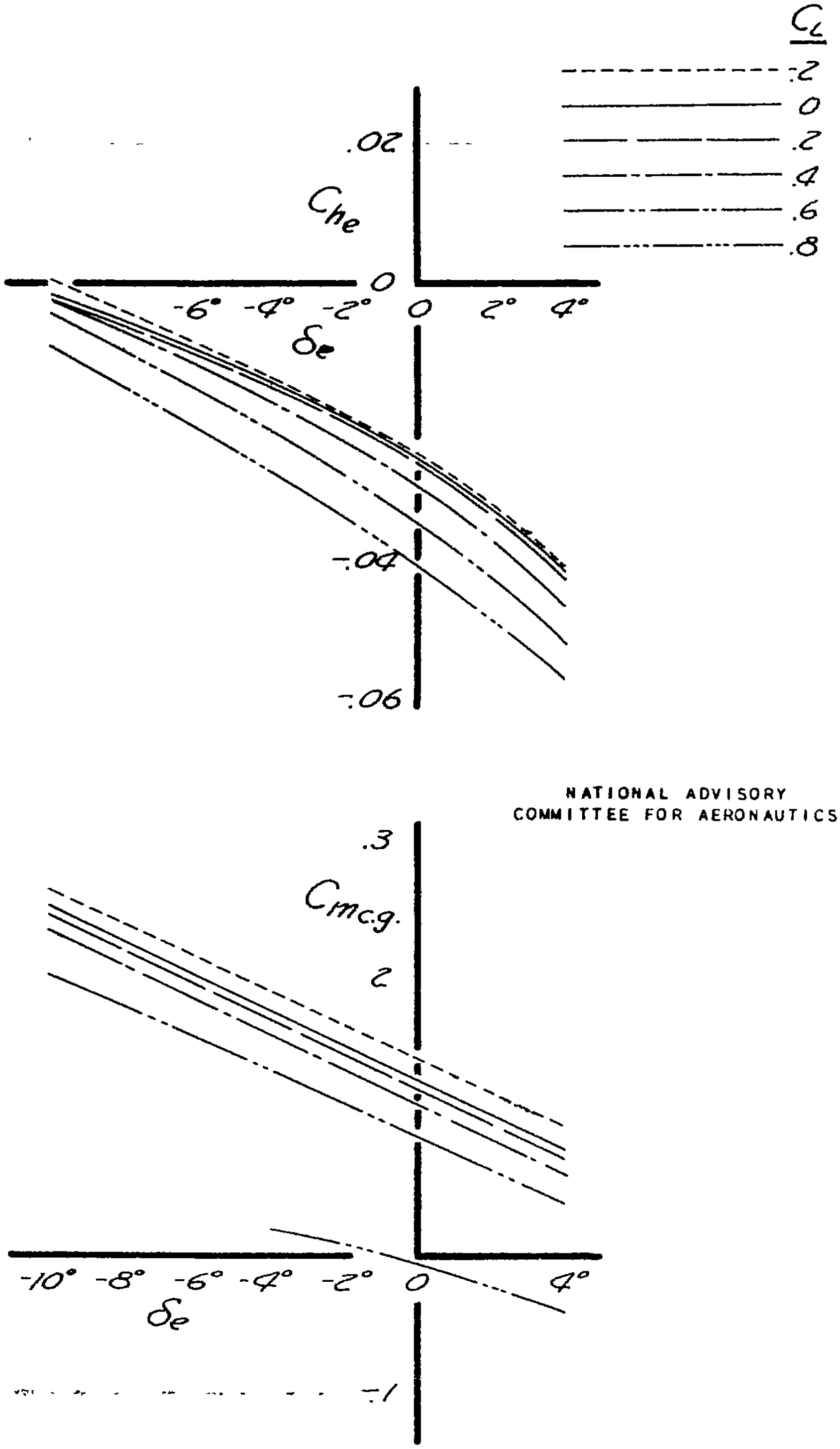

(b) M = 0.60

FIGURE 17.– (CONTINUED) 1.2-BY 12-INCH FLAPS DEFLECTED 60°

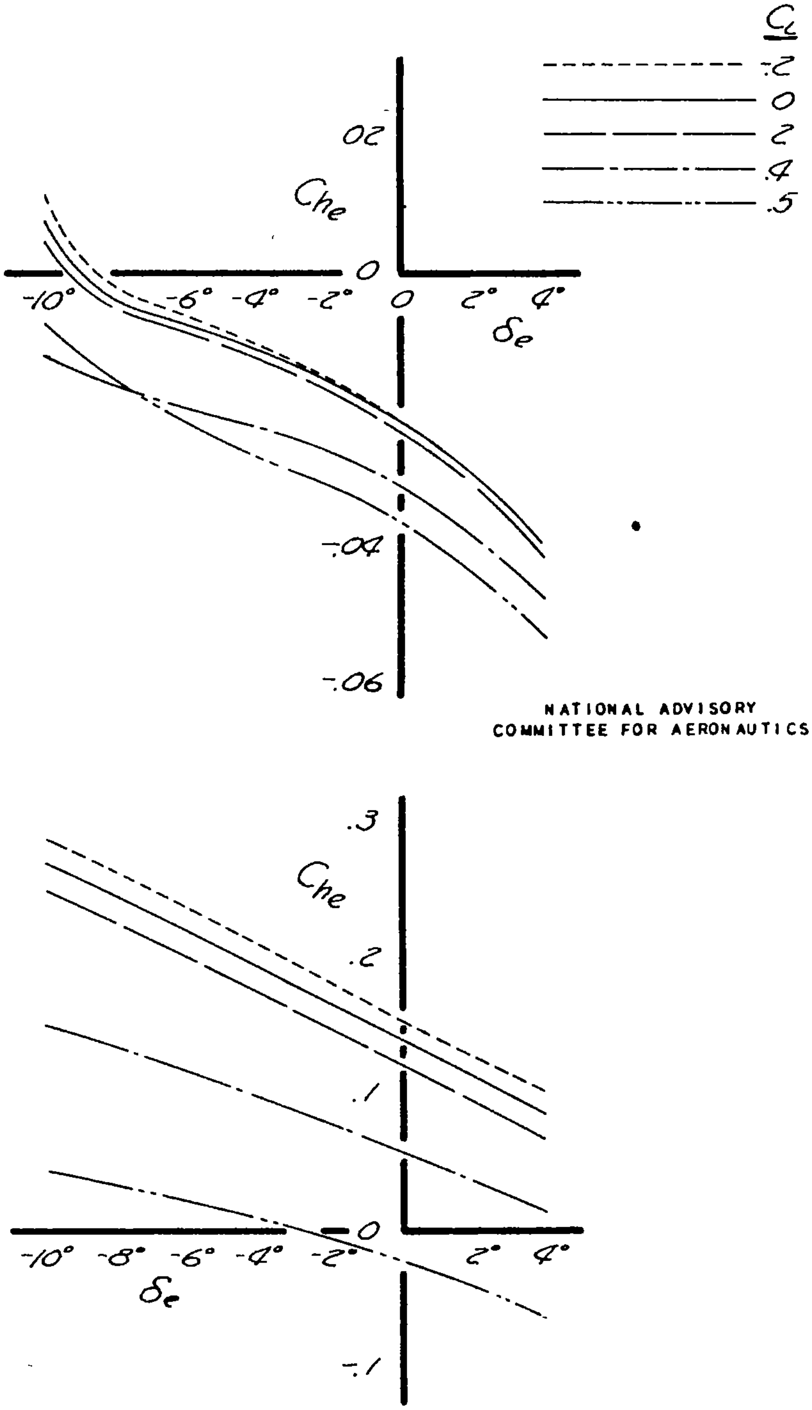

(c) $M = 0.74$

FIGURE 17.-(CONTINUED) 1.2-BY 12-INCH FLAPS DEFLECTED 60°

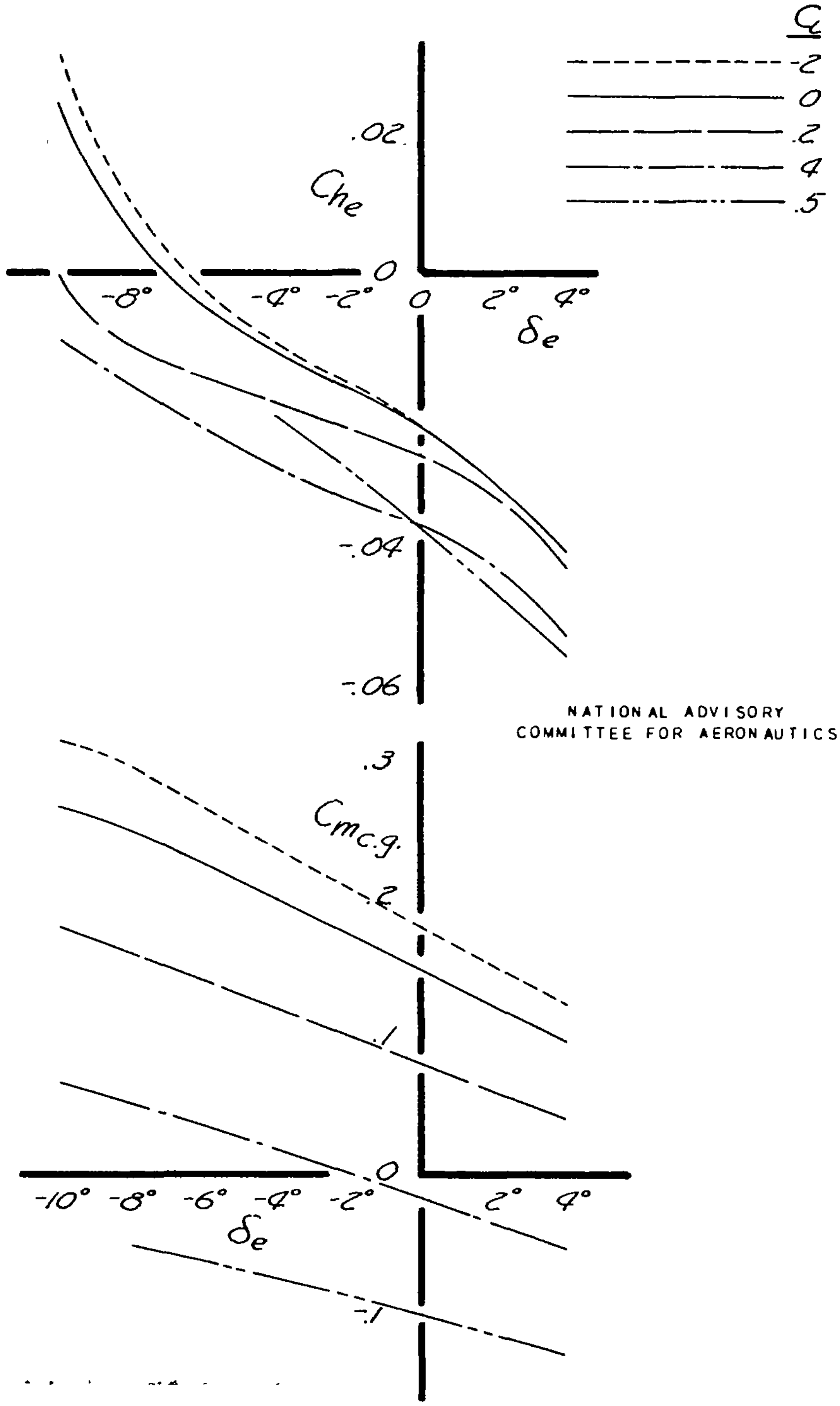

(d) M = 0.79

FIGURE 17.– (CONTINUED) 1.2-BY 12-INCH FLAPS DEFLECTED 60°

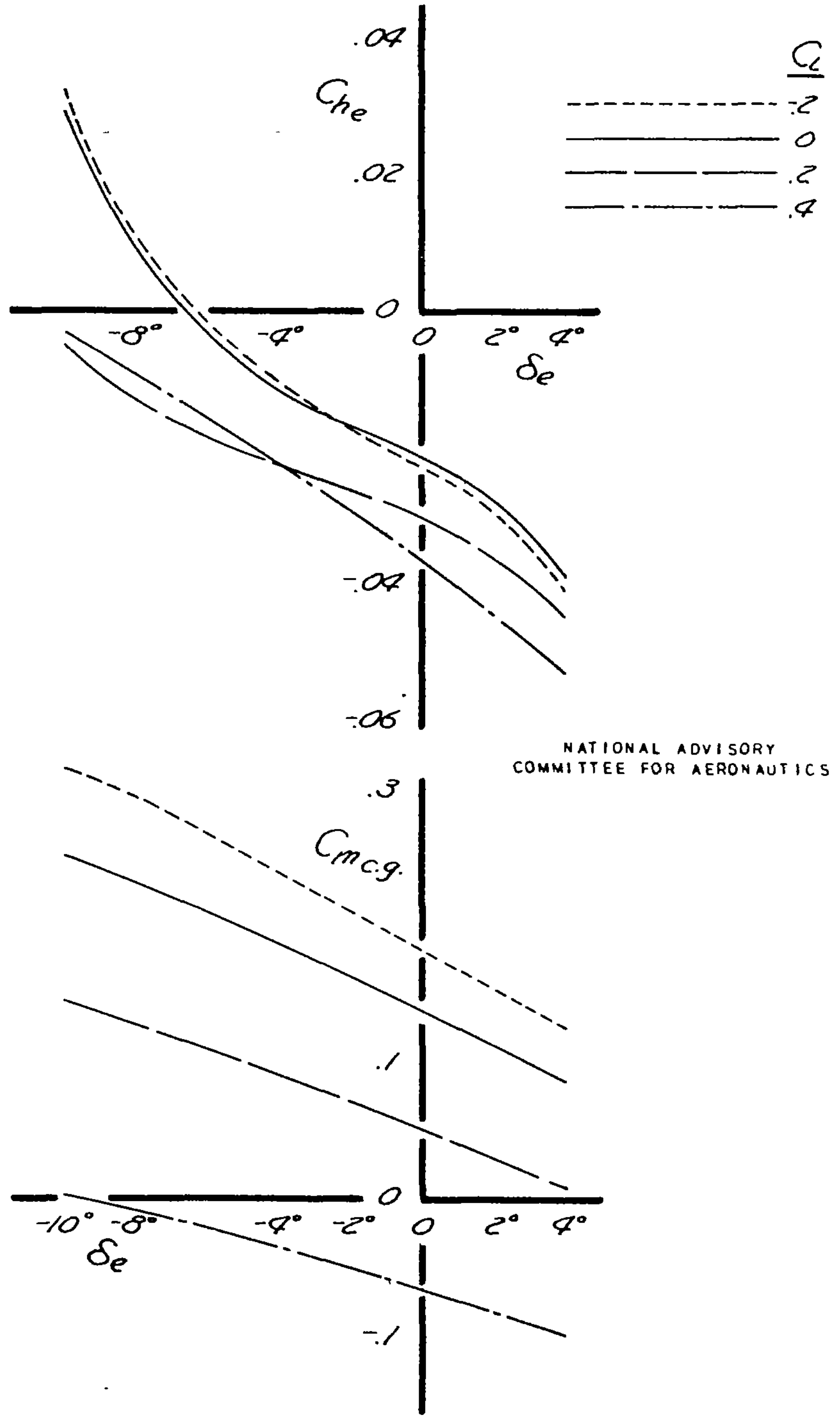

(e) $M = 0.815$

FIGURE 17.– (CONCLUDED) 1.2-BY 12-INCH FLAPS DEFLECTED 60°

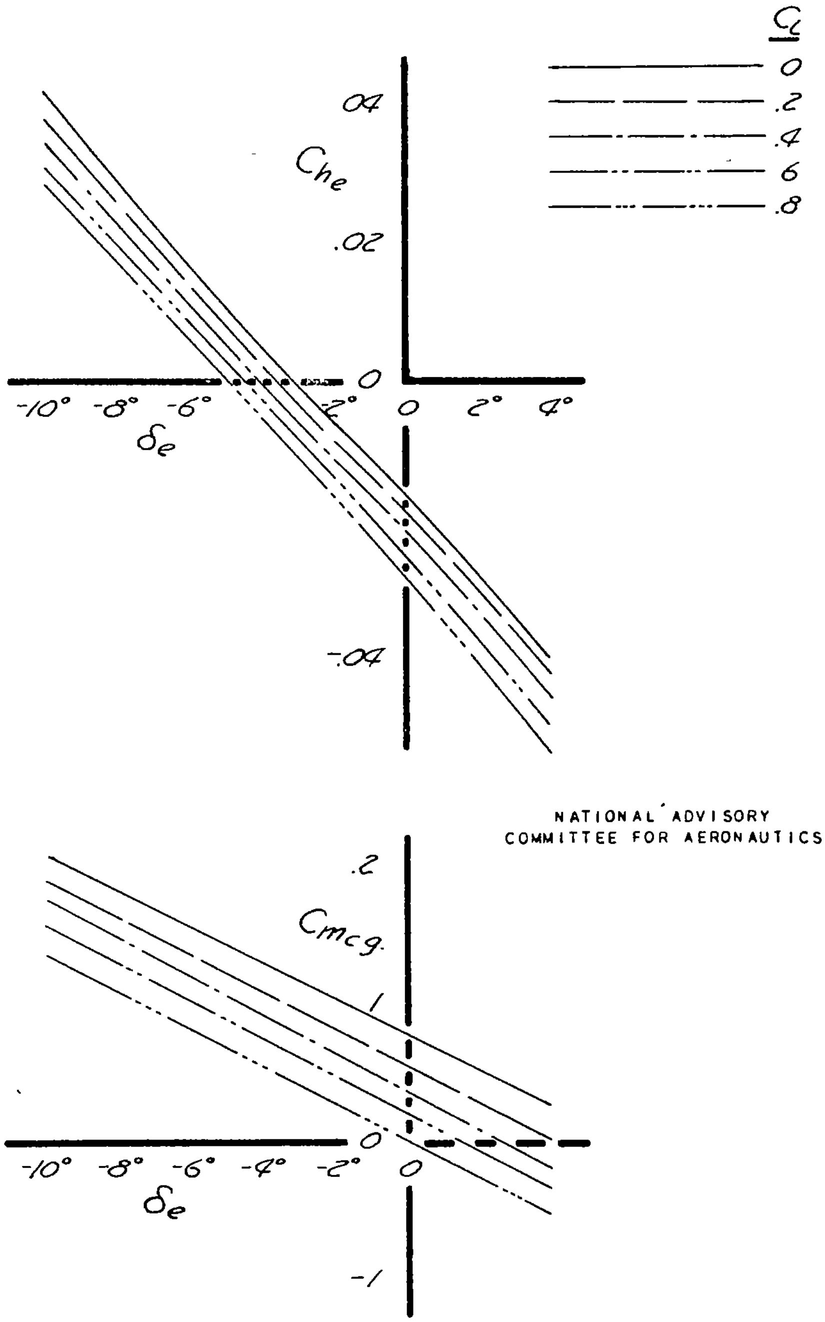

(a) M = 0.20

FIGURE 18.- ELEVATOR CHARACTERISTICS WITH THE 1.2-BY 12-INCH FLAPS WITH 0.4-INCH GAP DEFLECTED 45°

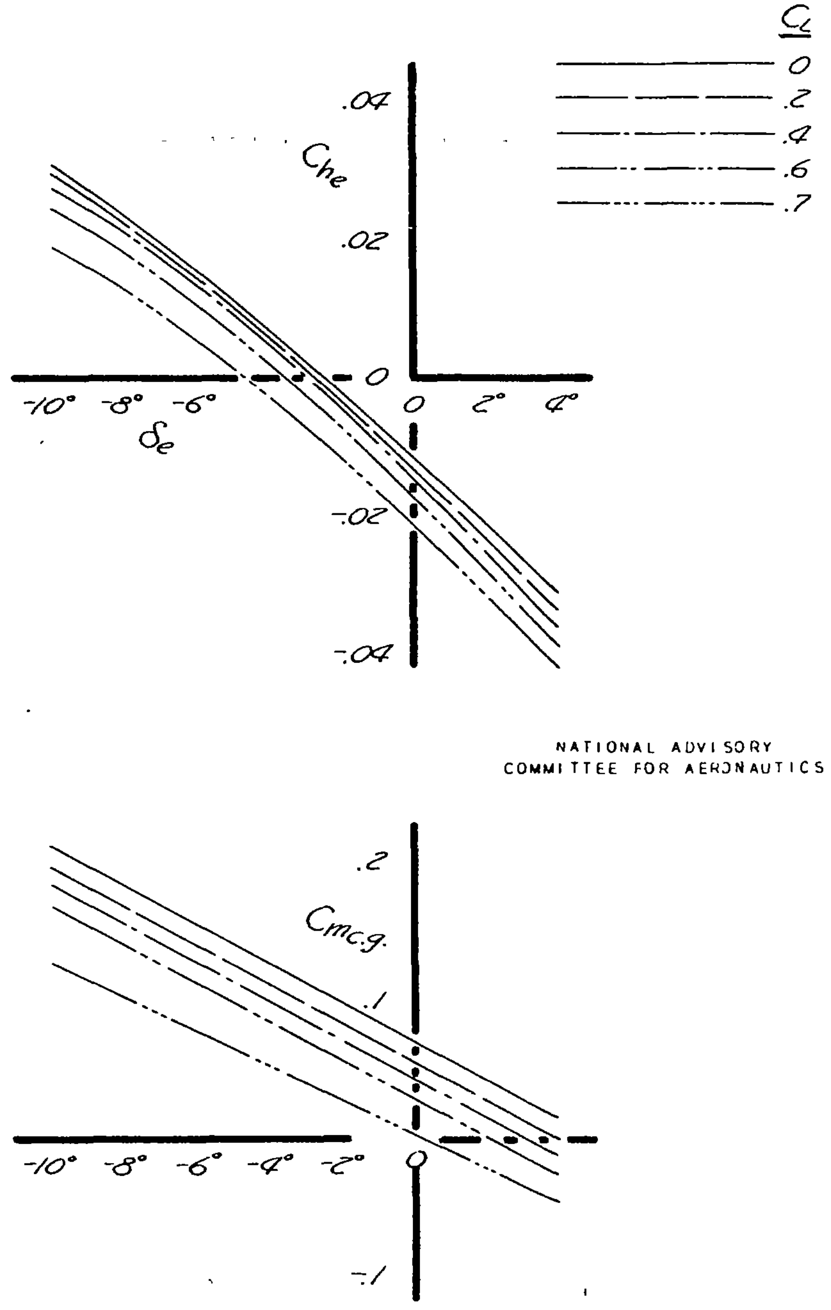

NATIONAL ADVISORY
COMMITTEE FOR AERONAUTICS

(b) M = 0.60

FIGURE 18.- (CONTINUED) 1.2-BY 12-INCH FLAPS WITH 0.4-INCH GAP DEFLECTED 45°

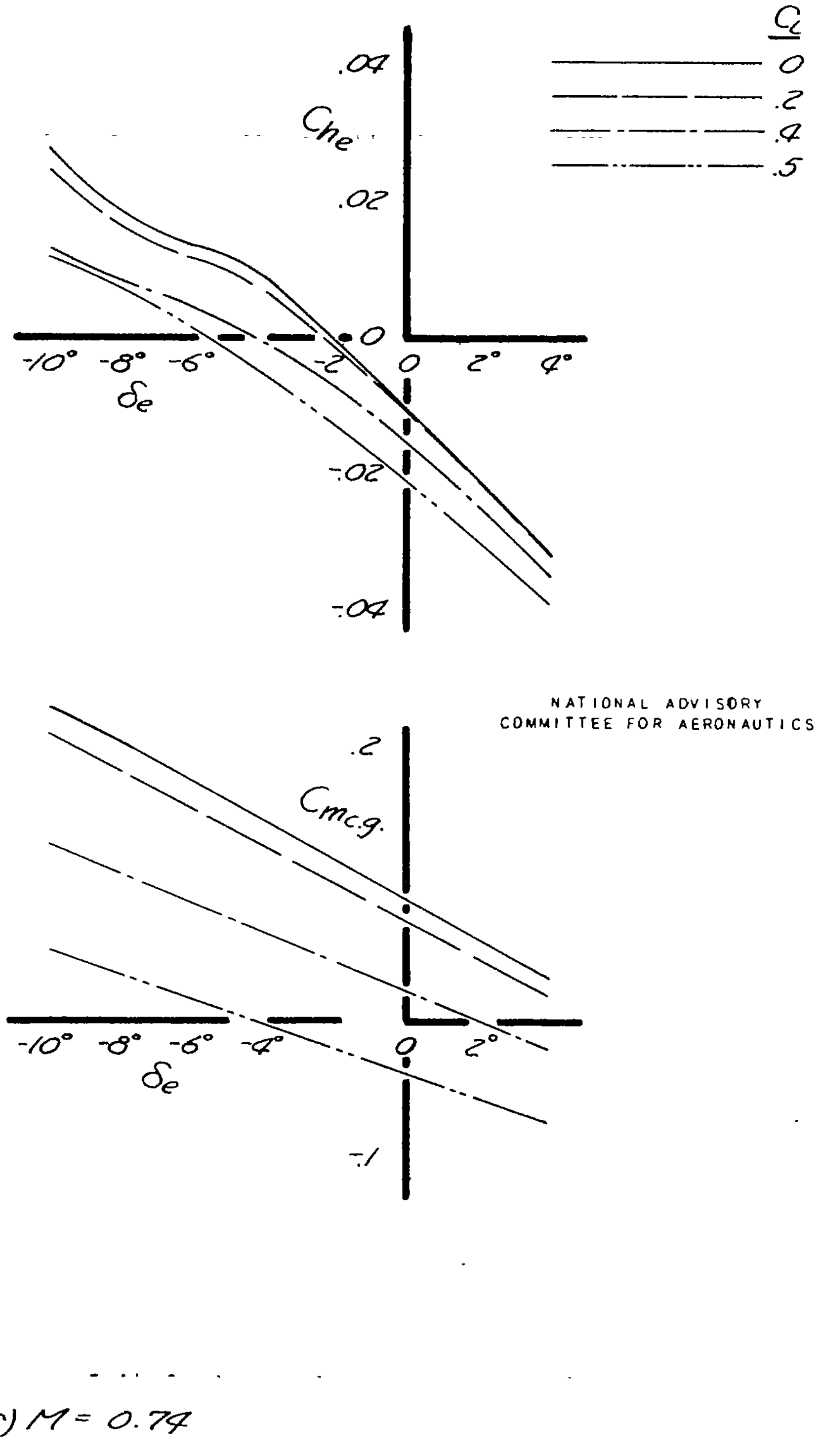

(c) $M = 0.74$

FIGURE 18.– (CONTINUED) 1.2-BY 12-INCH FLAPS WITH 0.4-INCH GAP DEFLECTED 45°

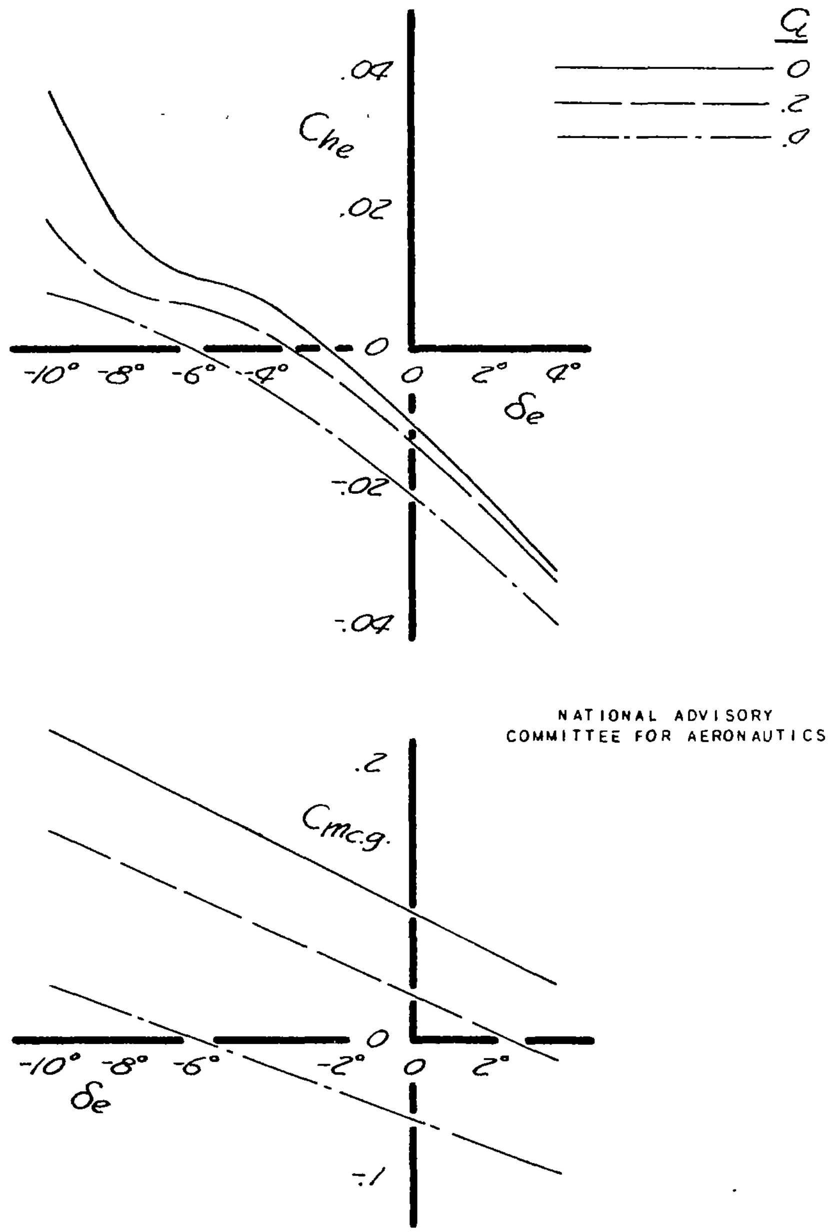

(d) M=0.79

FIGURE 18.– (CONTINUED) 1.2-BY 12-INCH FLAPS WITH 0.4-INCH GAP DEFLECTED 45°

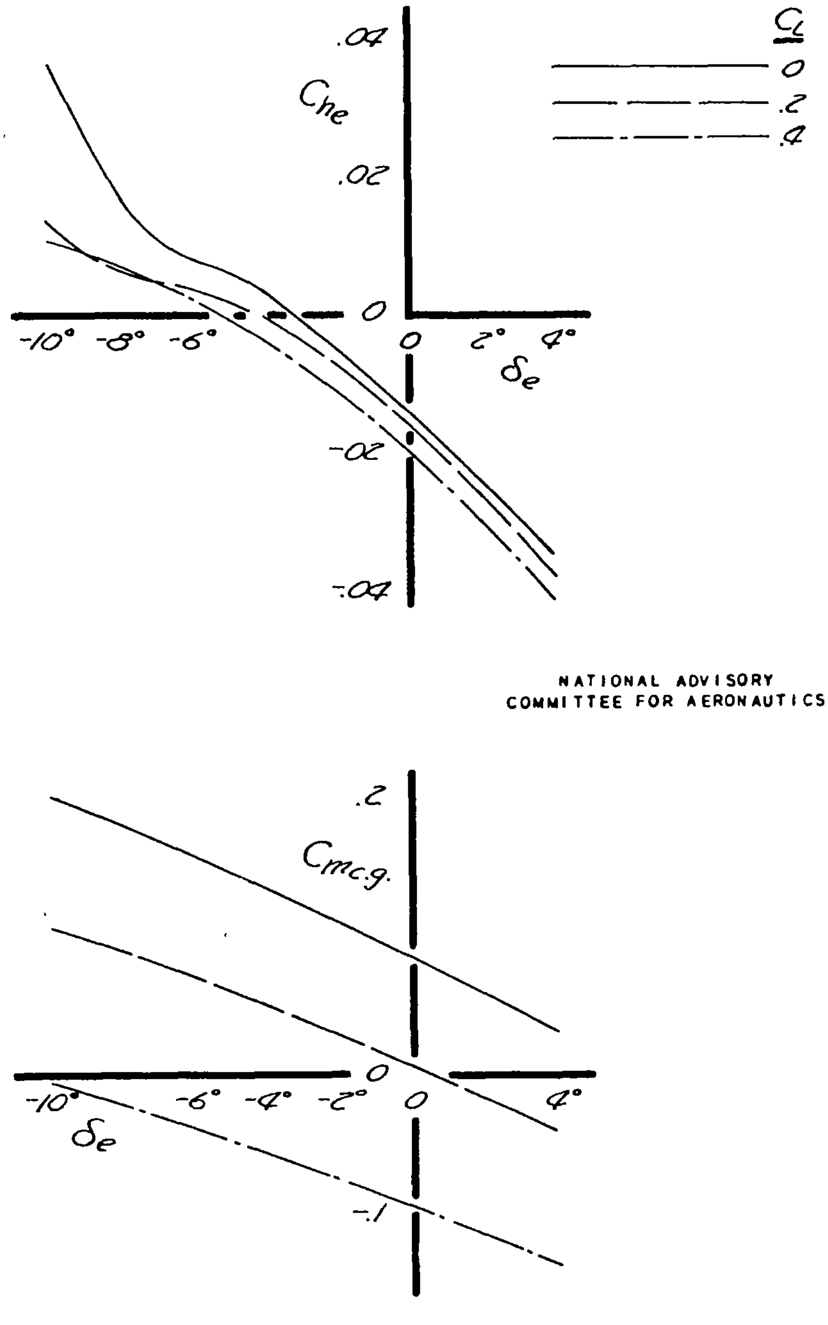

(e) M = 0.815

FIGURE 18.– (CONCLUDED) 1.2-BY 12-INCH FLAPS WITH 0.4-INCH GAP DEFLECTED 45°

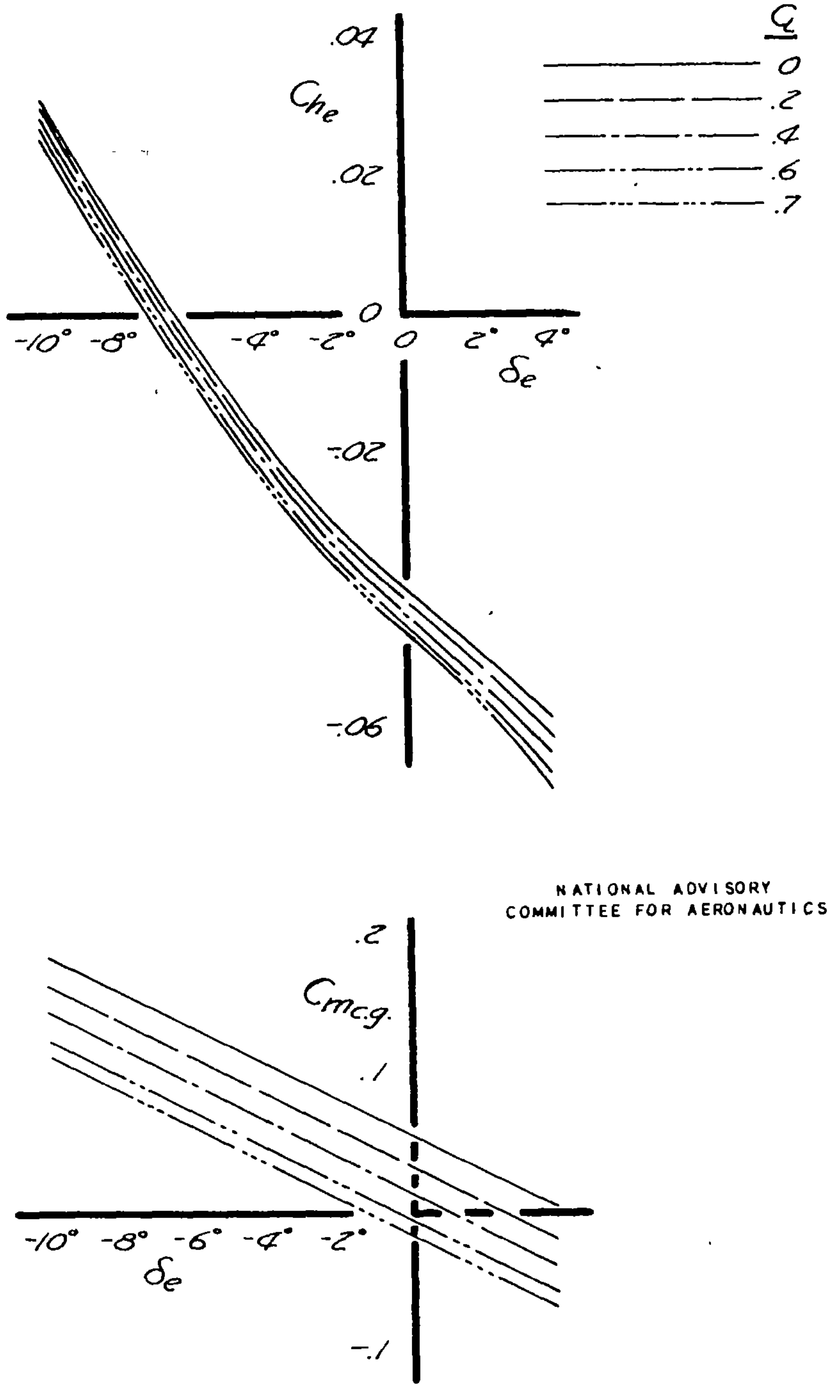

NATIONAL ADVISORY COMMITTEE FOR AERONAUTICS

(a) $M = 0.20$

FIGURE 19.- ELEVATOR CHARACTERISTICS WITH THE 1.2-BY 12-INCH FLAPS HINGED AT FLAP TRAILING EDGE AND DEFLECTED 30°

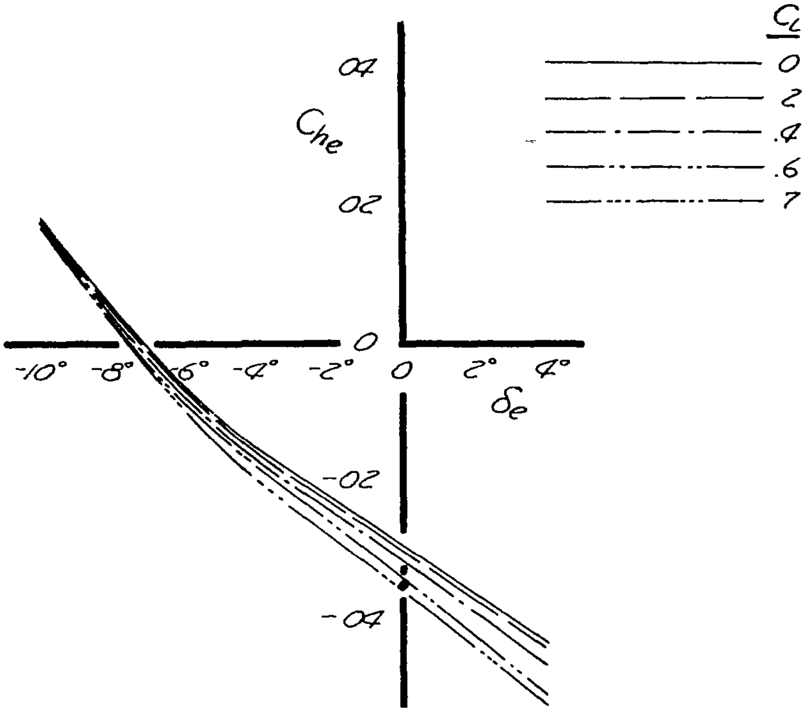

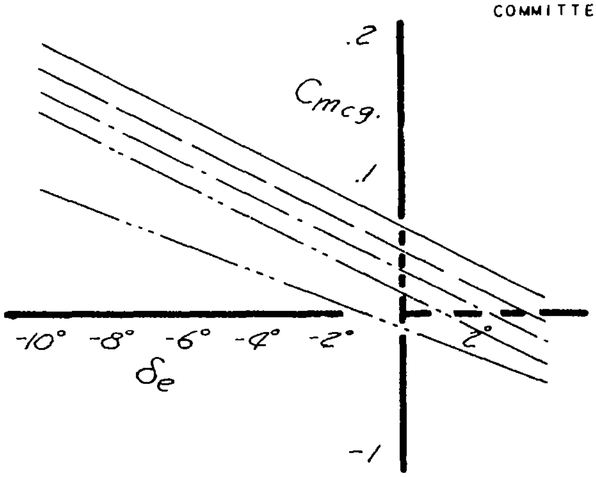

(b) M = 0.60

FIGURE 19.- (CONTINUED) 1.2-BY 12-INCH FLAPS HINGED AT FLAP TRAILING EDGE AND DEFLECTED 30°

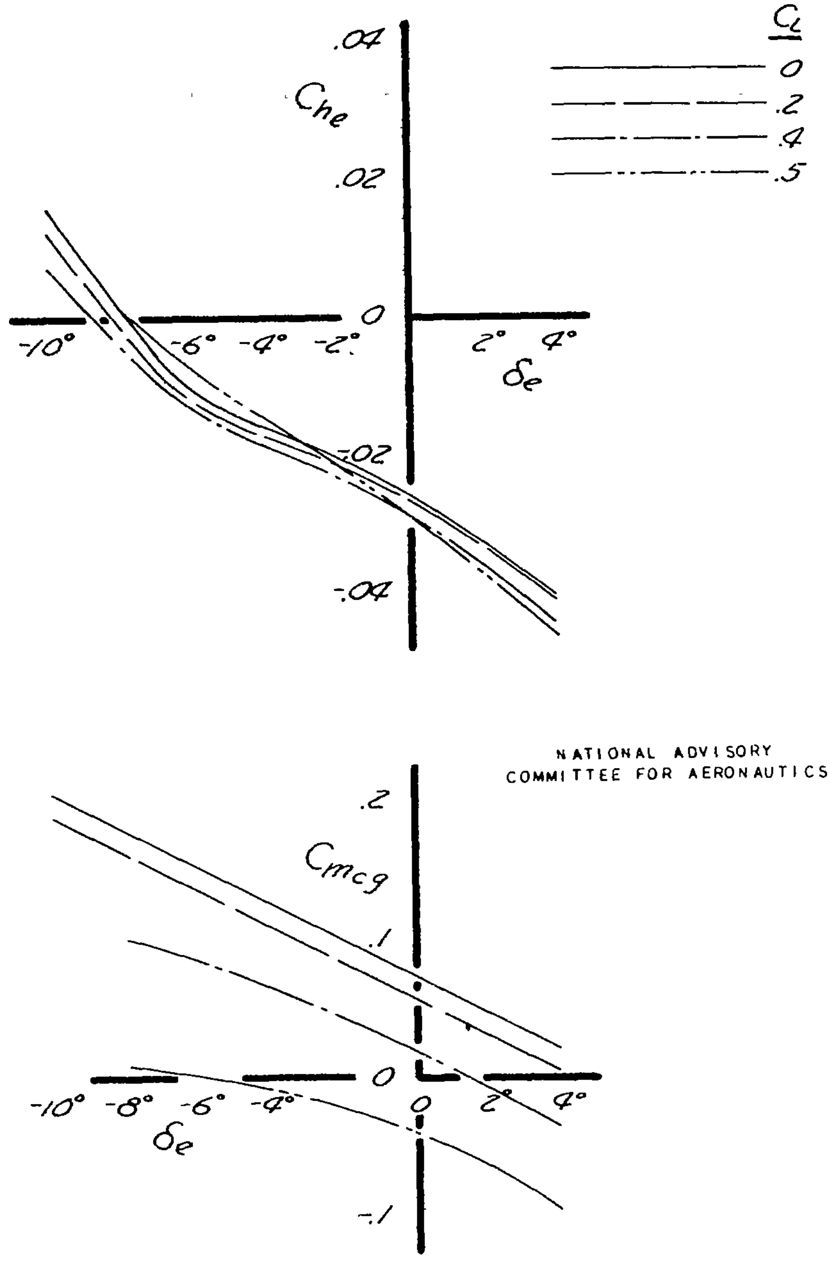

NATIONAL ADVISORY
COMMITTEE FOR AERONAUTICS

(c) M = 0.74

FIGURE 19.-(CONTINUED) 1.2-BY 12-INCH FLAPS HINGED AT FLAP TRAILING EDGE AND DEFLECTED 30°

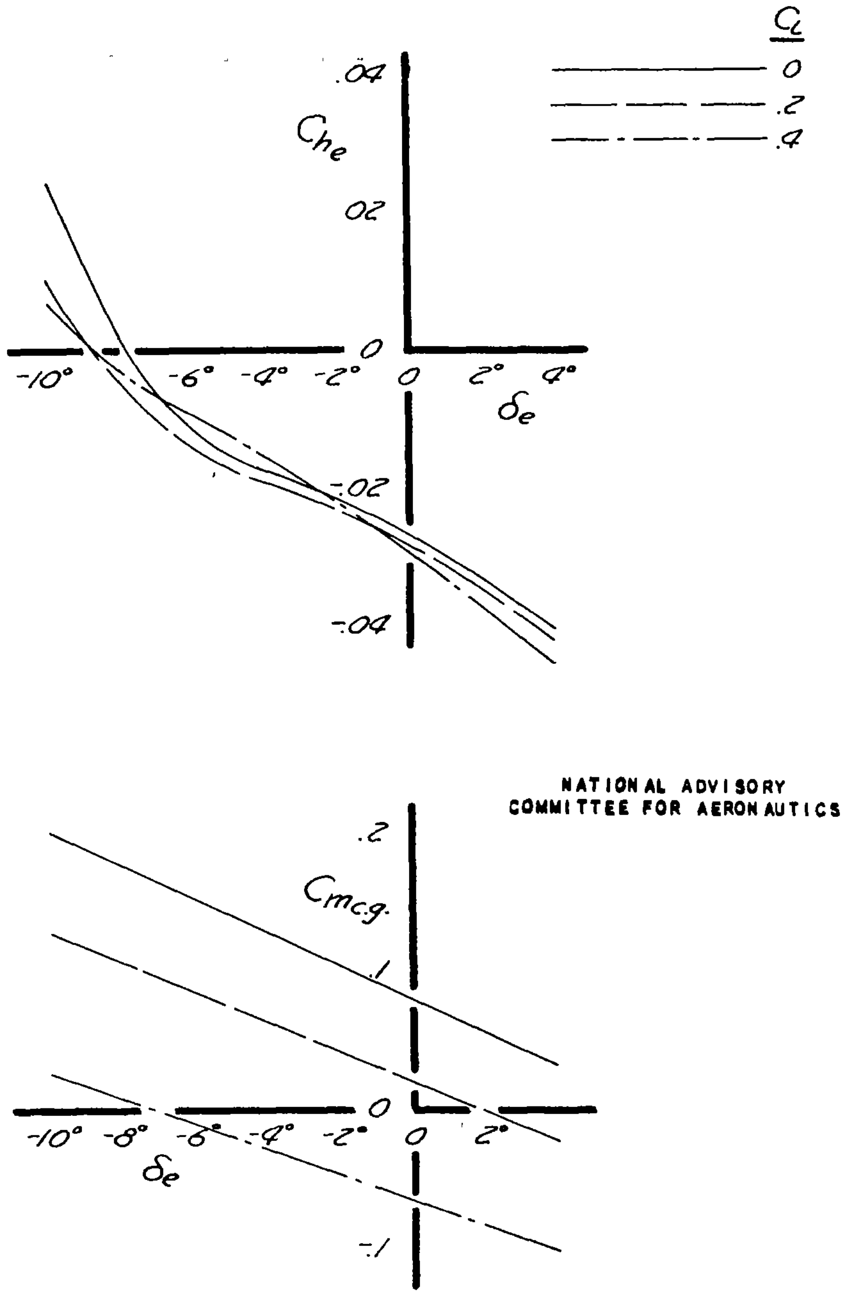

(d) M = 0.79

FIGURE 19.- (CONTINUED) 1.2-BY 12-INCH FLAPS HINGED AT FLAP TRAILING EDGE AND DEFLECTED 30°

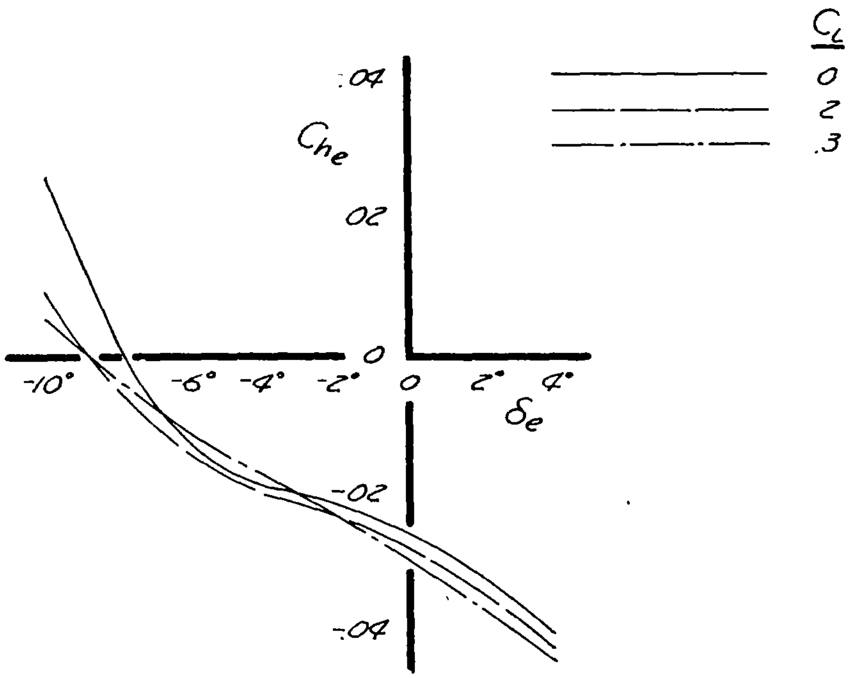

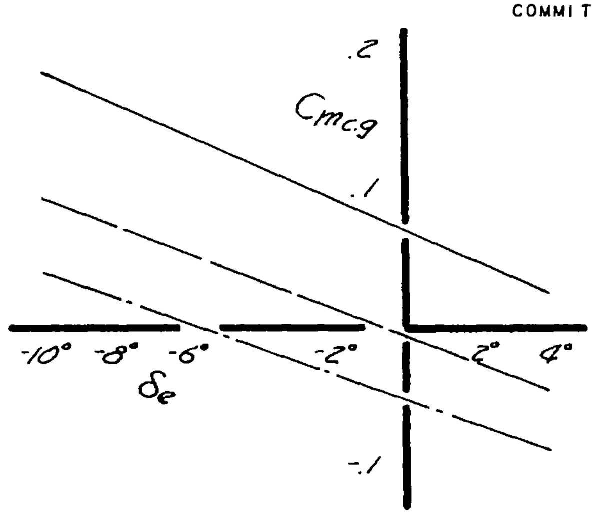

(e) $M = 0.815$

FIGURE 19.-(CONCLUDED) 12-BY 12-INCH FLAPS HINGED AT FLAP TRAILING EDGE AND DEFLECTED 30°

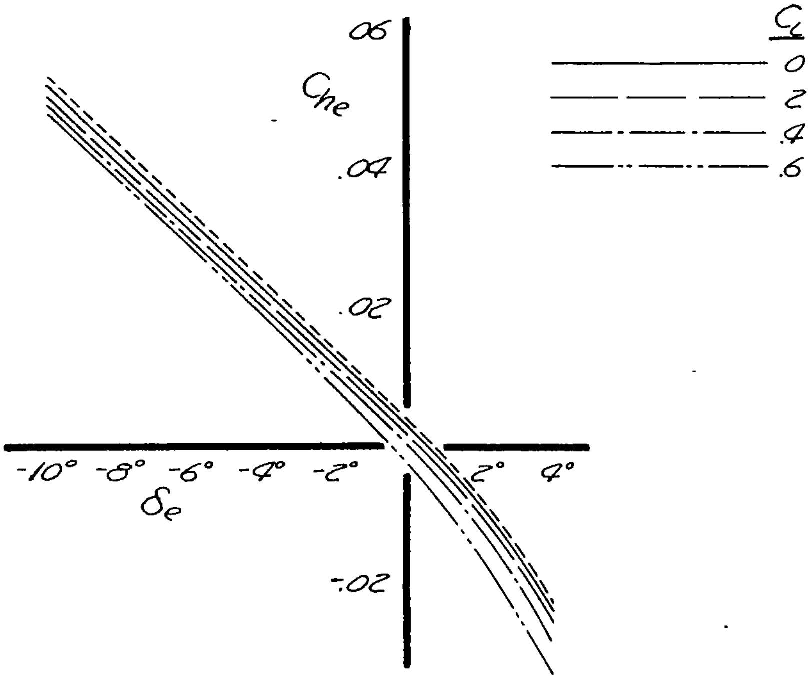

NATIONAL ADVISORY COMMITTEE FOR AERONAUTICS

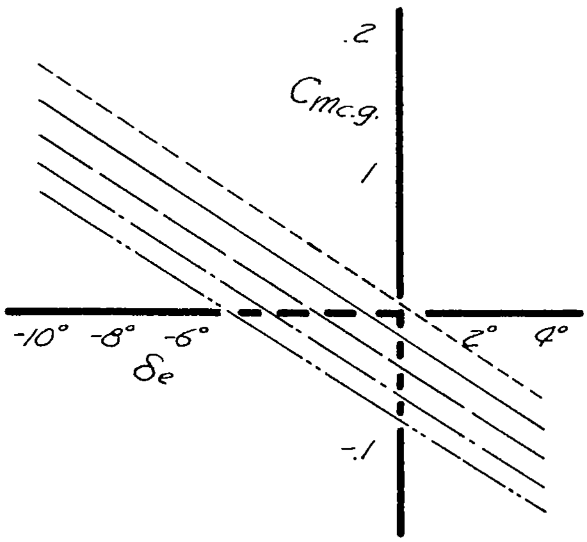

(a) M = 0.20

FIGURE 20.- ELEVATOR CHARACTERISTICS WITH THE 0.6-BY 12-INCH FLAPS DEFLECTED 7.5°

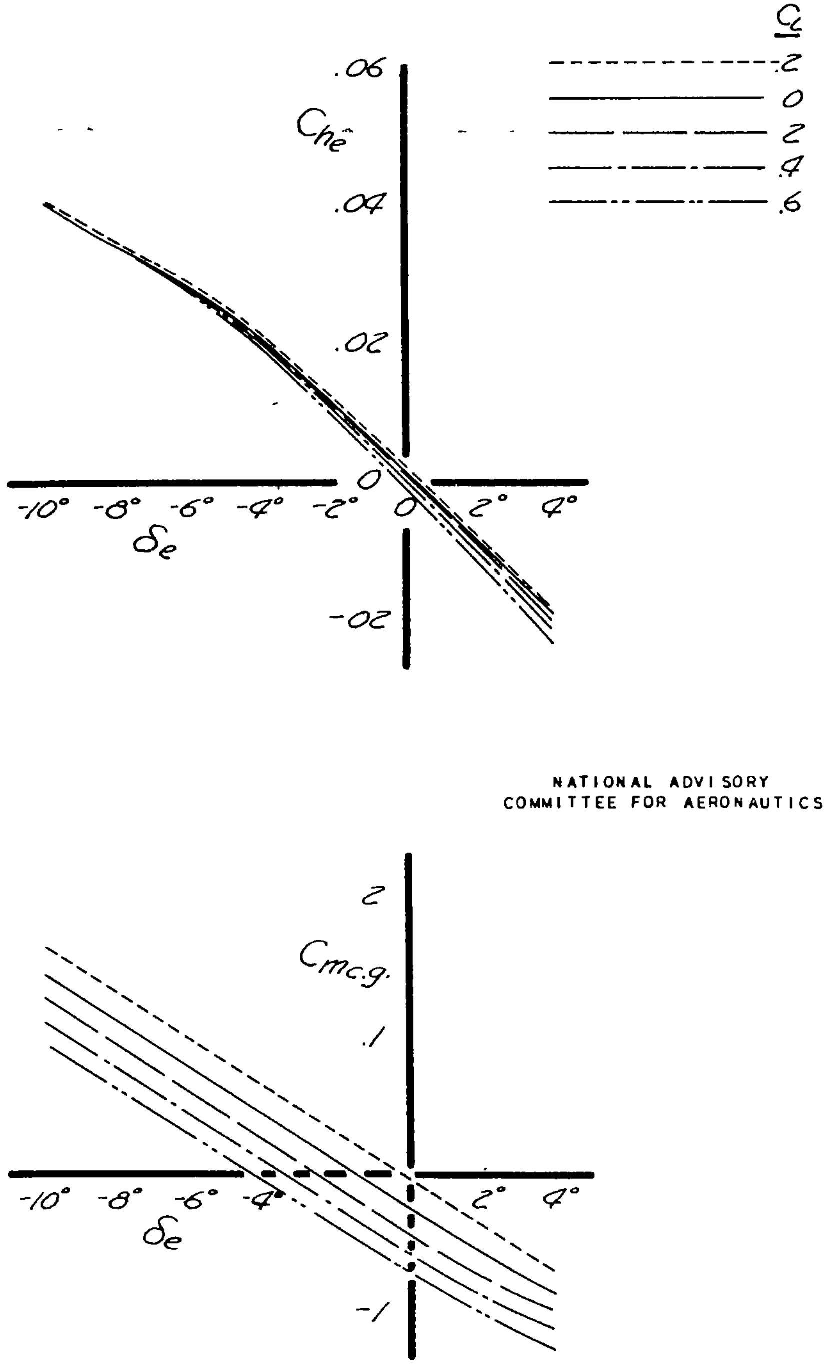

(b) $M = 0.60$

FIGURE 20.- (CONTINUED) 0.6-BY 12-INCH FLAPS DEFLECTED 7.5°

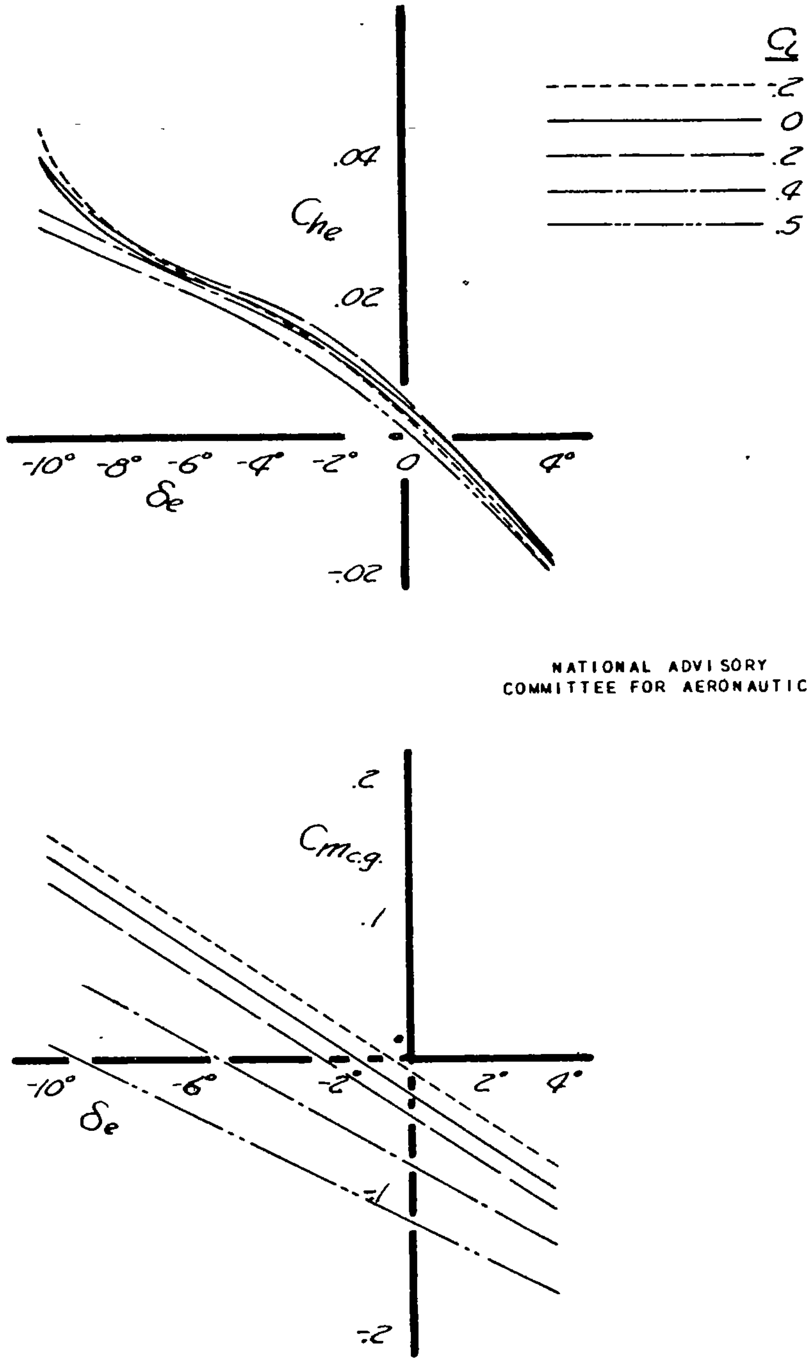

NATIONAL ADVISORY
COMMITTEE FOR AERONAUTICS

(c) $M = 0.74$

FIGURE 20.- (CONTINUED) 0.6-BY 12-INCH FLAPS DEFLECTED 7.5°

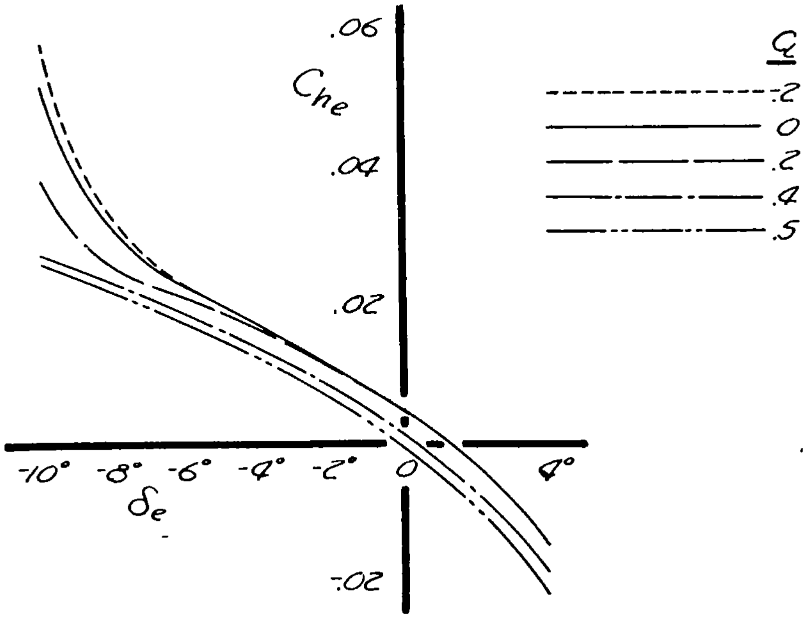

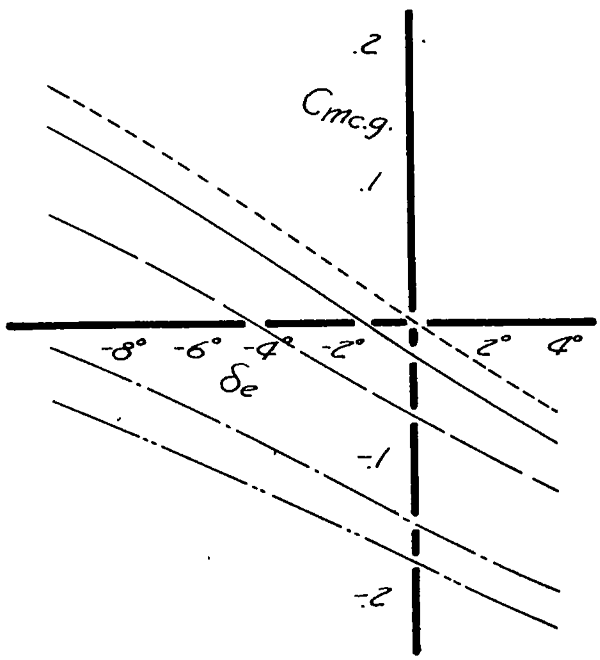

(d) M = 0.79

FIGURE 20.- (CONTINUED) 0.6-BY 12-INCH FLAPS DEFLECTED 7.5°

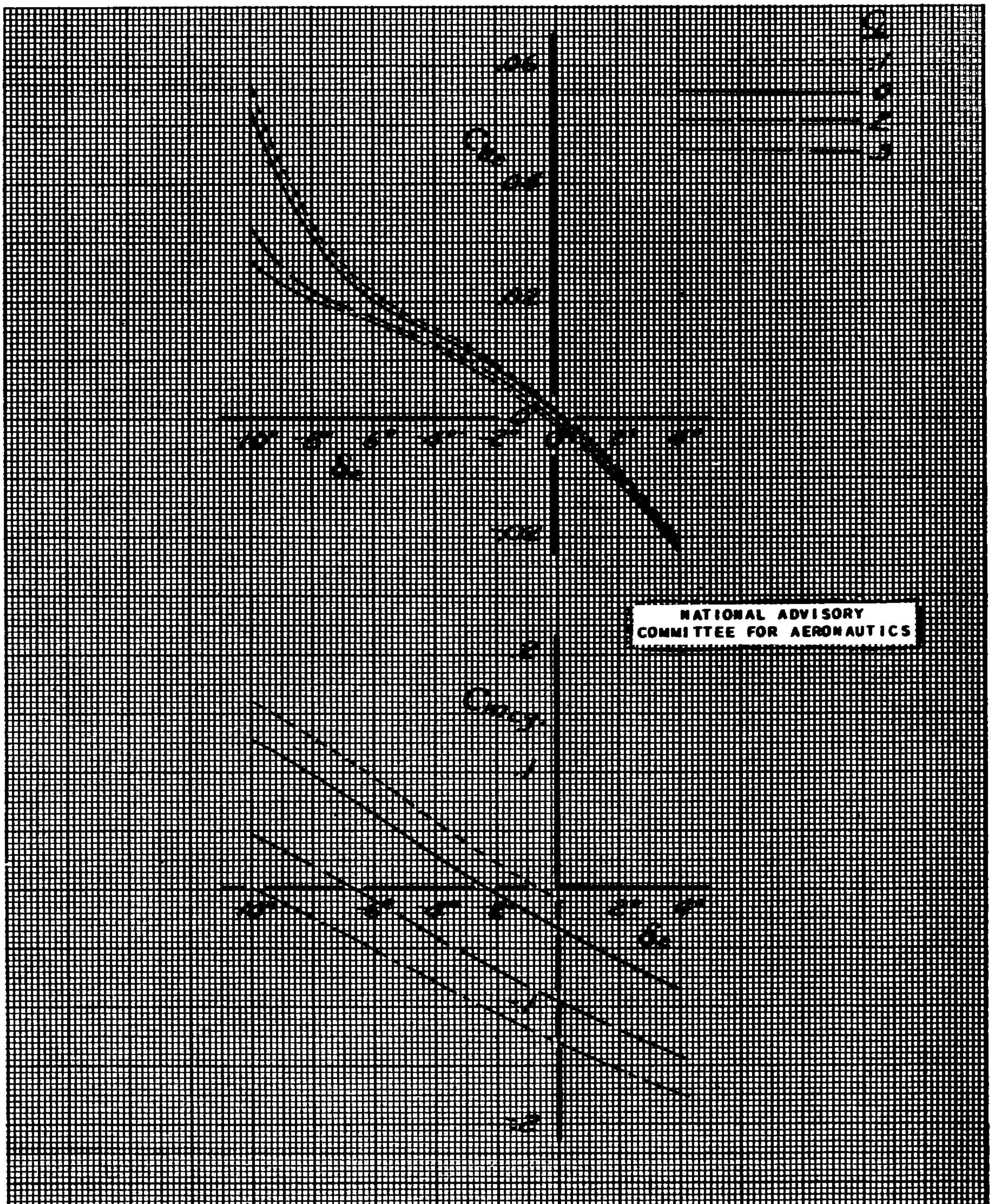

(e) M = 0.815

FIGURE 20.- (CONCLUDED) 0.6 BY 12-INCH FLAPS DEFLECTED

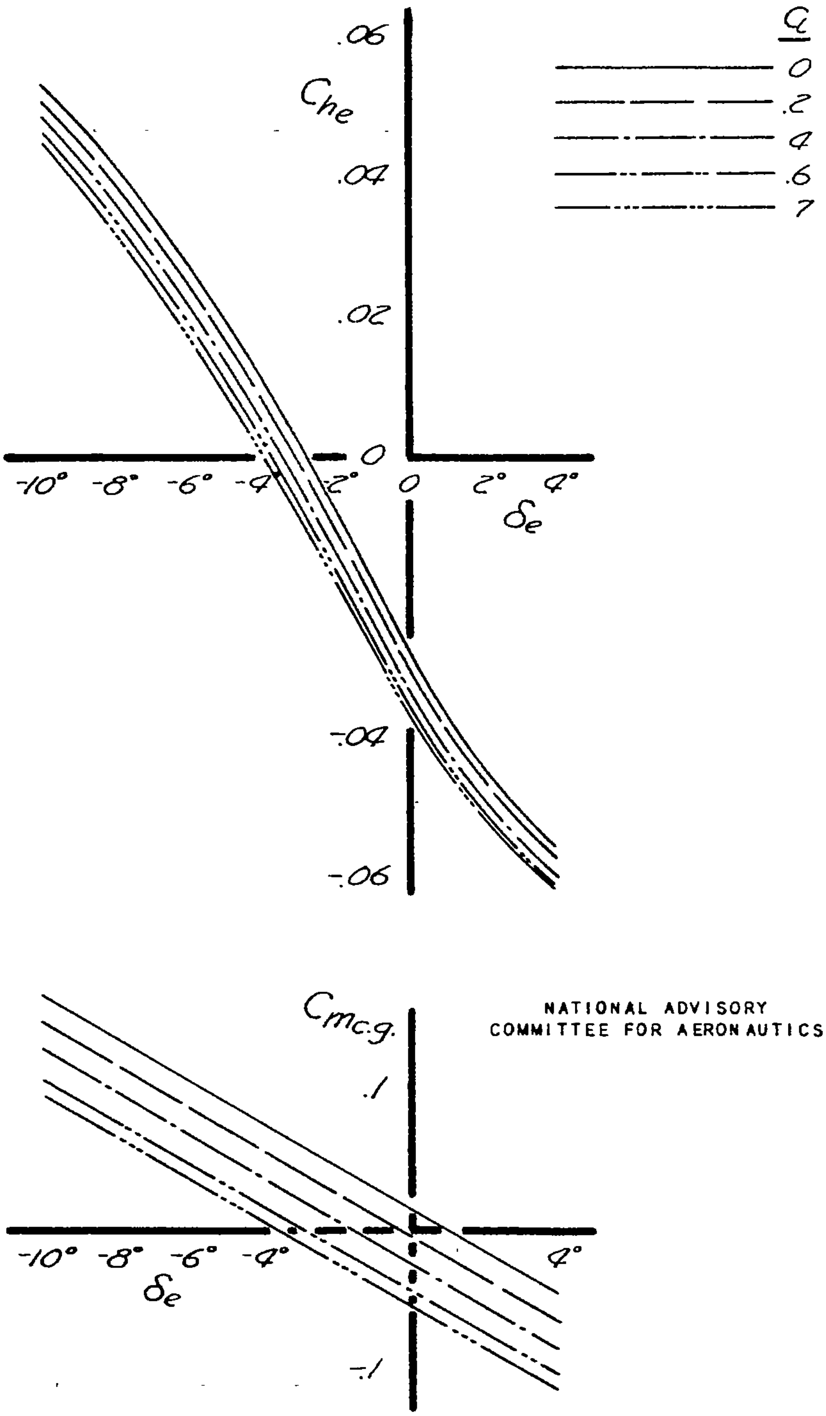

(a) M = 0.20

FIGURE 21.- ELEVATOR CHARACTERISTICS WITH THE 0.6- BY 12-INCH FLAPS DEFLECTED 30°

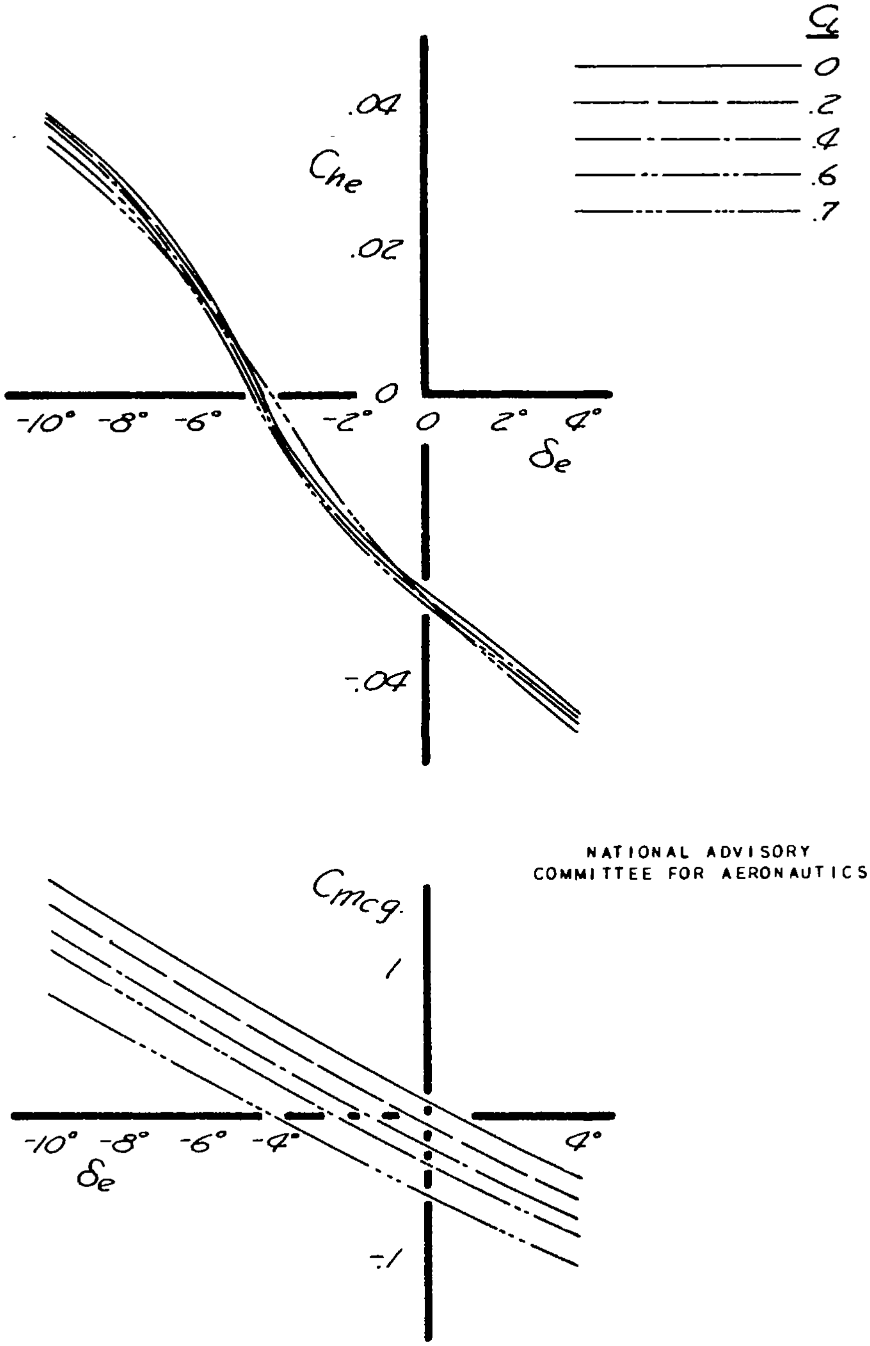

(b) M = 0.60

FIGURE 21. - (CONTINUED) 0.6-BY 12-INCH FLAPS DEFLECTED 30°

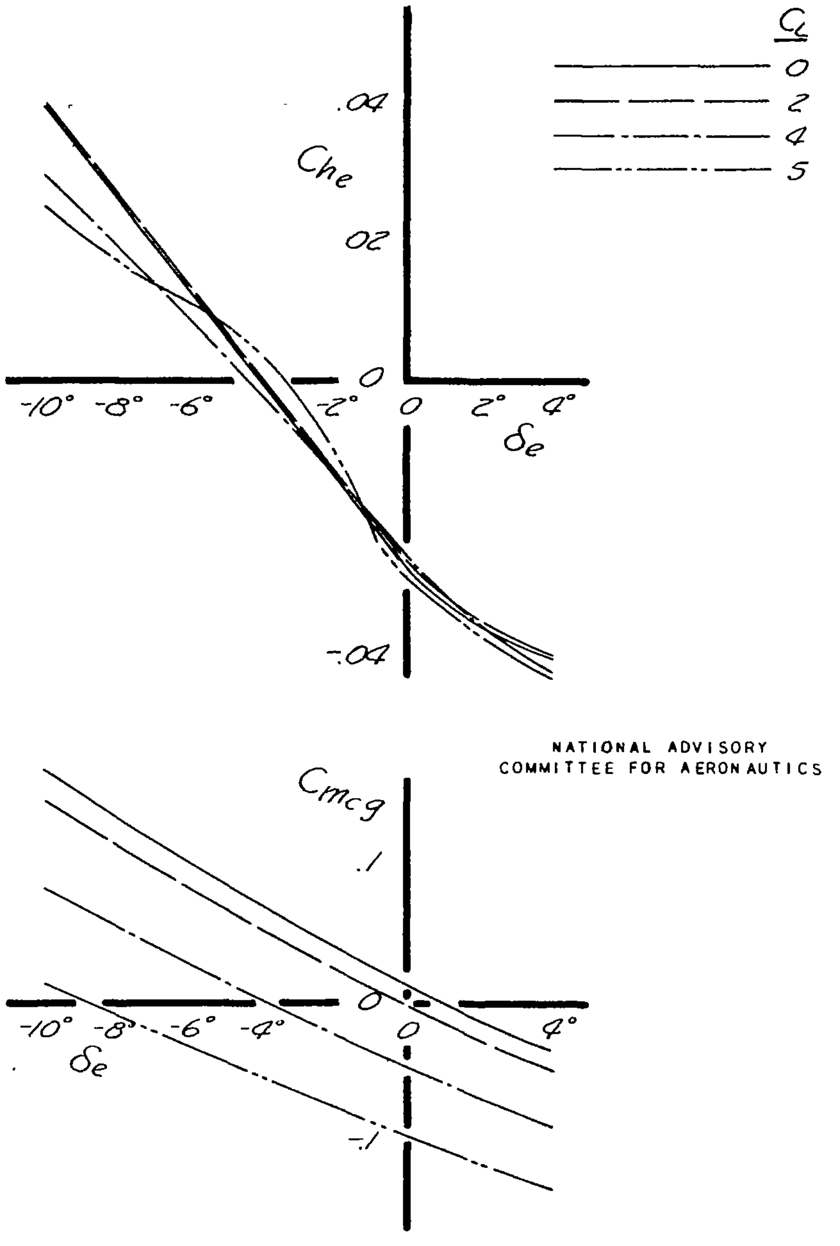

(c) M = 0.74

FIGURE 21.- (CONTINUED) 0.6-BY 12-INCH FLAPS DEFLECTED 30°

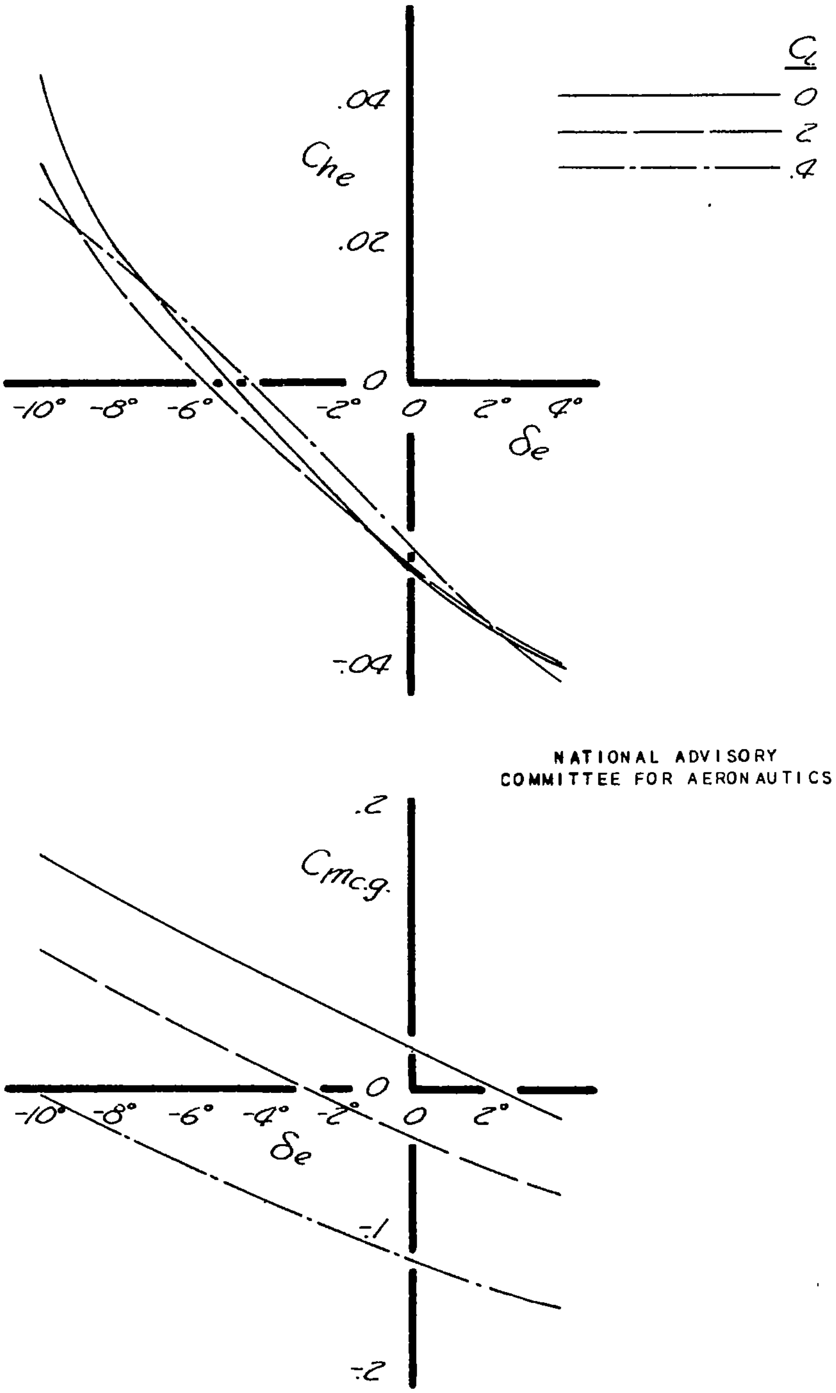

NATIONAL ADVISORY
COMMITTEE FOR AERONAUTICS

(d) M=0.79

FIGURE 21.- (CONTINUED) 0.6-BY 12-INCH FLAPS DEFLECTED 30°

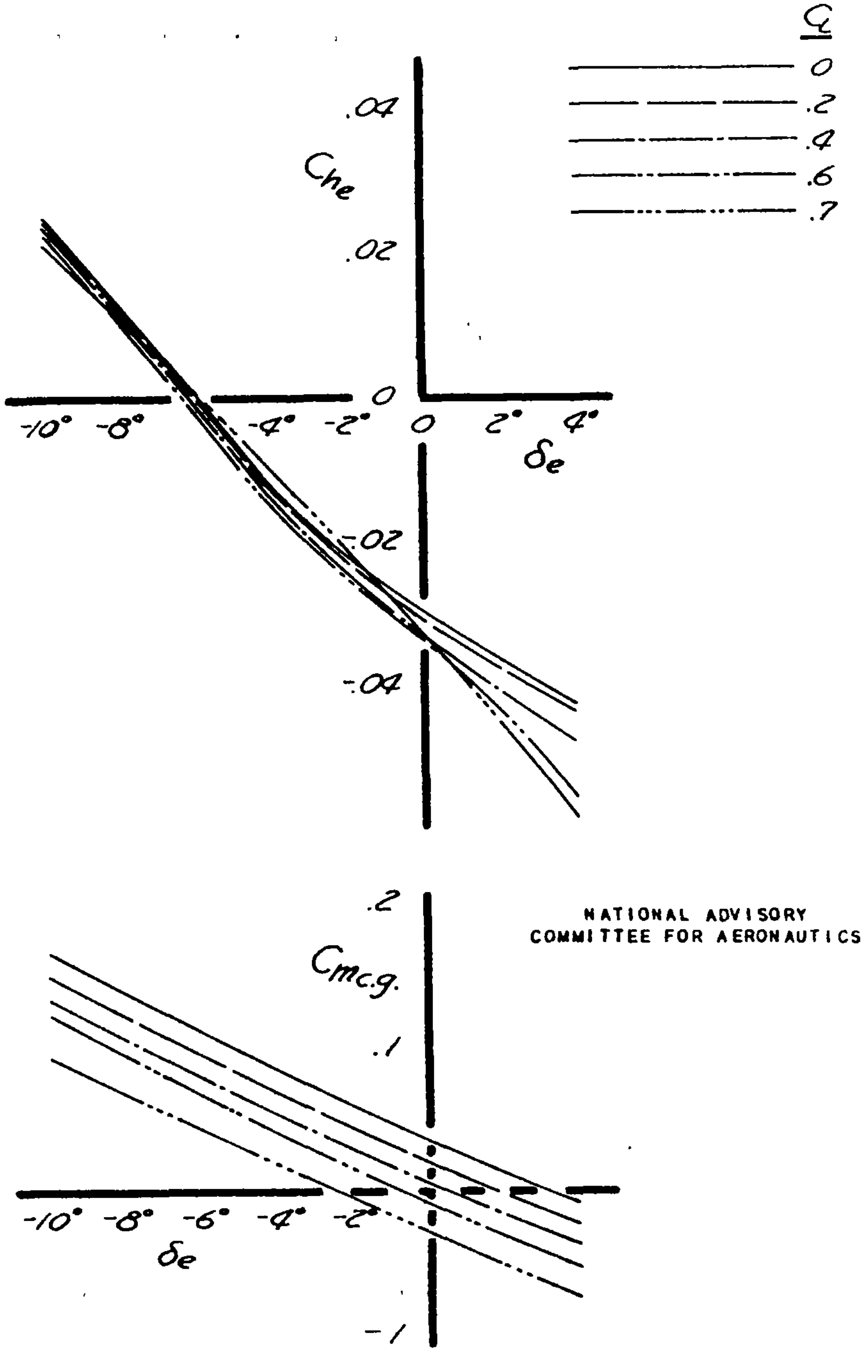

(b) M = 0.60

FIGURE 22.- (CONTINUED) 0.6-BY 12-INCH FLAPS DEFLECTED 45°

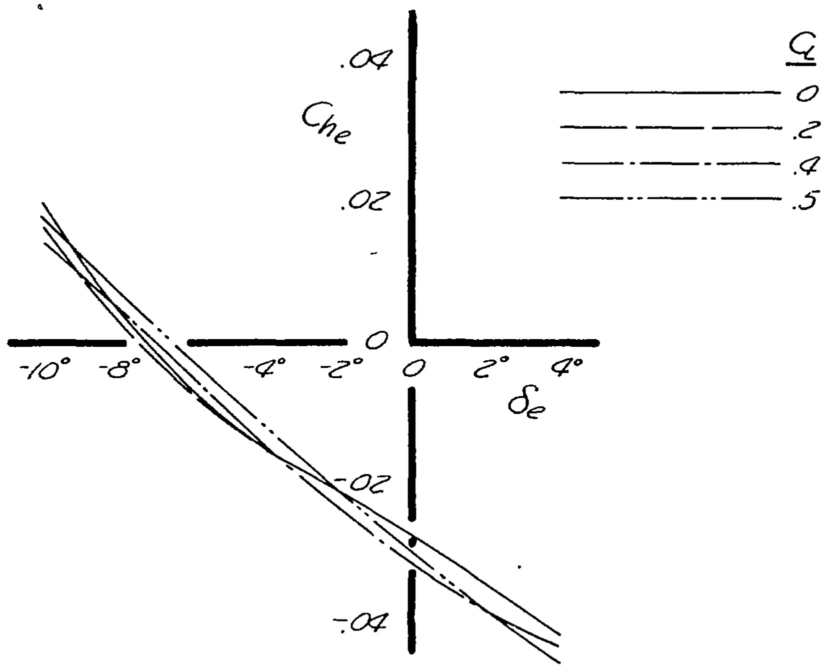

NATIONAL ADVISORY COMMITTEE FOR AERONAUTICS

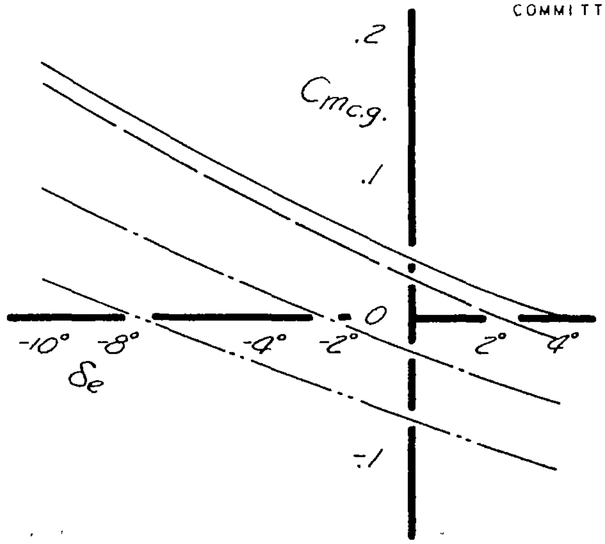

(c) M = 0.74

FIGURE 22.- (CONTINUED) 0.6-BY 12-INCH FLAPS DEFLECTED 45°

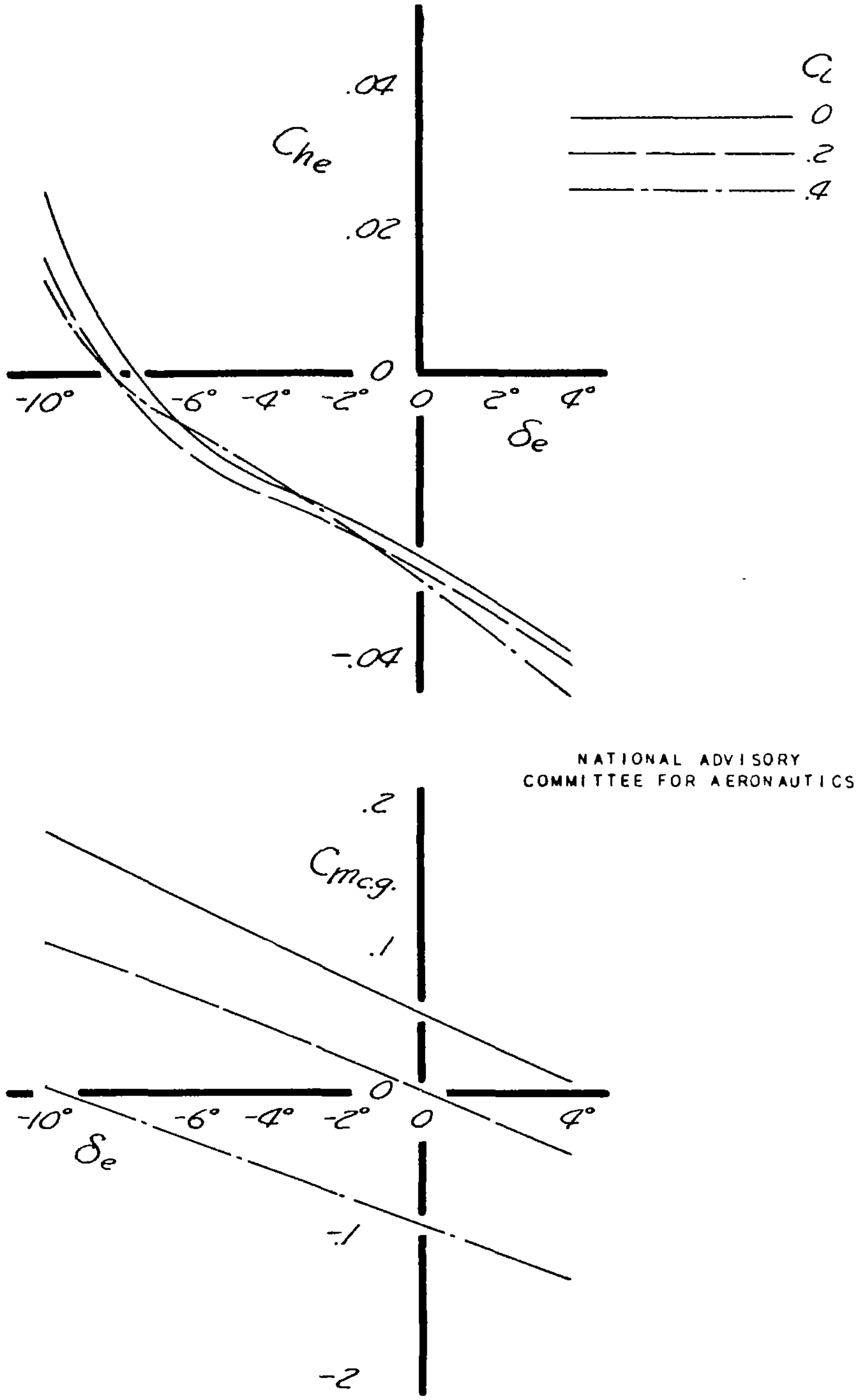

(d) M = 0.79

FIGURE 22.- (CONTINUED) 0.6-BY 12-INCH FLAPS DEFLECTED 45°

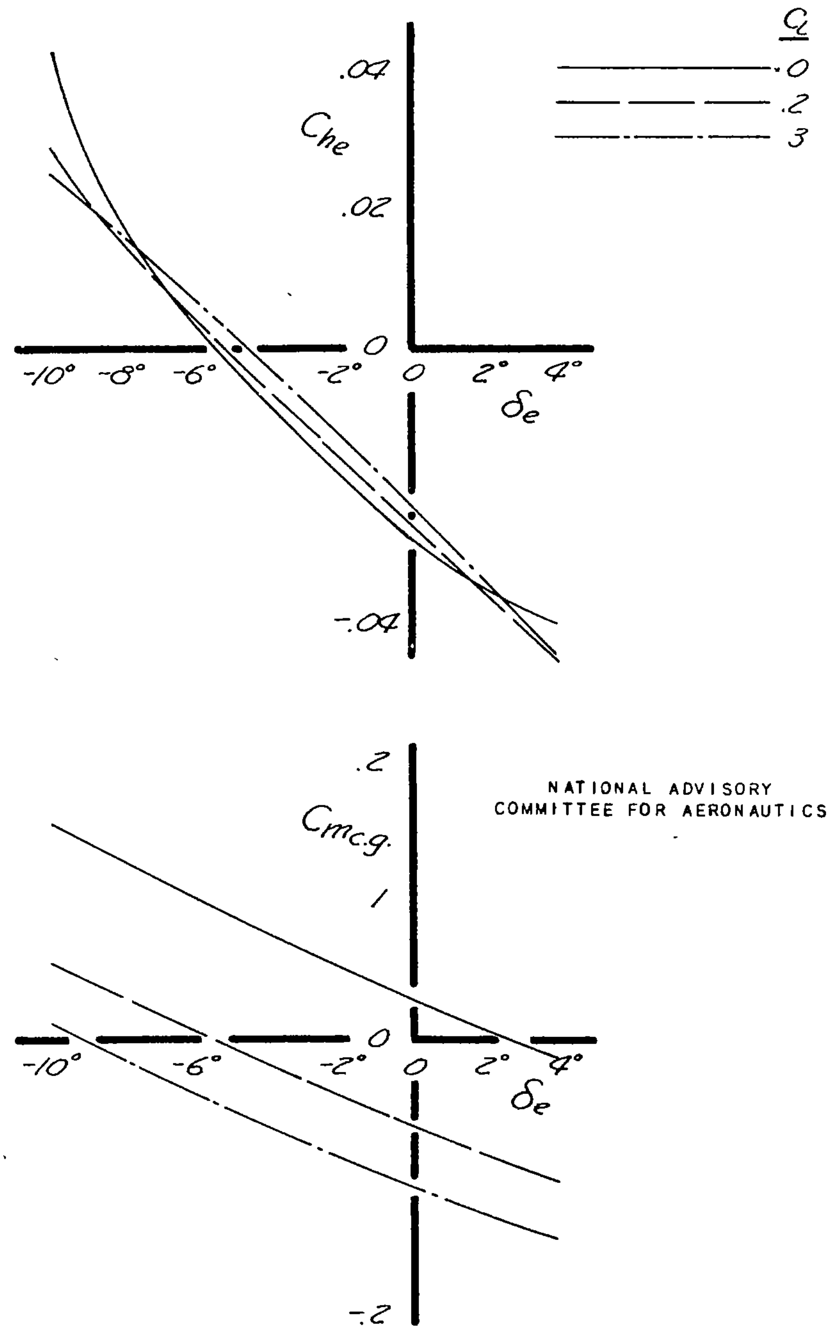

(e) $M = 0.815$

FIGURE 21.- (CONCLUDED) 0.6-BY 12-INCH FLAPS DEFLECTED 30°

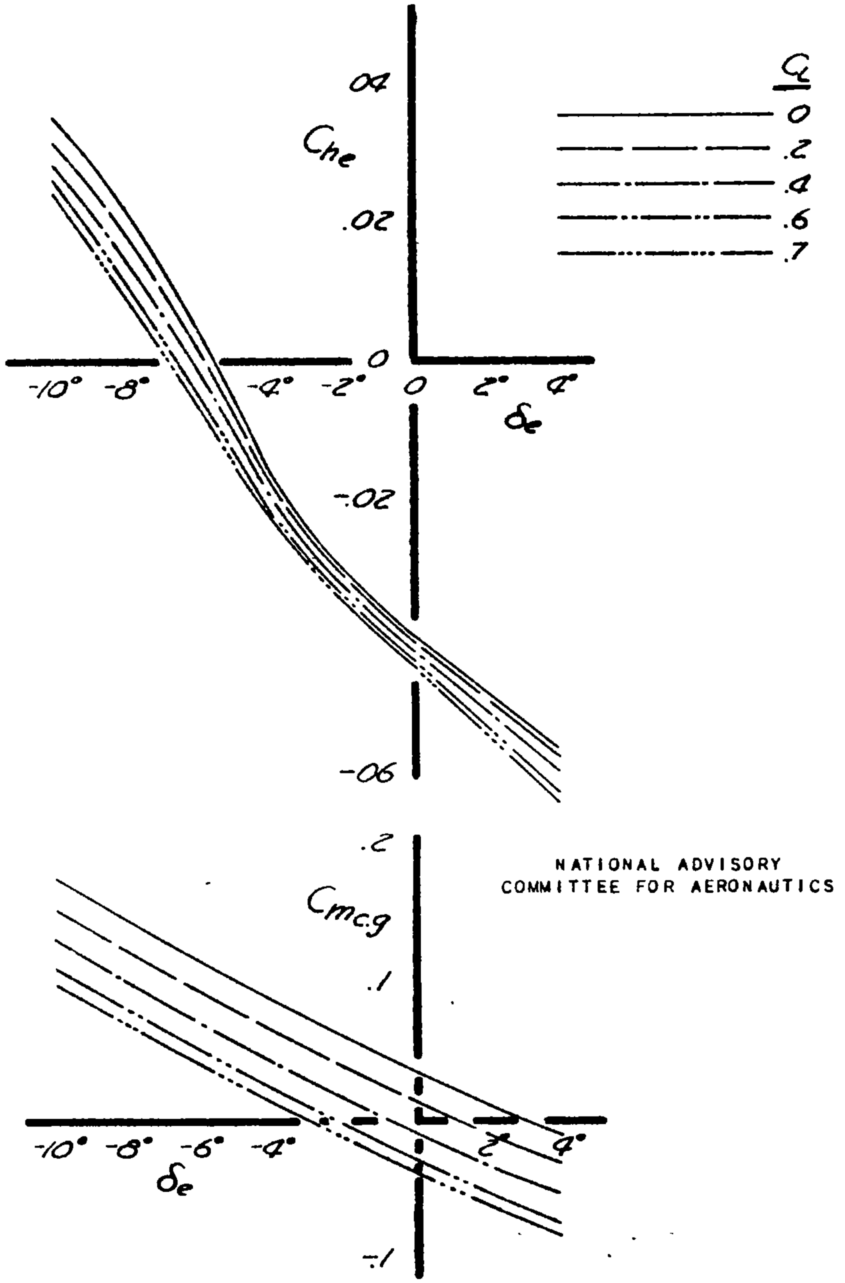

(a) M = 0.20

FIGURE 22.- ELEVATOR CHARACTERISTICS WITH THE 0.6-BY 12-INCH FLAPS DEFLECTED 45°

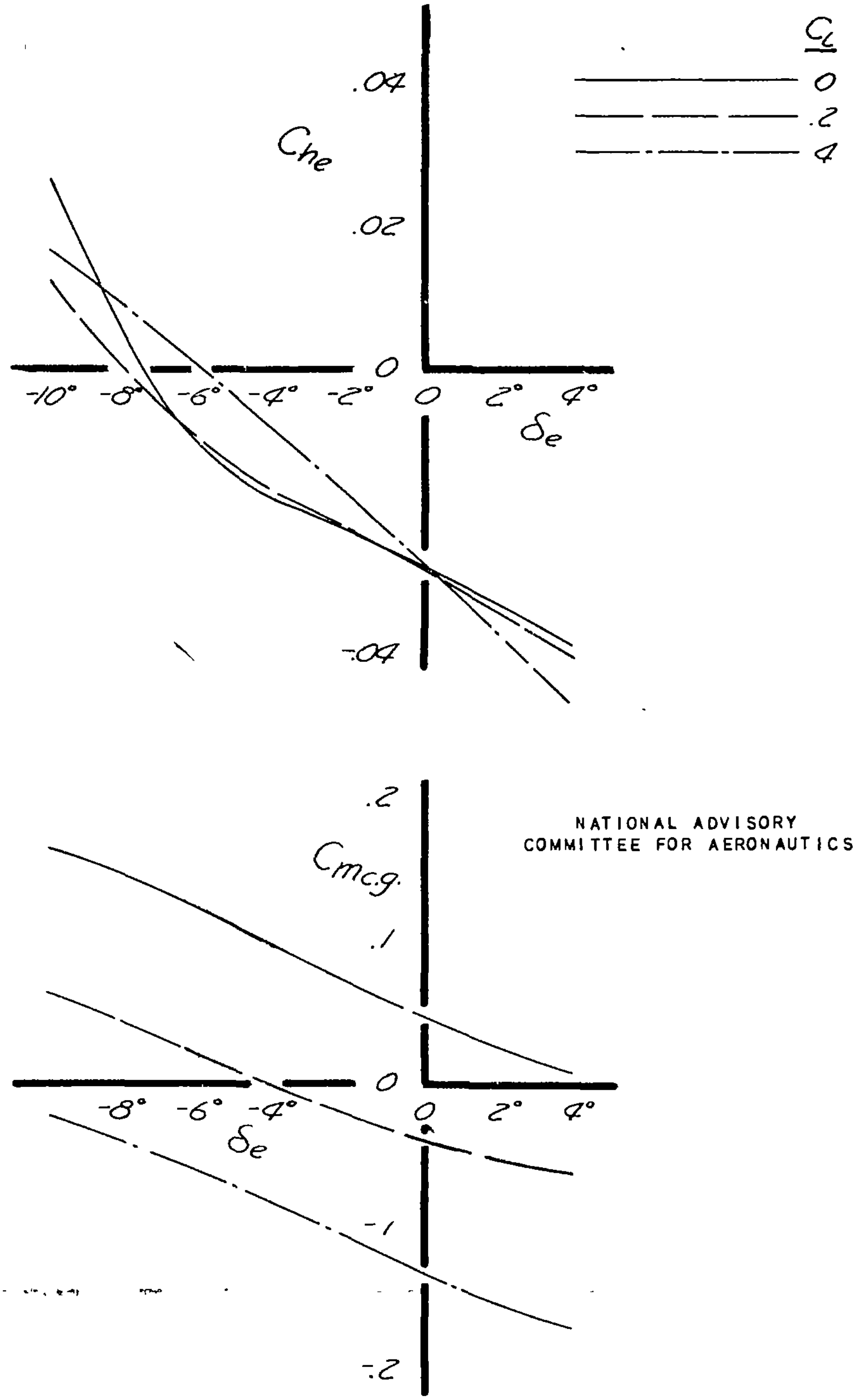

(e) $M = 0.815$

FIGURE 22.-(CONCLUDED) 0.6-BY 12-INCH FLAPS DEFLECTED 45°

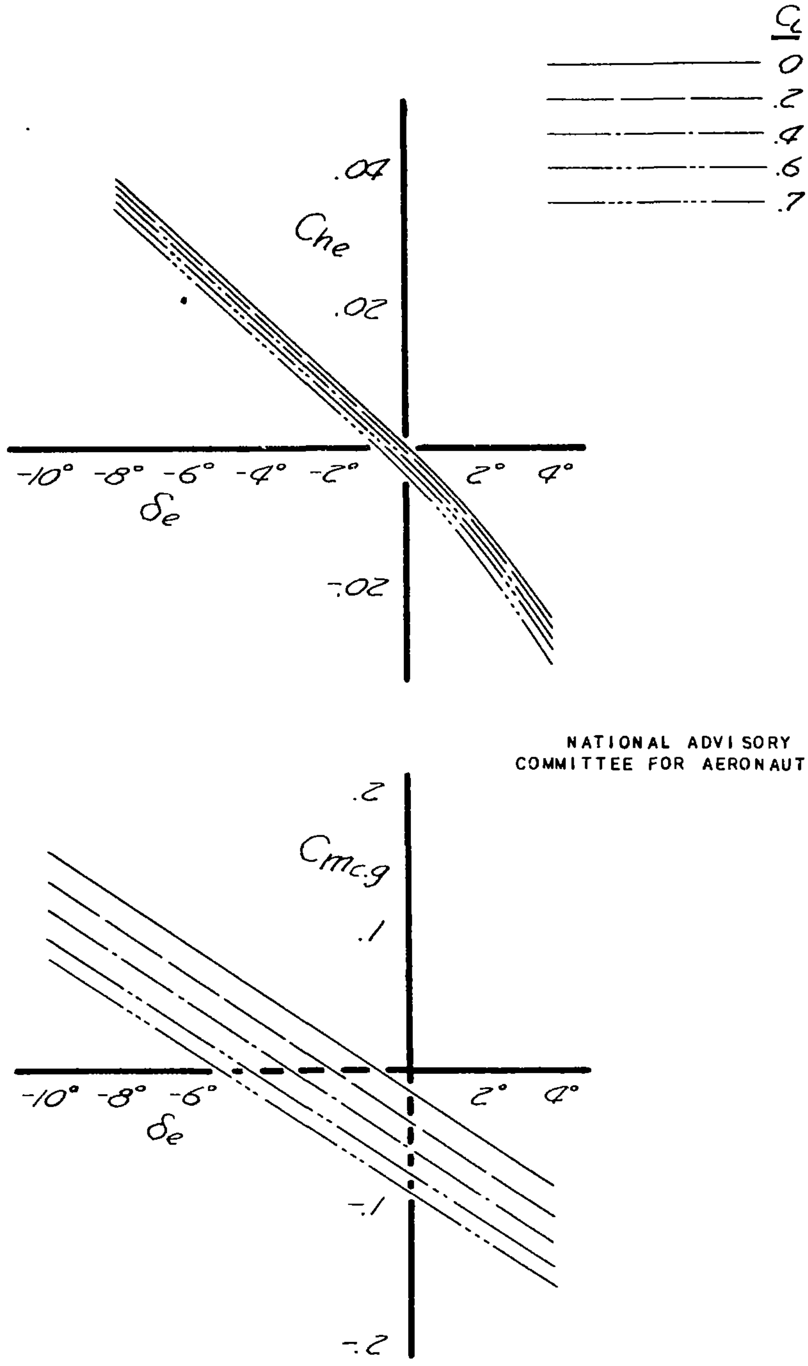

NATIONAL ADVISORY
COMMITTEE FOR AERONAUTICS

(a) M = 0.20

FIGURE 23.- ELEVATOR CHARACTERISTICS WITH THE 0.6-BY 6-INCH FLAPS DEFLECTED 7.5°

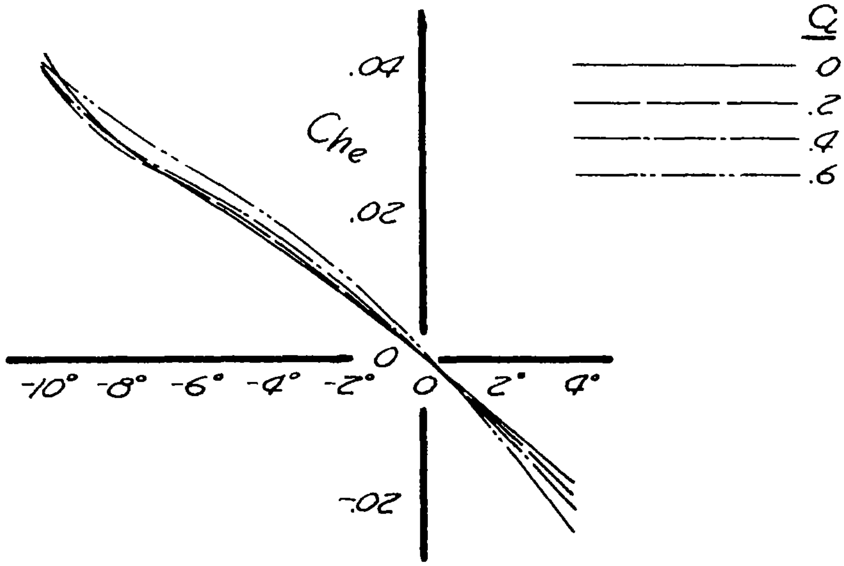

NATIONAL ADVISORY
COMMITTEE FOR AERONAUTICS

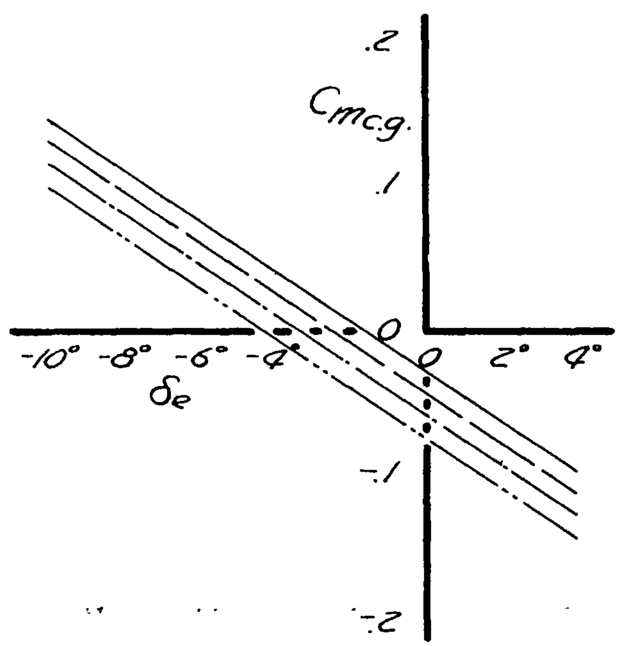

(b) M = 0.60

FIGURE 23.-(CONTINUED) 0.6-BY 6-INCH FLAPS DEFLECTED 7.5°

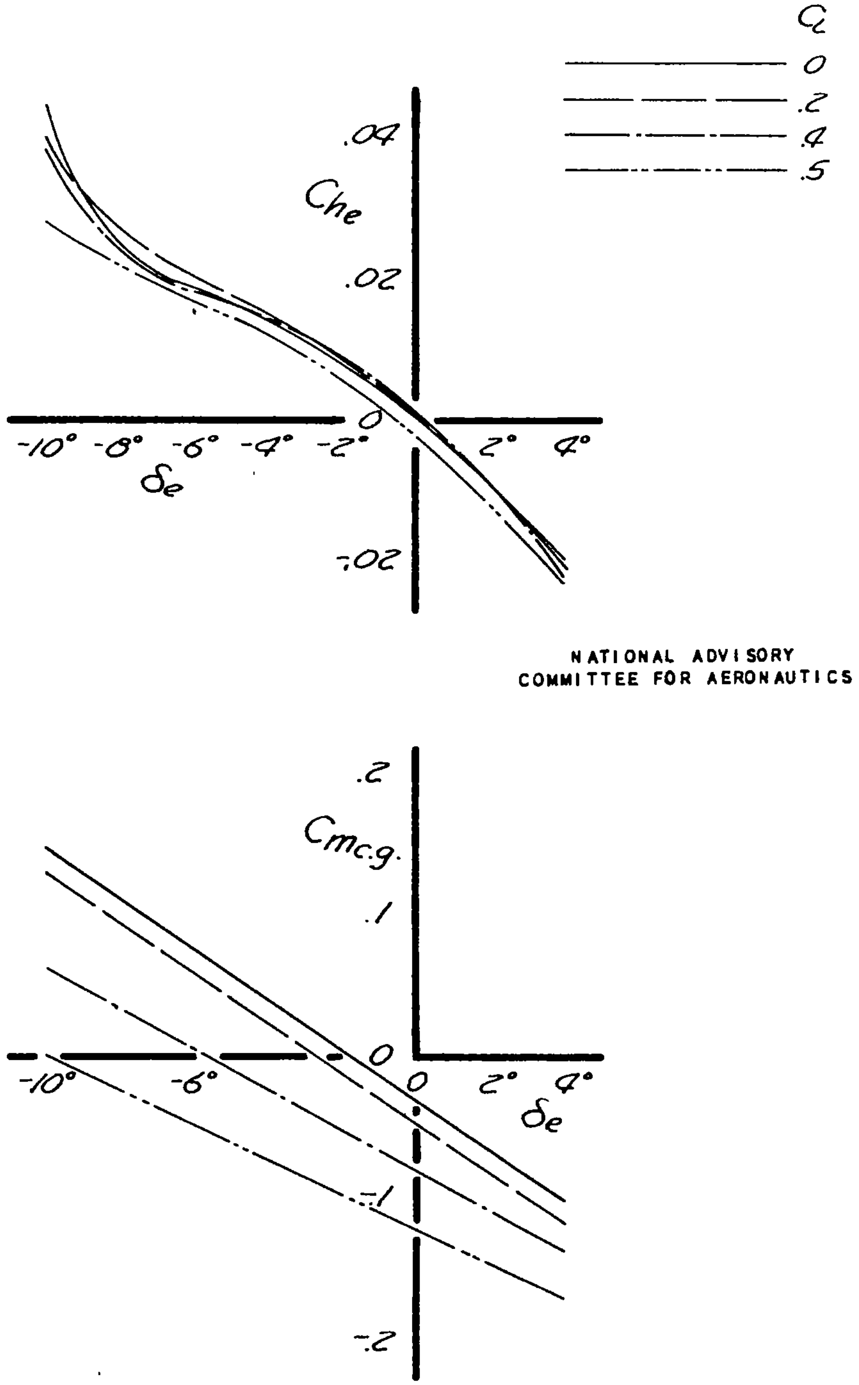

(c) M = 0.74

FIGURE 23.—(CONTINUED) 0.6-BY 6-INCH FLAPS DEFLECTED 7.5°

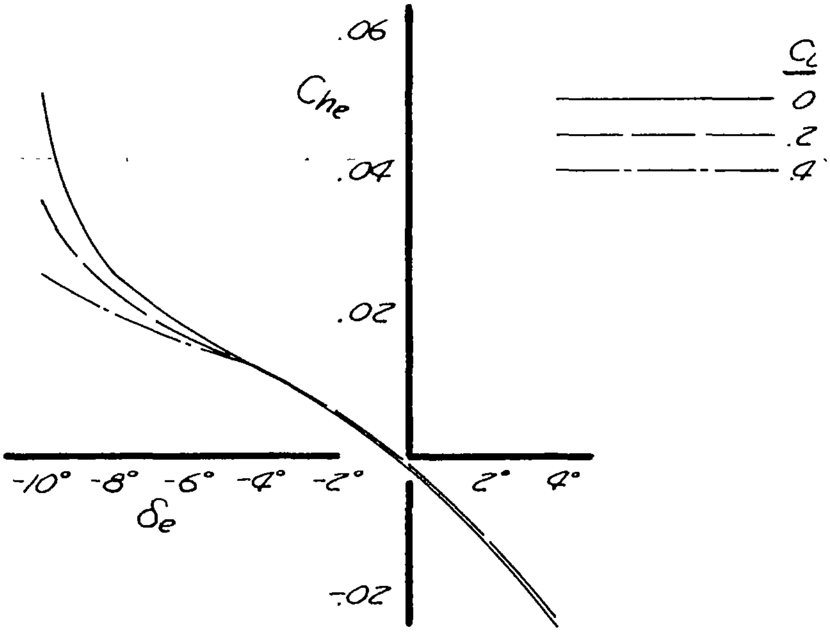

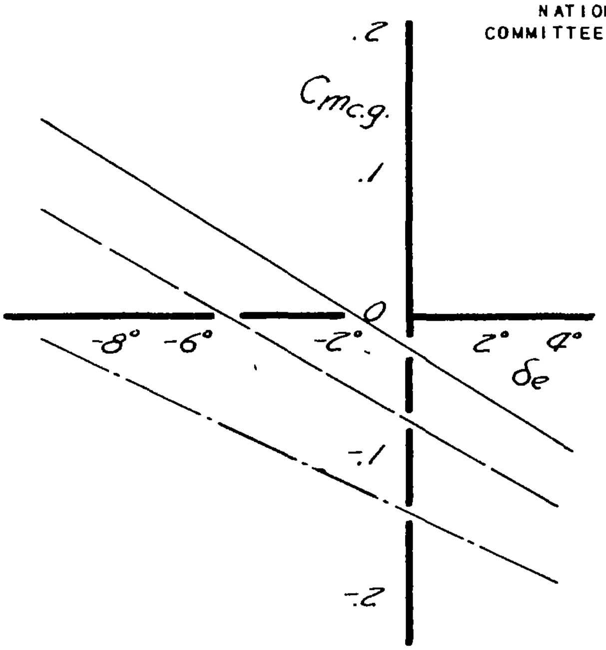

(d) M = 0.79

FIGURE 23.- (CONTINUED) 0.6-BY 6-INCH FLAPS DEFLECTED 7.5°

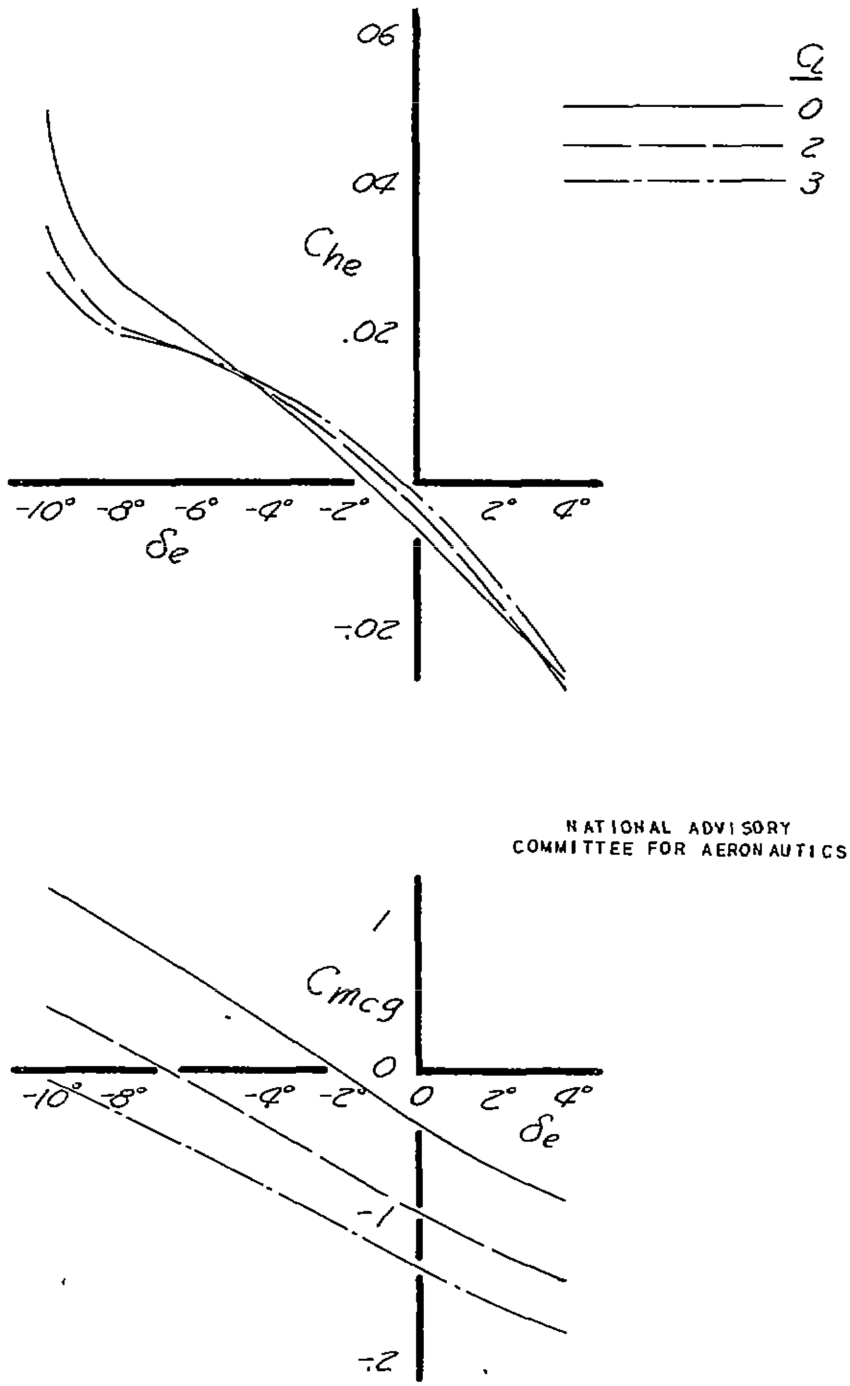

(e) M = 0.815

FIGURE 23 – (CONCLUDED) 0.6-BY 6-INCH FLAPS DEFLECTED 75°

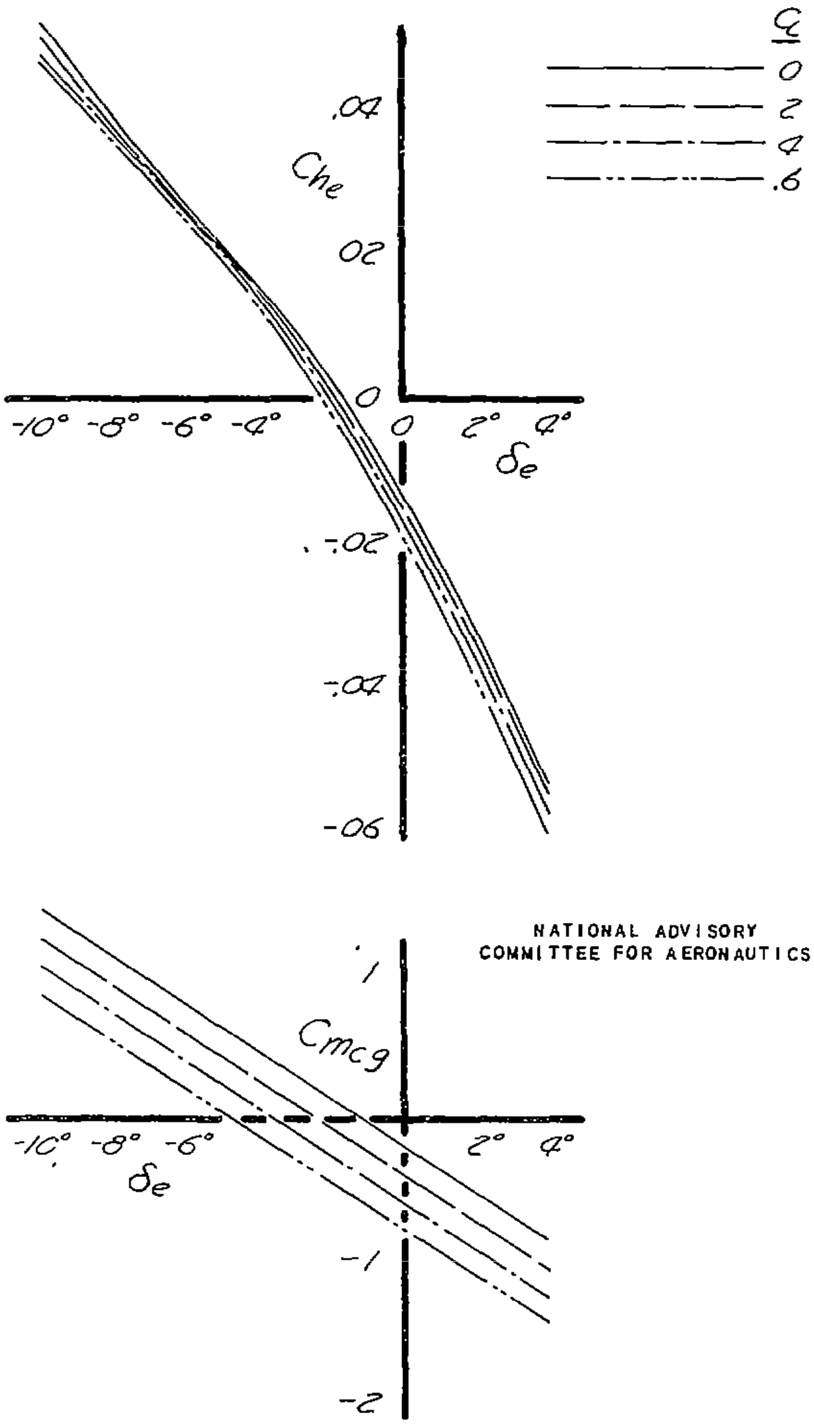

(a) M = 0.20

FIGURE 24 – ELEVATOR CHARACTERISTICS WITH THE 0.6-BY 6-INCH FLAPS DEFLECTED 30°

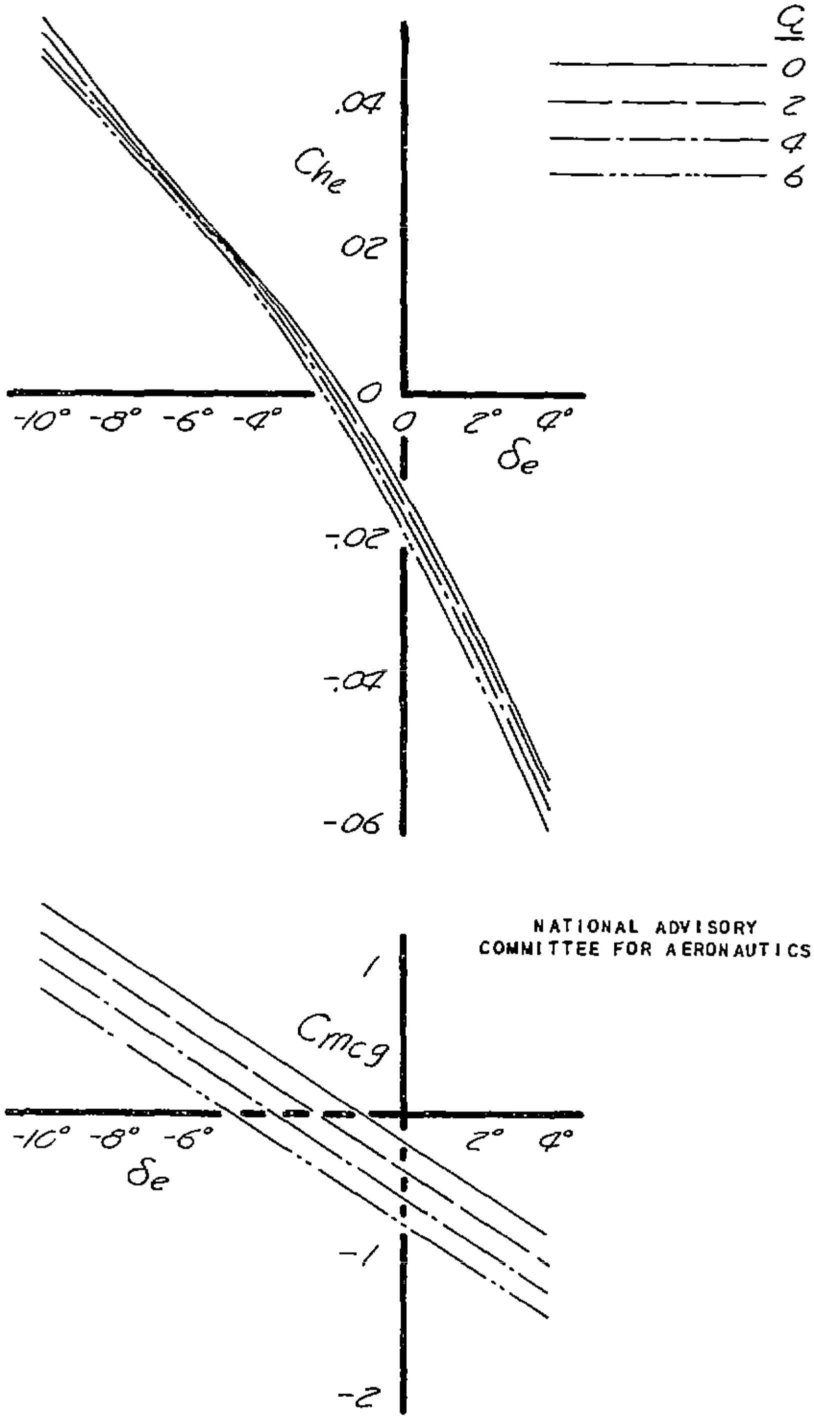

(a) M = 0.20

FIGURE 24 – ELEVATOR CHARACTERISTICS WITH THE 0.6-BY 6-INCH FLAPS DEFLECTED 30°

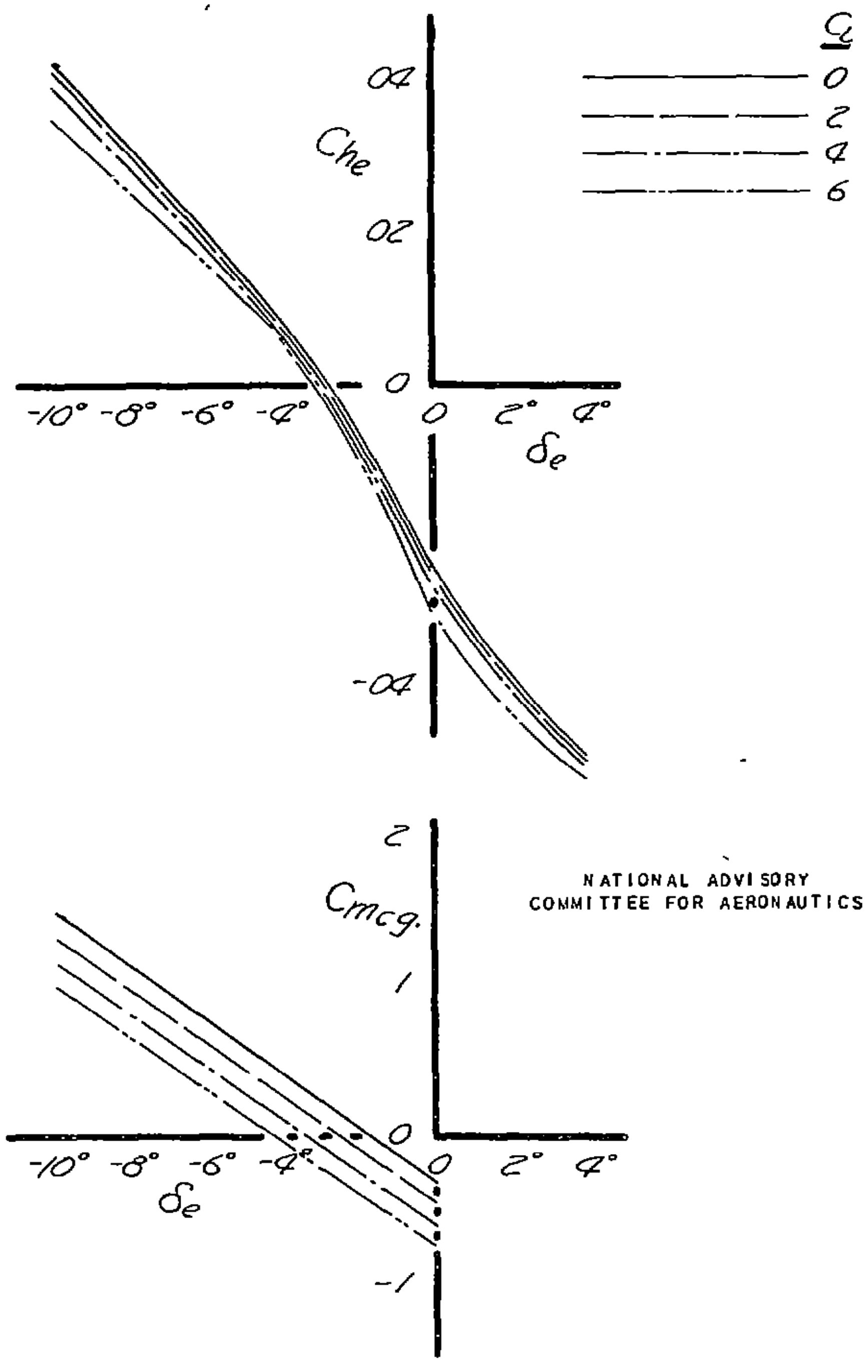

(b) M = 0.60

FIGURE 24.– (CONTINUED) 0.6-BY 6-INCH FLAPS DEFLECTED 30°

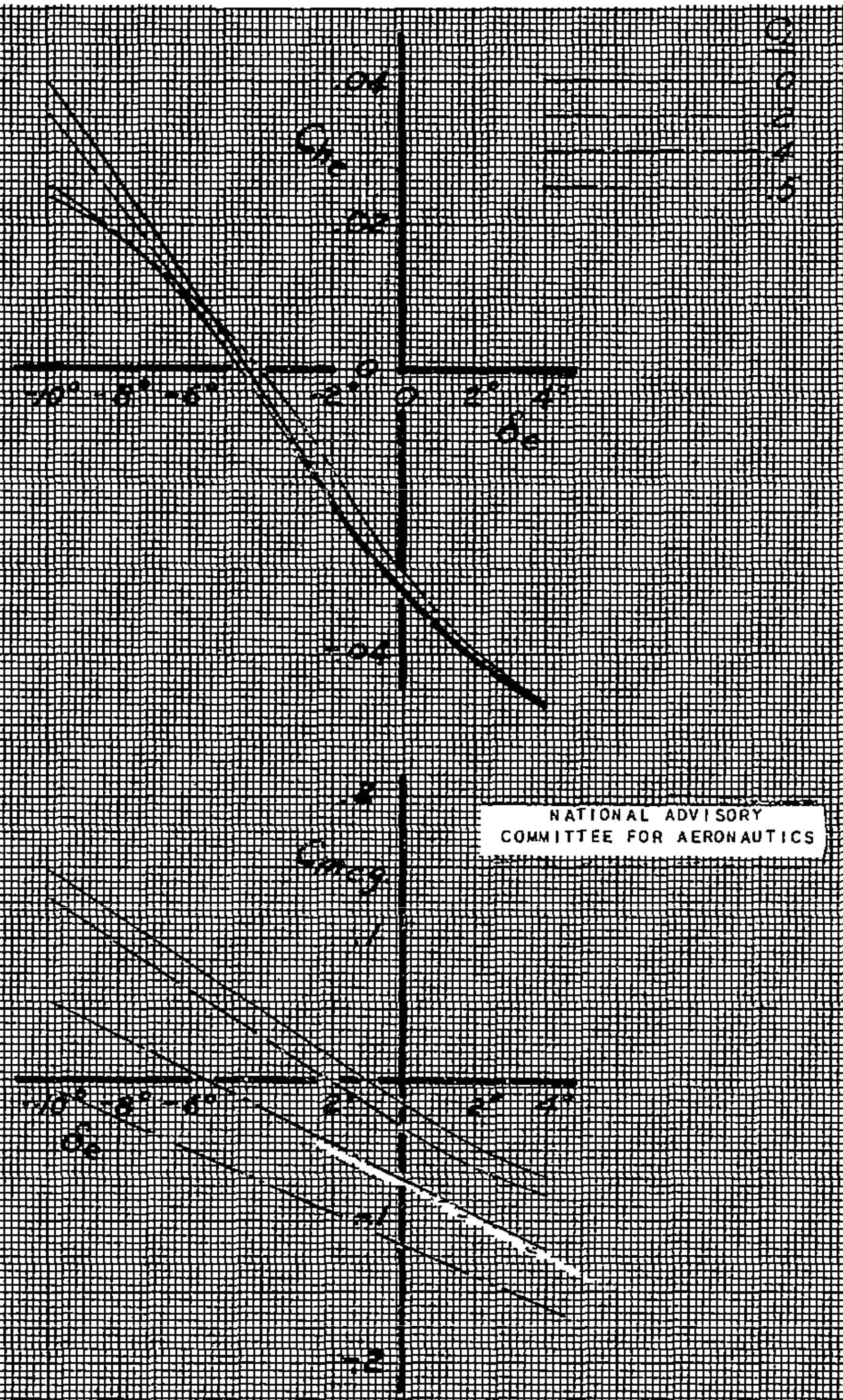

(c) M = 0.74

FIGURE 24 – (CONTINUED) 0.6- X 6-INCH FLAPS DEFLECTED 30°

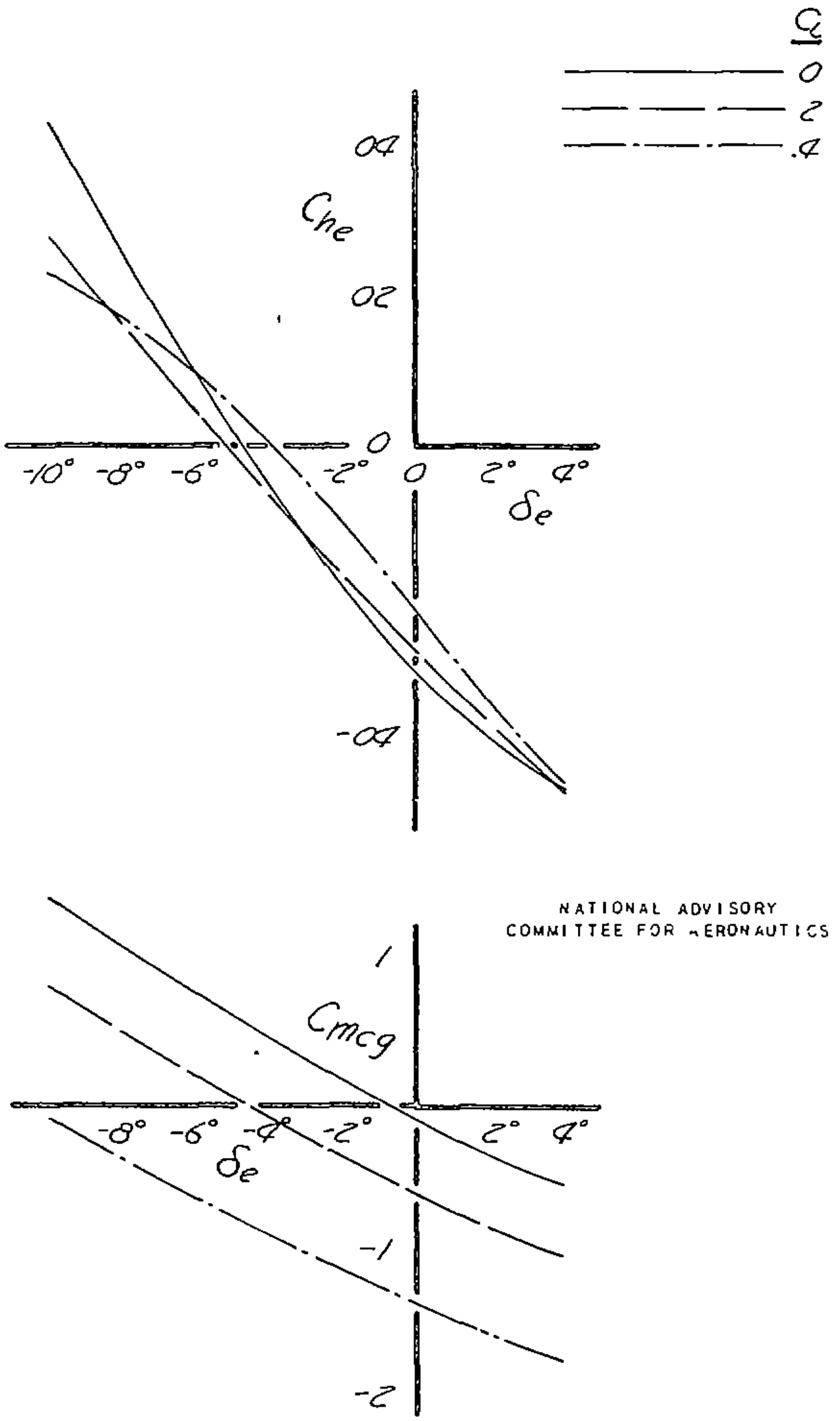

(d) M = 0.79

FIGURE 24 - (CONTINUED) 0.6-BY 6-INCH FLAPS DEFLECTED 30°

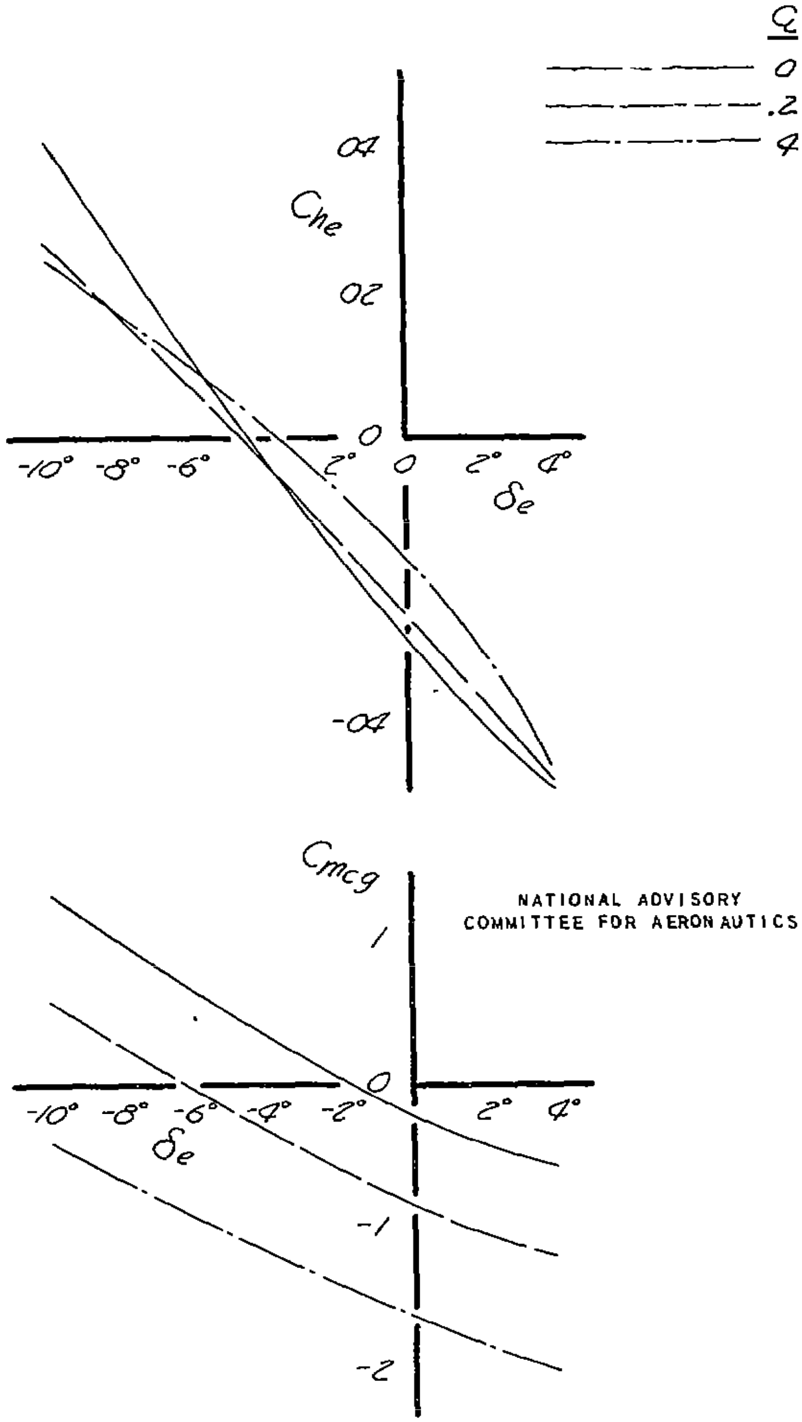

(e) M = 0.815

FIGURE 24.– (CONCLUDED) 0.6-BY 6-INCH FLAPS DEFLECTED 30°

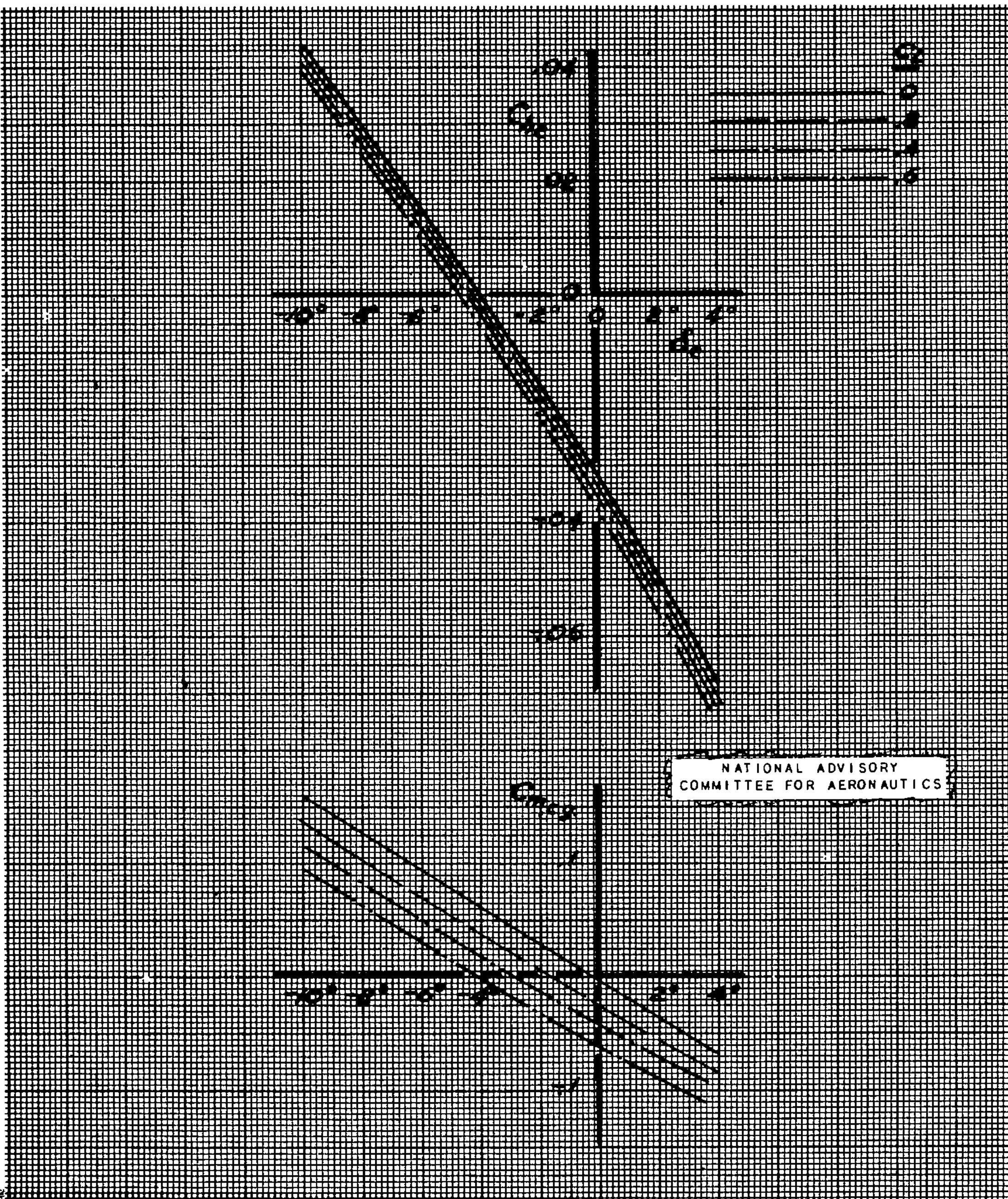

(a) M = 0.20

FIGURE 25.- ELEVATOR CHARACTERISTICS WITH THE 0.6-BY 6-INCH FLAPS DEFLECTED 45°

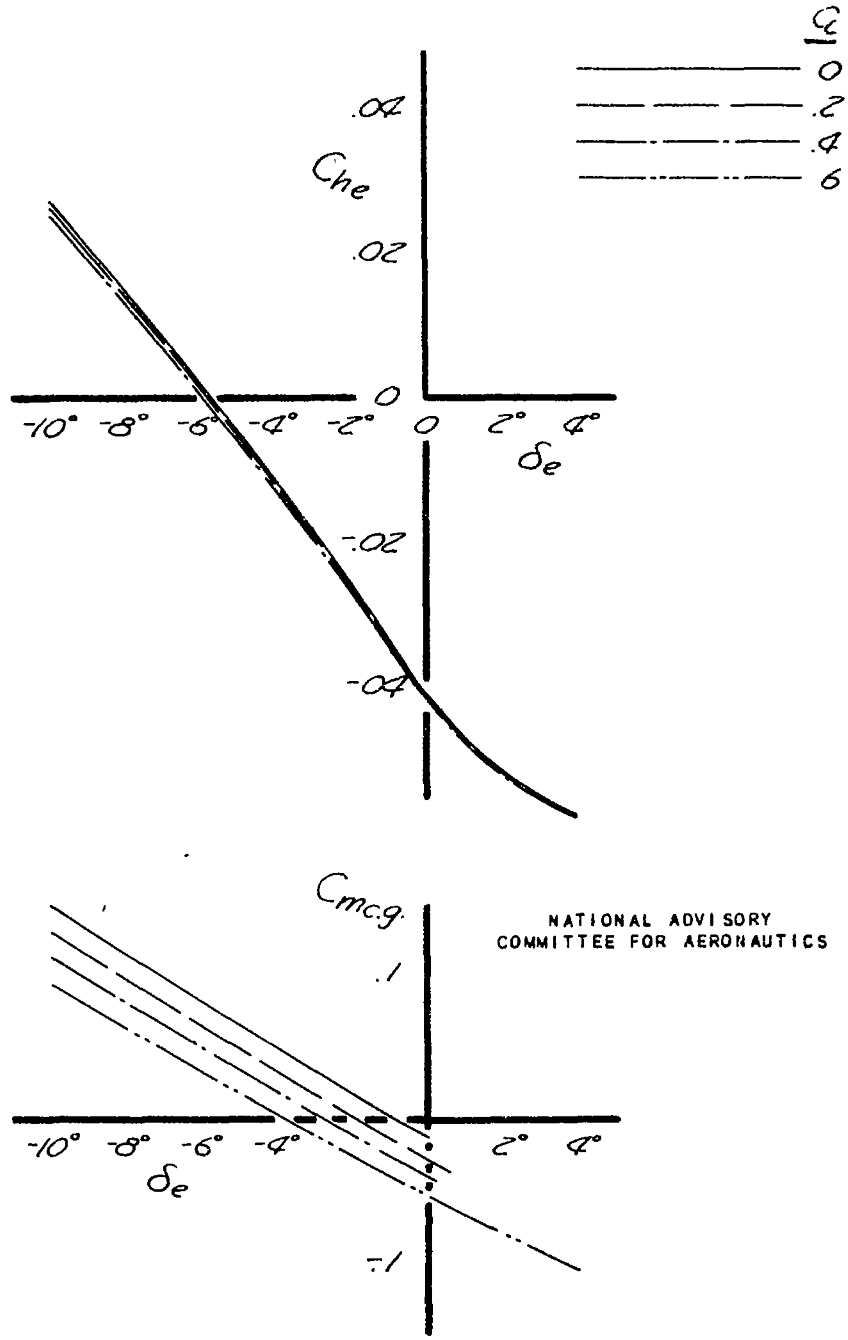

(b) $M = 0.60$

FIGURE 25.- (CONTINUED) 0.6-BY 6-INCH FLAPS DEFLECTED 45°

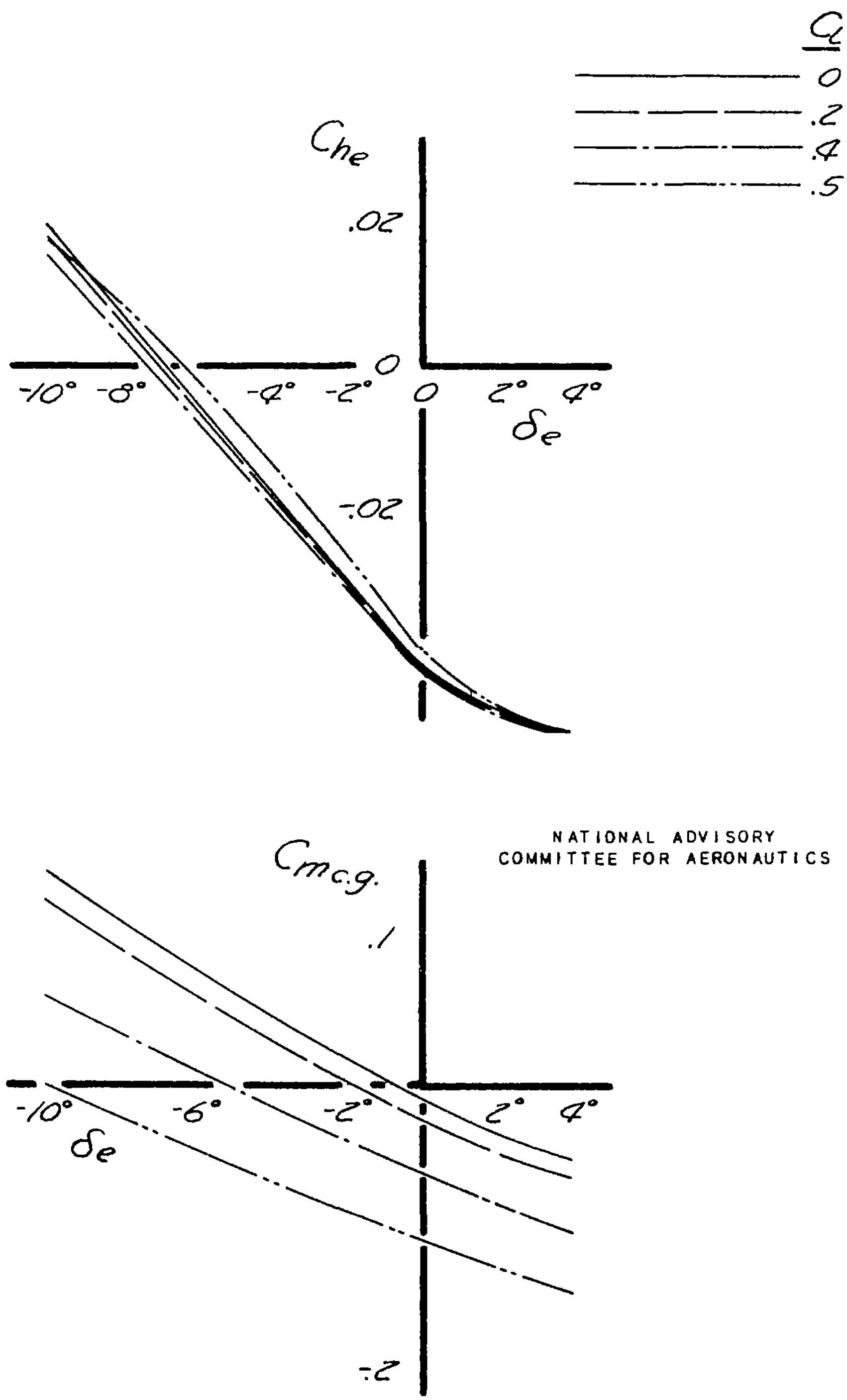

(c) $M = 0.74$

FIGURE 25.- (CONTINUED) 0.6-BY 6-INCH FLAPS DEFLECTED 45°

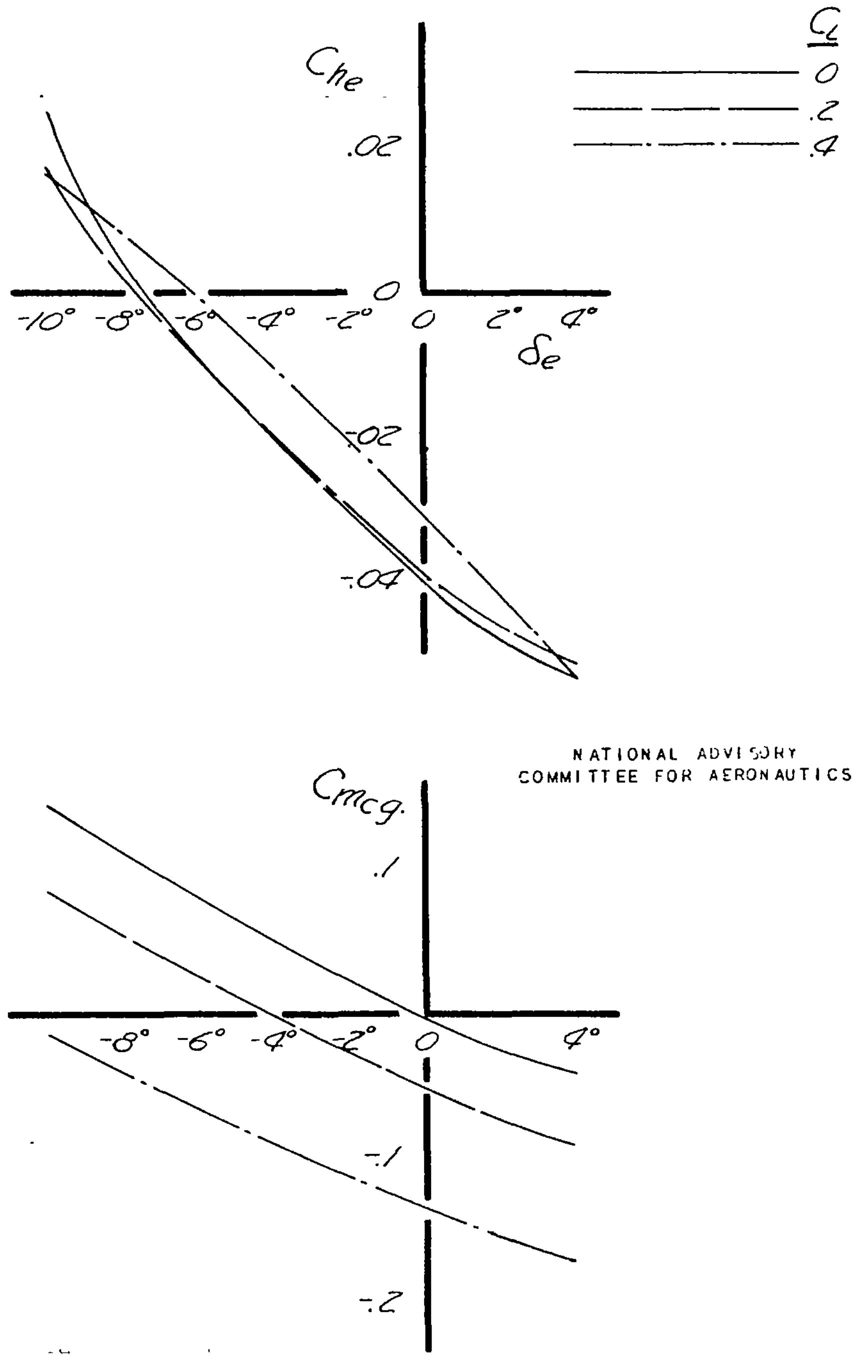

(d) M = 0.79

FIGURE 25.–(CONTINUED) 0.6-BY 6-INCH FLAPS DEFLECTED 45°

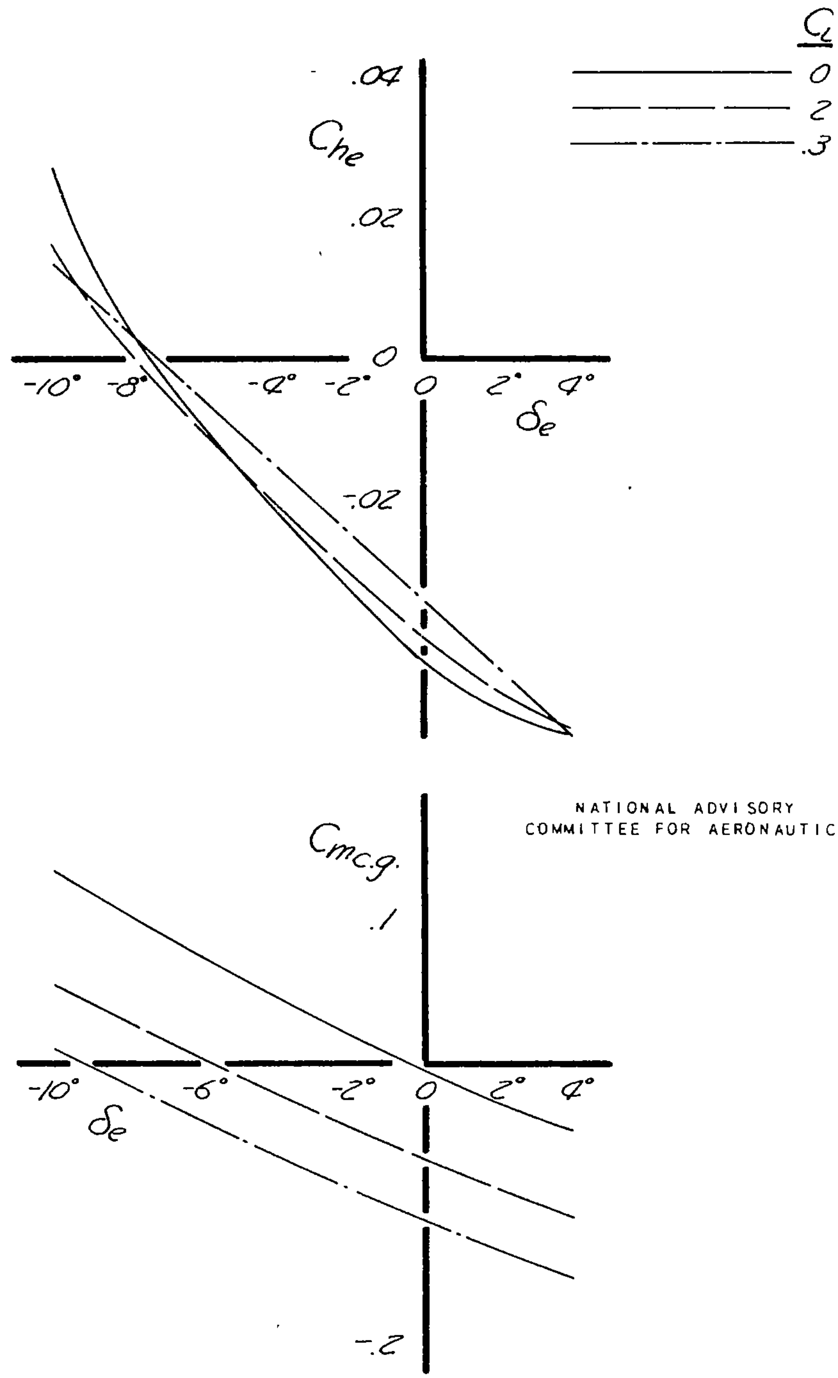

NATIONAL ADVISORY COMMITTEE FOR AERONAUTICS

(e) $M = 0.815$

FIGURE 25.-(CONCLUDED) 0.6-BY 6-INCH FLAPS DEFLECTED 45°

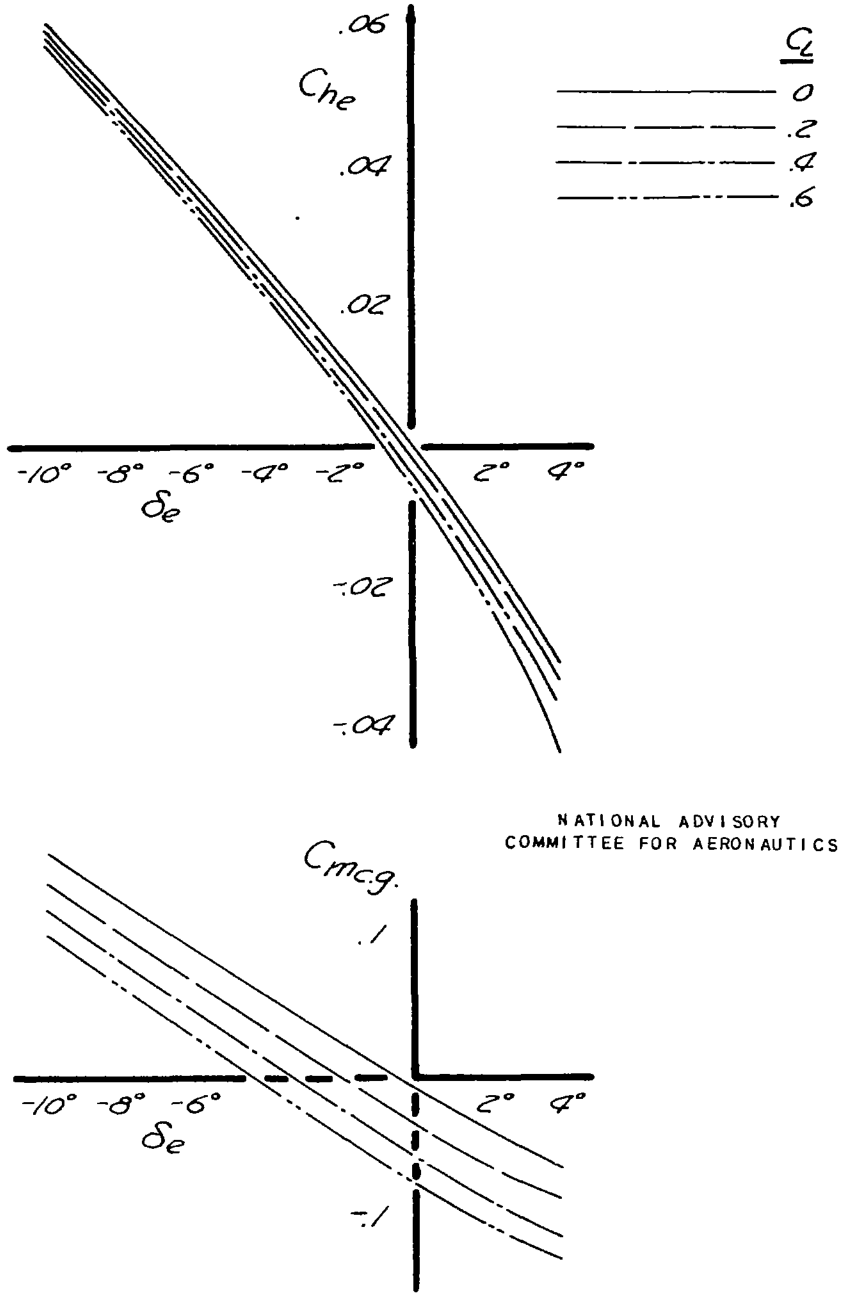

NATIONAL ADVISORY
COMMITTEE FOR AERONAUTICS

(a) M = 0.20

FIGURE 26.- ELEVATOR CHARACTERISTICS WITH THE 24-INCH-SPAN TAPERED SPOILERS PROJECTED 1 PERCENT AT THE INBOARD END

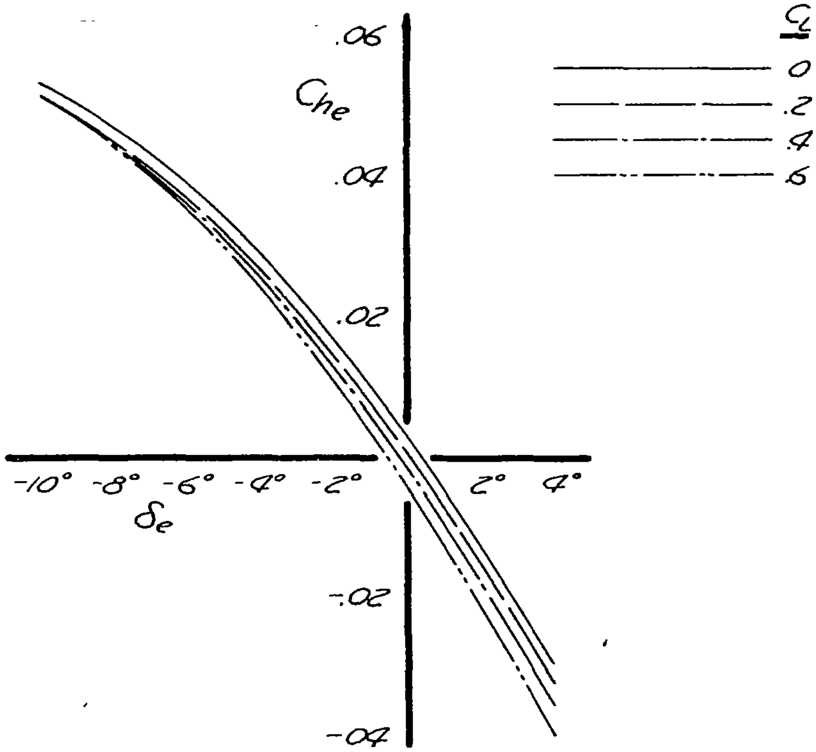

NATIONAL ADVISORY
COMMITTEE FOR AERONAUTICS

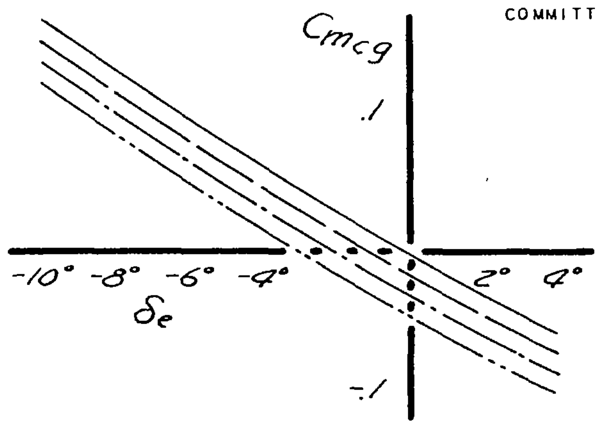

(b) $M = 0.60$

FIGURE 26.-(CONTINUED) 24-INCH-SPAN TAPERED SPOILERS PROJECTED 1 PERCENT AT THE INBOARD END.

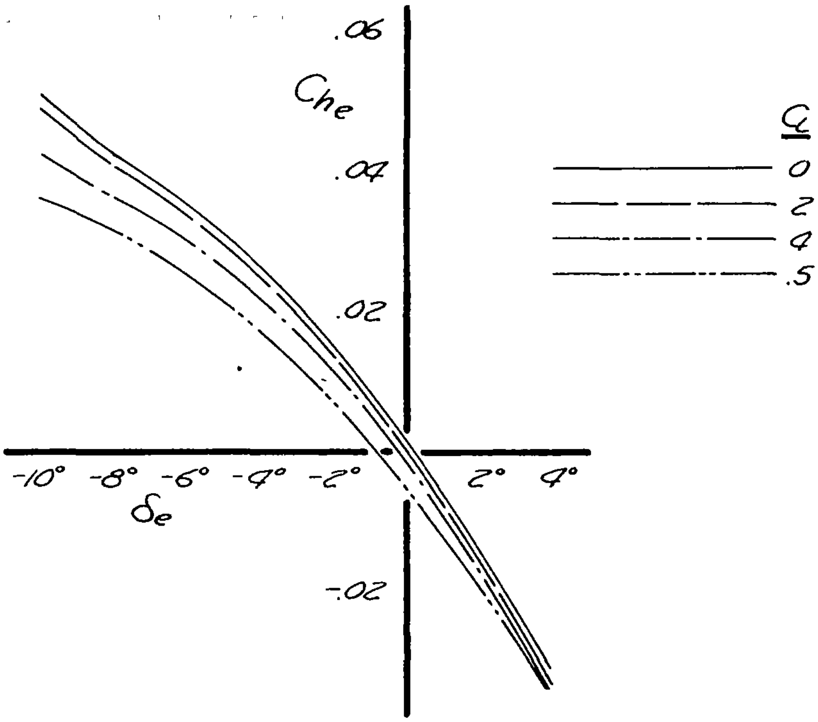

NATIONAL ADVISORY
COMMITTEE FOR AERONAUTICS

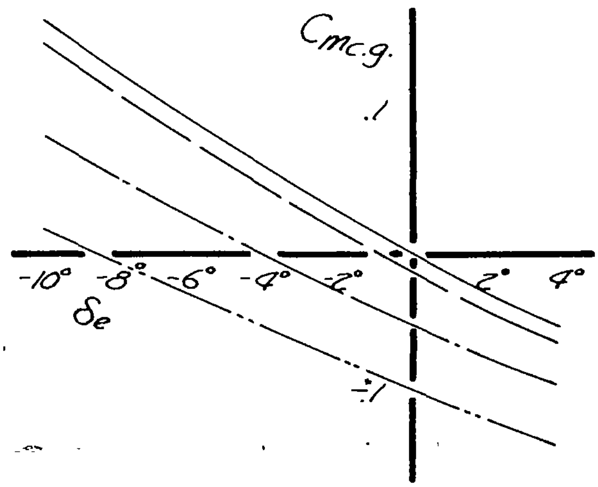

(c) $M = 0.74$

FIGURE 26.- (CONTINUED) 24-INCH-SPAN TAPERED SPOILERS PROJECTED 1 PERCENT AT THE INBOARD END.

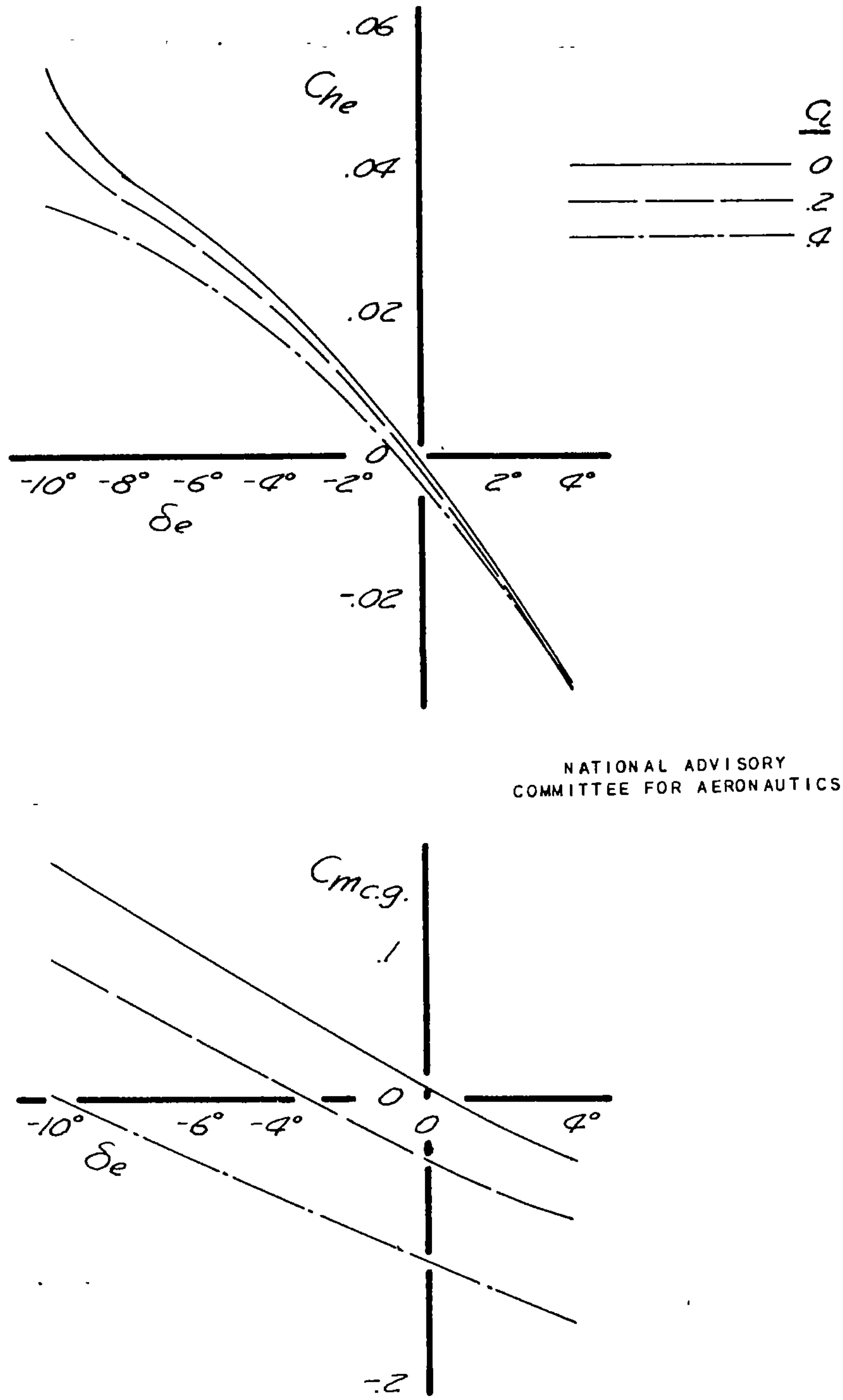

(d) M = 0.79

FIGURE 26.-(CONTINUED) 24-INCH-SPAN TAPERED SPOILERS PROJECTED 1 PERCENT AT THE INBOARD END.

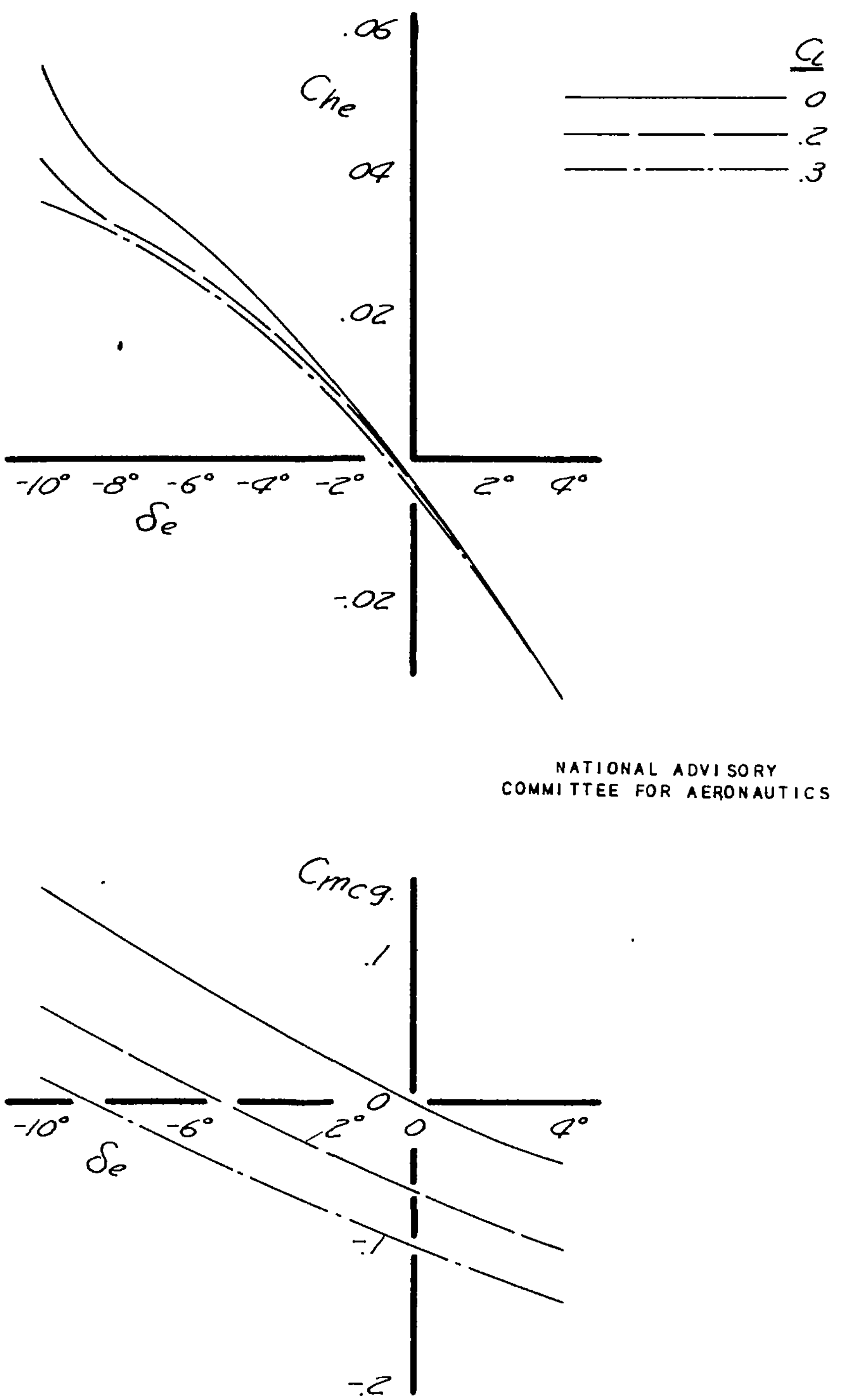

NATIONAL ADVISORY COMMITTEE FOR AERONAUTICS

(e) M = 0.815

FIGURE 26.- (CONCLUDED) 24-INCH-SPAN TAPERED SPOILERS PROJECTED 1 PERCENT AT THE INBOARD END.

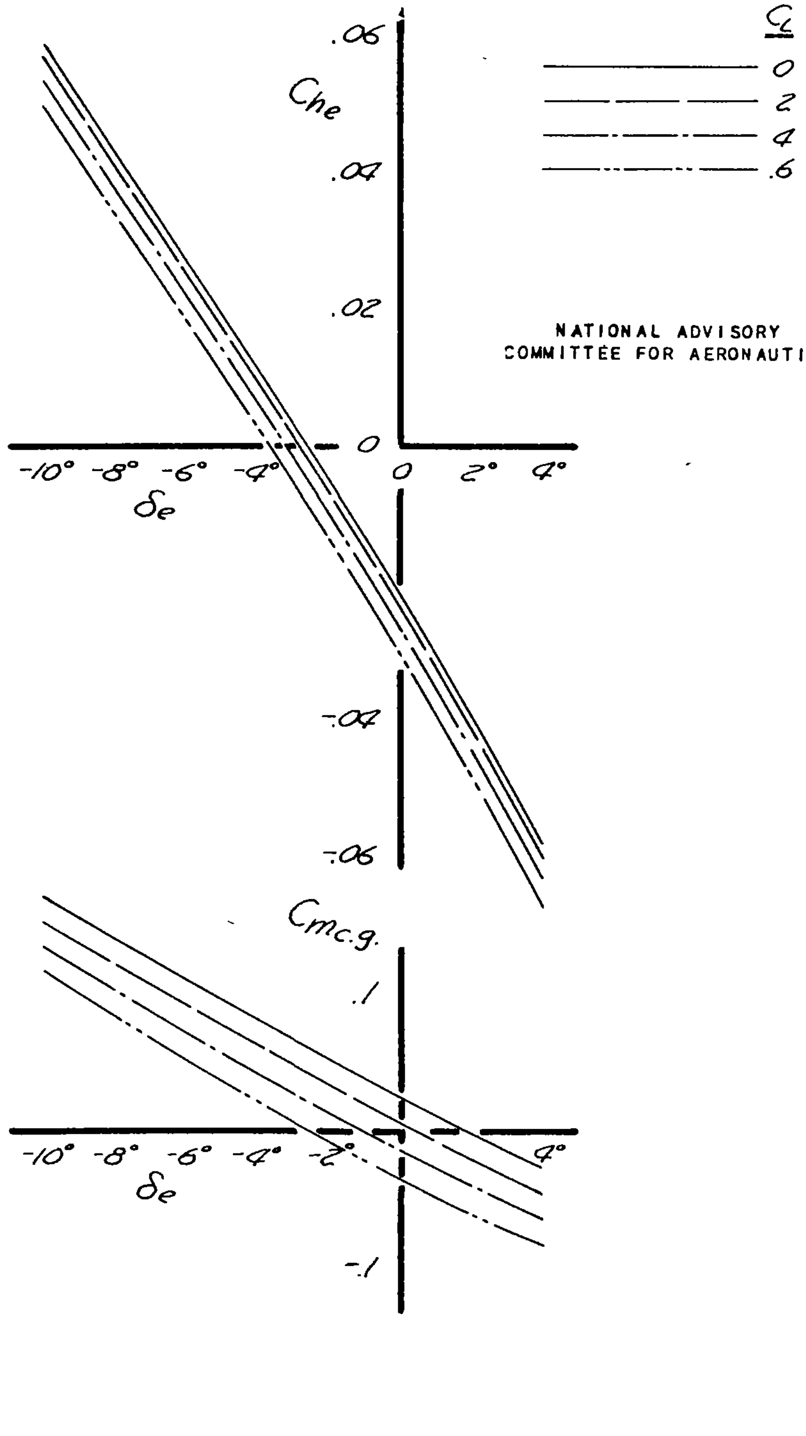

NATIONAL ADVISORY COMMITTEE FOR AERONAUTICS

FIGURE 27.– ELEVATOR CHARACTERISTICS WITH THE 24-INCH-SPAN TAPERED SPOILERS PROJECTED 2 PERCENT AT THE INBOARD END.

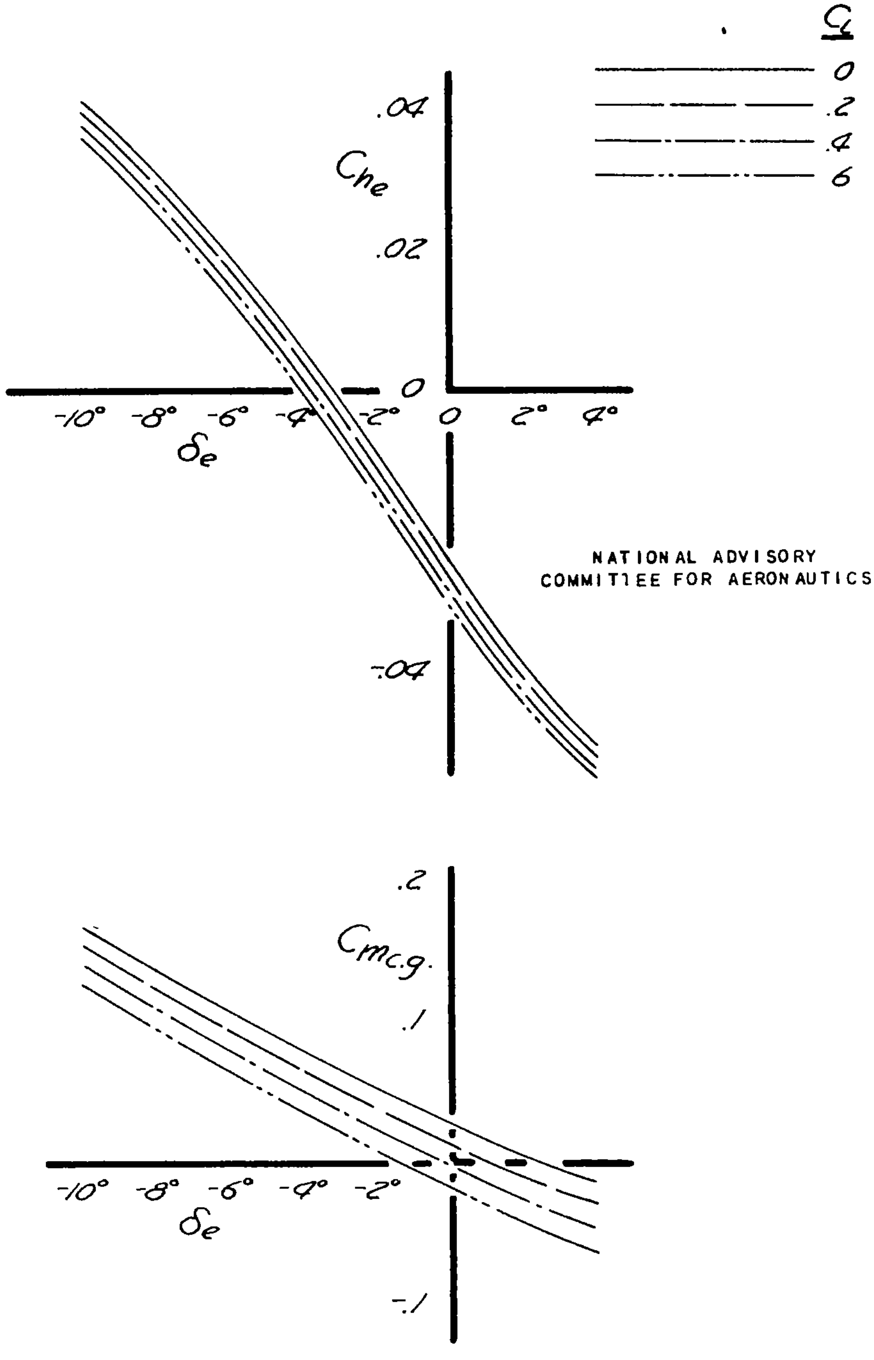

(b) $M = 0.60$

FIGURE 27.- (CONTINUED) 24-INCH-SPAN TAPERED SPOILERS PROJECTED 2 PERCENT AT THE INBOARD END.

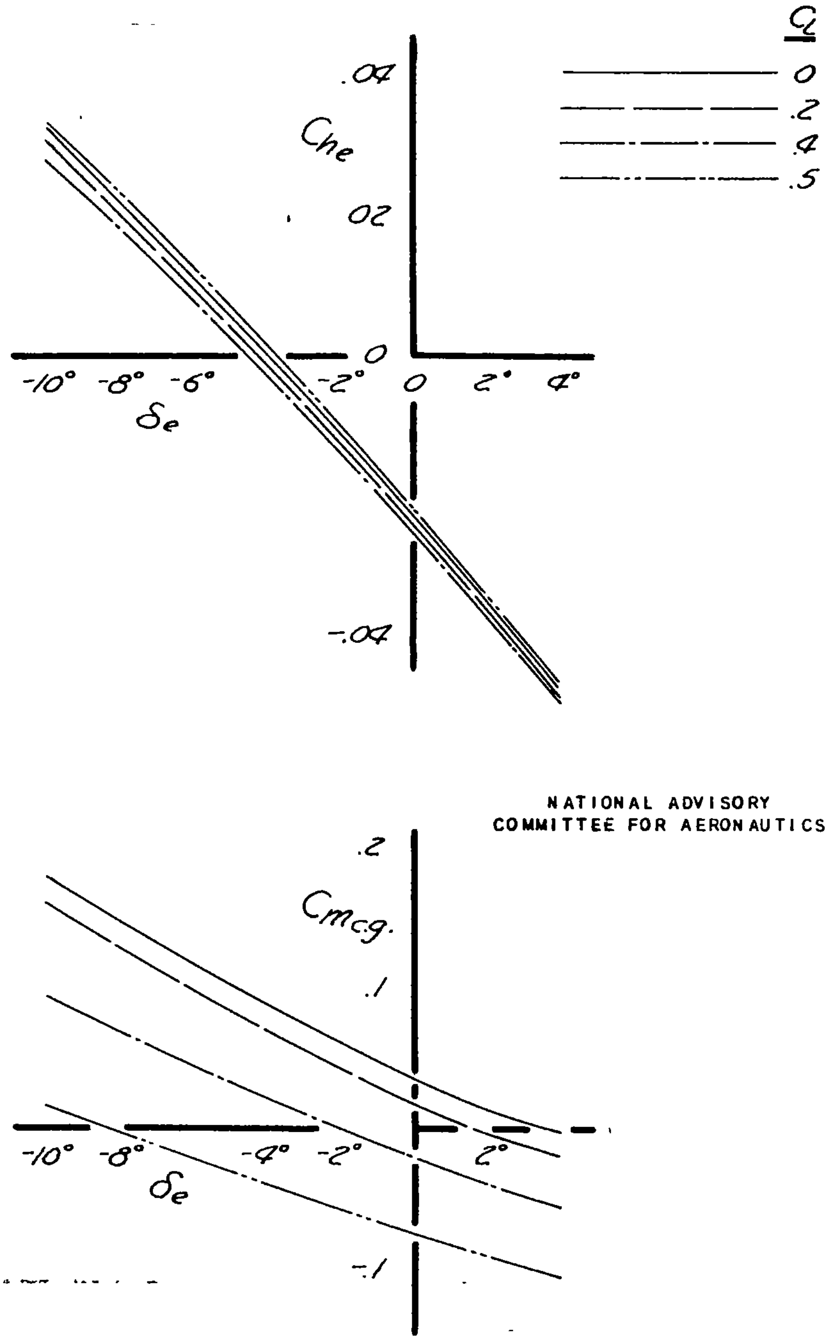

(c) $M = 0.74$

FIGURE 27.- (CONTINUED) 24-INCH-SPAN TAPERED SPOILERS PROJECTED 2 PERCENT AT THE INBOARD END.

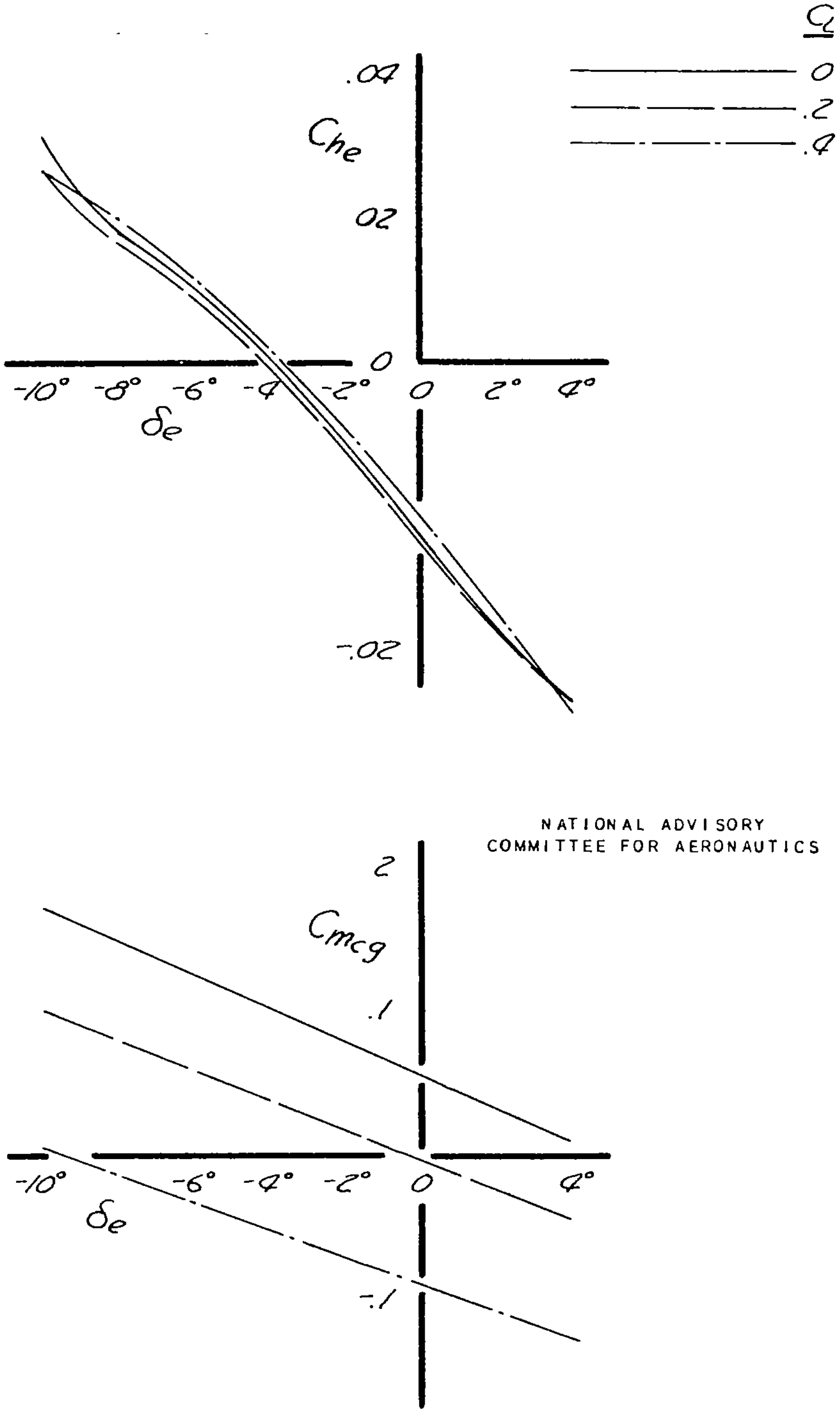

(d) M = 0.79

FIGURE 27.- (CONTINUED) 24-INCH-SPAN TAPERED SPOILERS PROJECTED 2 PERCENT AT THE INBOARD END.

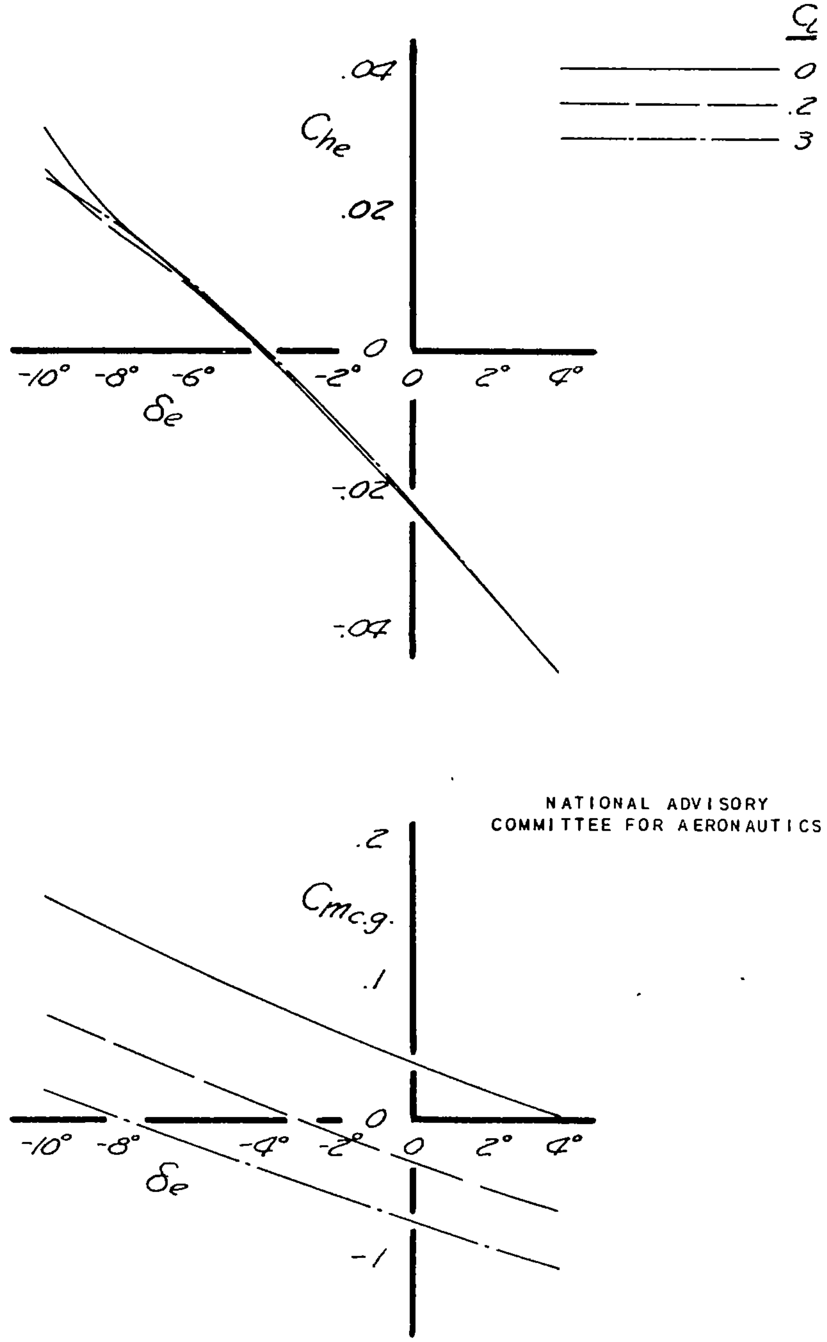

(e) $M = 0.815$

FIGURE 27.- (CONCLUDED) 24-INCH-SPAN TAPERED SPOILERS PROJECTED 2 PERCENT AT THE INBOARD END.

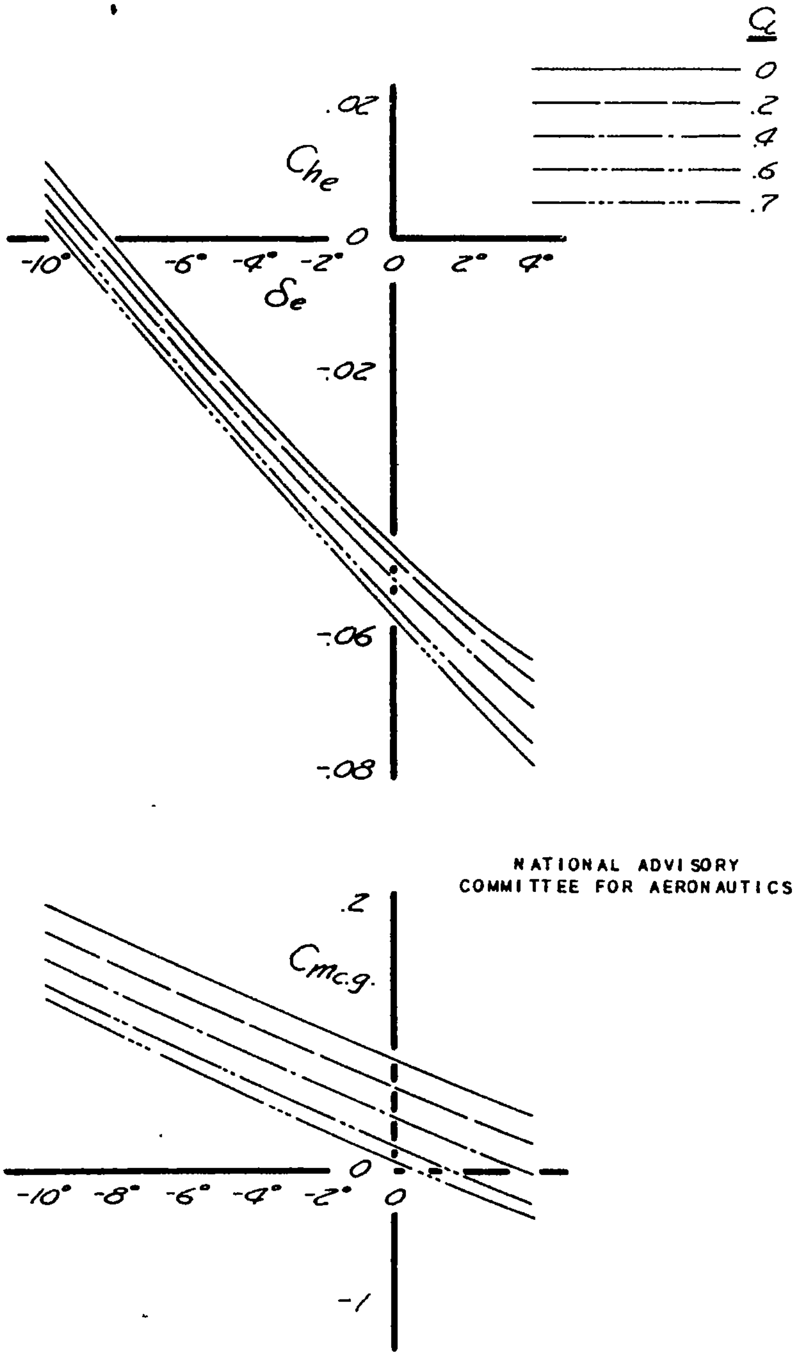

(a) M = 0.20

FIGURE 28.- ELEVATOR CHARACTERISTICS WITH THE 24-INCH-SPAN TAPERED SPOILERS PROJECTED 4 PERCENT AT THE INBOARD END.

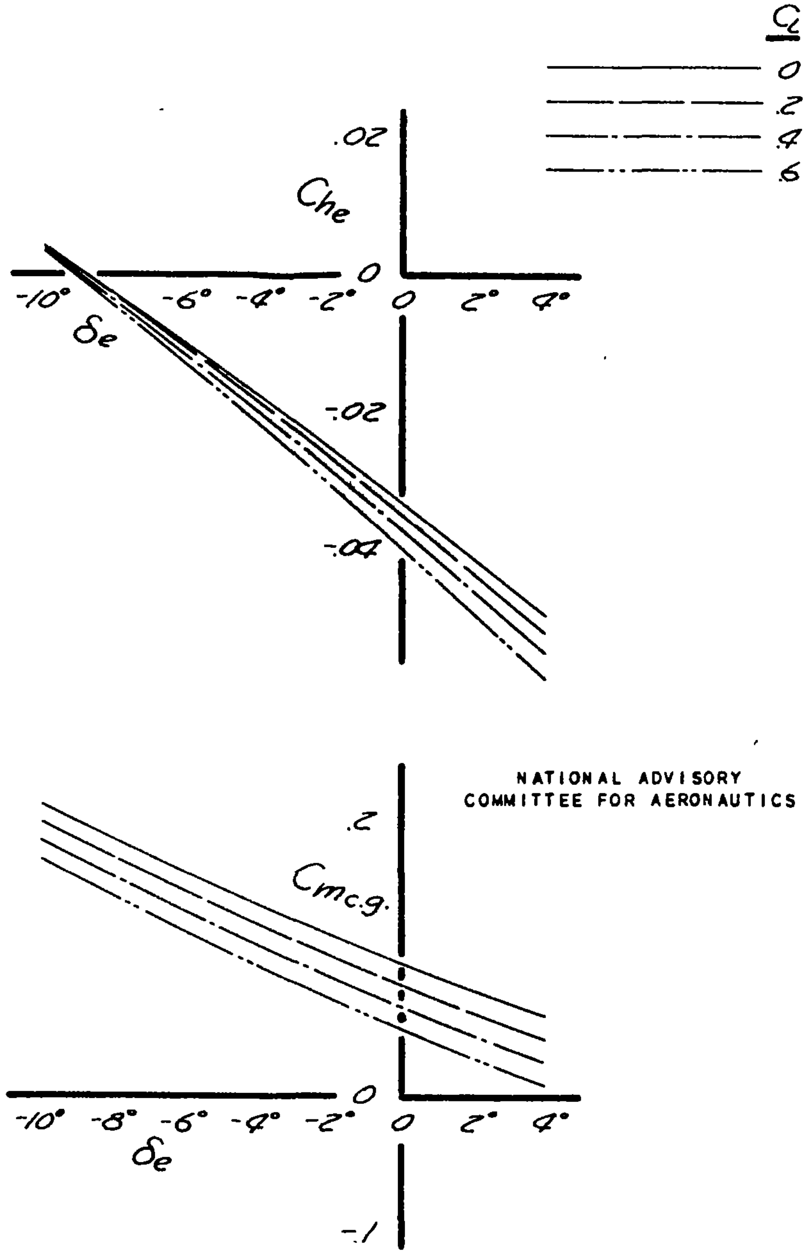

(b) M = 0.60

FIGURE 28.-(CONTINUED) 24-INCH-SPAN TAPERED SPOILERS PROJECTED 4 PERCENT AT THE INBOARD END.

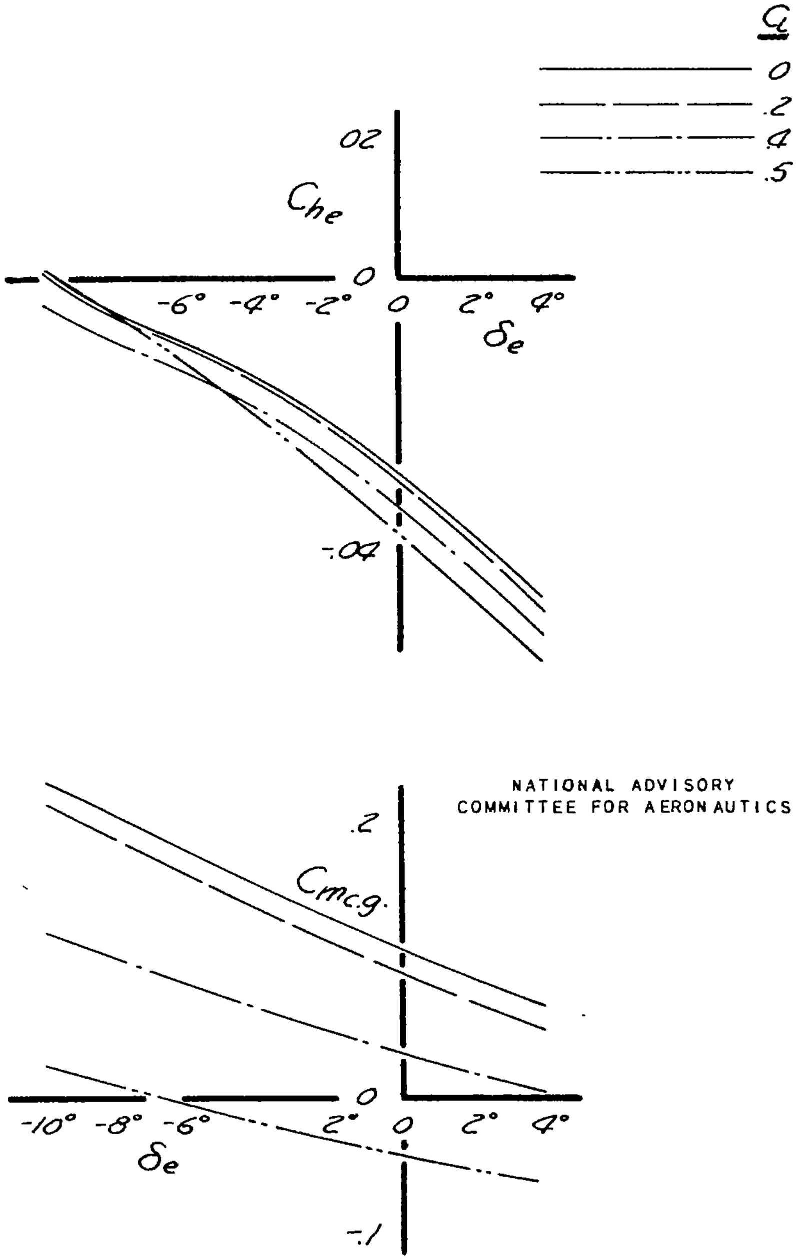

(c) M = 0.74

FIGURE 28.-(CONTINUED) 24-INCH-SPAN TAPERED SPOILERS PROJECTED 4 PERCENT AT THE INBOARD END.

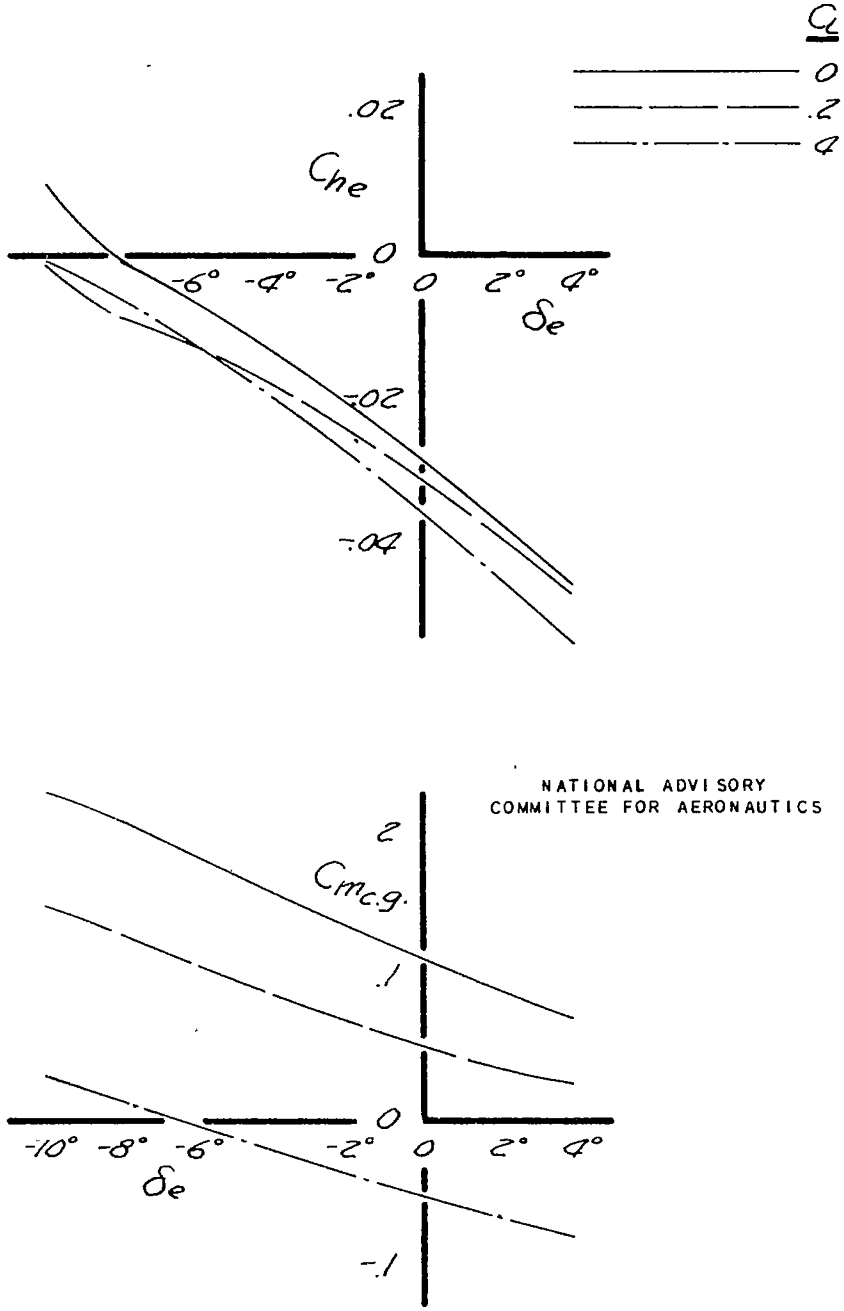

(d) M = 0.79

FIGURE 28 - (CONTINUED) 24-INCH-SPAN TAPERED SPOILERS PROJECTED 4 PERCENT AT THE INBOARD END.

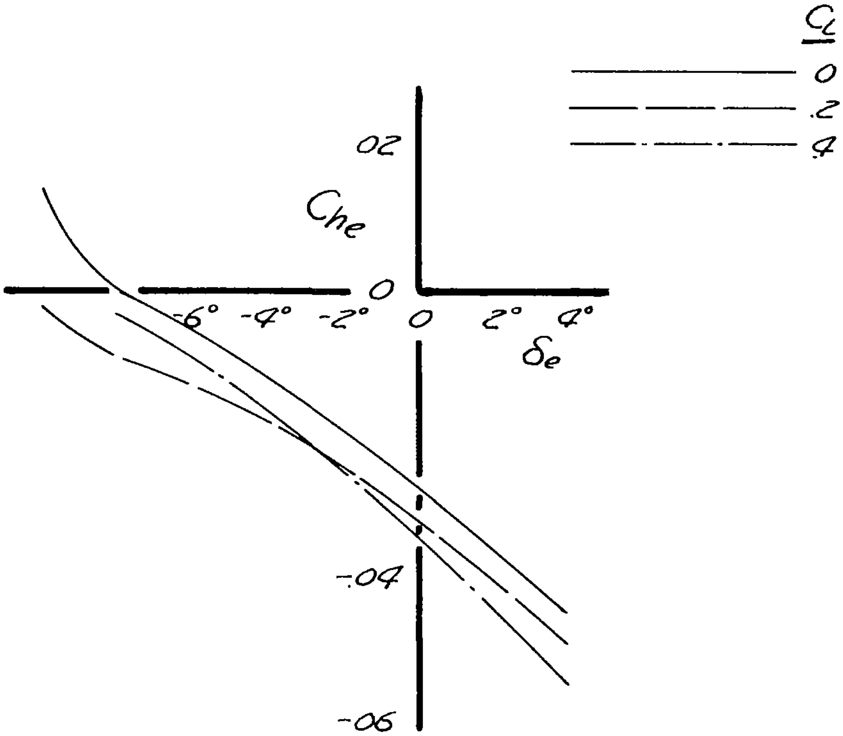

NATIONAL ADVISORY
COMMITTEE FOR AERONAUTICS

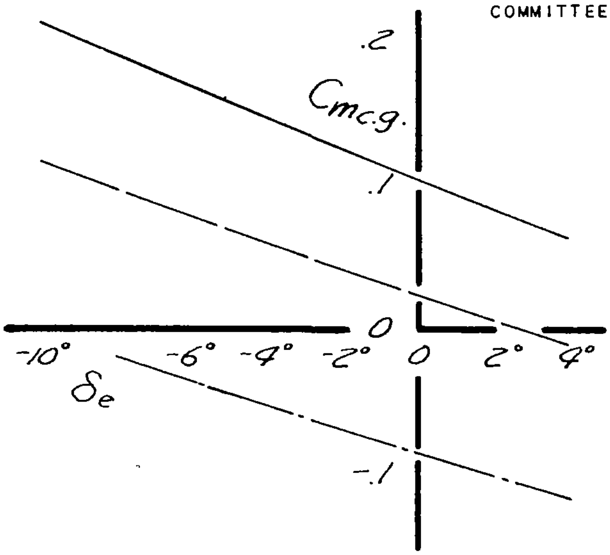

(e) $M = 0.815$

FIGURE 28.- (CONCLUDED) 24-INCH-SPAN TAPERED SPOILERS PROJECTED 4 PERCENT AT THE INBOARD END.

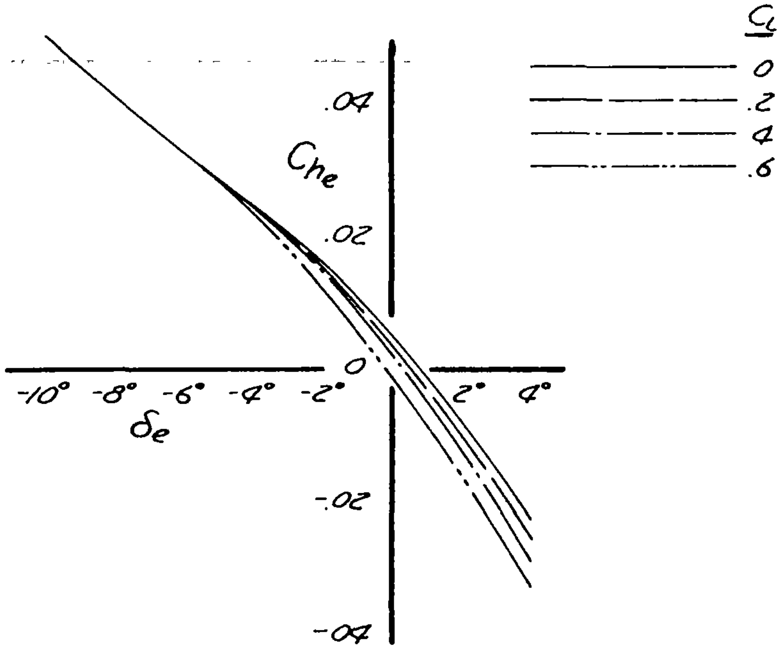

NATIONAL ADVISORY
COMMITTEE FOR AERONAUTICS

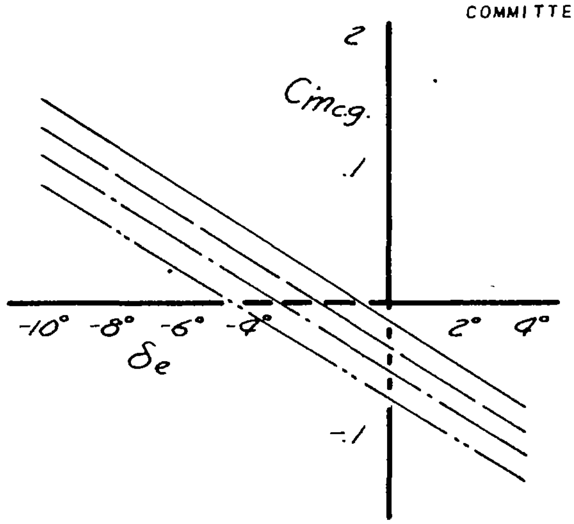

(a) M = 0.20

FIGURE 29.- ELEVATOR CHARACTERISTICS WITH THE 24-INCH-SPAN CONSTANT-PERCENT-CHORD SPOILERS PROJECTED 0.5 PERCENT

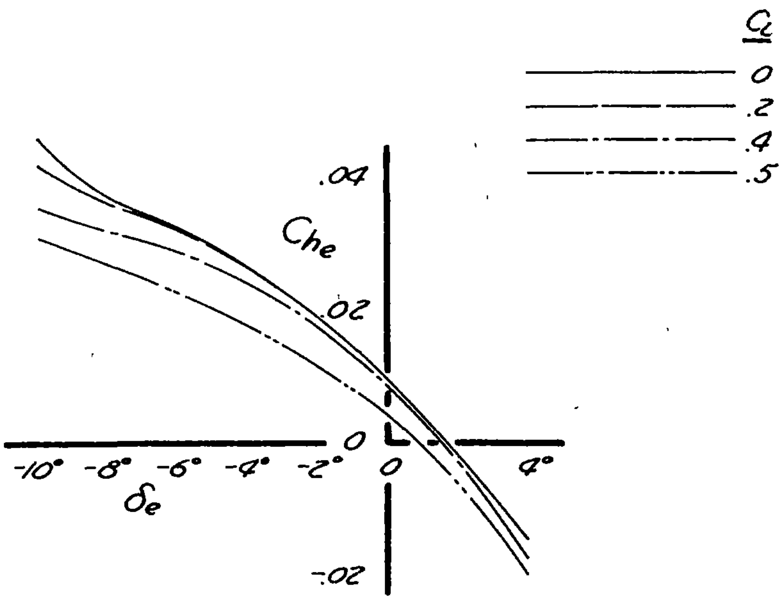

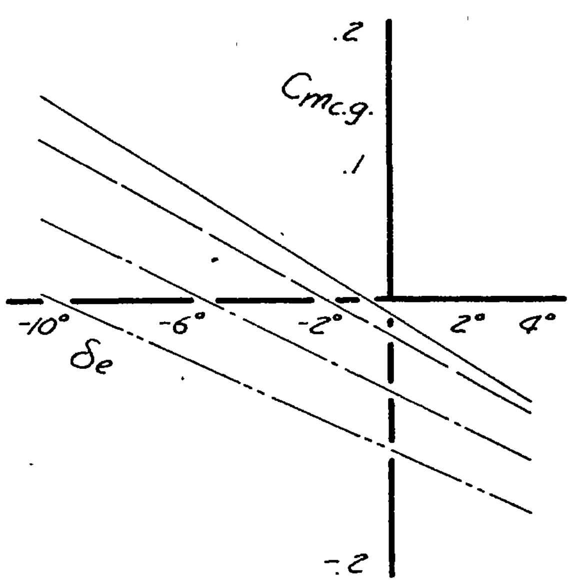

(b) M = 0.74

FIGURE 29.-(CONTINUED) 24-INCH-SPAN CONSTANT-PERCENT-CHORD SPOILERS PROJECTED 0.5 PERCENT.

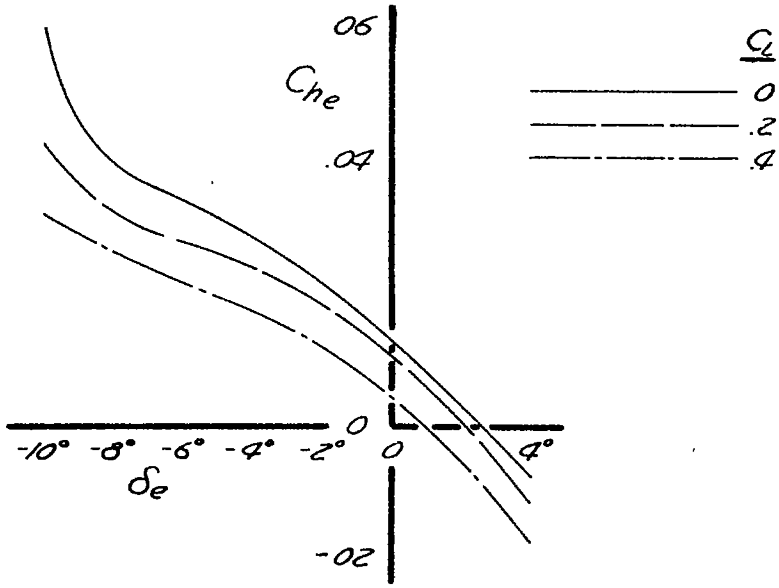

NATIONAL ADVISORY
COMMITTEE FOR AERONAUTICS

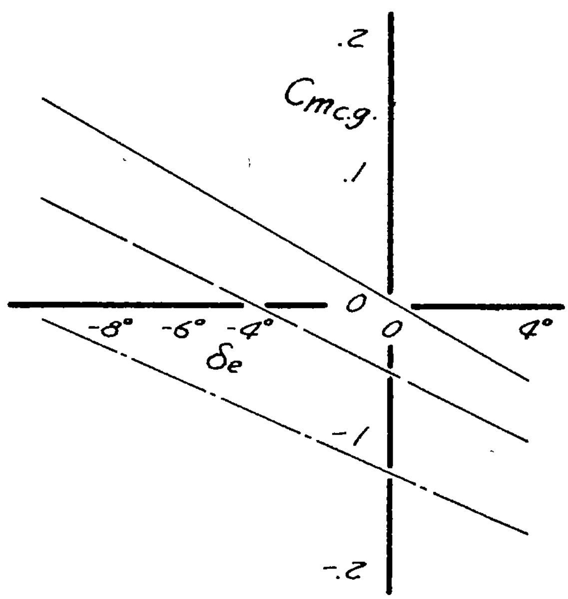

(c) M = 0.79

FIGURE 29.-(CONCLUDED) 24-INCH-SPAN CONSTANT-PERCENT-CHORD SPOILERS PROJECTED 0.5 PERCENT.

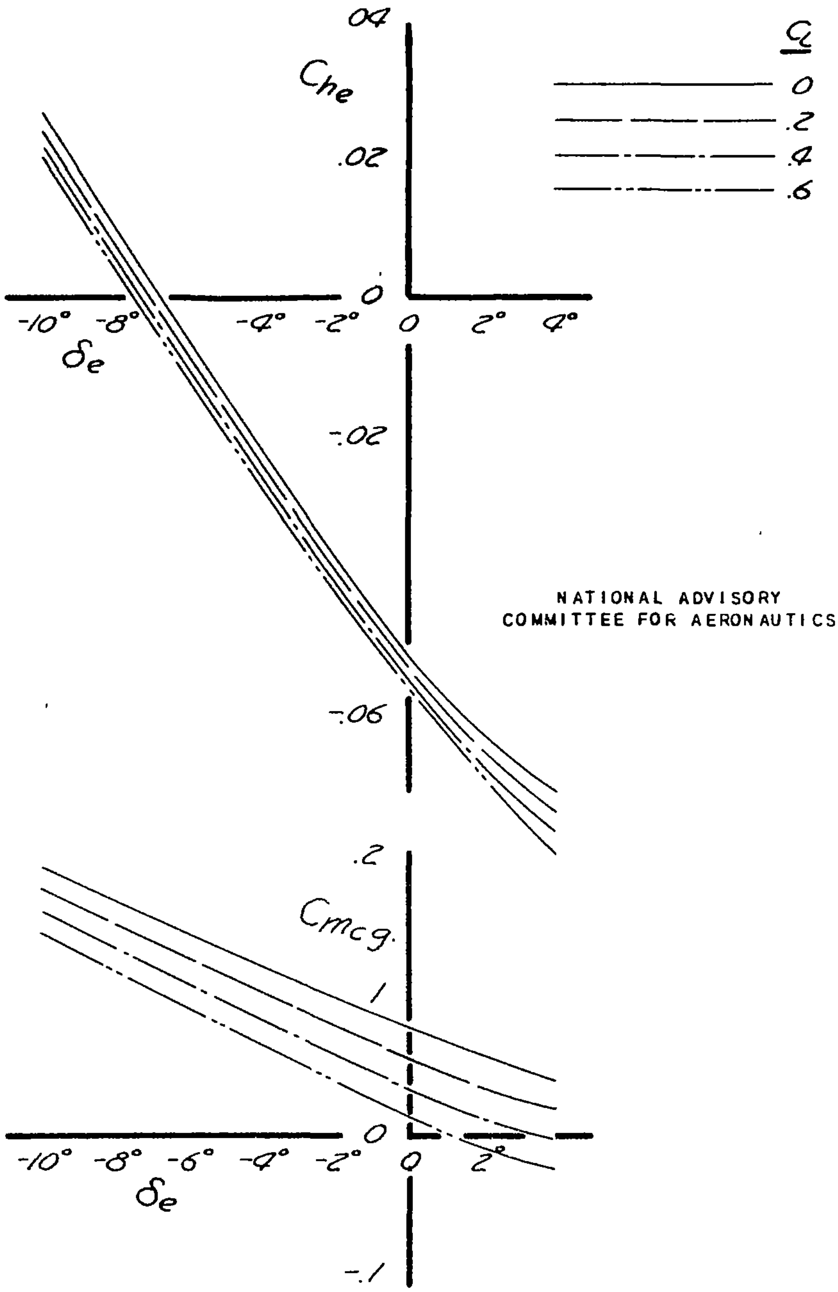

(a) $M = 0.20$

FIGURE 30.– ELEVATOR CHARACTERISTICS WITH THE 24-INCH-SPAN CONSTANT-PERCENT-CHORD SPOILERS PROJECTED 2 PERCENT.

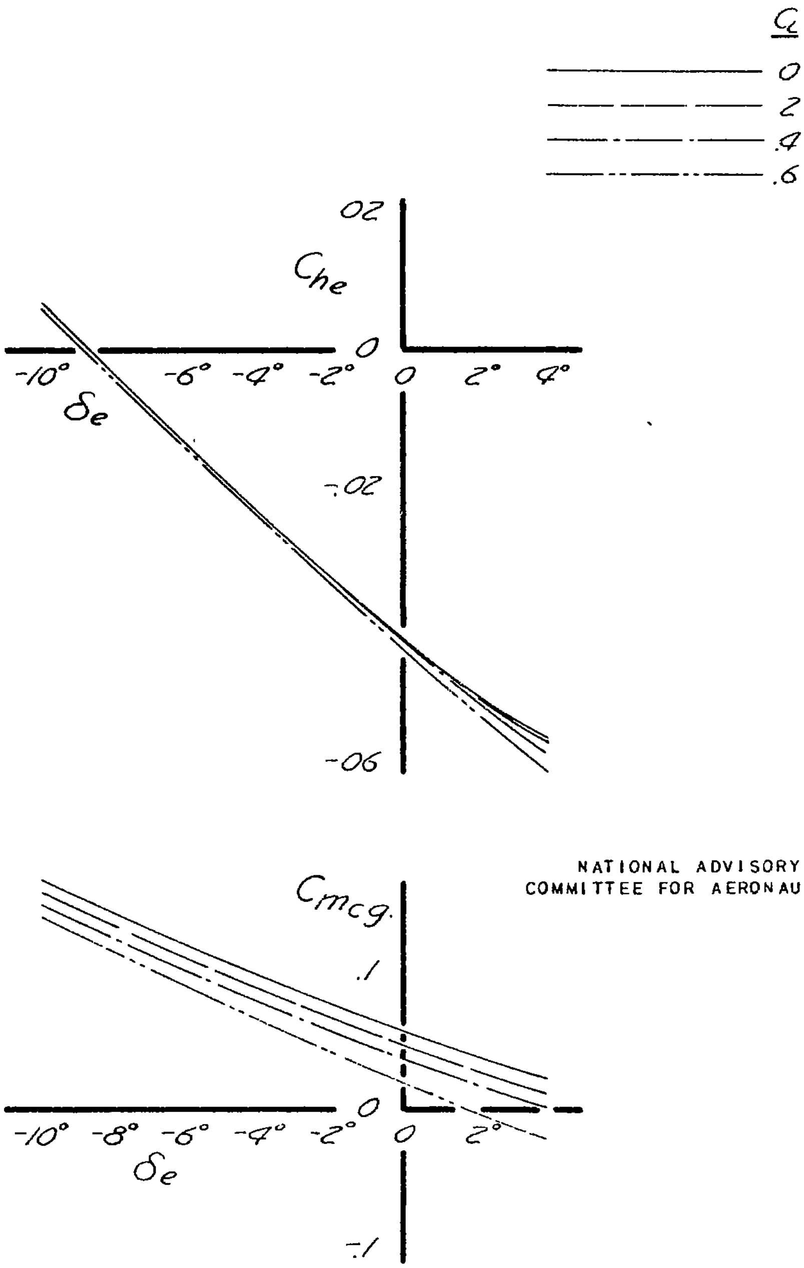

NATIONAL ADVISORY COMMITTEE FOR AERONAUTICS

(b) M = 0.60

FIGURE 30 .-(CONTINUED) 24-INCH-SPAN CONSTANT-PERCENT-CHORD SPOILERS PROJECTED 2 PERCENT.

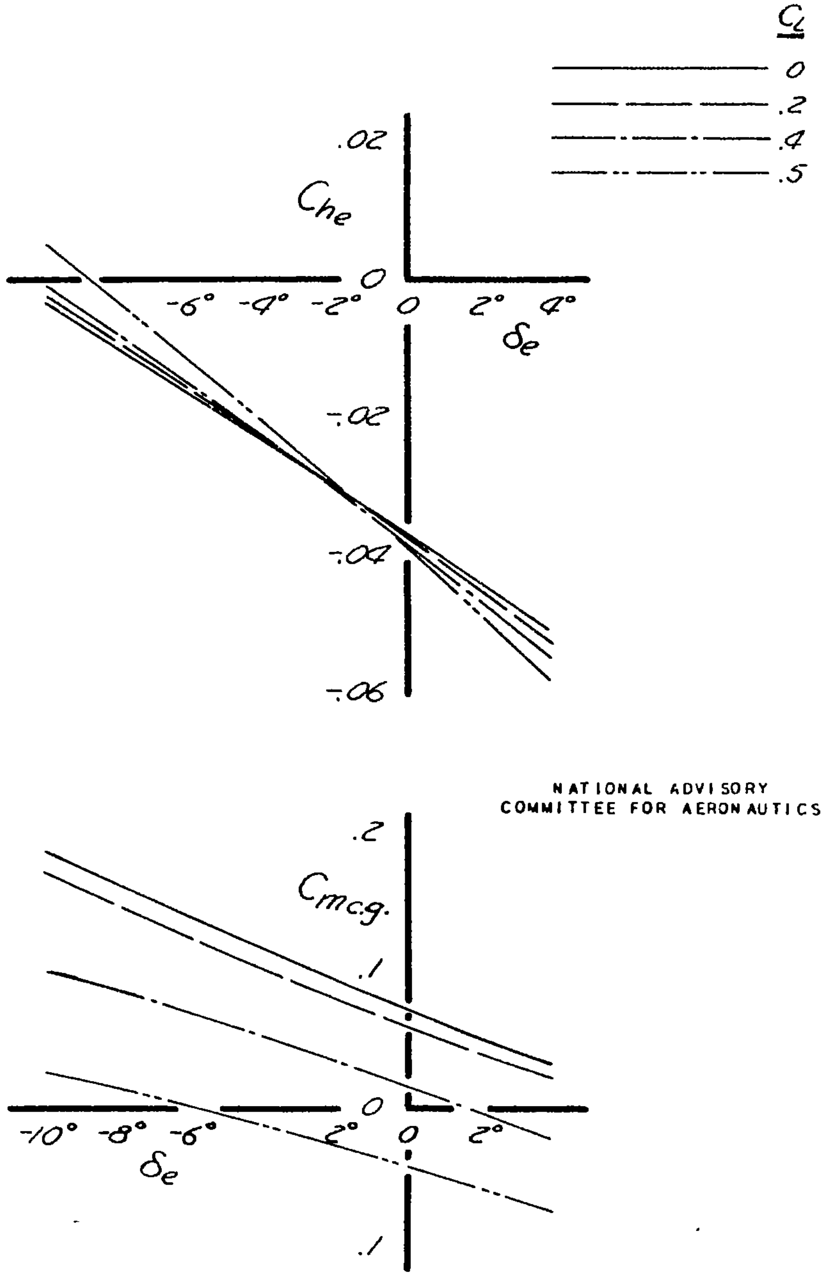

(c) M= 0.74

FIGURE 30.- (CONTINUED) 24-INCH-SPAN CONSTANT-PERCENT-CHORD SPOILERS PROJECTED 2 PERCENT

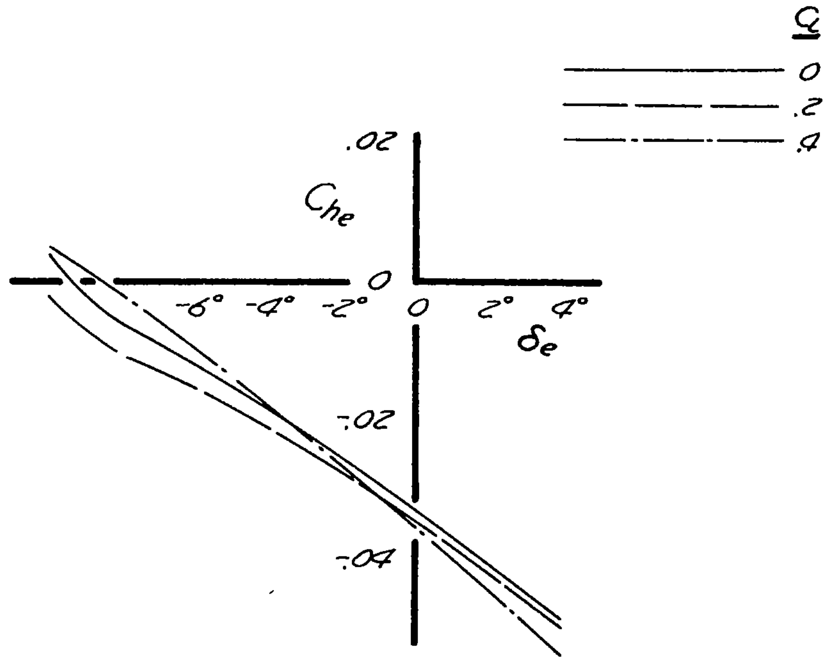

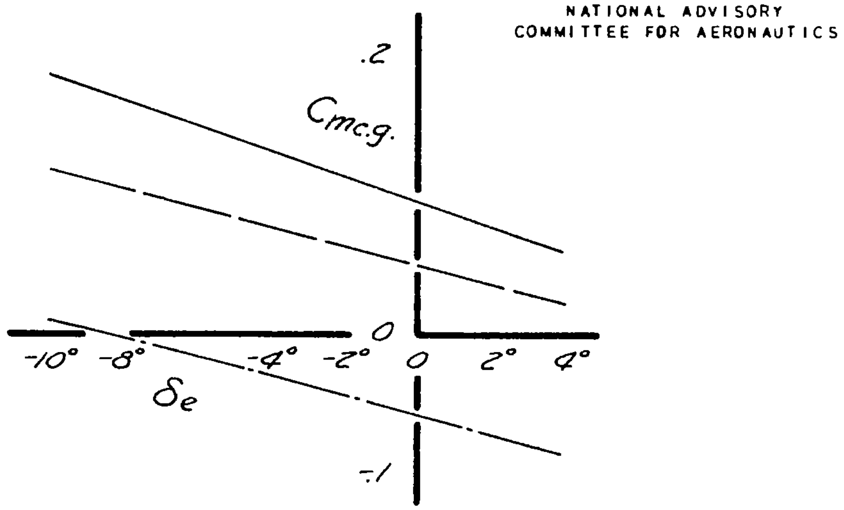

(d) M = 0.79

FIGURE 30.– (CONTINUED) 24-INCH-SPAN CONSTANT-PERCENT-CHORD SPOILERS PROJECTED 2 PERCENT

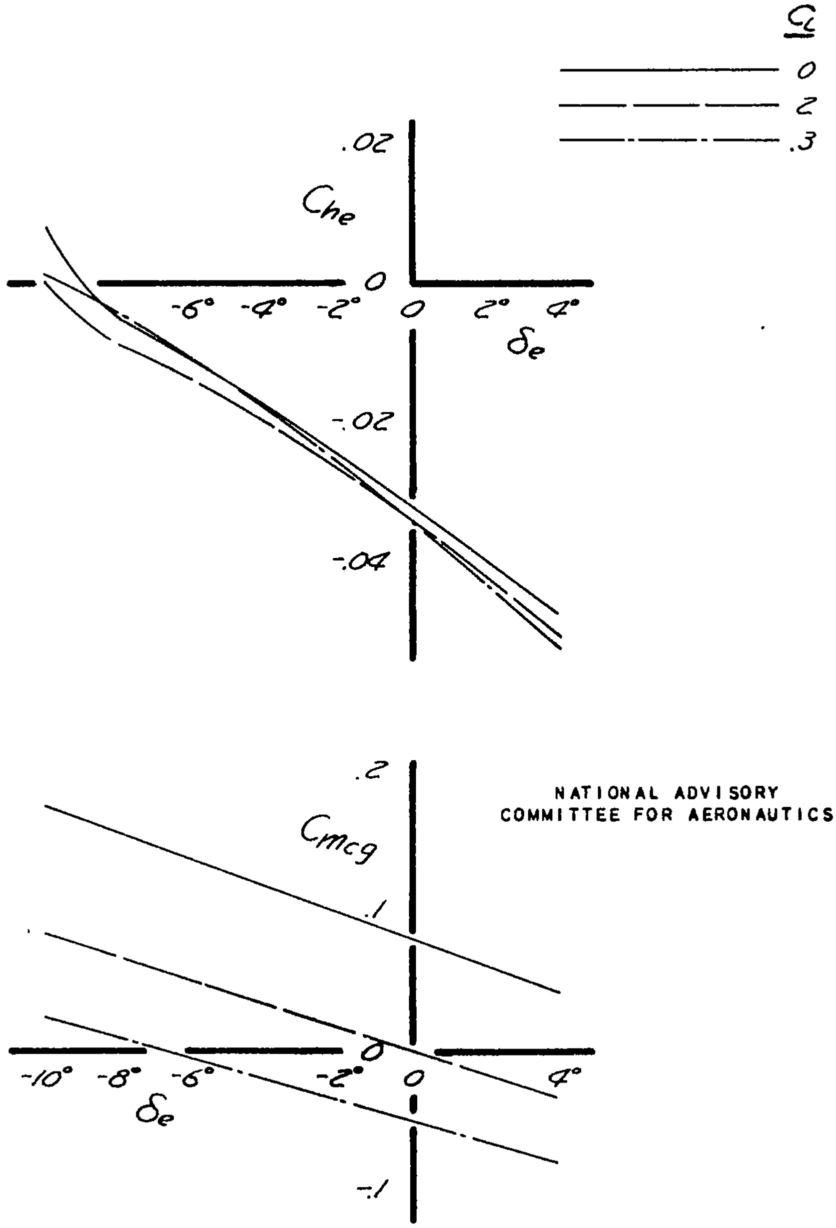

NATIONAL ADVISORY COMMITTEE FOR AERONAUTICS

(e) M = 0.815

FIGURE 30.- (CONCLUDED) 24-INCH-SPAN CONSTANT-PERCENT-CHORD SPOILERS PROJECTED 2 PERCENT

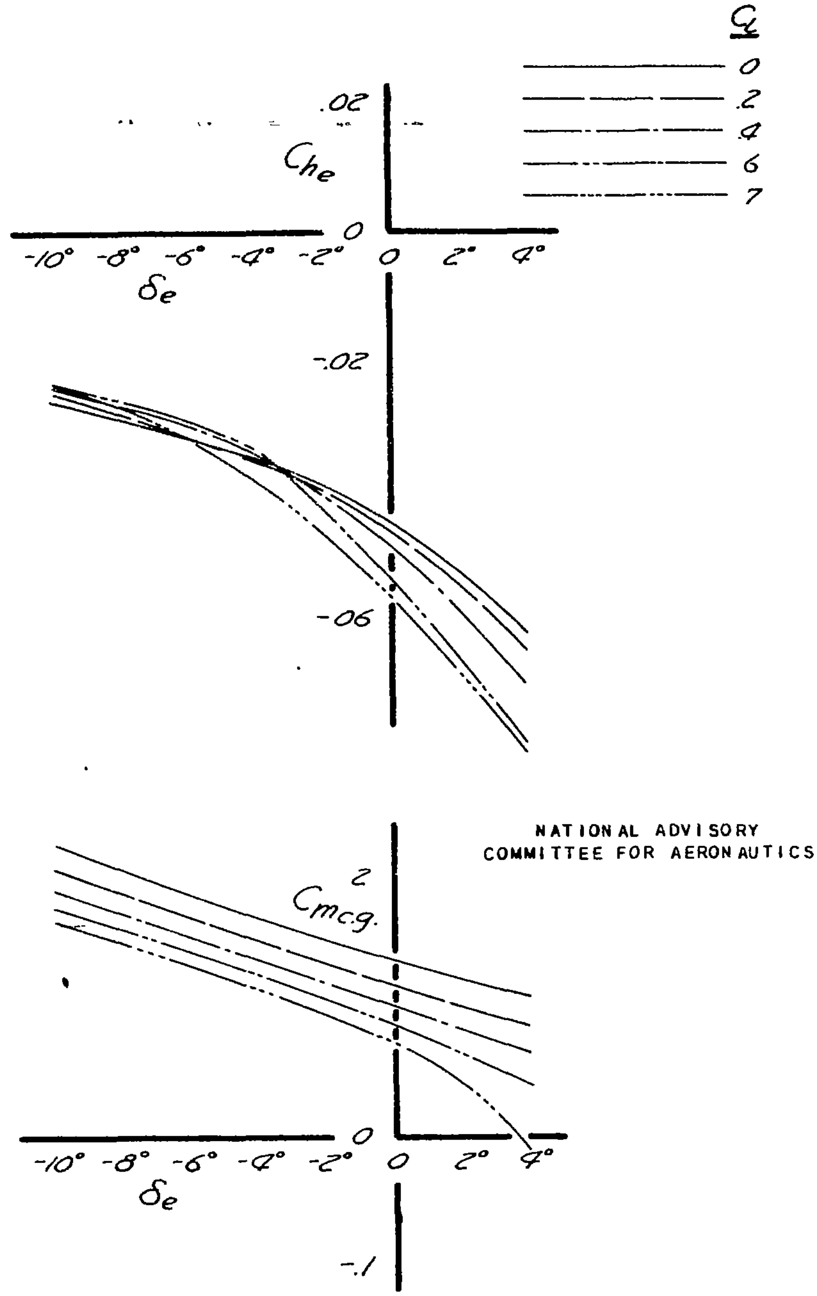

NATIONAL ADVISORY COMMITTEE FOR AERONAUTICS

FIGURE 31.—ELEVATOR CHARACTERISTICS WITH THE 24-INCH-SPAN CONSTANT-PERCENT-CHORD SPOILERS PROJECTED 4 PERCENT. MACH NUMBER OF 0.20

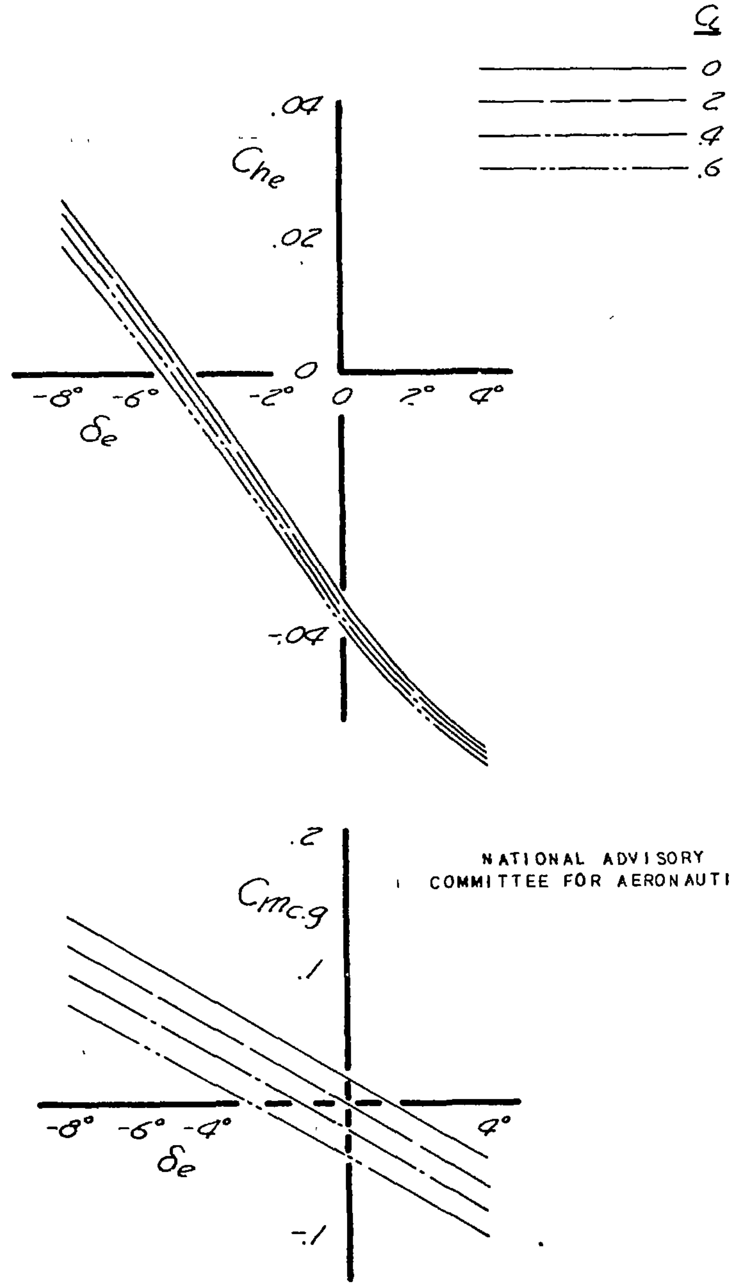

NATIONAL ADVISORY COMMITTEE FOR AERONAUTICS

(a) M = 0.20

FIGURE 32.- ELEVATOR CHARACTERISTICS WITH THE 12-INCH-SPAN CONSTANT-PERCENT-CHORD SPOILERS PROJECTED 2 PERCENT

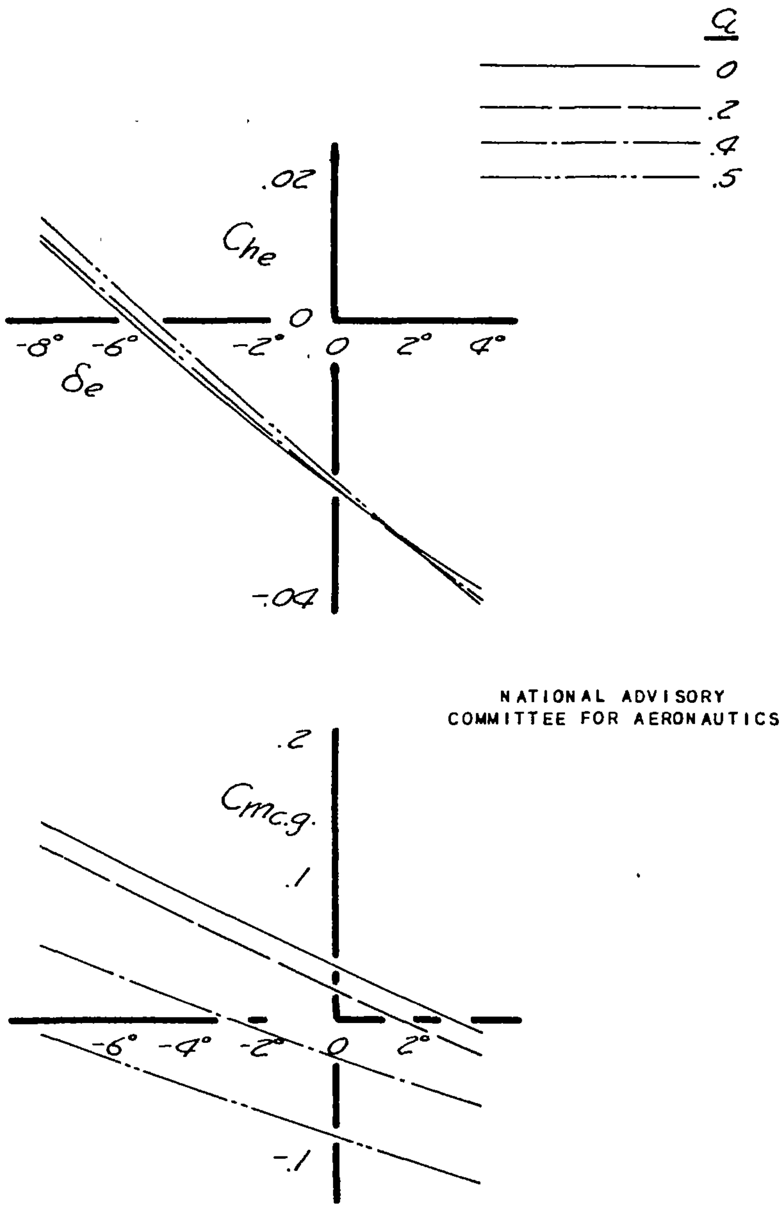

(b) M = 0.74

FIGURE 32.-(CONTINUED) 12-INCH-SPAN CONSTANT-PERCENT-CHORD SPOILERS PROJECTED 2 PERCENT.

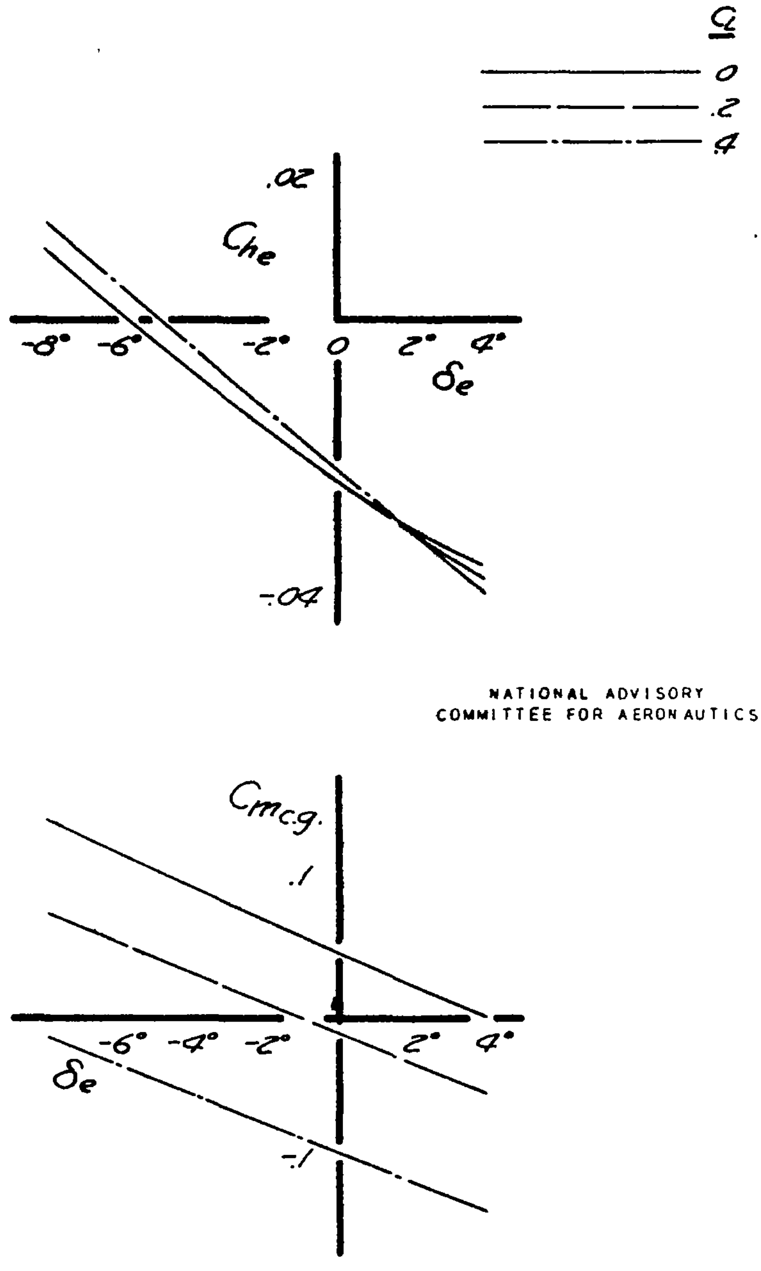

(c) M = 0.79.

FIGURE 32.-(CONTINUED) 12-INCH-SPAN CONSTANT-PERCENT-CHORD SPOILERS PROJECTED 2 PERCENT.

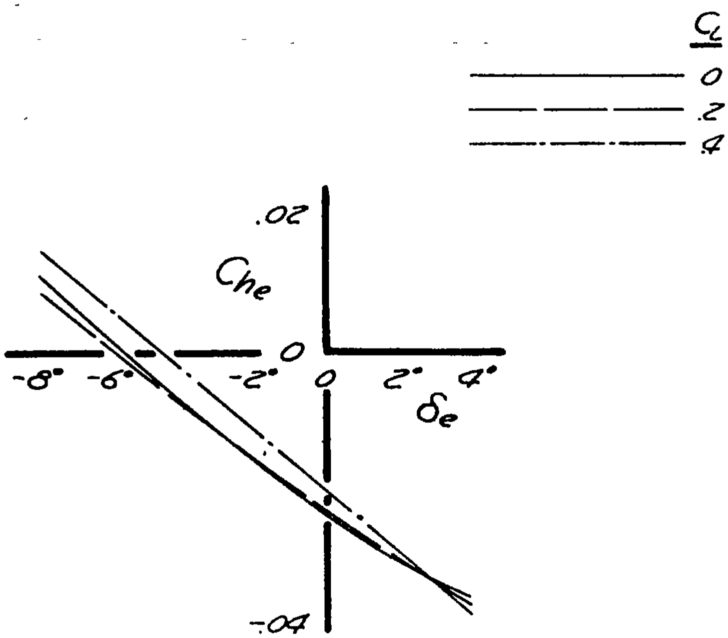

NATIONAL ADVISORY
COMMITTEE FOR AERONAUTICS

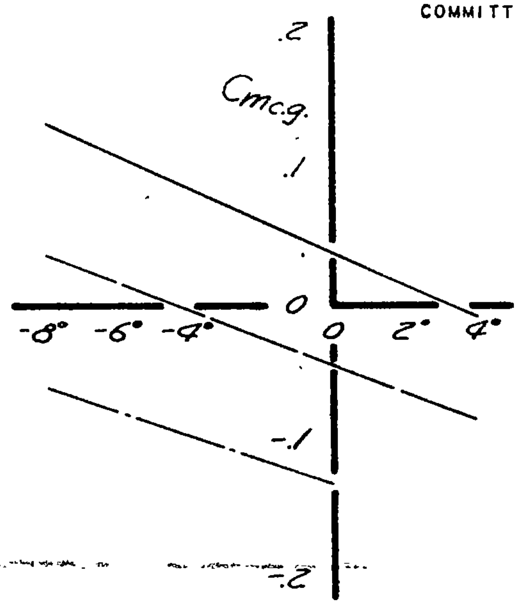

(d) M = 0.815

FIGURE 32.- (CONCLUDED) 12-INCH-SPAN CONSTANT-PERCENT-CHORD SPOILERS PROJECTED 2 PERCENT.

———— Using data from tests of spoilers and 0.6-inch-chord flaps. Projected normal heights of approximately 2 percent of the tail chord, various spans.
— — — 1.2-by 12-inch flaps, various deflections
- - - - - 0.6-by 12-inch flaps, various deflections

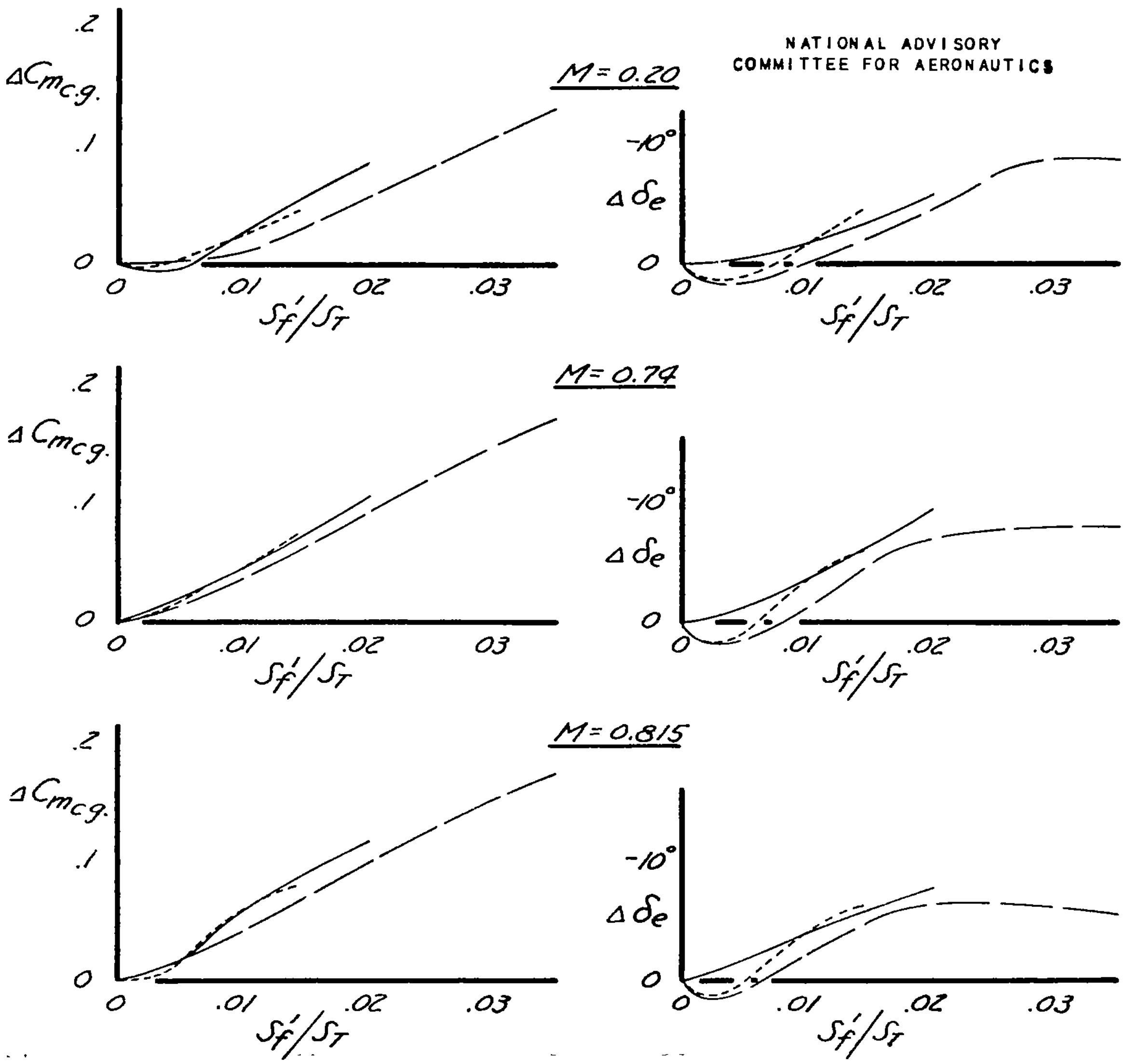

Figure 33.– Increment of pitching-moment coefficient at $C_L = 0$ and $\delta_e = 0$, and of elevator floating angle at $C_L = 0$, as a function of the projected area of the flaps normal to the stabilizer surface.

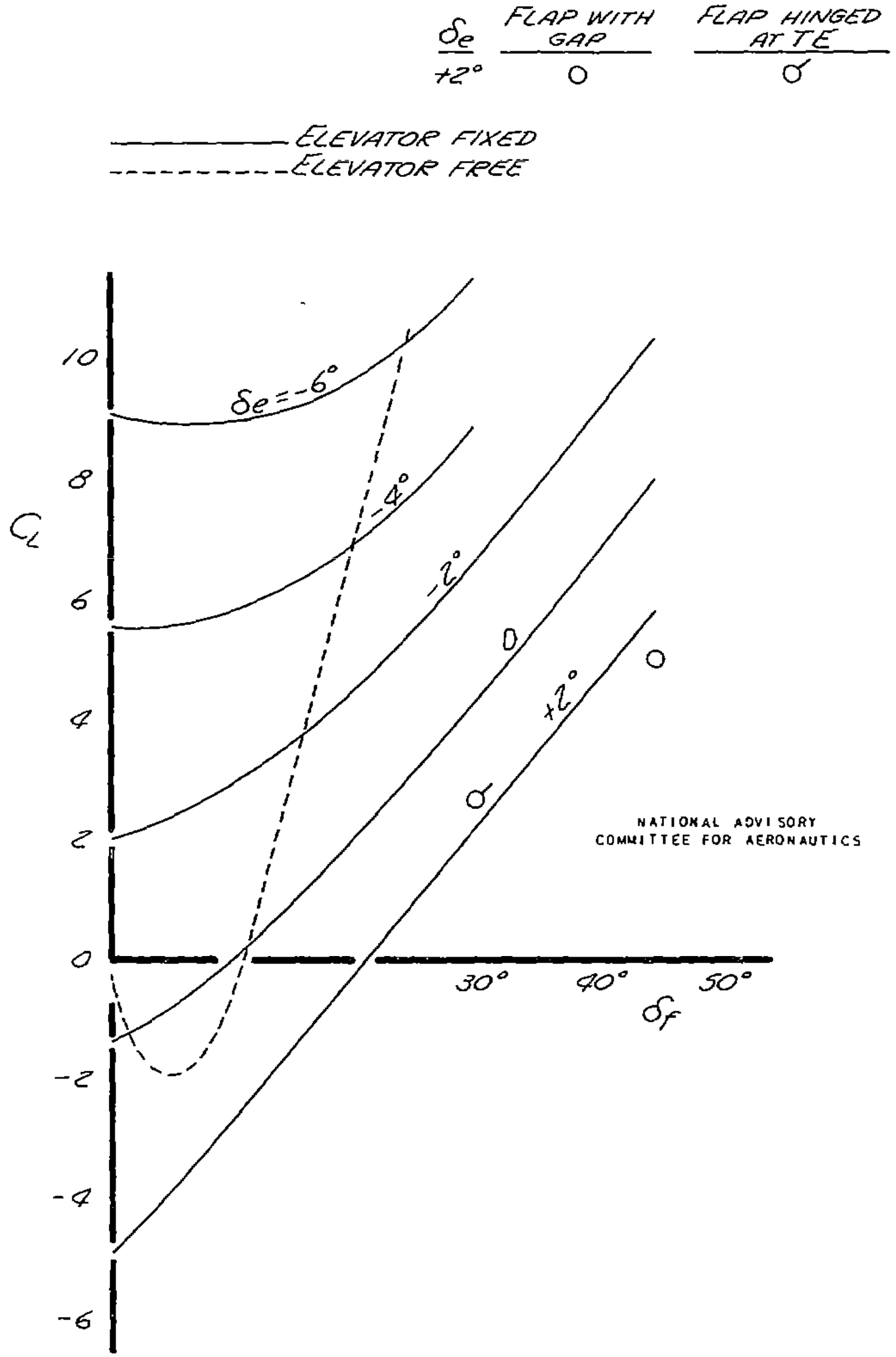

(a) M = 0.20

FIGURE 34 - VARIATION OF BALANCE LIFT COEFFICIENT WITH DEFLECTION OF THE 1.2- BY 12-INCH FLAPS

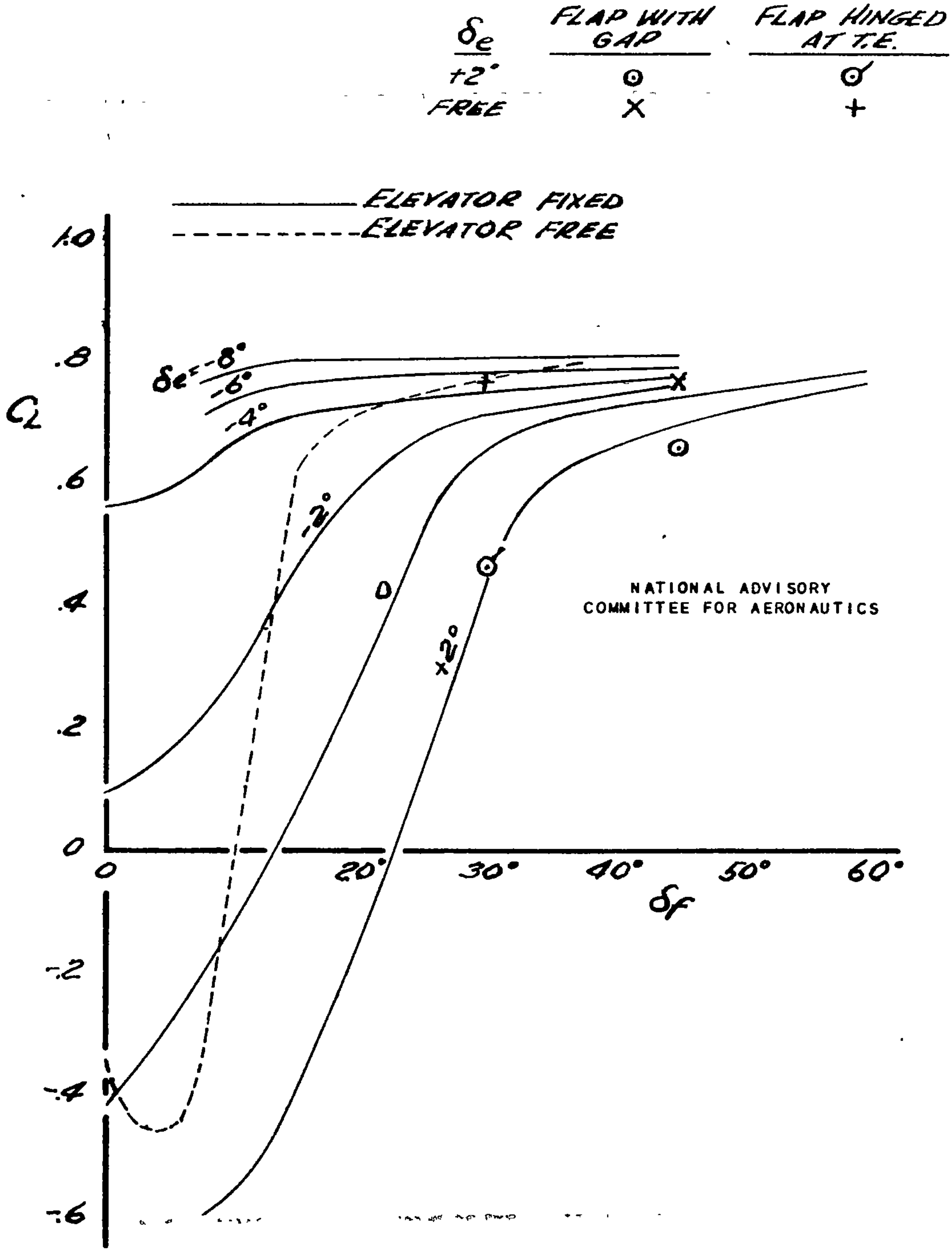

(b) M = 0.60

FIGURE 34.-(CONTINUED) 1.2-BY 12-INCH FLAPS

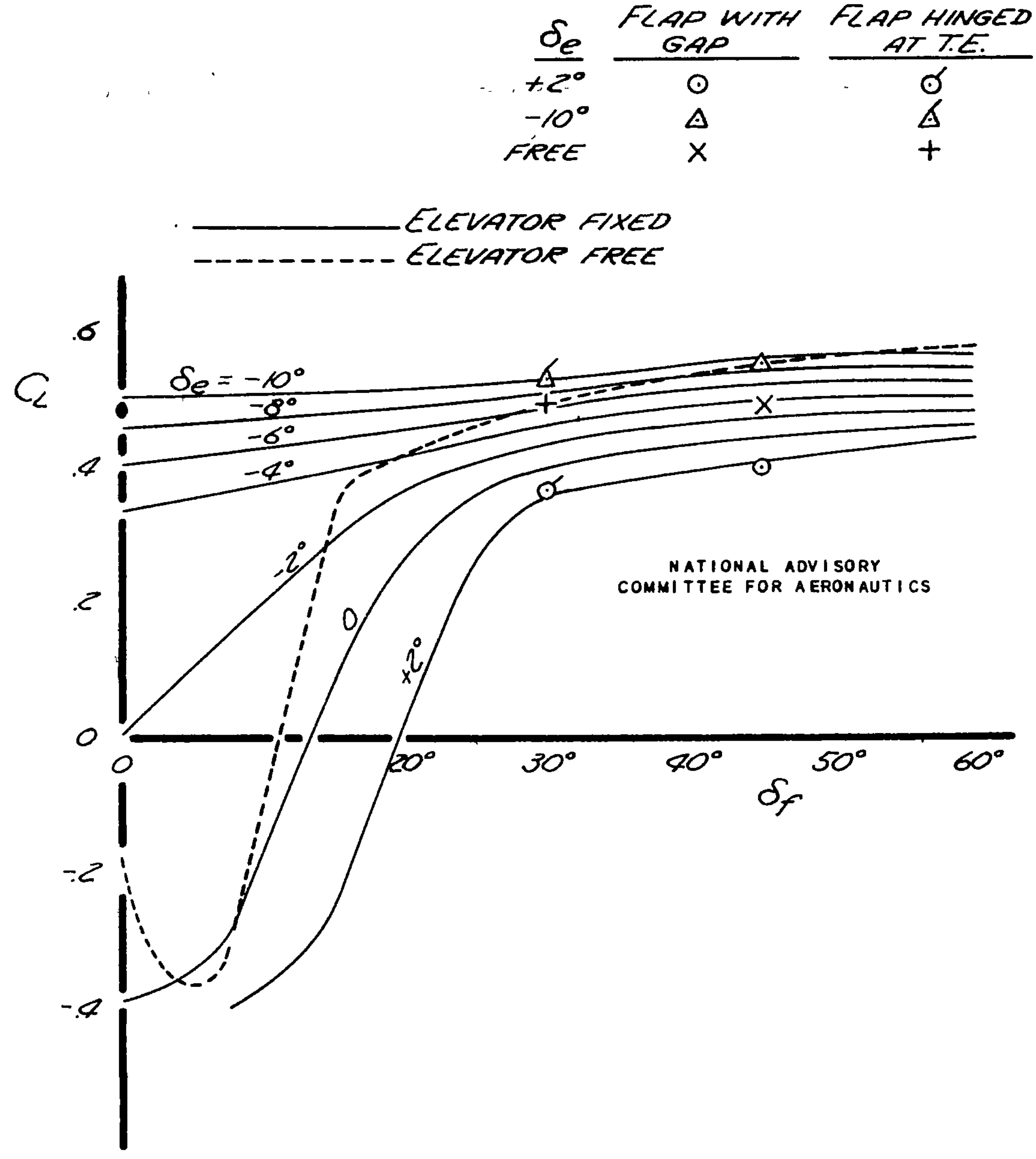

(c) M = 0.74

FIGURE 34.- (CONTINUED) 1.2- BY 12-INCH FLAPS

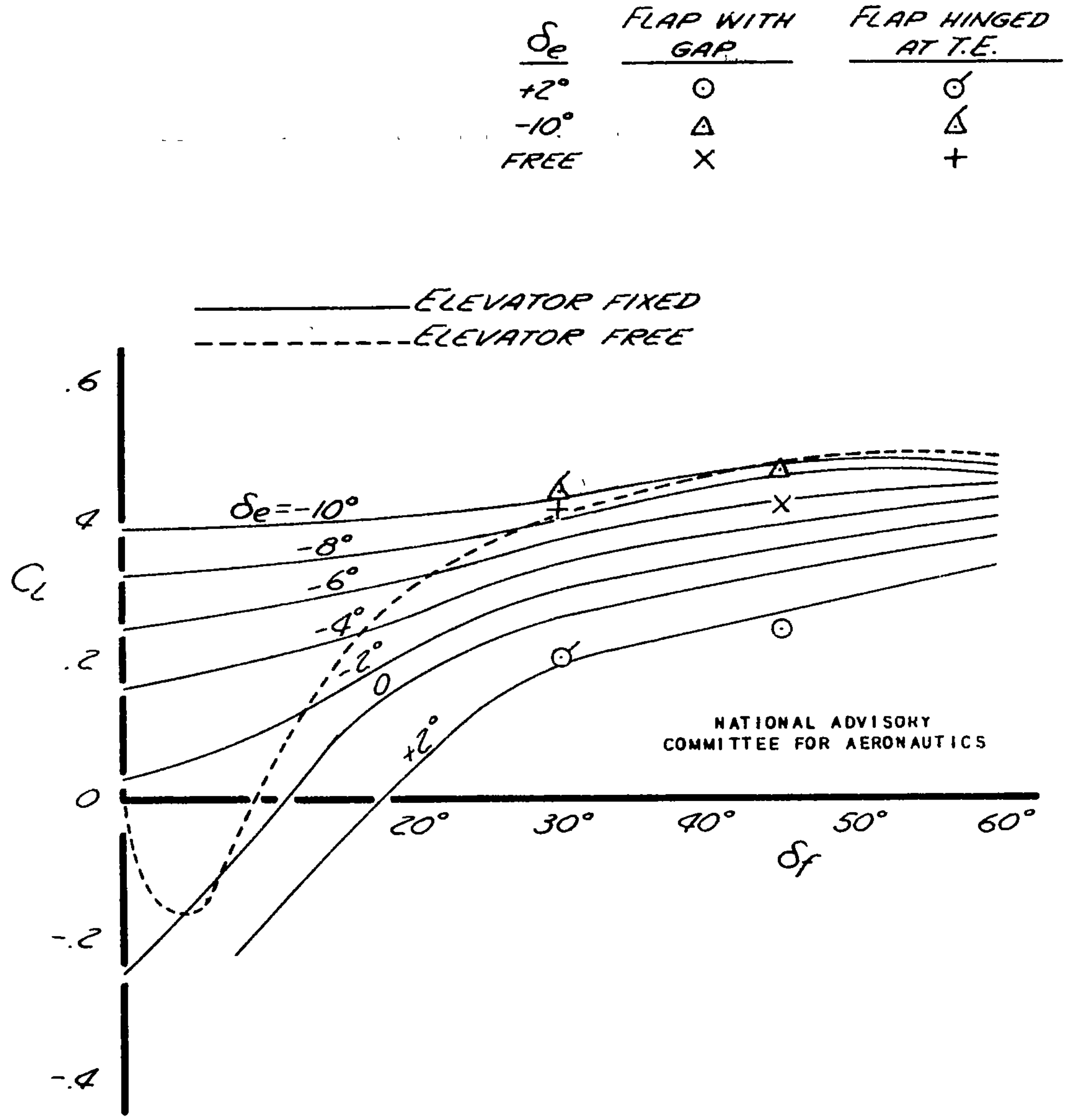

(d) M = 0.79

FIGURE 39.- (CONTINUED) 1.2- BY 12-INCH FLAPS

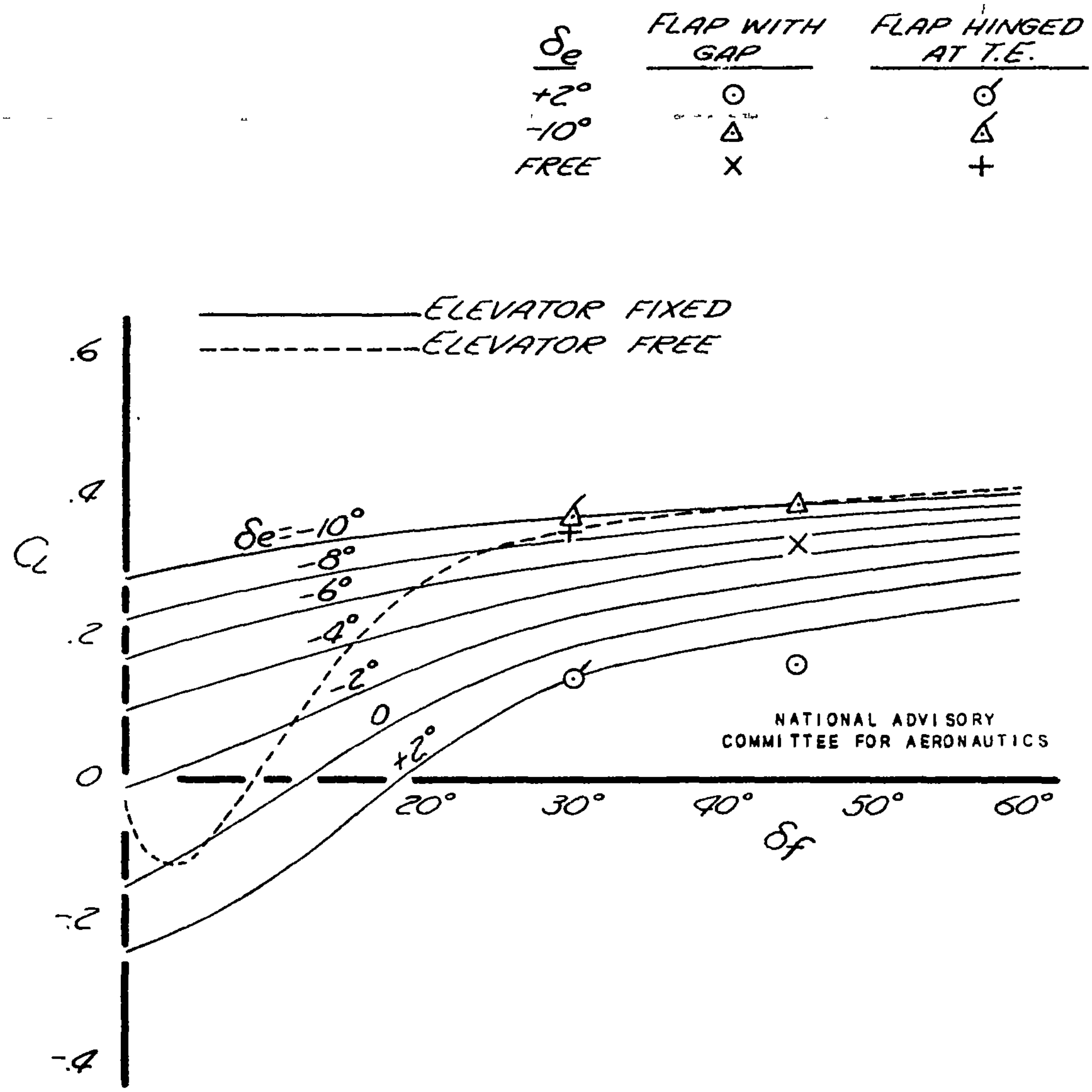

(e) M = 0.815

FIGURE 34.-(CONCLUDED) 1.2- BY 12-INCH FLAPS

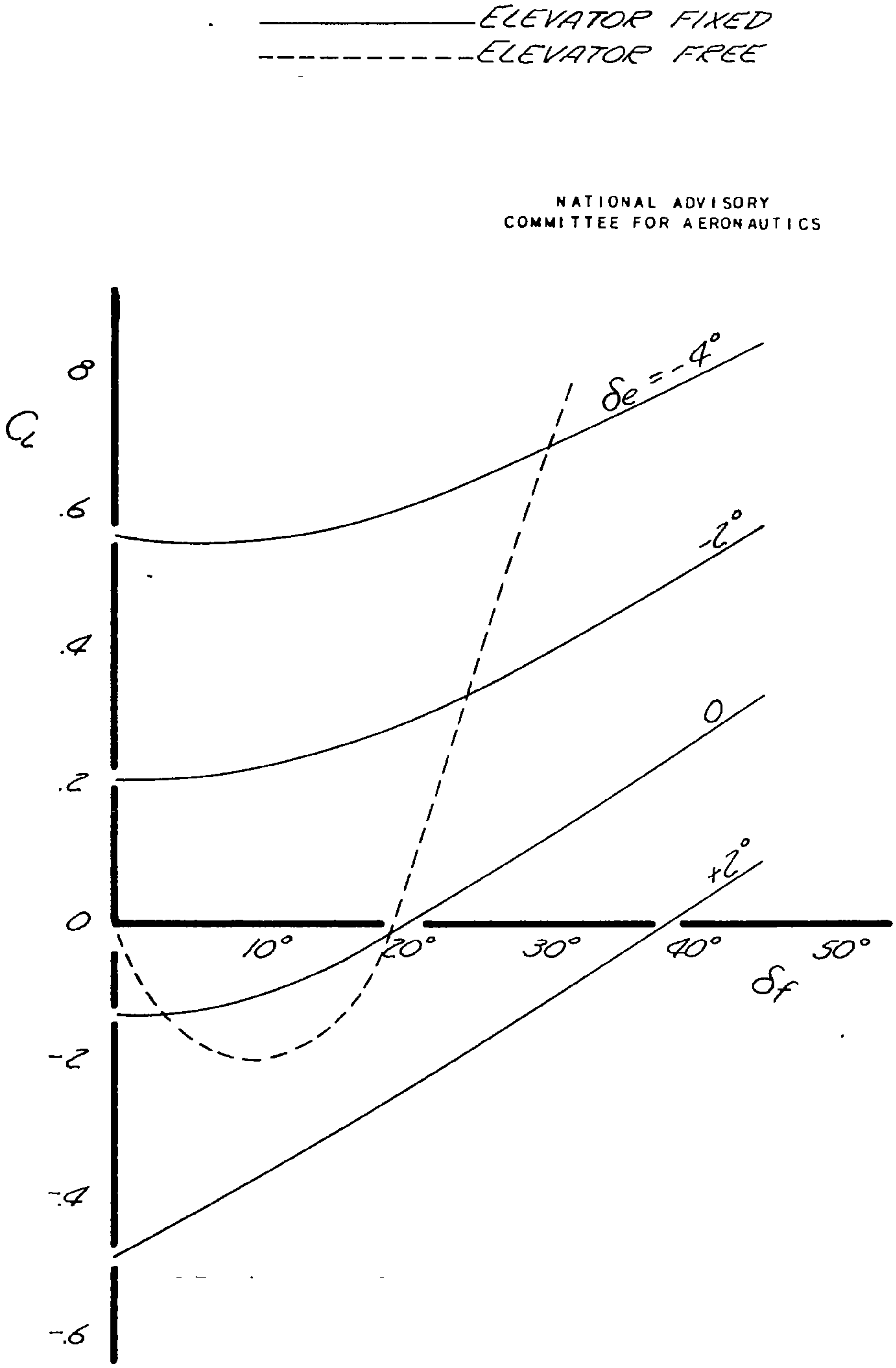

(a) M = 0.20

FIGURE 35.- VARIATION OF BALANCE LIFT COEFFICIENT WITH DEFLECTION OF THE 0.6- BY 12-INCH FLAPS

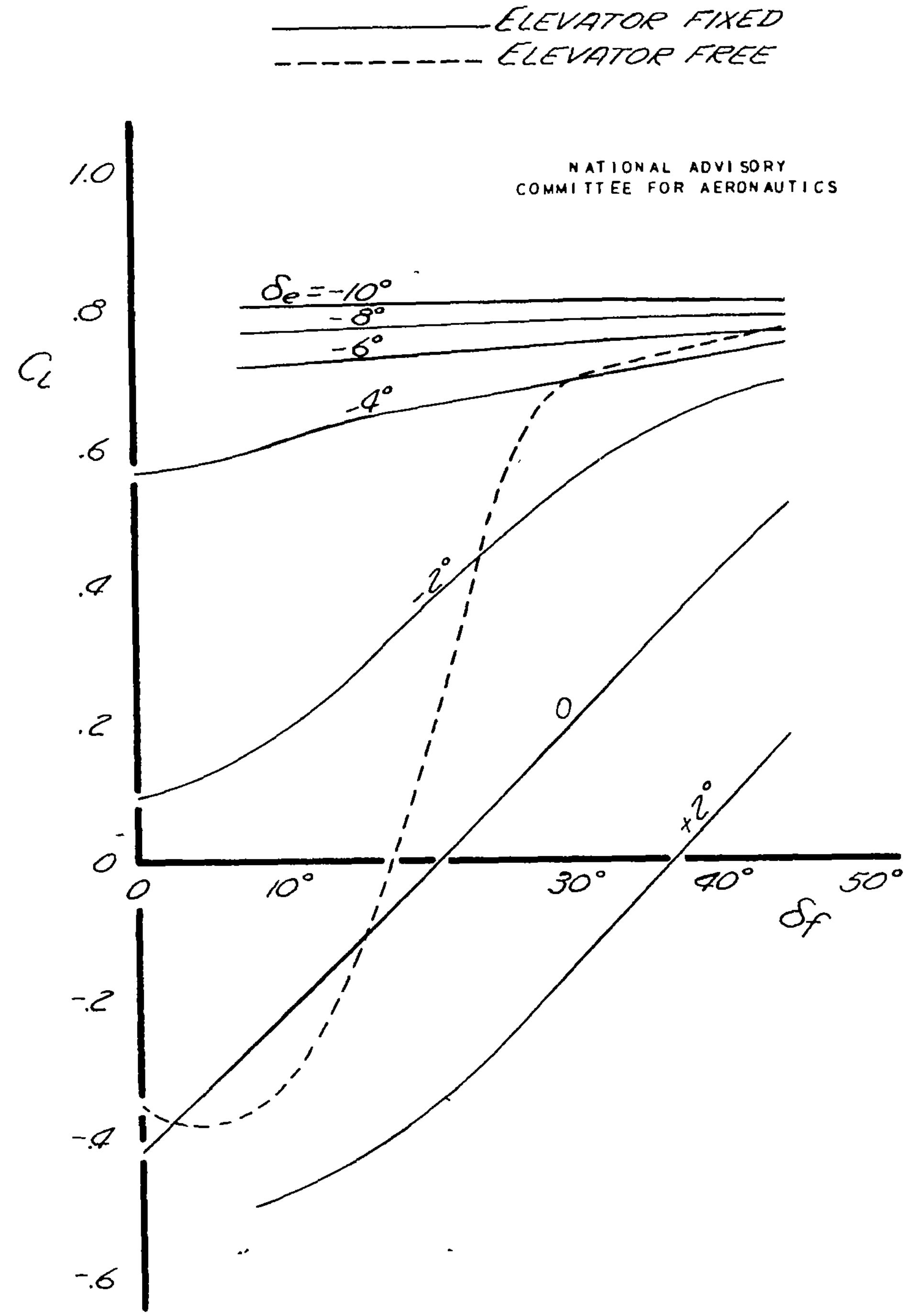

(b) M = 0.60

FIGURE 35.-(CONTINUED) 0.6- BY 12-INCH FLAPS

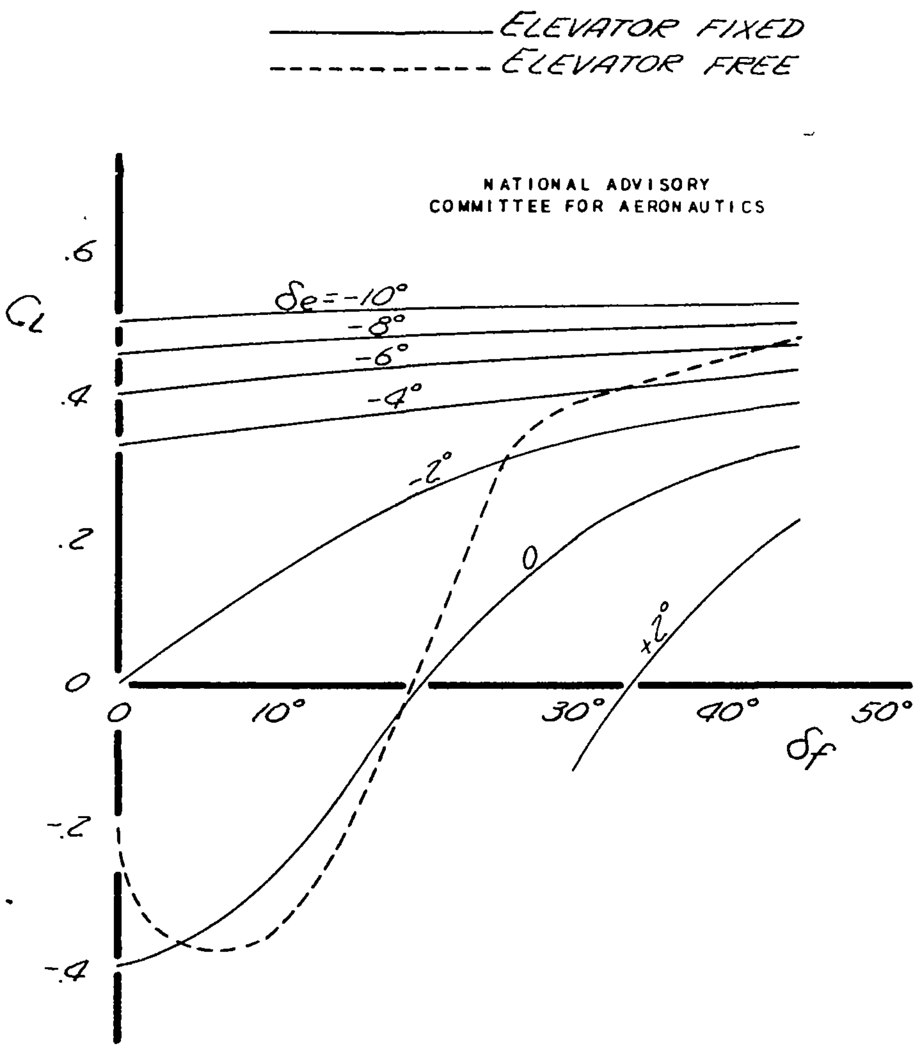

(c) $M = 0.74$

FIGURE 35.- (CONTINUED) 0.6- BY 12- INCH FLAPS

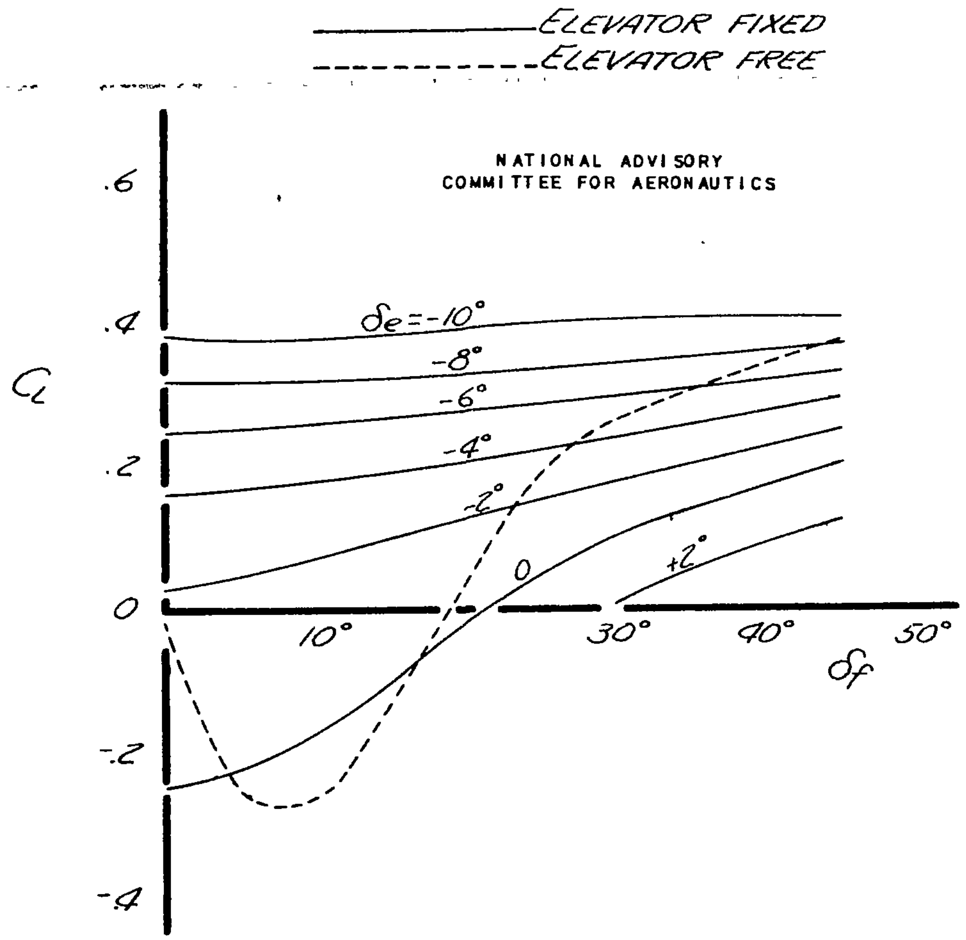

(d) $M = 0.79$

FIGURE 35.—(CONTINUED) 0.6-BY 12-INCH FLAPS

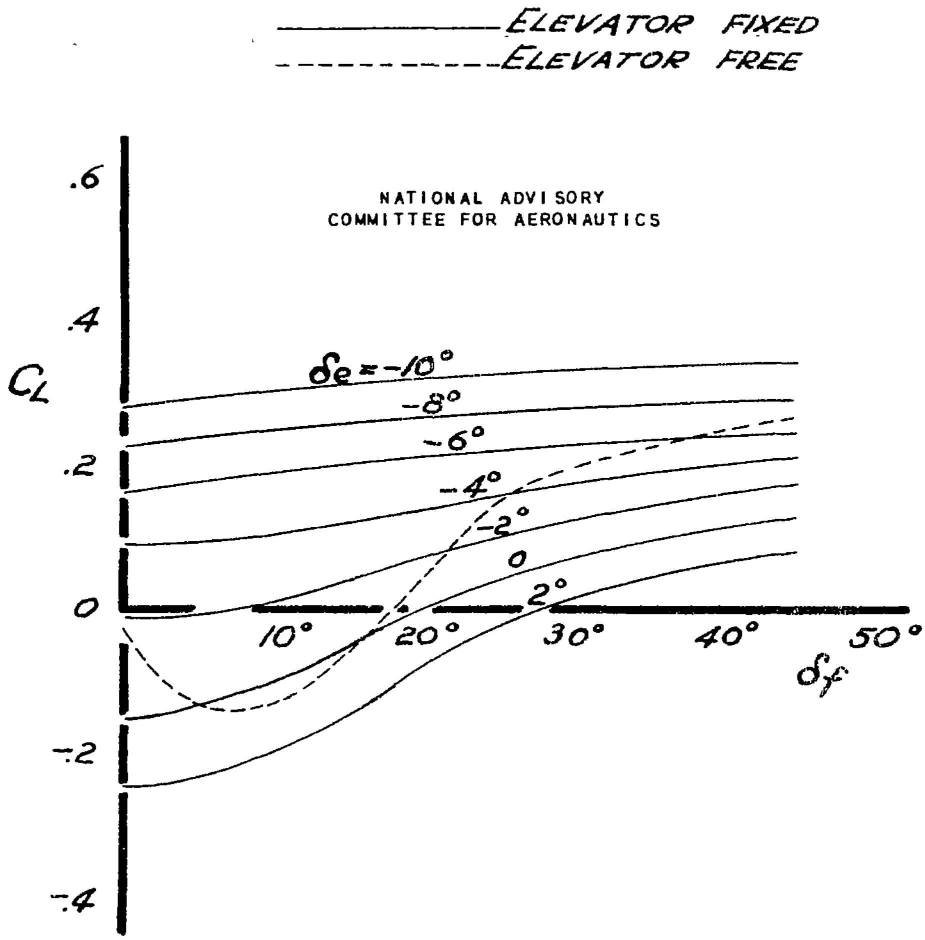

(e) $M = 0.815$

FIGURE 35.-(CONCLUDED) 0.6- BY 12-INCH FLAPS.

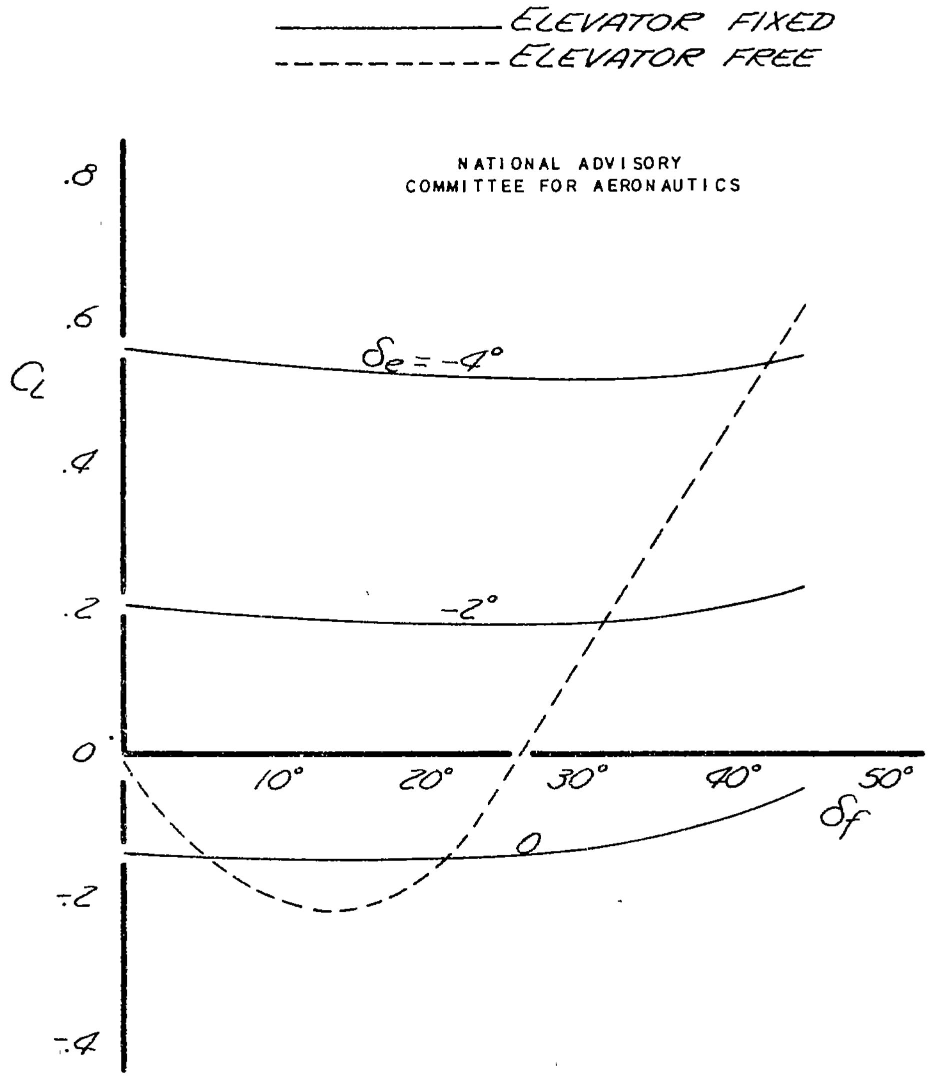

(a) M = 0.20

FIGURE 36.- VARIATION OF BALANCE LIFT COEFFICIENT WITH DEFLECTION OF THE 0.6- BY 6-INCH FLAPS

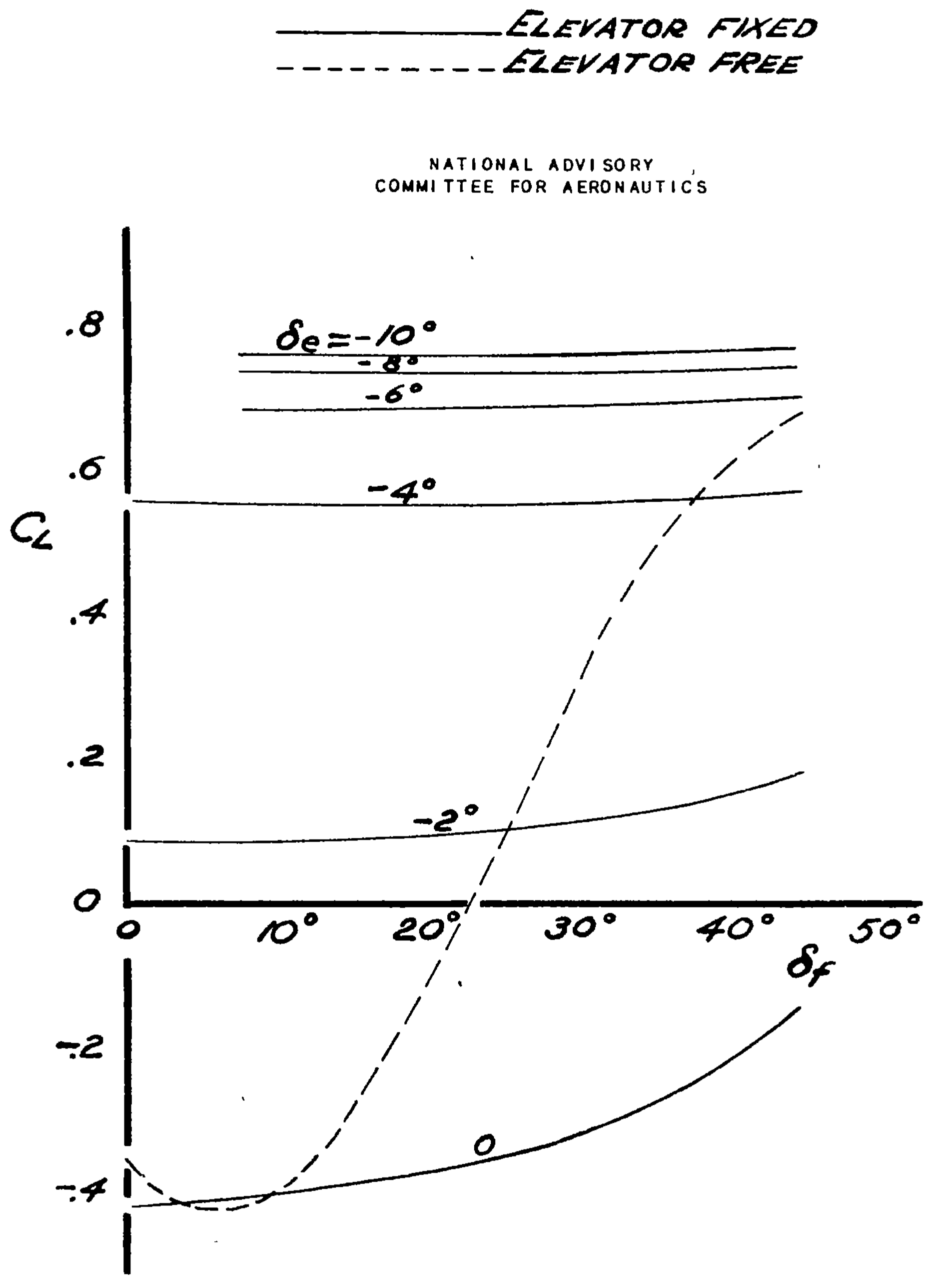

(b) M = 0.60

FIGURE 36.- (CONTINUED) 0.6-BY 6-INCH FLAPS

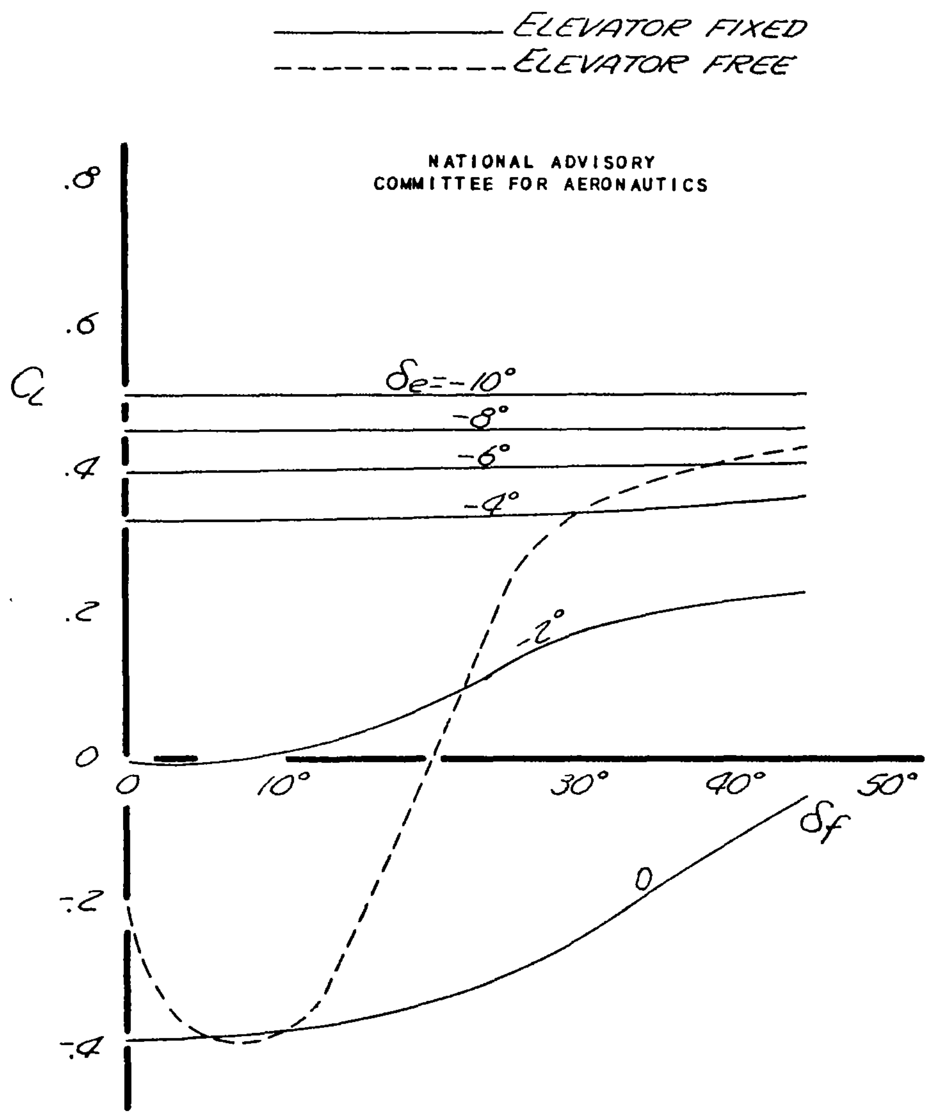

(c) $M = 0.74$

FIGURE 36.- (CONTINUED) 0.6- BY 6-INCH FLAPS

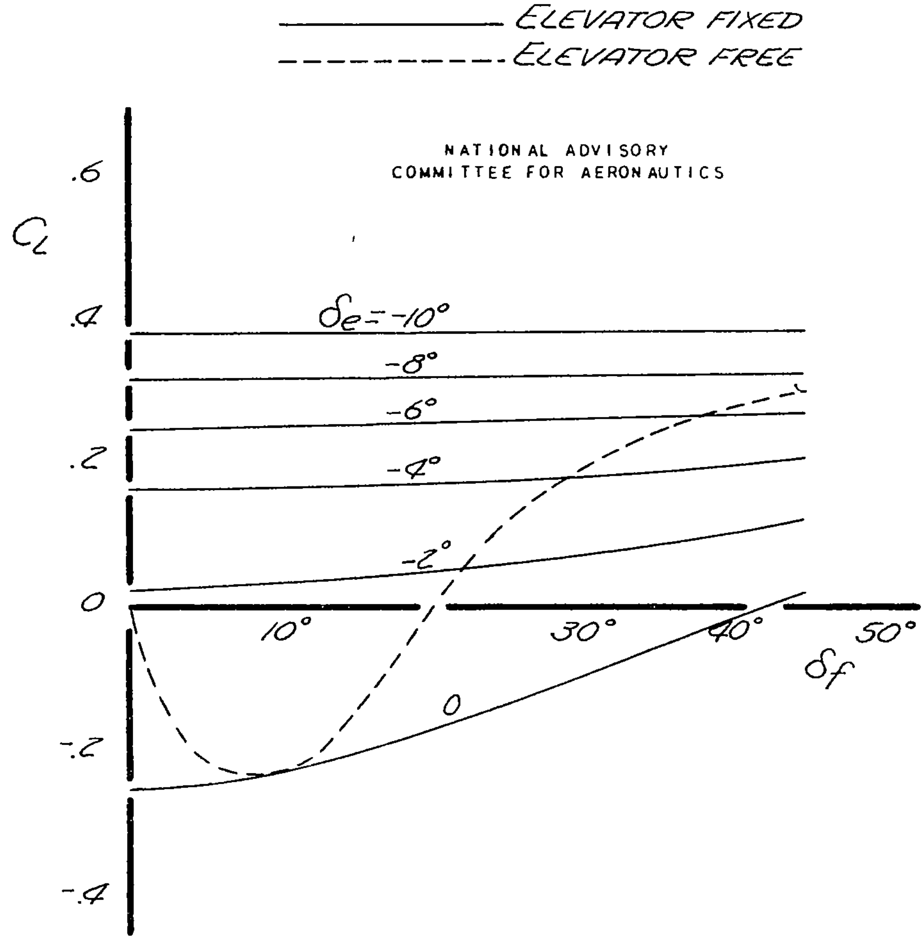

(d) M = 0.79

FIGURE 36.- (CONTINUED) 0.6-BY 6-INCH FLAPS

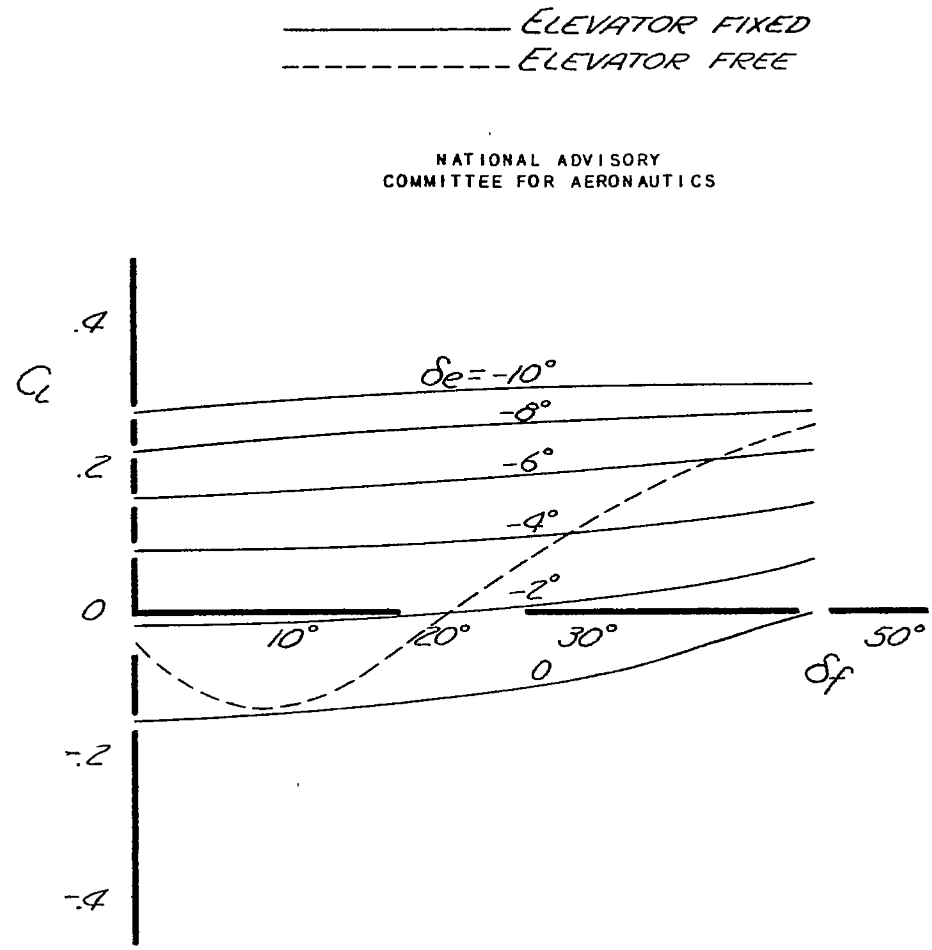

(e) M = 0.815

FIGURE 36.- (CONCLUDED) 0.6-BY 6-INCH FLAPS

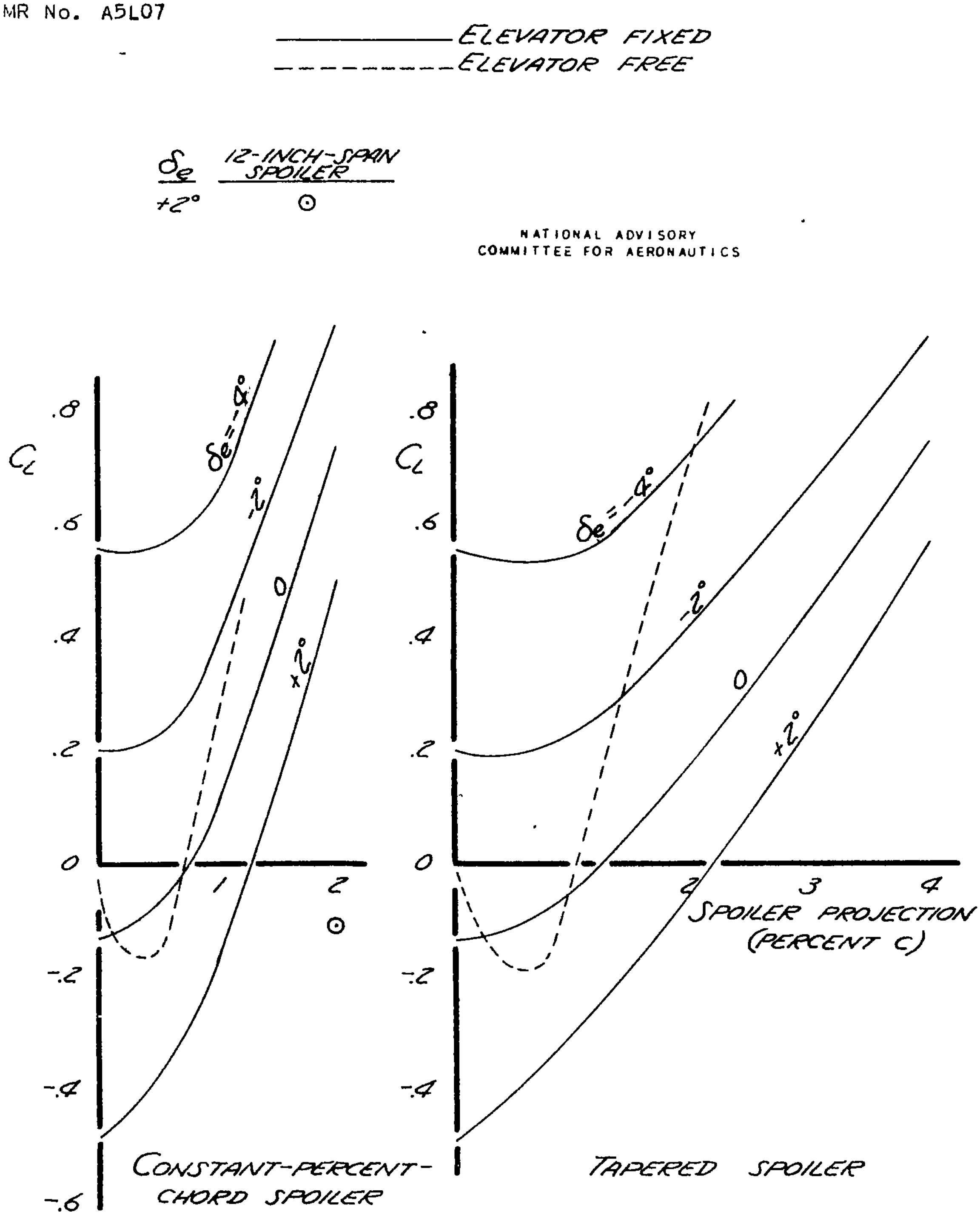

(a) M = 0.20

FIGURE 37.- VARIATION OF BALANCE LIFT COEFFICIENT WITH PROJECTION OF THE 24-INCH SPAN SPOILERS.

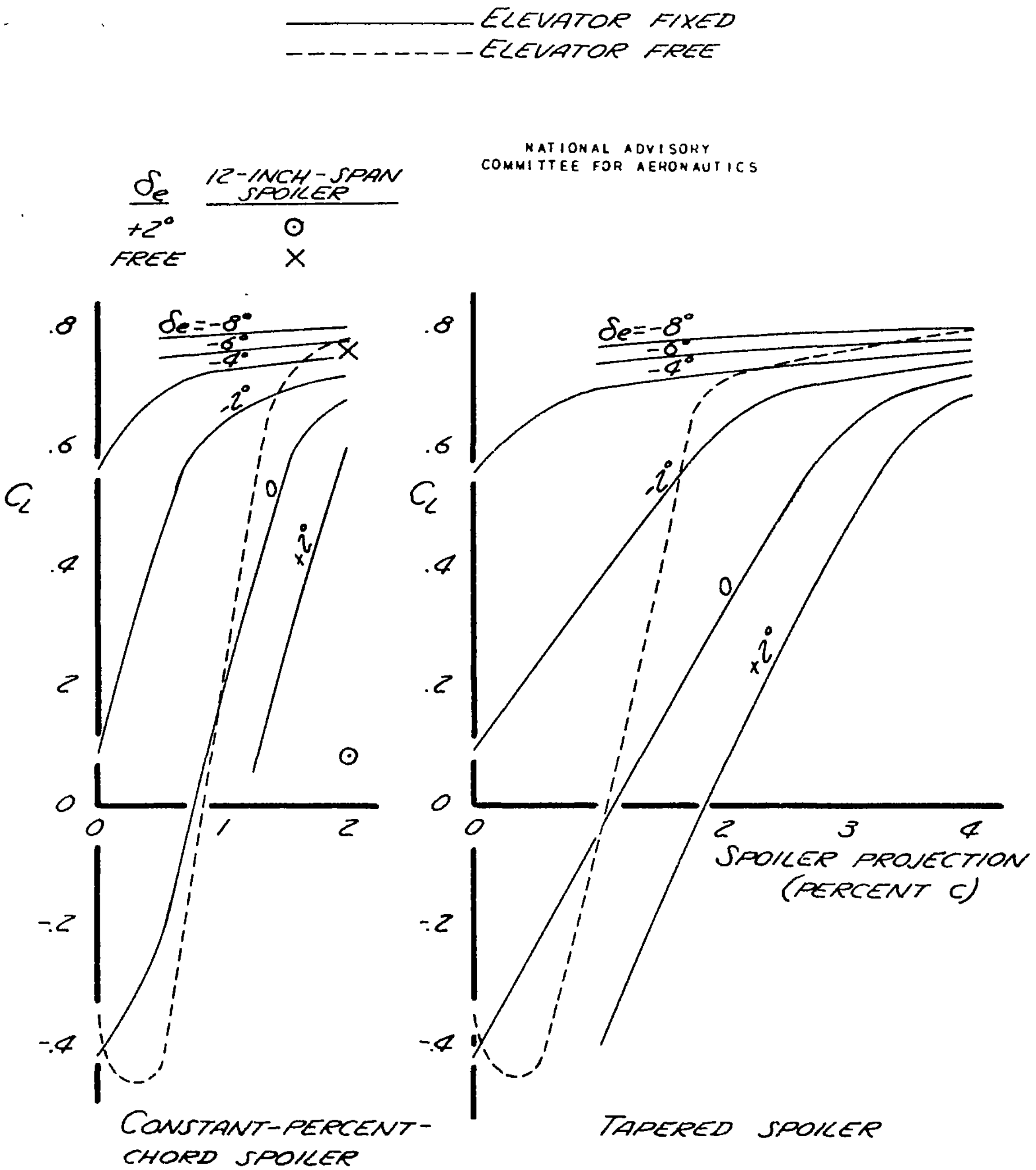

(b) M = 0.60

FIGURE 37.- (CONTINUED) 24-INCH-SPAN SPOILERS

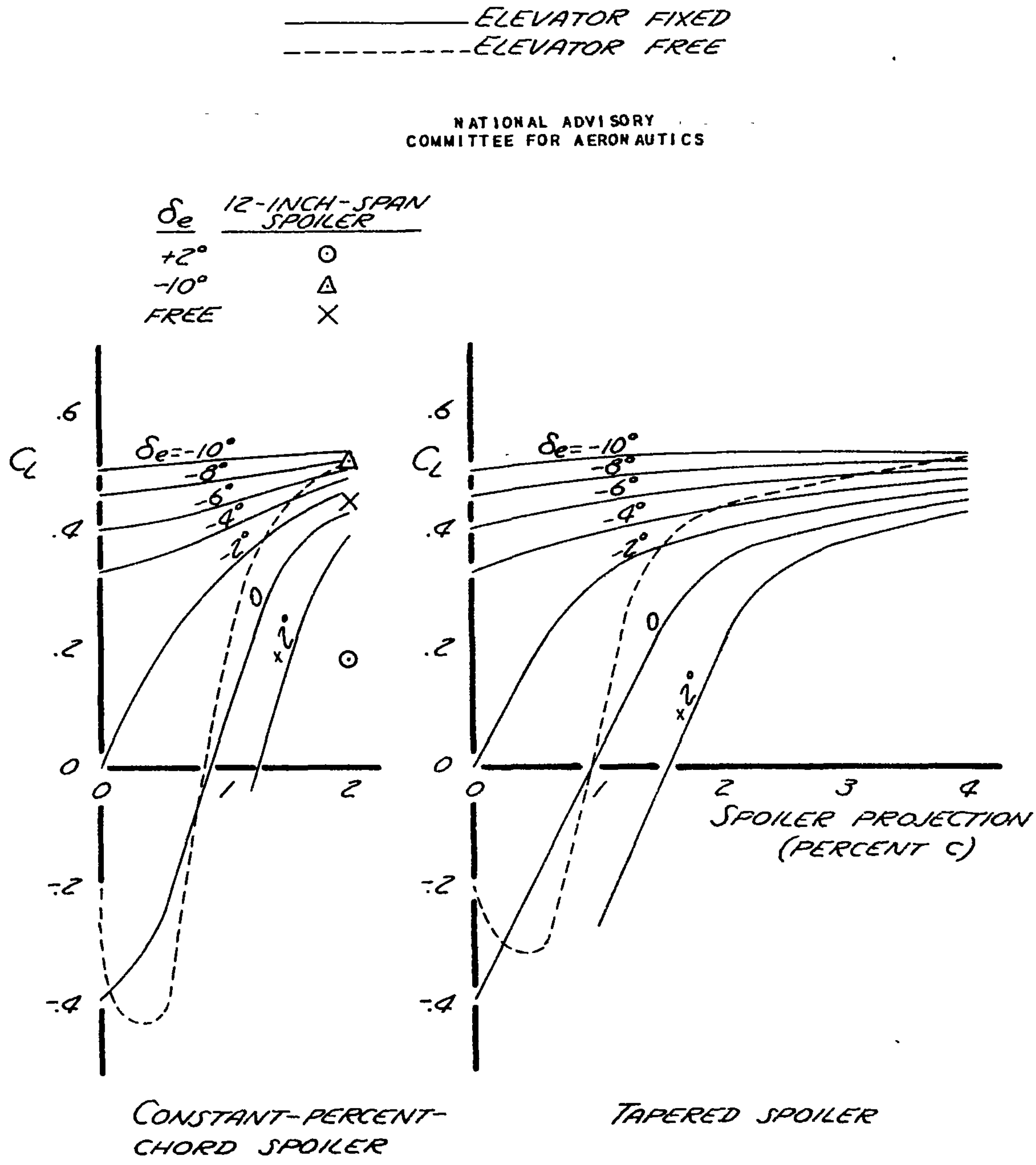

(c) M = 0.74

FIGURE 37.-(CONTINUED) 24-INCH SPAN SPOILERS

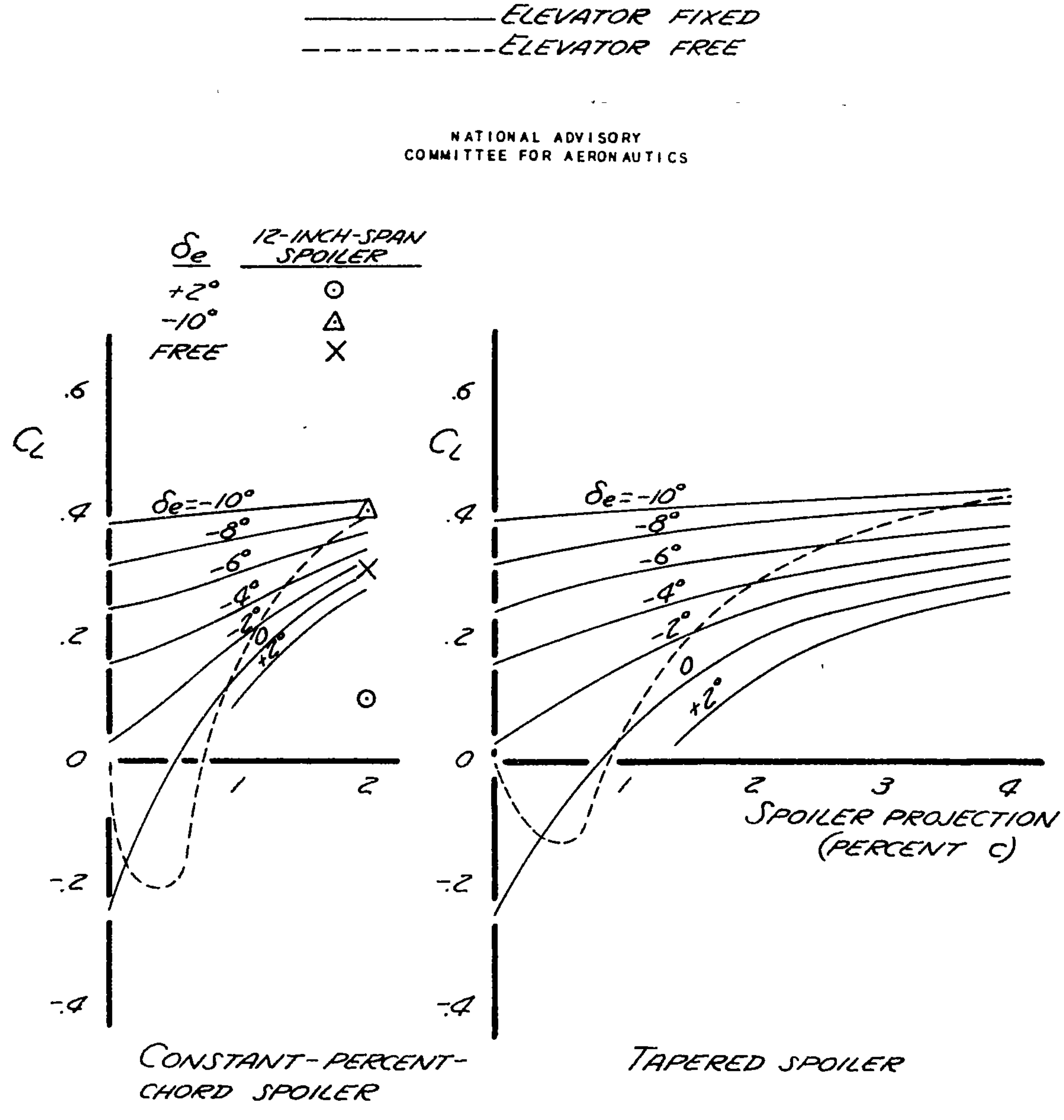

(d) M = 0.79

FIGURE 37.- (CONTINUED) 24-INCH-SPAN SPOILERS

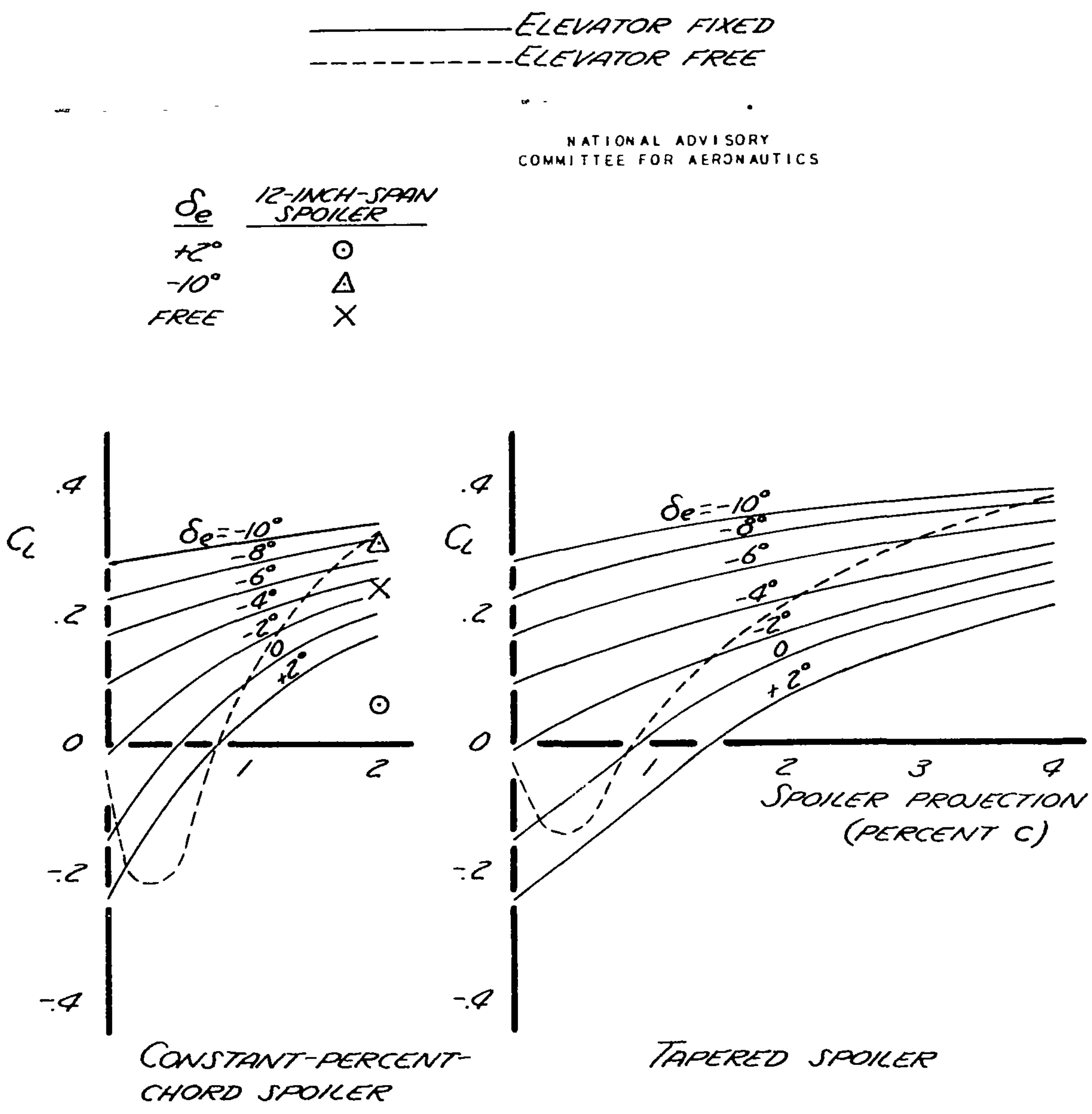

(e) M = 0.815

FIGURE 37.-(CONCLUDED) 24-INCH-SPAN SPOILERS

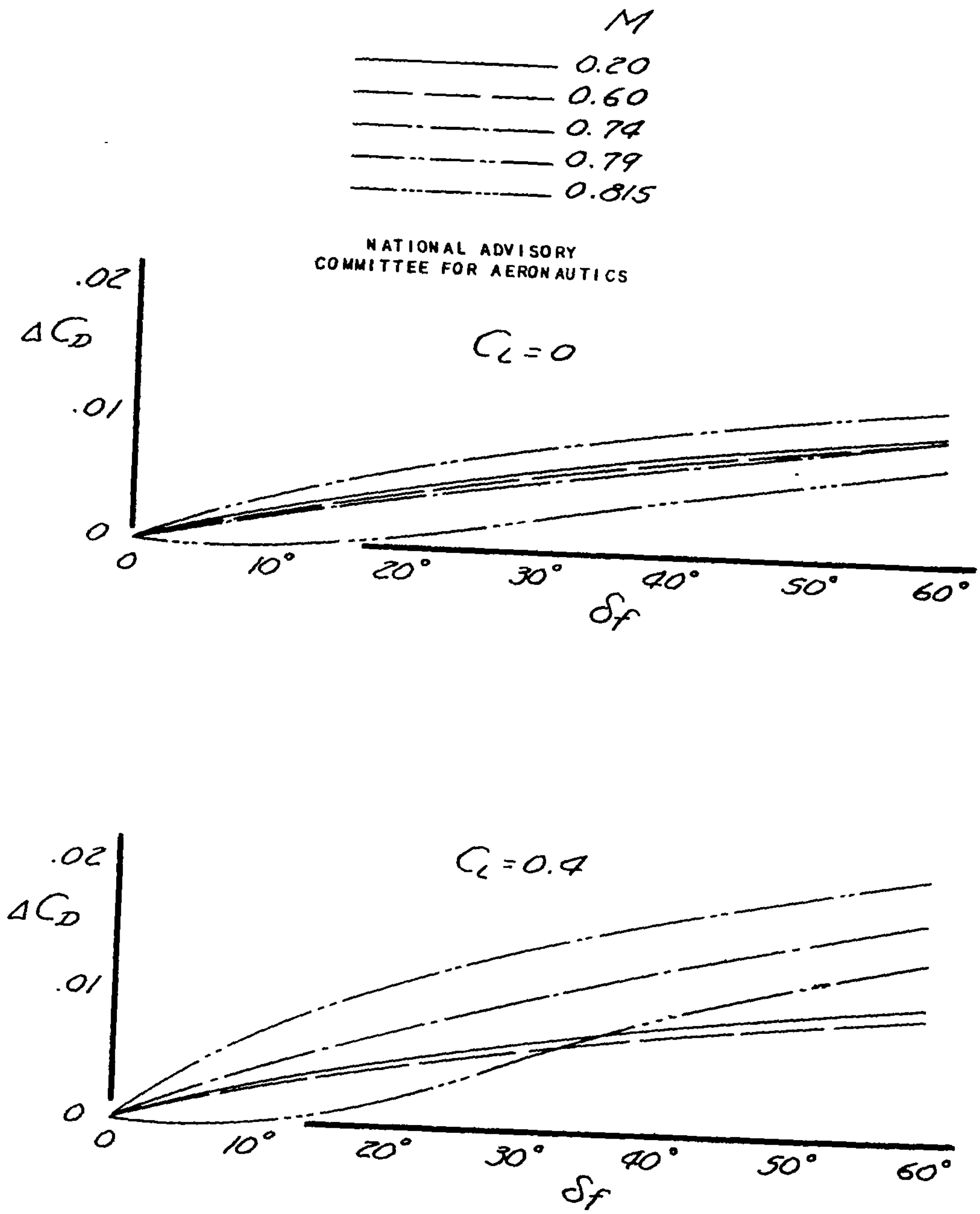

FIGURE 38.- INCREASE OF DRAG COEFFICIENT DUE TO DEFLECTION OF THE 1.2- BY 12-INCH FLAPS, $\delta_e = 0°$

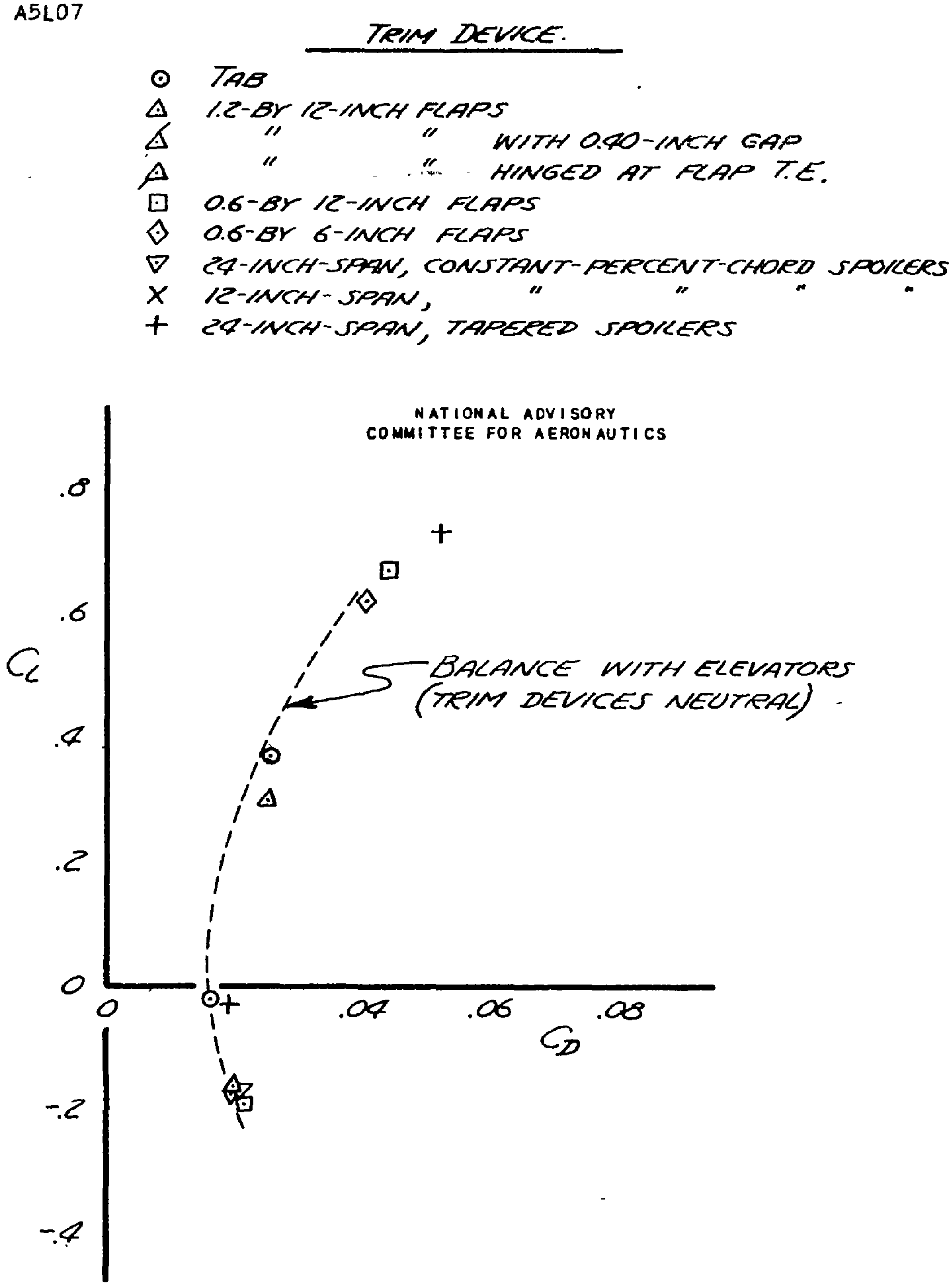

(a) $M = 0.20$

FIGURE 39.- VARIATION OF DRAG COEFFICIENT WITH TRIM LIFT COEFFICIENT.

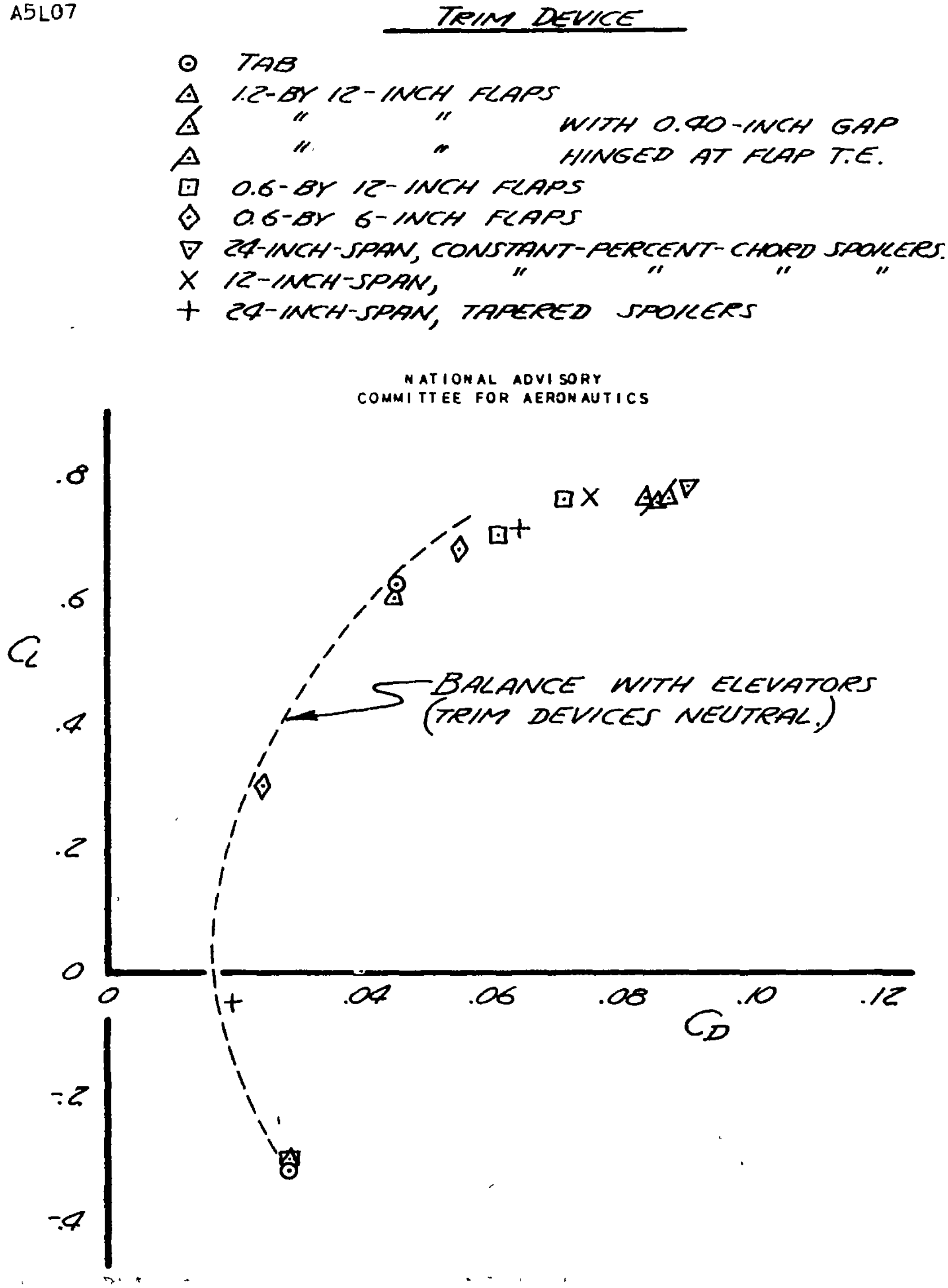

(b) M = 0.60

FIGURE 39.- (CONTINUED)

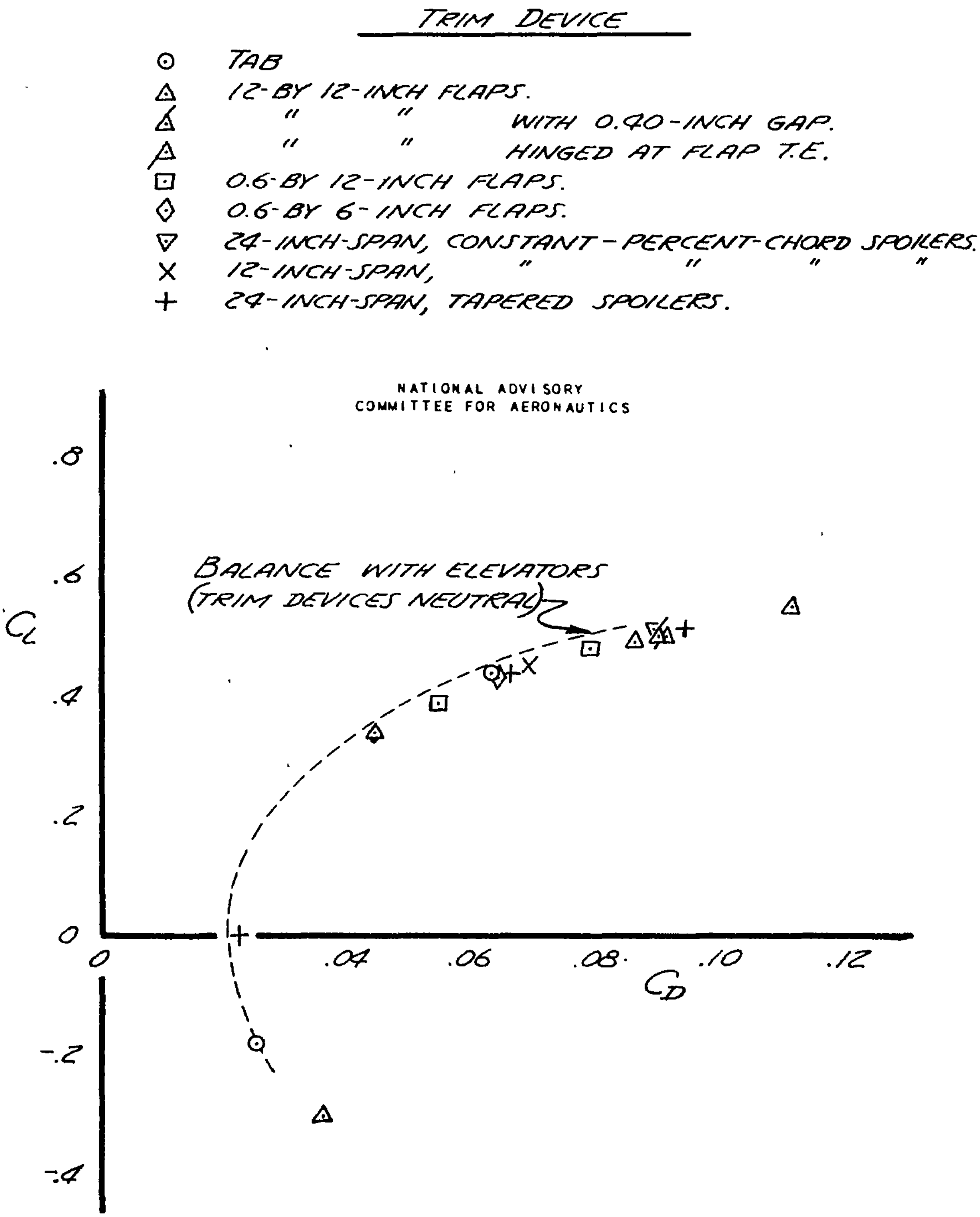

(c) M = 0.74

FIGURE 39.- (CONTINUED)

TRIM DEVICE

⊙	TAB
△	1.2-BY 12-INCH FLAPS.
△	" " WITH 0.40-INCH GAP.
△	" " HINGED AT FLAP T.E.
⊡	0.6-BY 12-INCH FLAPS.
◇	0.6-BY 6-INCH FLAPS.
▽	24-INCH-SPAN, CONSTANT-PERCENT-CHORD SPOILERS.
X	12-INCH-SPAN, " " " "
+	24-INCH-SPAN, TAPERED SPOILERS.

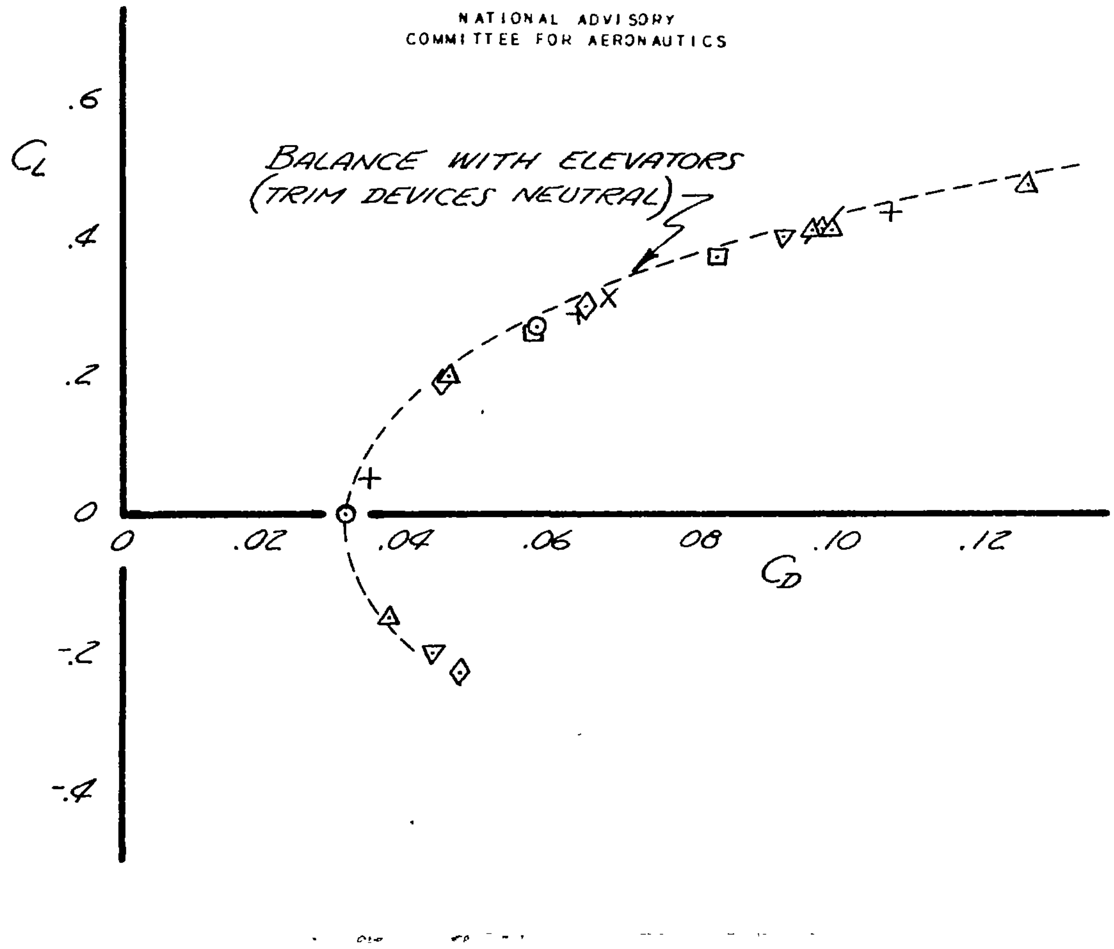

(d) M = 0.79

FIGURE 39.-(CONTINUED)

TRIM DEVICE

- ⊙ TAB
- △ 1.2- BY 12-INCH FLAPS
- △ " " WITH 0.40-INCH GAP
- △ " " HINGED AT FLAP T.E.
- ⊡ 0.6- BY 12-INCH FLAPS
- ◈ 0.6- BY 6-INCH FLAPS
- ▽ 24-INCH-SPAN, CONSTANT-PERCENT-CHORD SPOILERS
- × 12-INCH-SPAN, " " " "
- \+ 24-INCH-SPAN, TAPERED SPOILERS.

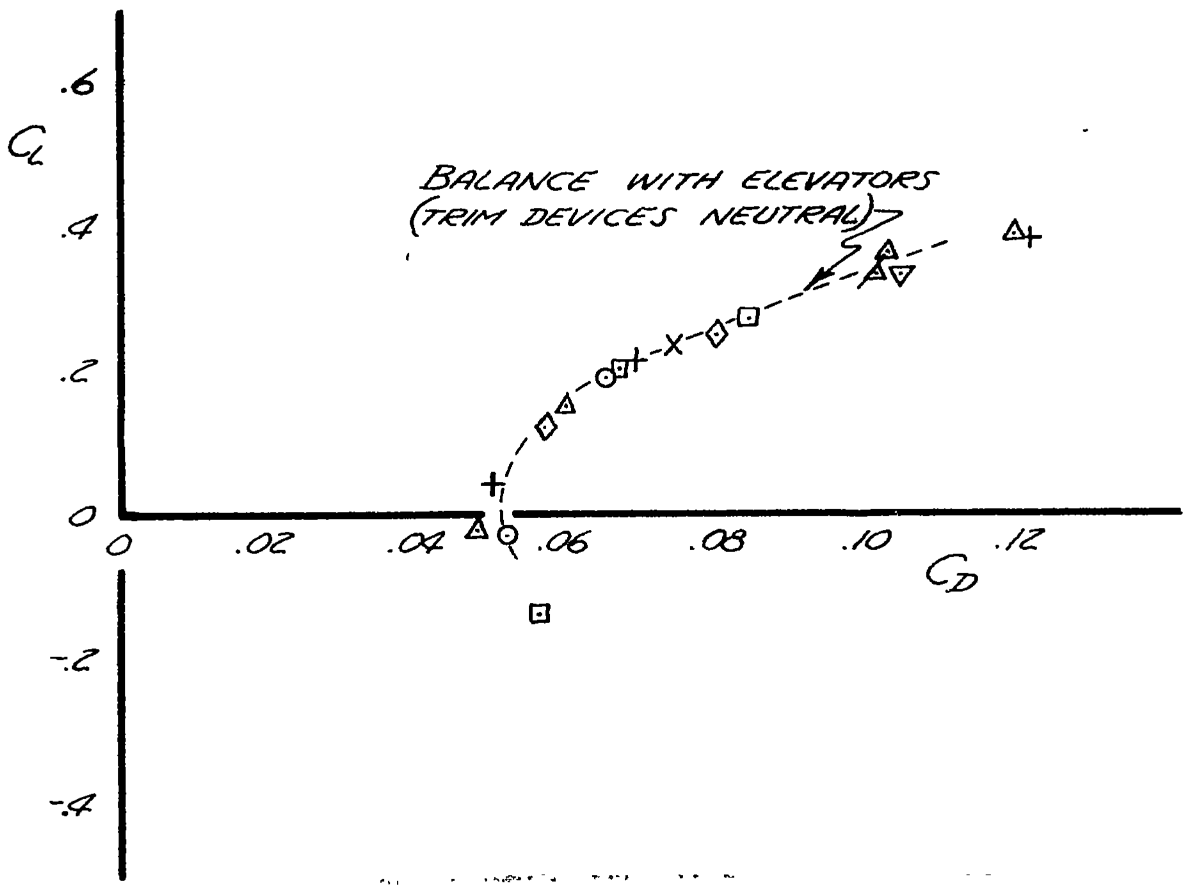

(e) $M = 0.815$

FIGURE 39.- (CONCLUDED)

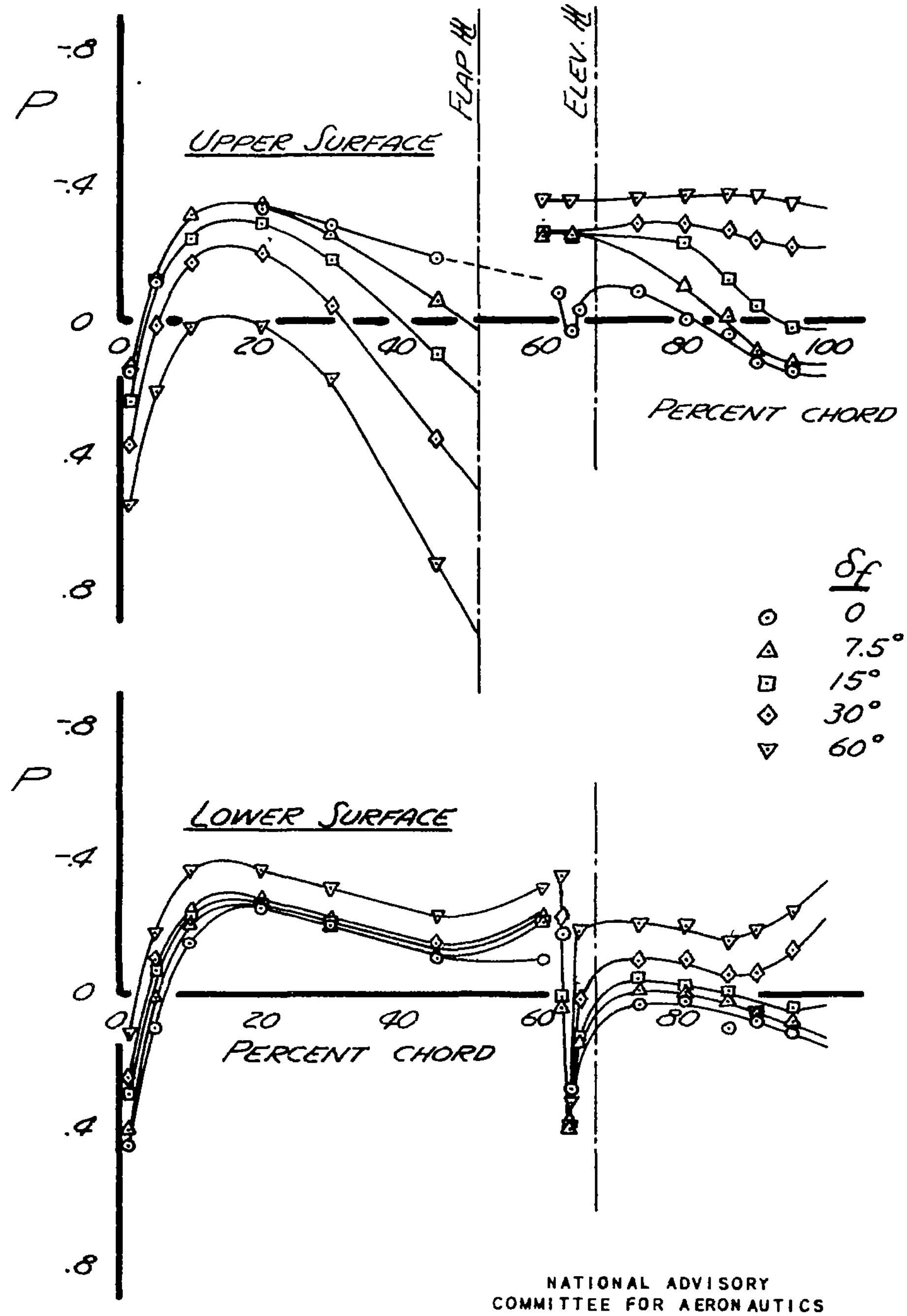

NATIONAL ADVISORY
COMMITTEE FOR AERONAUTICS

(a) $M = 0.20$, $\alpha_0 = 1°$

FIGURE 40.- PRESSURE DISTRIBUTION AT STATION 10.0 OF THE HORIZONTAL TAIL FOR SEVERAL DEFLECTIONS OF THE 1.2- BY 12-INCH FLAPS. $\delta_e = 0$

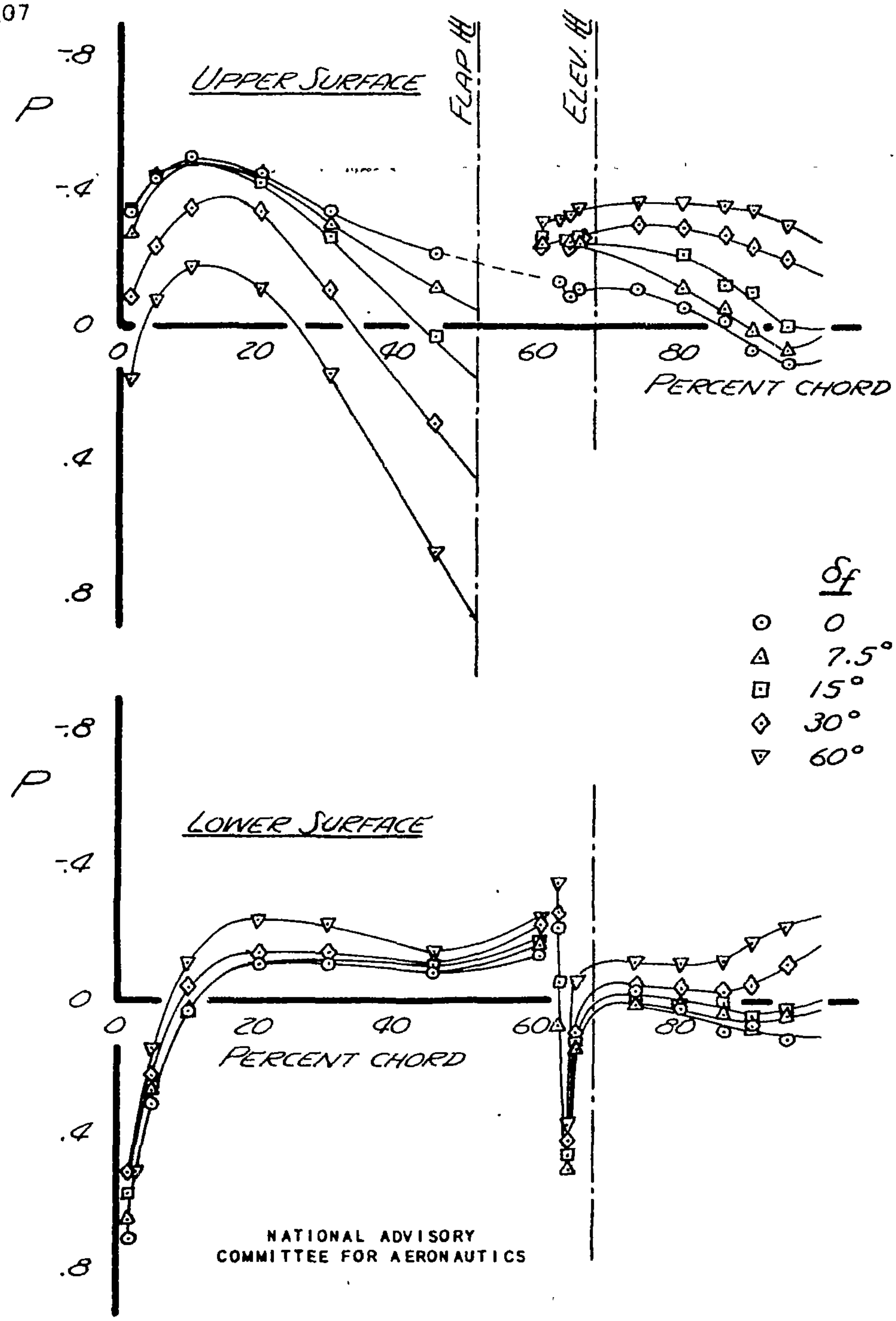

(b) $M=0.20$, $\alpha_u=5°$

FIGURE 40.- (CONTINUED)

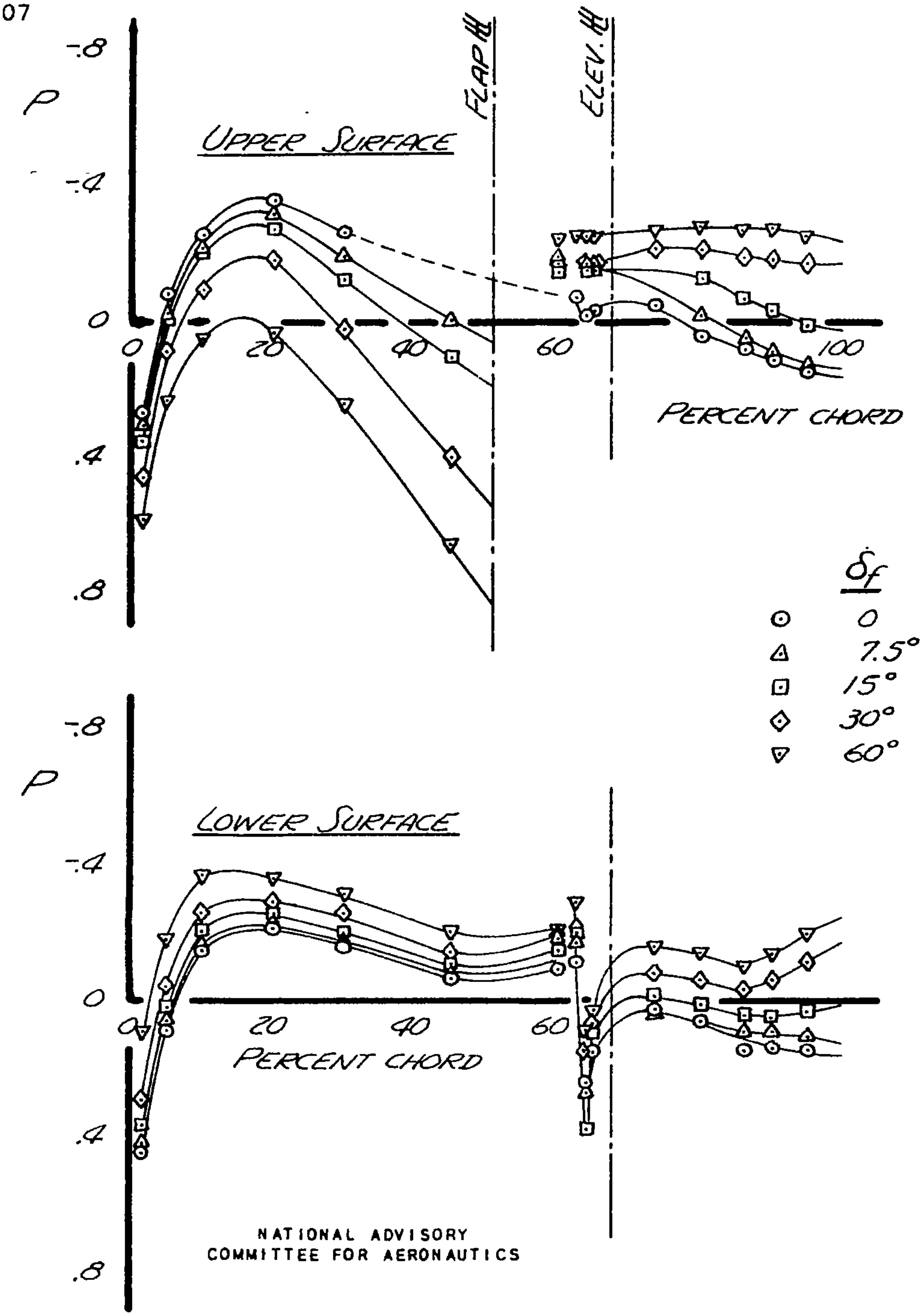

(c) $M = 0.60$, $\alpha_0 = 1°$

FIGURE 40.- (CONTINUED)

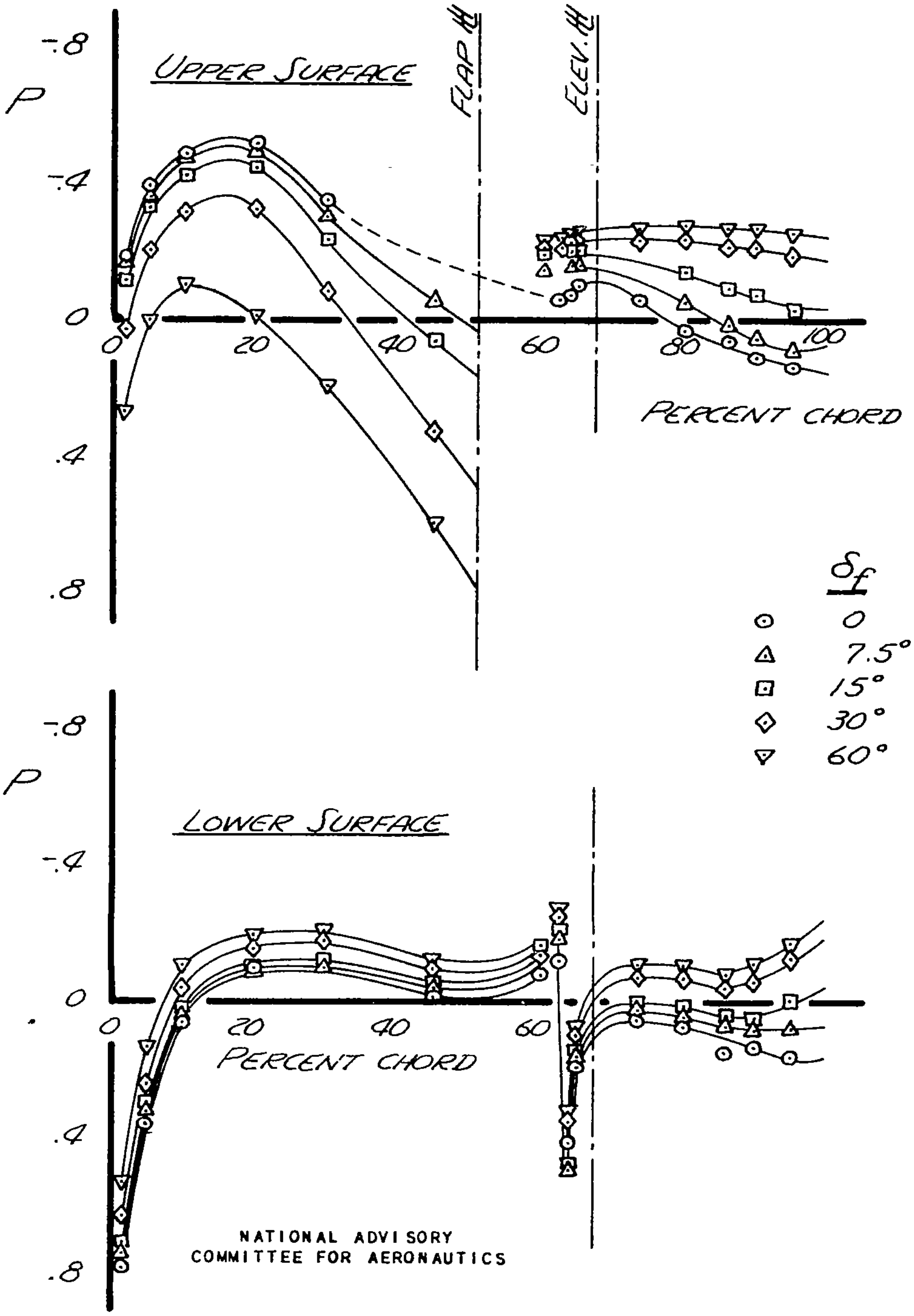

(d) $M = 0.60$, $\alpha_u = 5°$

FIGURE 40.- (CONTINUED)

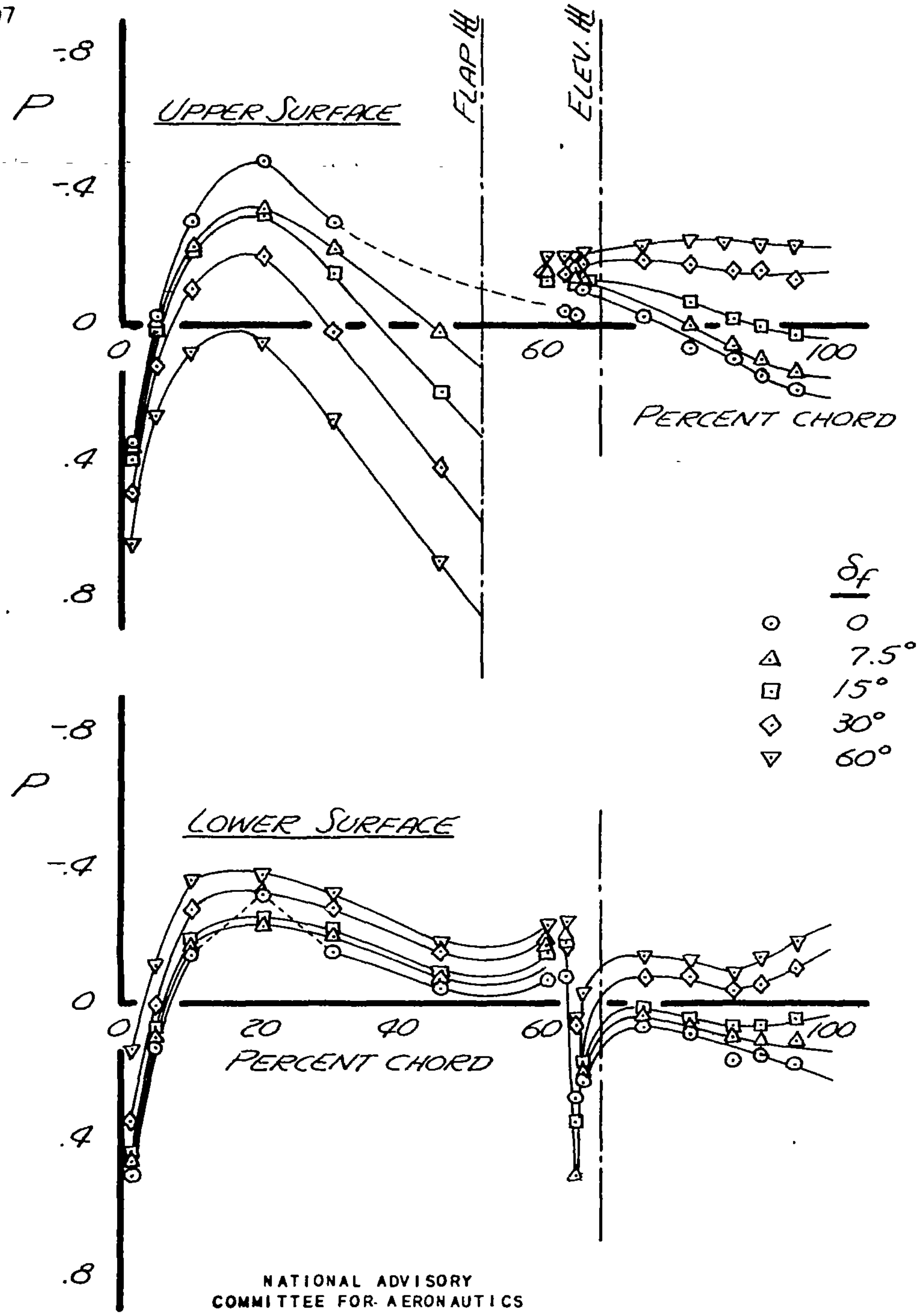

(e) $M = 0.74,\ \alpha_u = 1°$

FIGURE 40.-(CONTINUED)

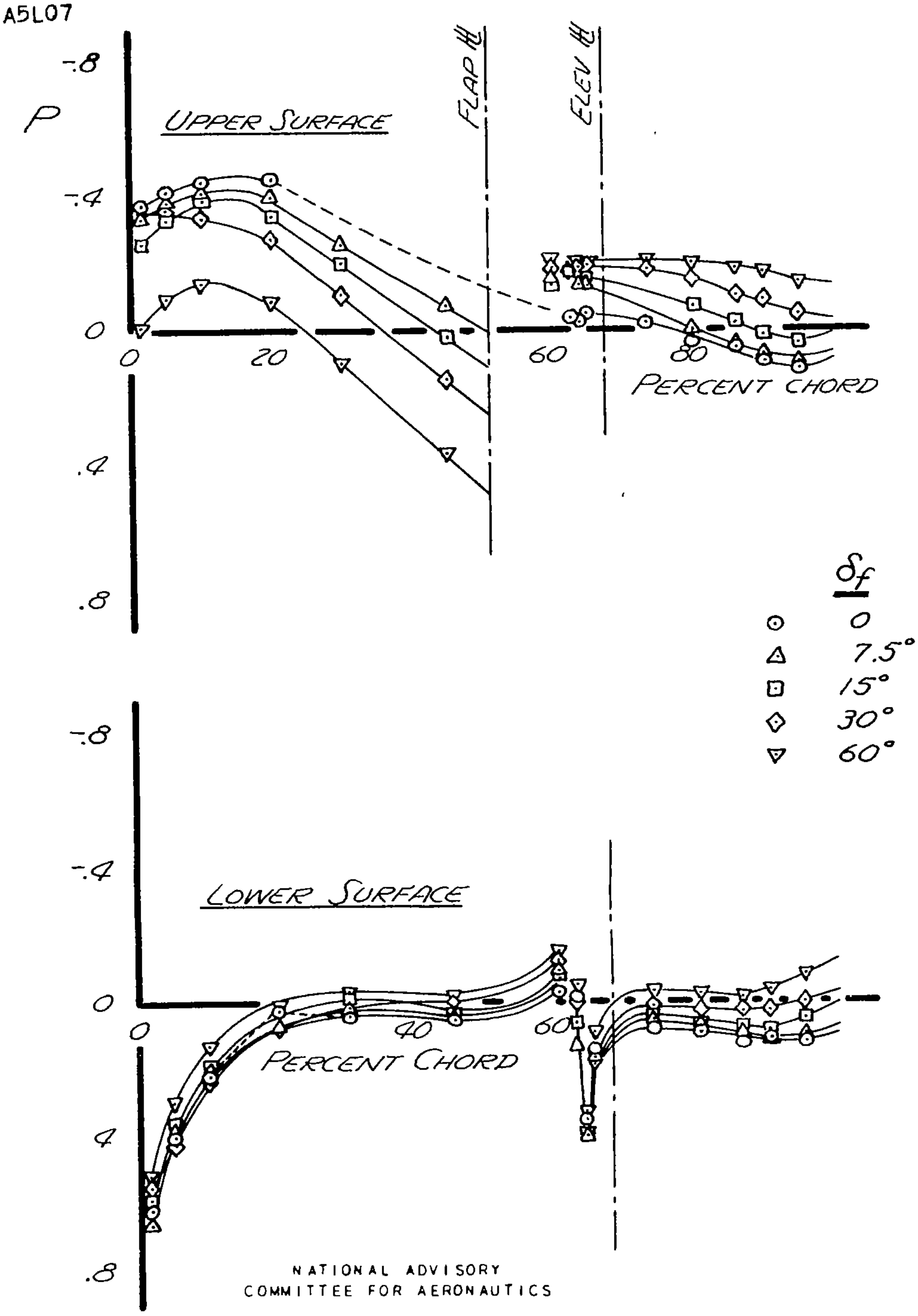

NATIONAL ADVISORY COMMITTEE FOR AERONAUTICS

(f) $M = 0.74,\ \alpha_u = 5°$

FIGURE 40.-(CONTINUED)

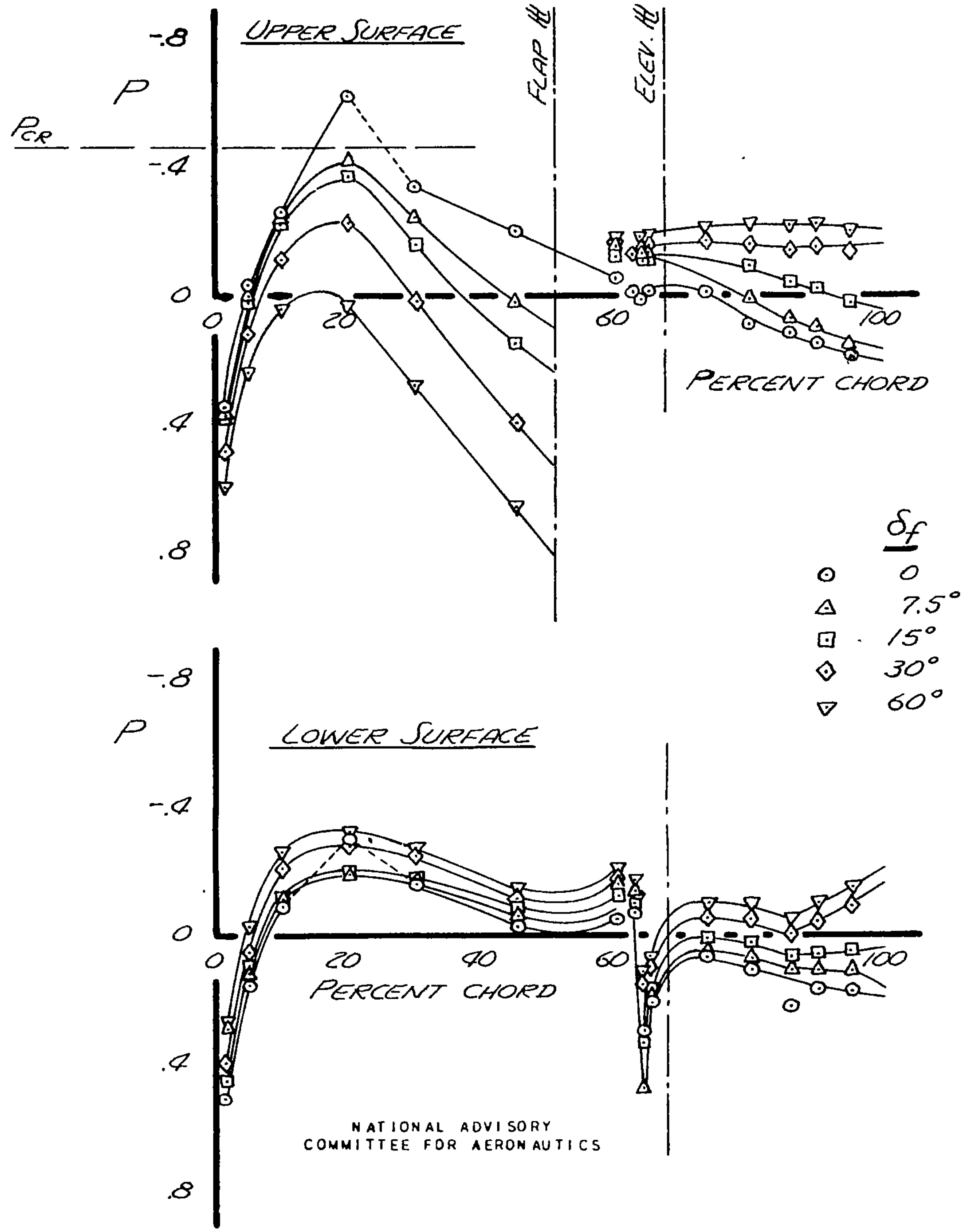

NATIONAL ADVISORY
COMMITTEE FOR AERONAUTICS

(g) M = 0.79, α_u = 1°

FIGURE 40.- (CONTINUED) 1.2- BY 12-INCH FLAPS

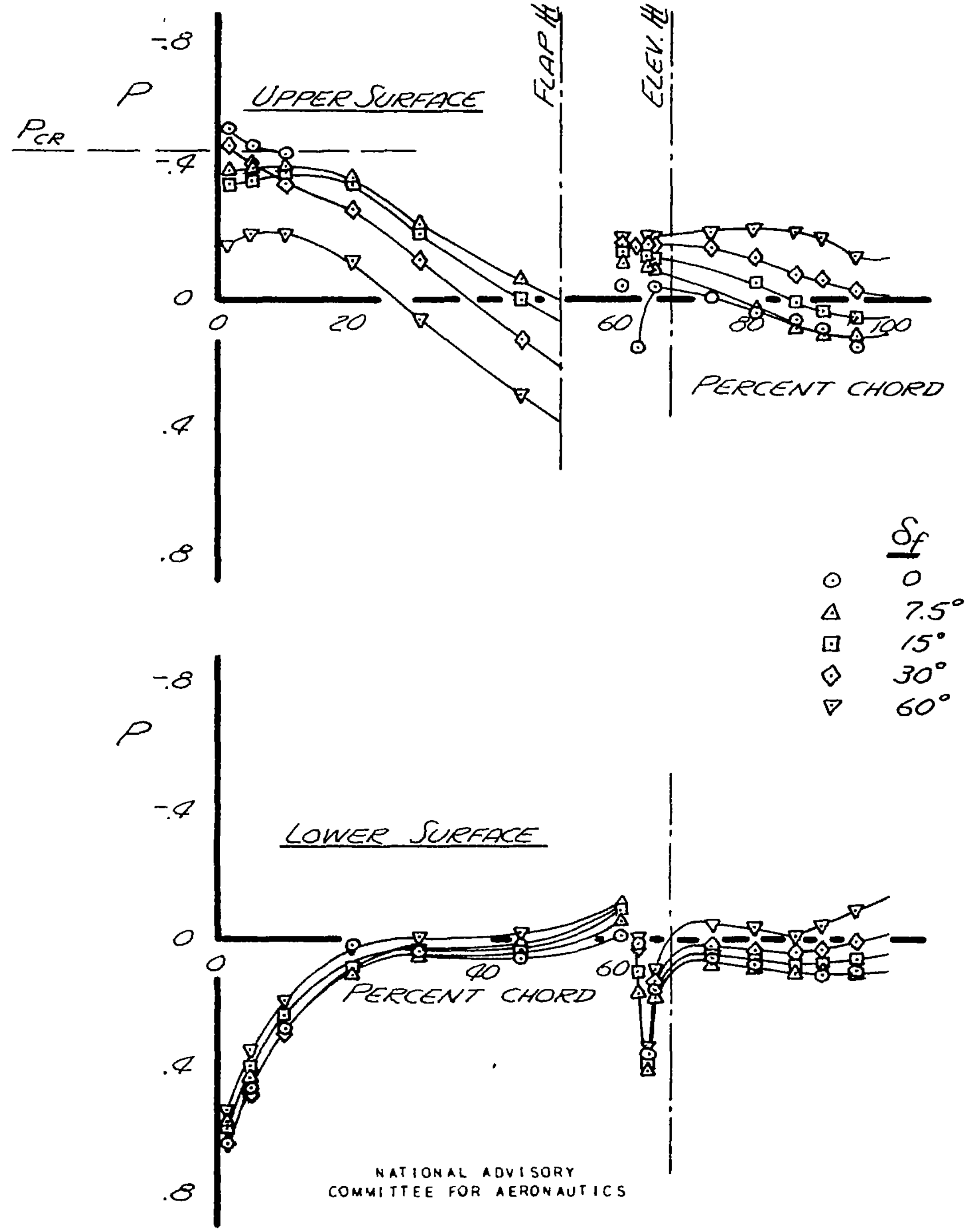

(h) $M = 0.79$, $\alpha_0 = 5°$

FIGURE 40.- (CONTINUED)

MR No. A5L07

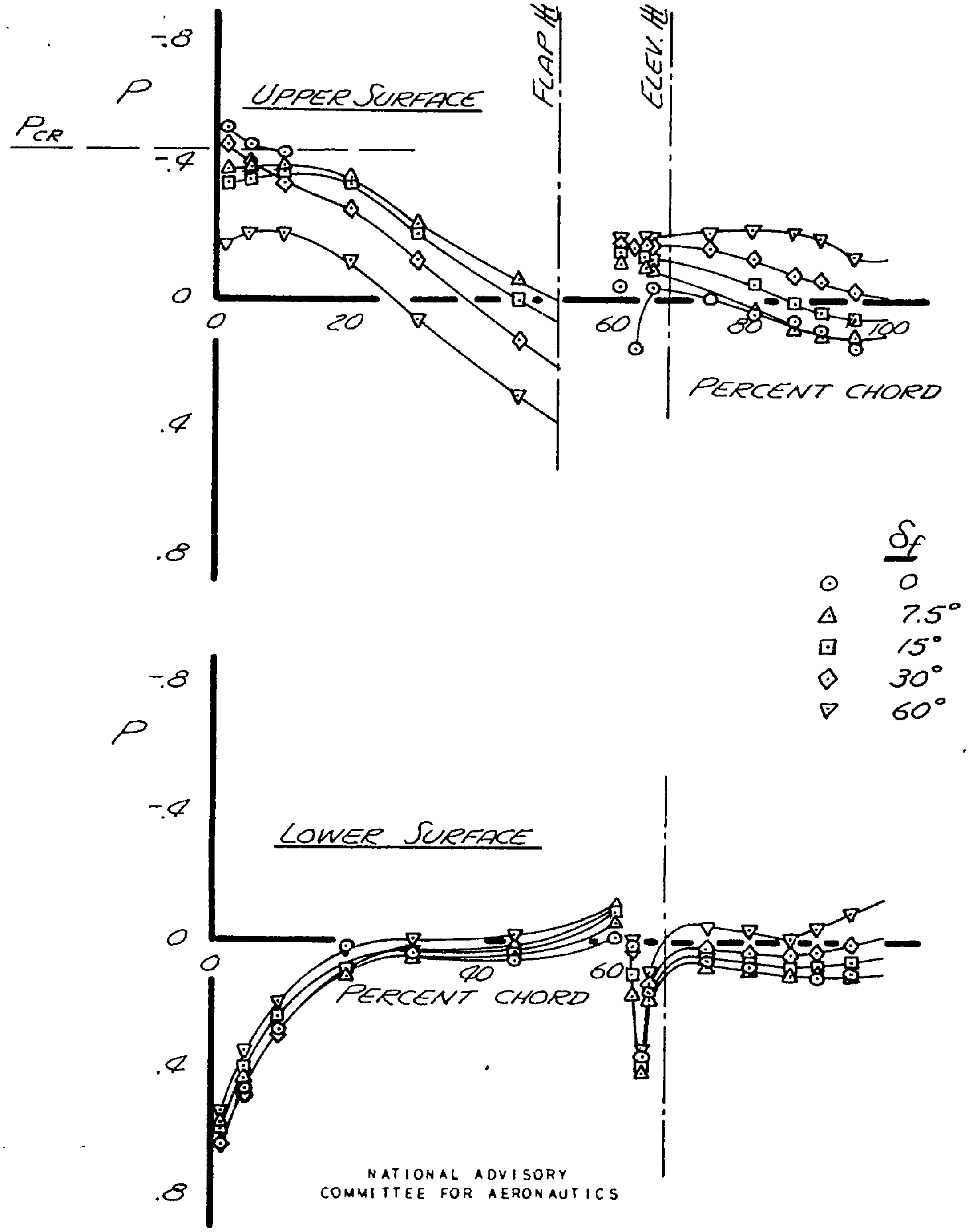

(h) $M = 0.79$, $\alpha_0 = 5°$

FIGURE 40.-(CONTINUED)

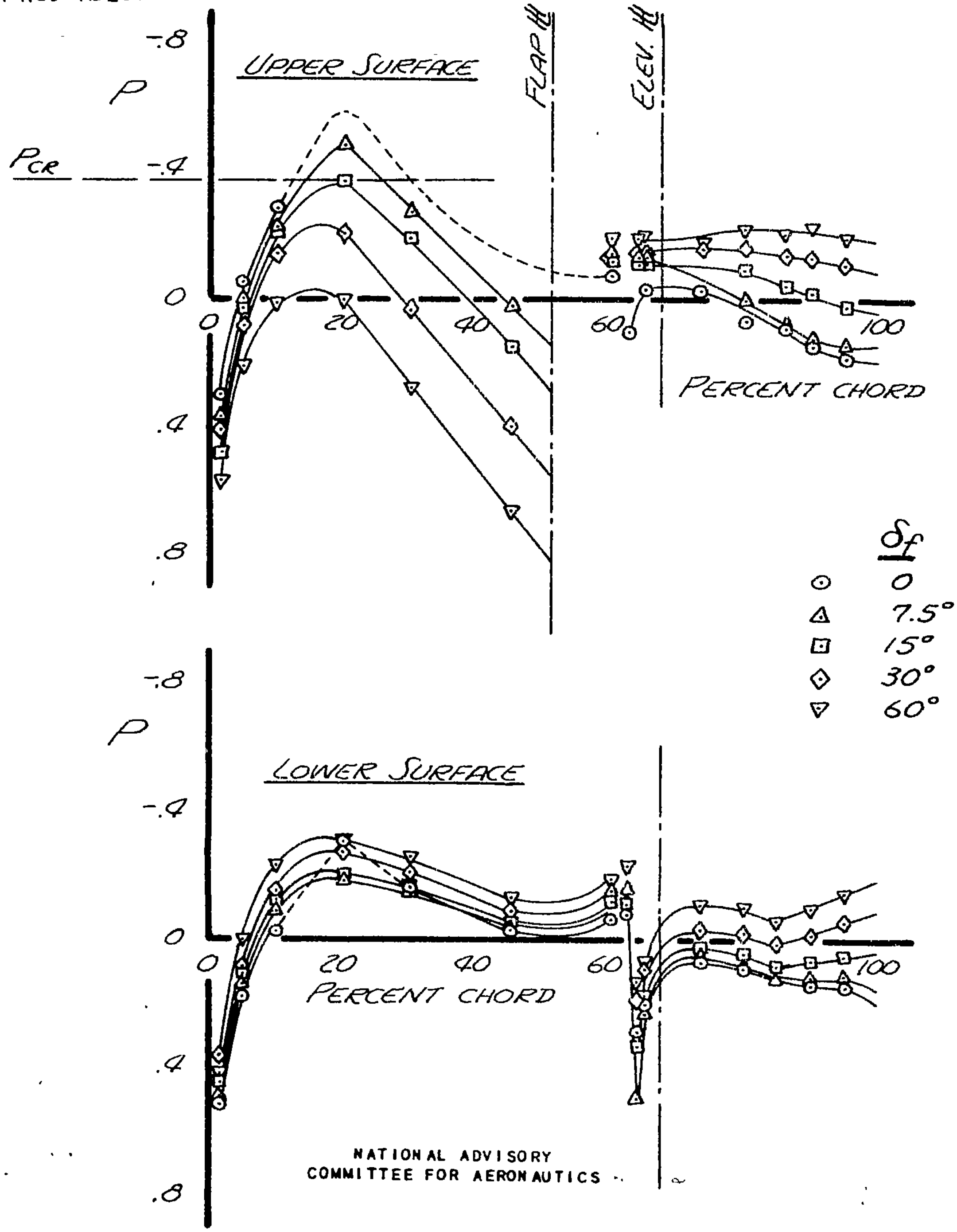

(i) $M = 0.815$, $\alpha_u = 1°$

FIGURE 40.- (CONTINUED)

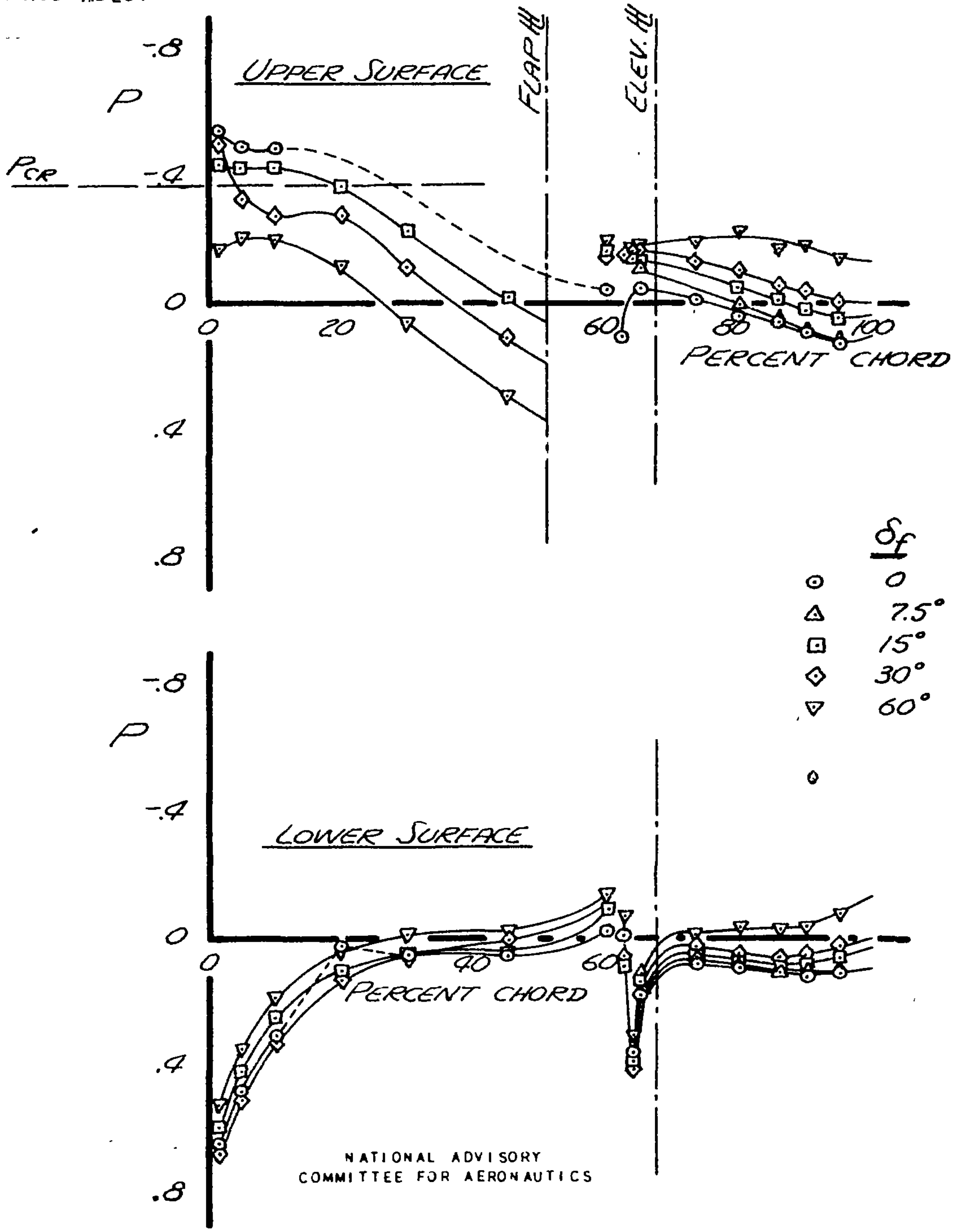

(j) $M = 0.815$, $\alpha_0 = 5°$

FIGURE 40.- (CONCLUDED)

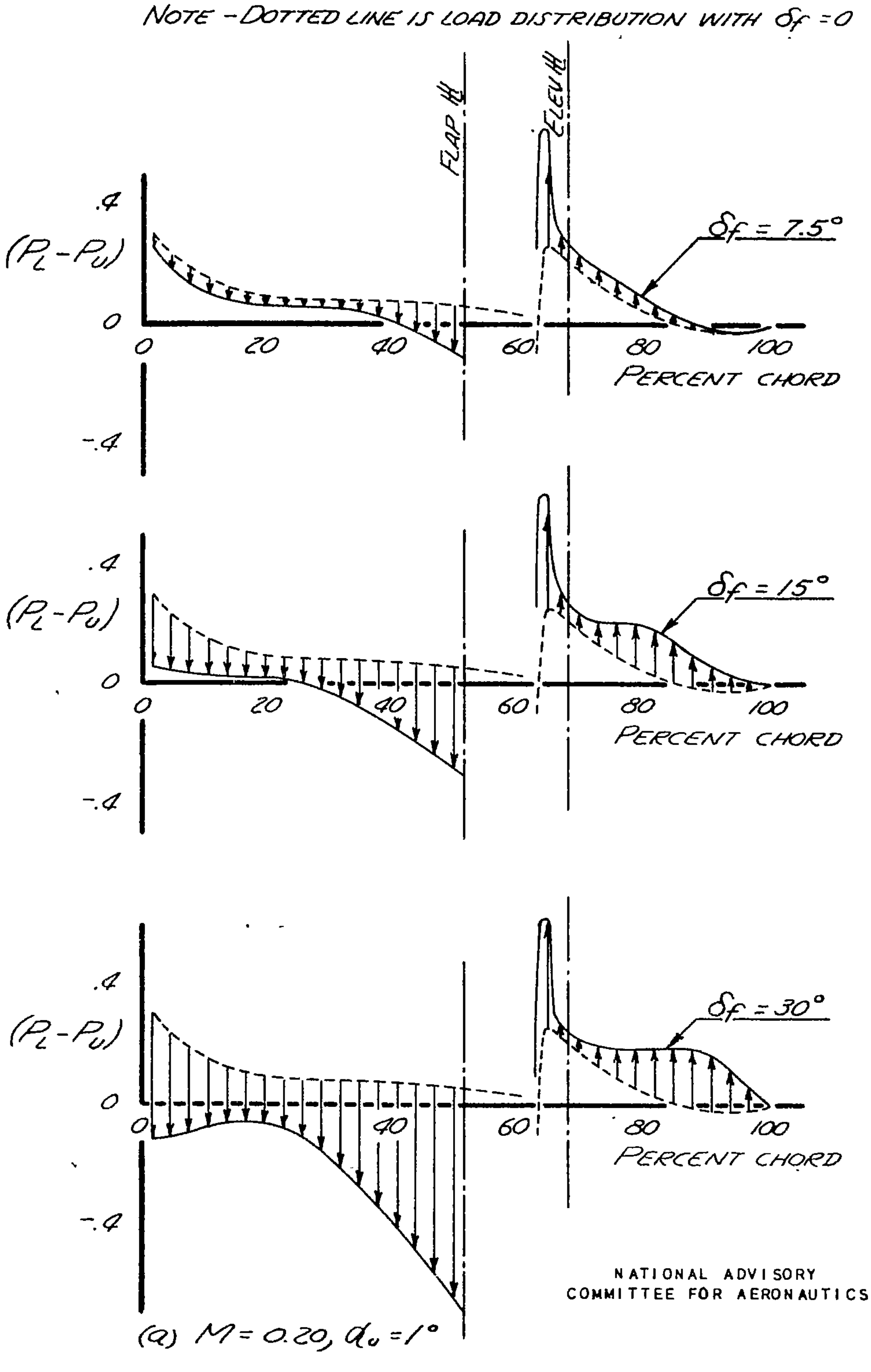

FIGURE 41.- LOAD DISTRIBUTION AT STATION 10.0 OF THE HORIZONTAL TAIL FOR SEVERAL DEFLECTIONS OF THE 1.2- BY 12-INCH FLAPS. $\delta_e = 0$

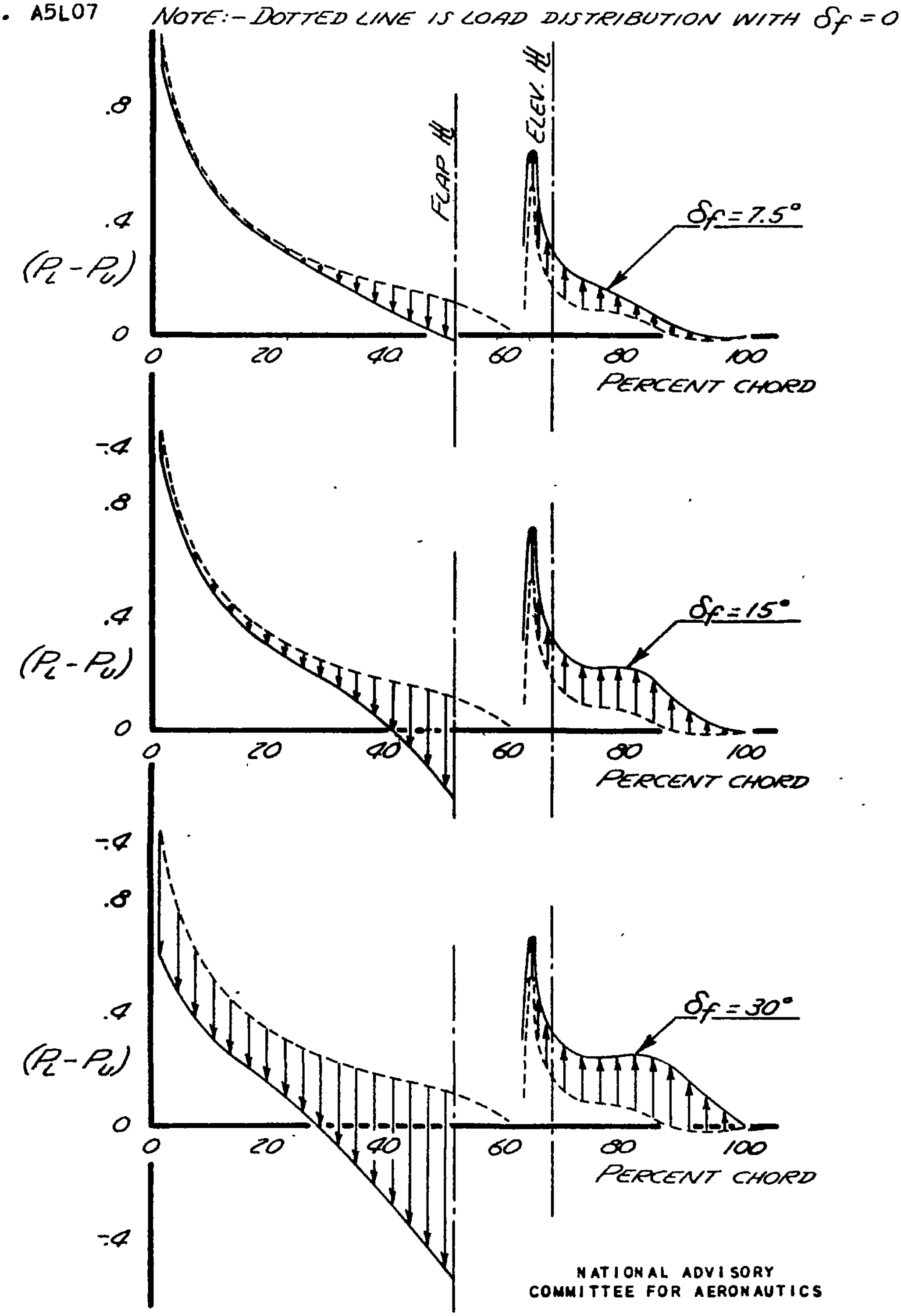

NATIONAL ADVISORY COMMITTEE FOR AERONAUTICS

(b) $M = 0.20$, $\alpha_u = 5°$

FIGURE 41.- (CONTINUED)

NOTE:-DOTTED LINE IS LOAD DISTRIBUTION WITH $\delta_f = 0$

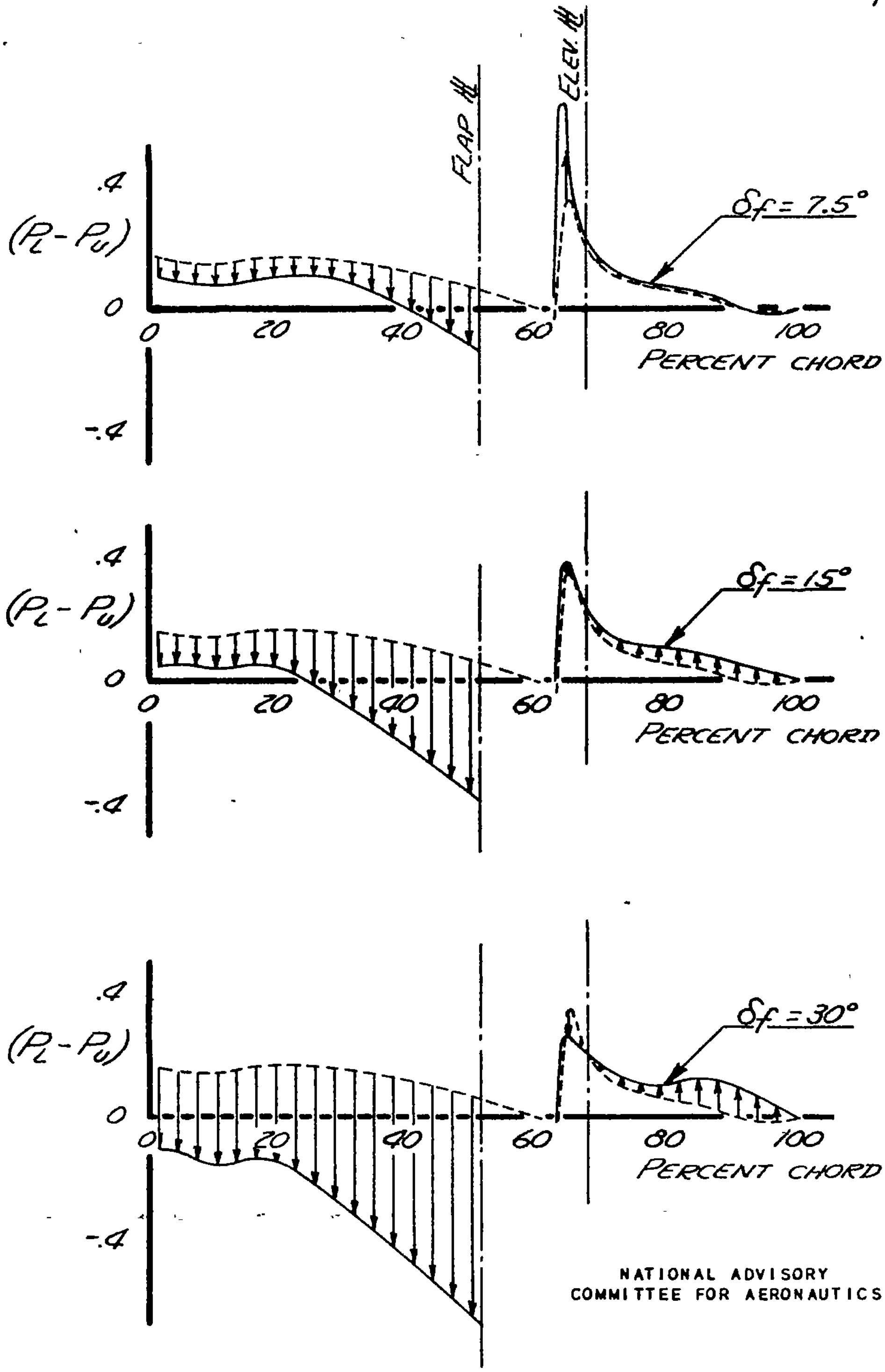

(c) $M = 0.74$, $\alpha_u = 1$

FIGURE 41.- (CONTINUED)

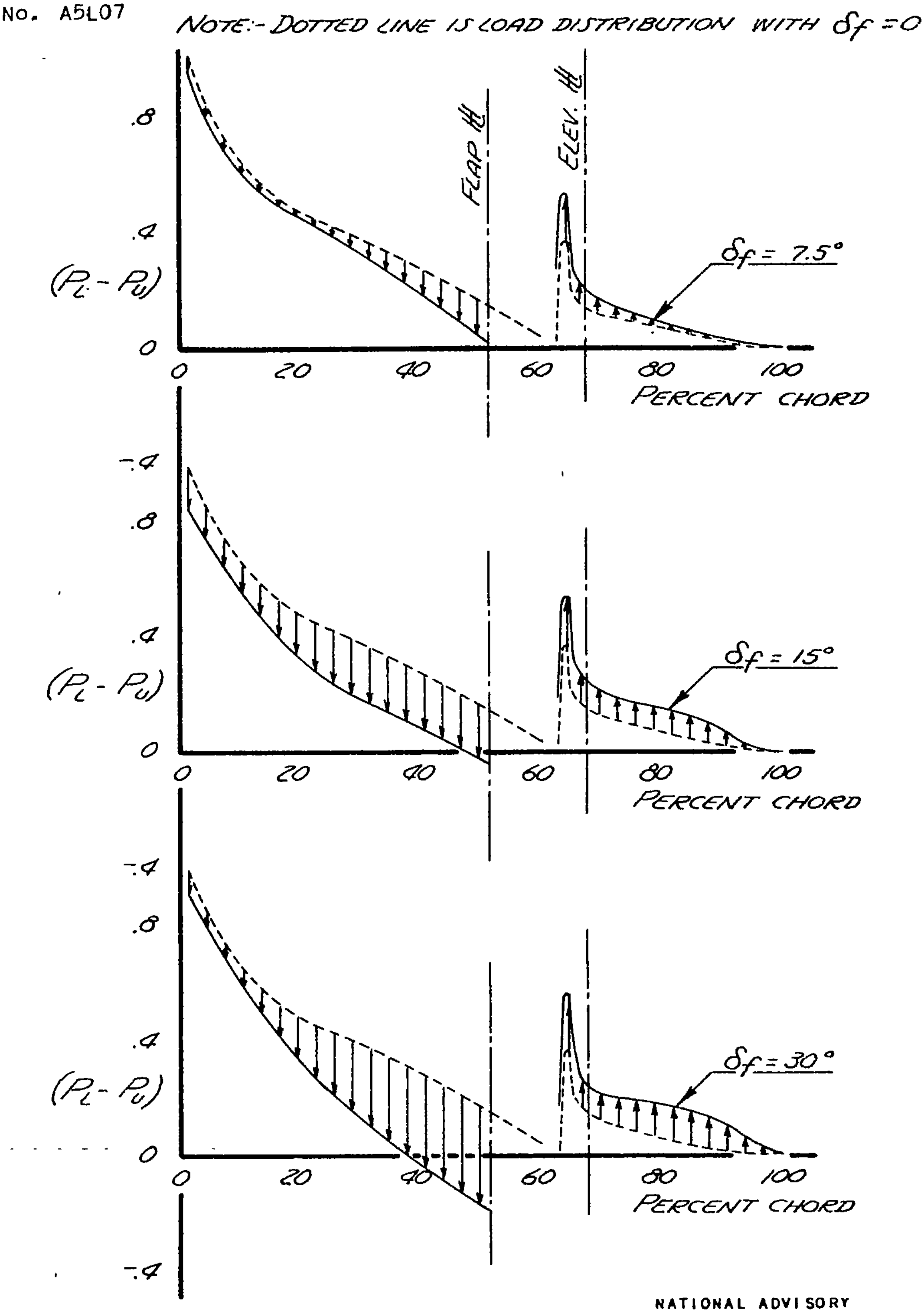

(d) M = 0.74, αu = 5°

FIGURE 41.- (CONTINUED)

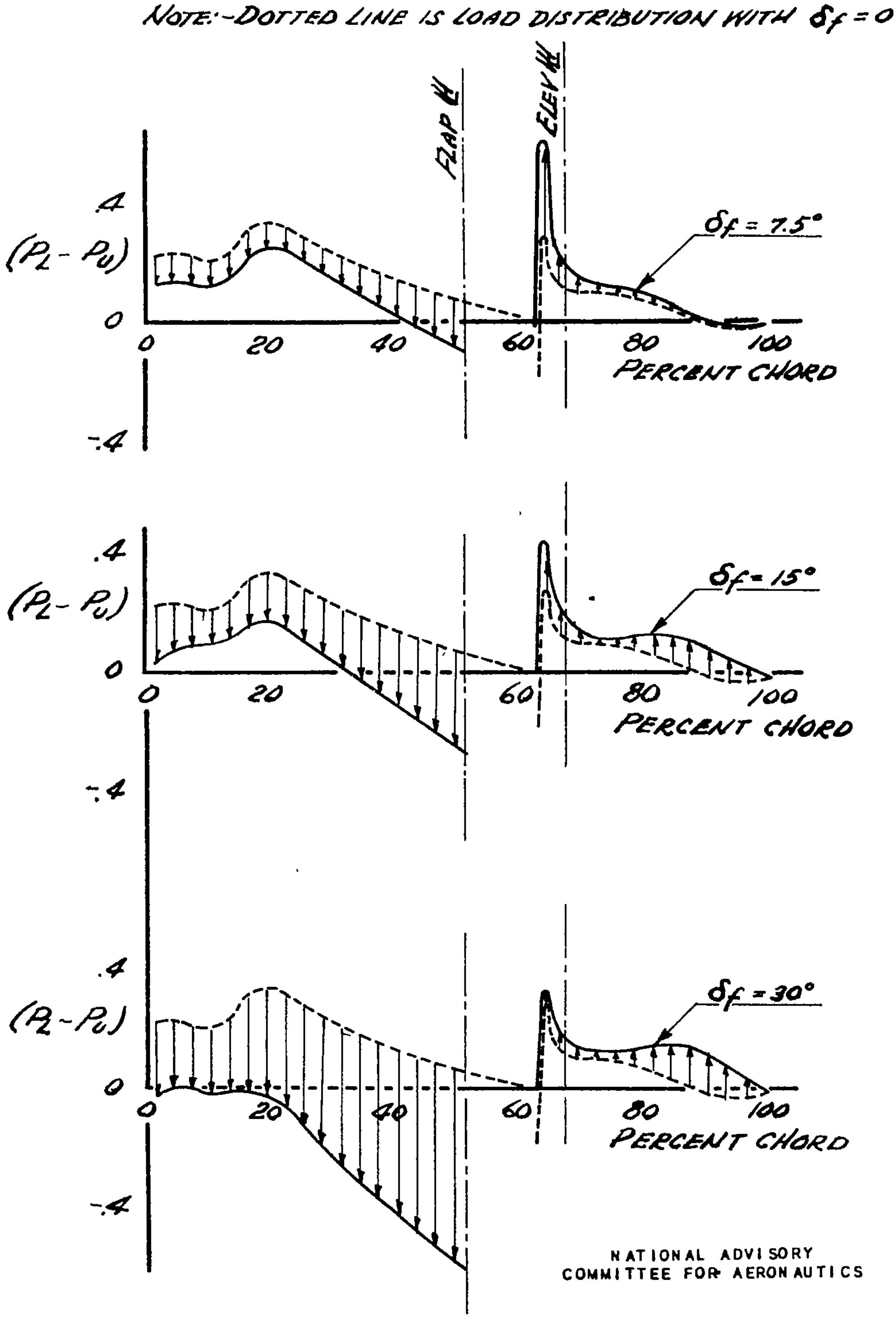

(e) $M = 0.815$, $\alpha_u = 1°$

FIGURE 41.- (CONTINUED)

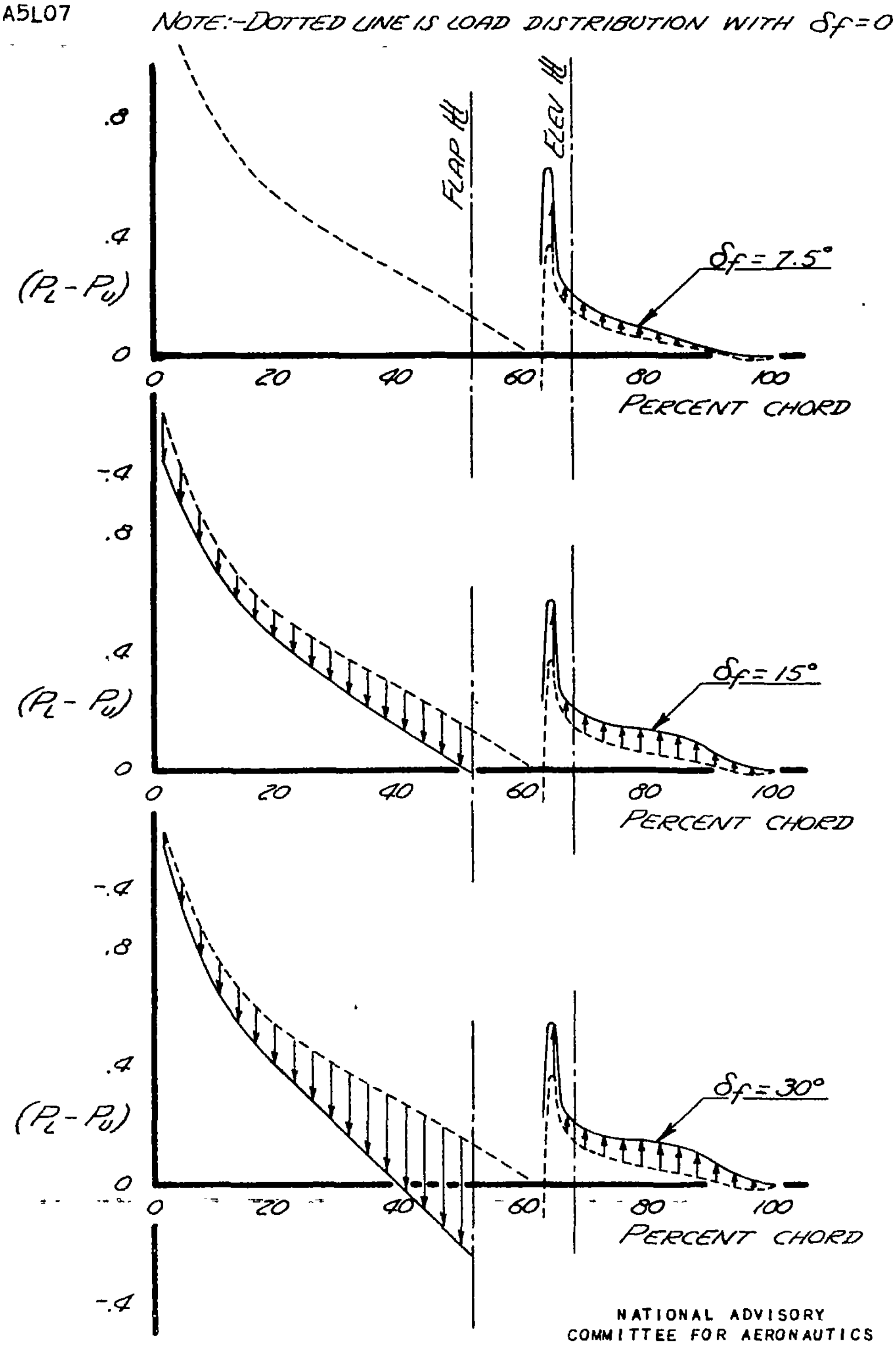

NATIONAL ADVISORY
COMMITTEE FOR AERONAUTICS

(f) $M = 0.815$, $\alpha_u = 5°$

FIGURE 41.-(CONCLUDED)

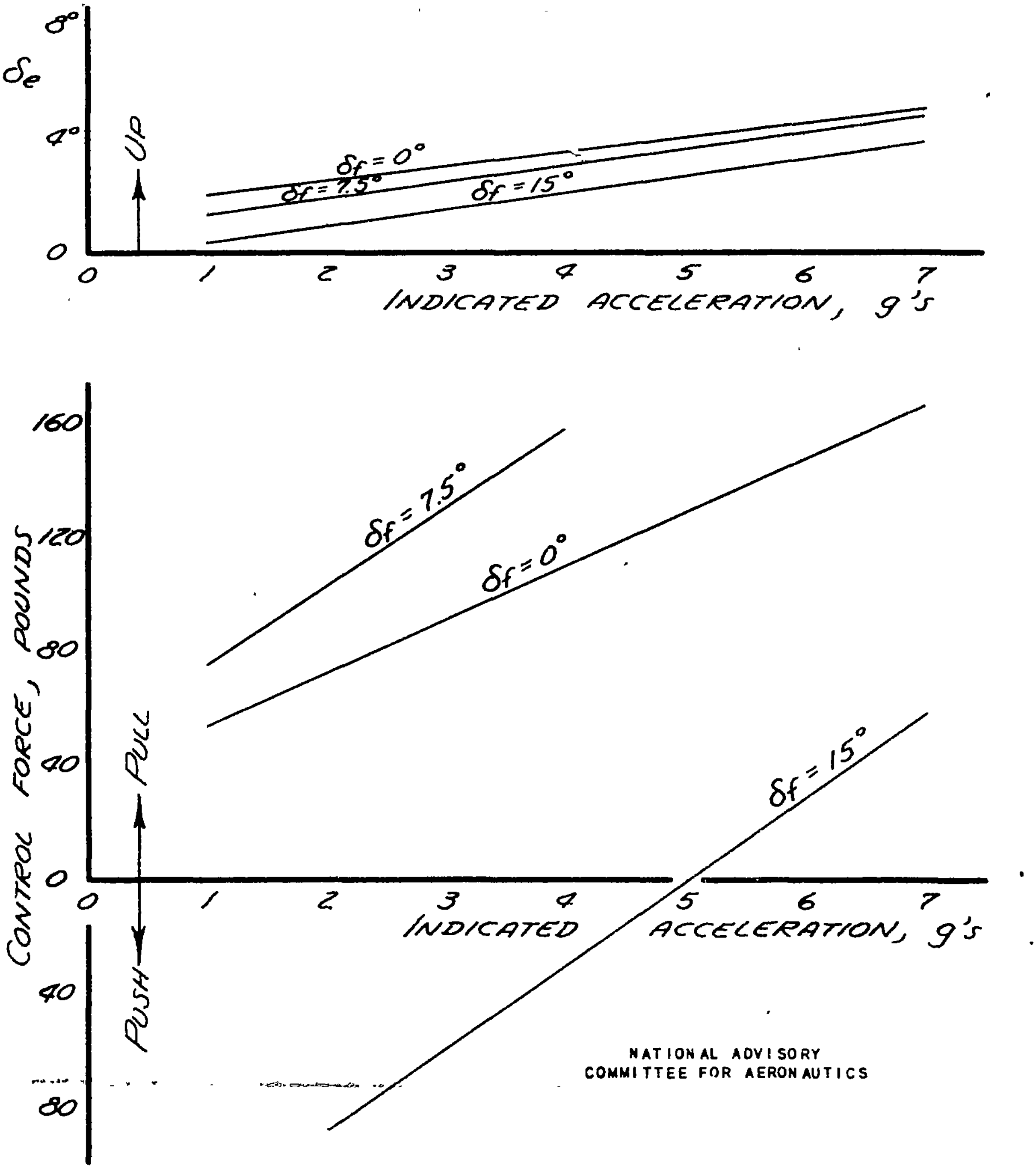

(a) $M = 0.60$, $V = 460$ mph

FIGURE 42.- ESTIMATED VARIATION OF ELEVATOR ANGLE AND CONTROL FORCE WITH INDICATED NORMAL ACCELERATION OF THE PURSUIT AIRPLANE AT SEA LEVEL FOR SEVERAL DEFLECTIONS OF THE 1.2- BY 12-INCH FLAPS (MODEL SIZE). WING LOADING OF 45 POUNDS PER SQUARE FOOT. $\delta_t = 0°$

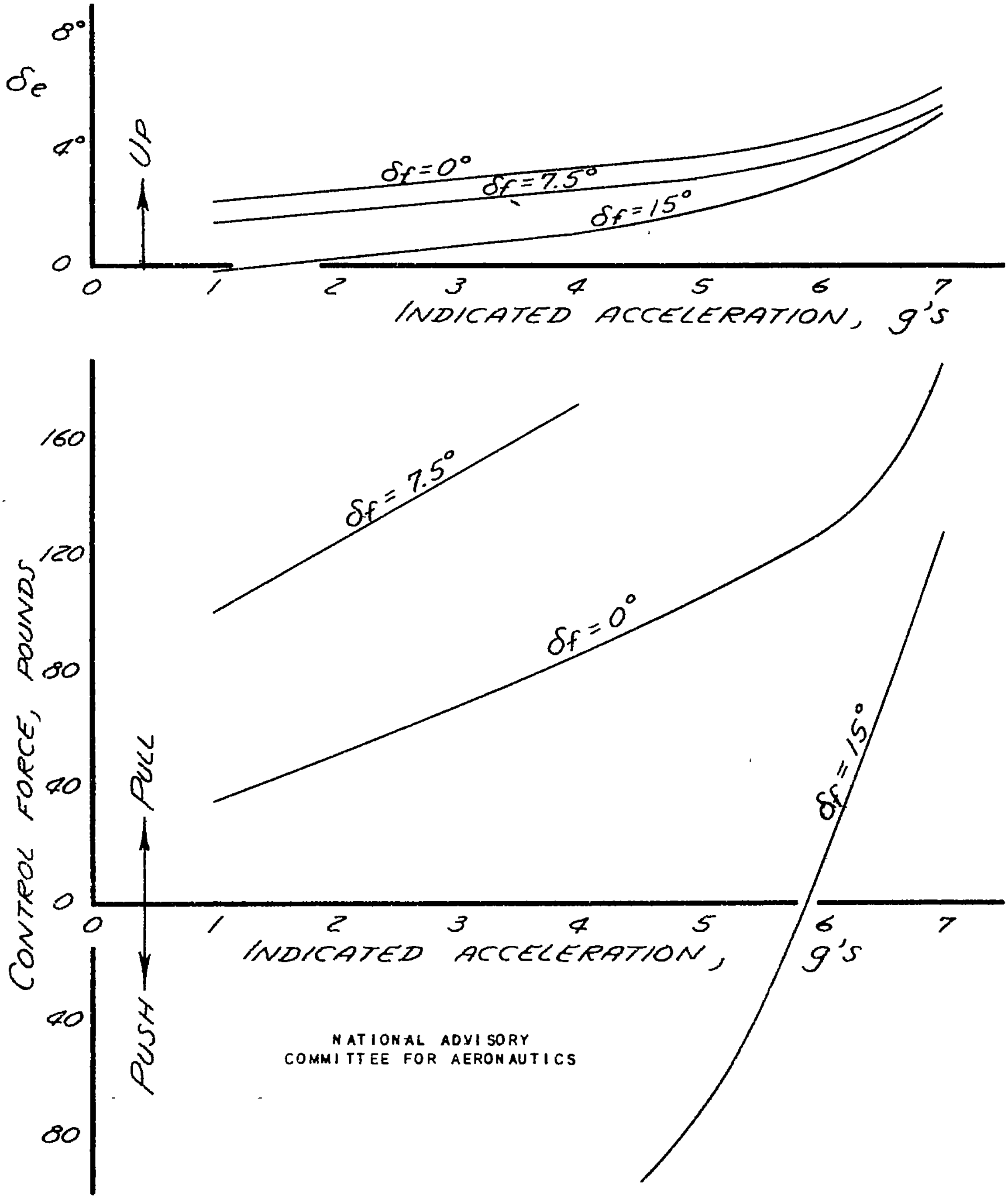

(b) M = 0.74, V = 565 mph

FIGURE 42.-(CONTINUED)

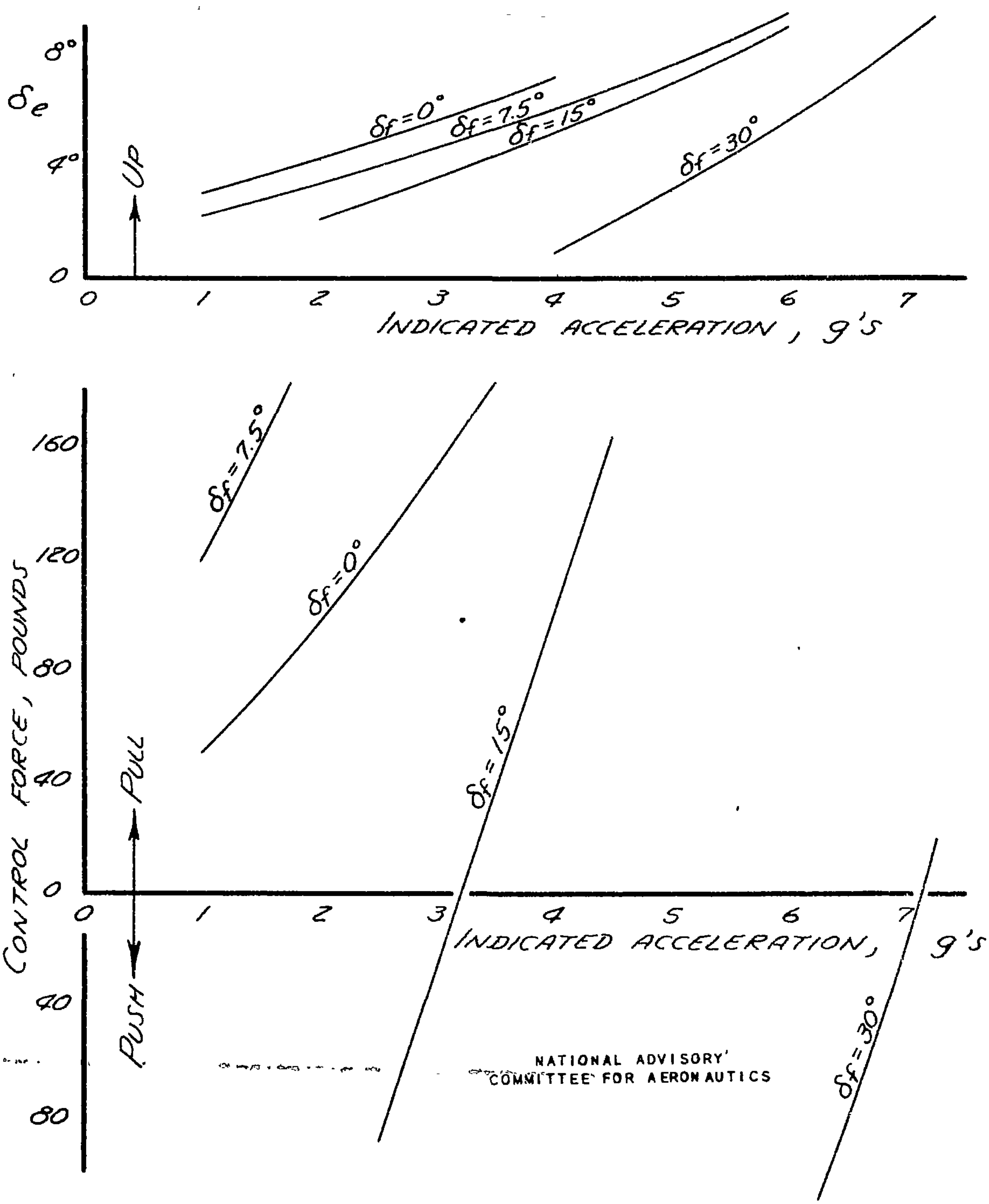

(c) $M = 0.815$, $V = 625$ mph

FIGURE 42.-(CONCLUDED)

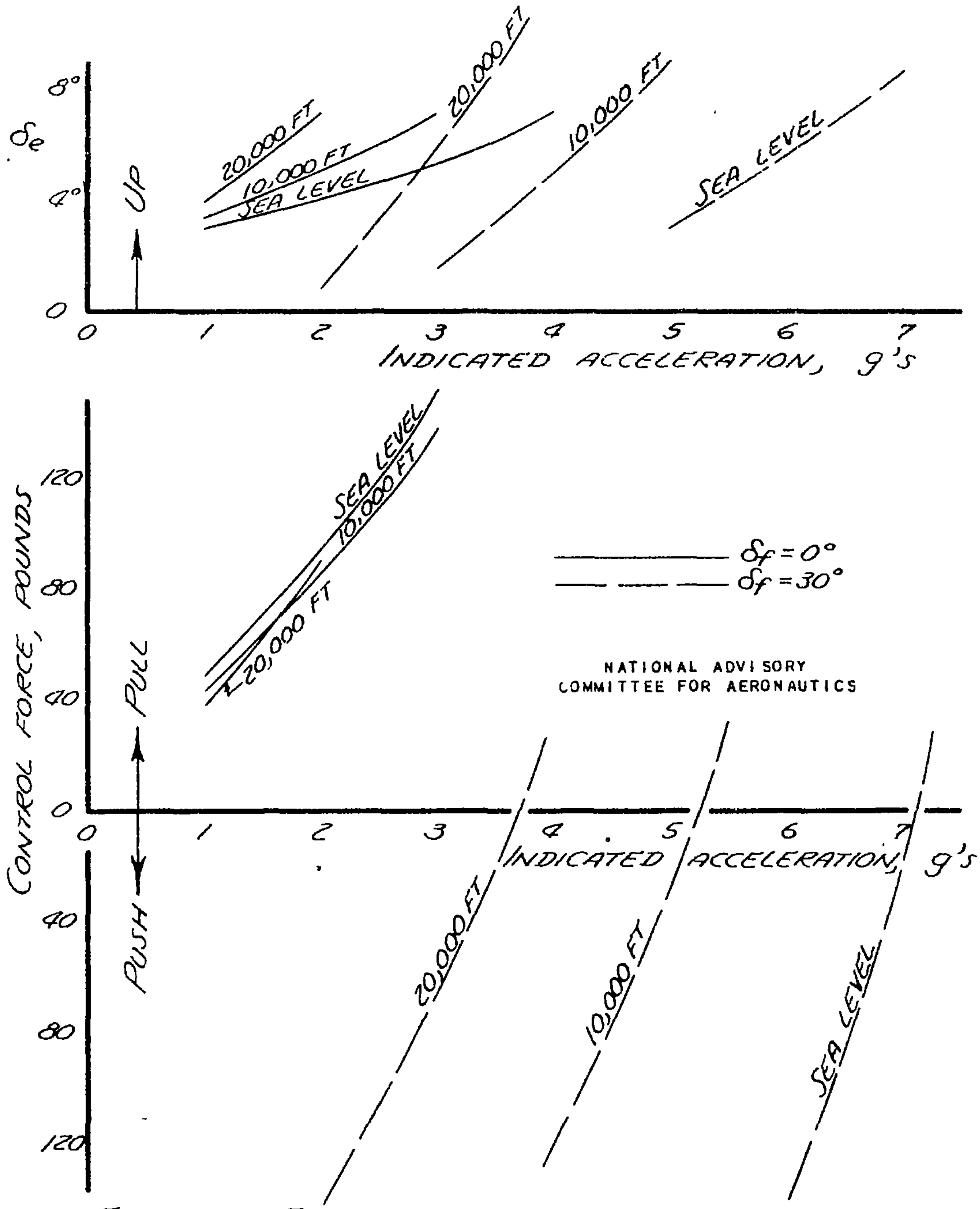

FIGURE 43.–ESTIMATED VARIATION OF ELEVATOR ANGLE AND CONTROL FORCE WITH INDICATED NORMAL ACCELERATION OF THE PURSUIT AIRPLANE AT SEVERAL ALTITUDES FOR 0° AND 30° DEFLECTION OF THE 12- BY 12-INCH FLAPS (MODEL SIZE). WING LOADING OF 45 POUNDS PER SQUARE FOOT. $\delta_t = 0°$. MACH NUMBER OF 0.815

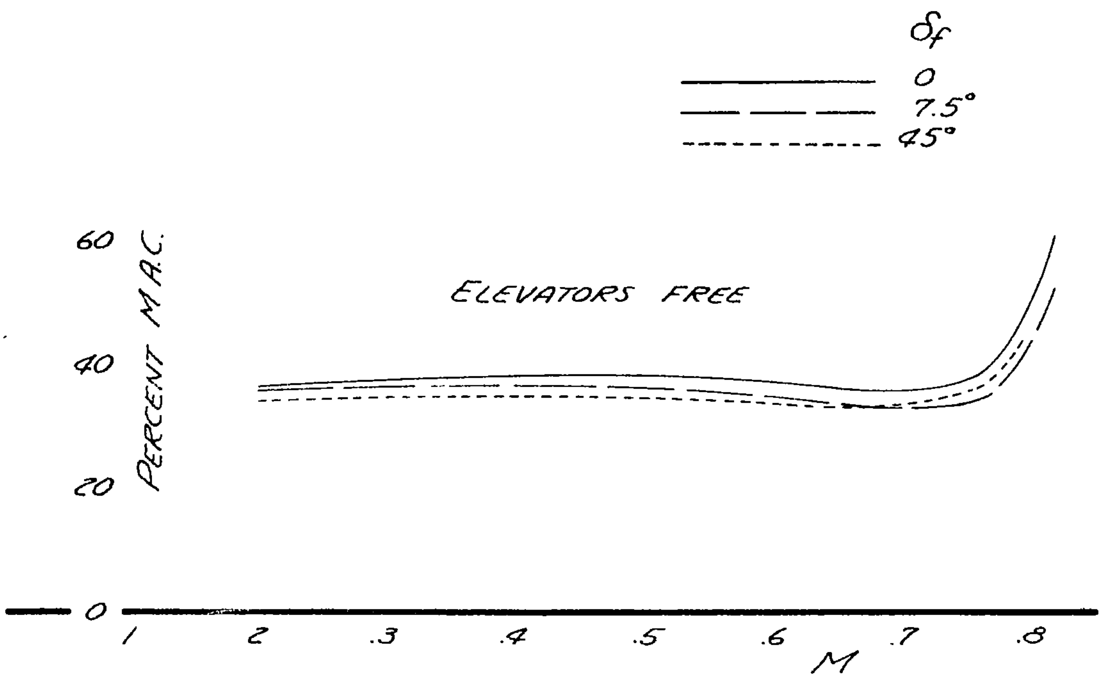

NATIONAL ADVISORY
COMMITTEE FOR AERONAUTICS

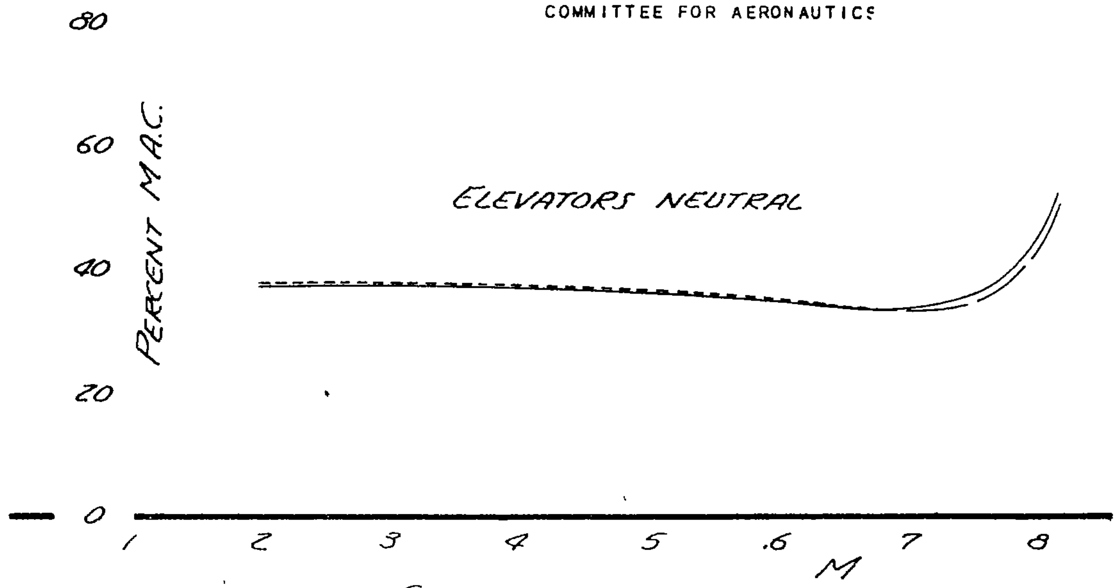

(a) $C_L = 0$

FIGURE 44.- STICK-FREE AND STICK-FIXED NEUTRAL POINT FOR SEVERAL DEFLECTIONS OF THE 1.2- BY 12-INCH FLAPS

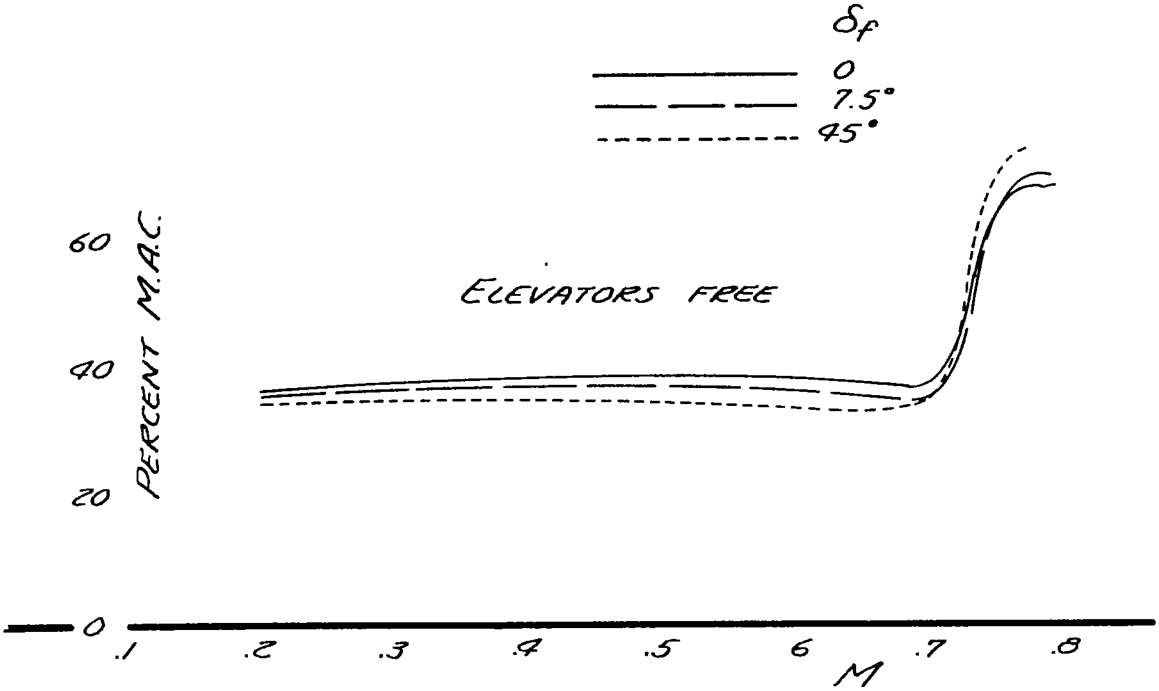

NATIONAL ADVISORY
COMMITTEE FOR AERONAUTICS

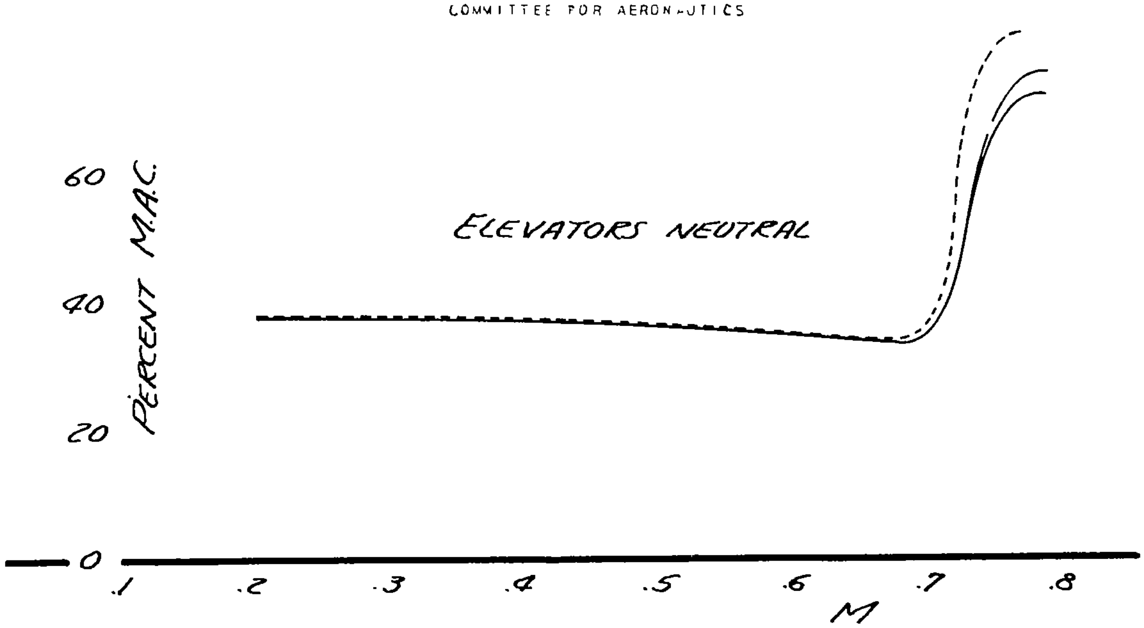

(b) $C_L = 0.40$

FIGURE 44.- (CONCLUDED)